FUNDAMENTAL STUDIES OF VITAMIN DIFFUSIONAL MOBILITY IN HIGH-SOLID HYDROCOLLOID MATRICES

A Thesis submitted in fulfillment of the requirements for

the degree of Doctor of Philosophy

Naksit Panyoyai

B.Sc. (Honours), M.Sc.

(Food Science and Technology)

School of Science

College of Science, Engineering and Health (SEH)

RMIT University

MELBOURNE-AUSTRALIA

APRIL 2016

DECLARATION

I, Naksit Panyoyai, certify that except where due acknowledgement has been made, the work is that of the author alone; the work has not been submitted previously, in whole or in part, to qualify for any other academic award; the content of the Thesis is the result of work which has been carried out since the official commencement due of the approval research program; any editorial work, paid or unpaid, carried out by a third party is acknowledged; and, ethics procedures and guidelines has been followed.

Naksit Panyoyai

1 April 2016

DEDICATION

This Thesis is dedicated to my loved ones,

My parents

Saman and Khemthong Panyoyai

For giving me life and love

&

My sister

Vimuthita Panyoyai

For without their love, support, friendship, understanding, and sacrifices,

This Thesis would not have come to fruition.

In loving memory of my grandmothers and grandfathers,

Nuan and Nan Panyoyai
Boonyowng and Kammee Palee

Life is suffering.

Gautama Buddha

Founder of Buddhism

ACKNOWLEDGEMENTS

Success in completing my doctoral degree was destined to be a challenging journey and it would not have been possible to do experimental work at RMIT University and write this Thesis without advice, encouragement and support from many people and organisations. Although the cover of this Thesis mentions only my name, I acknowledge everyone from deep within for helping me to complete this research successfully.

First and foremost, I express my gratitude to principal supervisor, Professor Stefan Kasapis, who made my study abroad possible through the supervision, smart and endless wisdom and thoughts as well as scientific insight in rheology and food biophysics to the highest publication standards. This continually inspired and motivated me to complete the hard work.

I express my heartfelt appreciation to my second supervisor, Associate Professor Darryl M. Small, for his continuous guidance, invaluable assistance, thoughtfulness and giving me plentiful of academic resources throughout the food chemistry and PhD course of the study. Your gentleness, politeness, and humanity as co-supervisor really impressed me on both an academic and a personal view.

A word of gratitude also goes to Dr Anna Bannikova, who so patiently offered her time, kindness, enthusiastic attitude, suggestions and critical outlook in manuscripts for publication and through this research during my PhD program. Her invaluable contribution as my co-supervisor and in providing practical solutions in my research helped me to be on track during my candidature.

I thankfully acknowledge the Thai Government Scholarship awarded by the Cooperation of Office of The Civil Service Commission and Coordinating Centre for Thai Government Science and Technology made it possible to commence and continue the journey. The conference grant, academic and technical support of RMIT University,

particularly including the School of Graduate Research, School of Applied Sciences and International teams is also gratefully acknowledged. The library and computer facilities of the University have also been indispensable. I thank Emeritus Professor Robert A. Shanks for his kindness and support related to principle and instrumentation in dynamic mechanical analysis. In addition, I thank Professor Gary Bryant, Dr Lisa Dias, Dr Emma Goethals and Alexandra Radywonik within the School of Applied Sciences for valuable suggestions. Special thank to Lita Katopo for her excellent proofreading.

Also I owe thanks to Kaewta Srisung, ex-Minister Counselor (Education), Kamonwan Sattayayut, Minister Counselor (Education) and Somchitr Wattanatassi, Ploypaphat Ruanwong, Kewalee Somboon, official staff at Office of Educational Affairs, Royal Thai Embassy, ACT. I also acknowledge Visa Saetea and Thilak Cheurpang at the Cooperation of Office of The Civil Service Commission and Coordinating Centre for Thai Government Science and Technology. I express my thanks and respect to Assistant Professor Ruangdej Wongla, Associate Professor Prapan Thammachai, Associate Professor Supachai Sritiwong, Assistant Professor Supot Boonrang, and Assistant Professor Tanya Tapingkae as well as academic and official staff at Chiang Mai Rajabhat University, my workplace in Thailand.

Special thanks goes to the Technical Services Coordinator, Chemistry, Karl Lang, Senior Technical Service Coordinator of Food Science, Julianne Aloe, Laboratory Manager of Bioscience, David Heathcote, and Technical Officers within Food Science, Lillian Chuang, Yan Chen, Deesha Makwana, Fiona De-Mendonca and Mary Karagiozakis for their help and offering me technical support, training for the analytical instruments both in the laboratory and pilot plant including resources required for running my experiments and also for their kindness, friendship and support.

I extend my sincere gratitude towards academic staff, Professor Harsharn Gill (Discipline Head), Associate Professor Benu Adhikari (Higher Degree by Research

Coordinator), Dr Jeffery Hughes, Ms Elisabeth Gorczyca, Dr Bee May and John Glass whose stimulating suggestions helped throughout the entire process. For technical staff, I thank Phil Francis, Peter Rummel and Duty Microscopists within the RMIT Microscopy and Microanalysis Facility, Frank Antolasic at RMIT Vibrational Spectroscopy and X-ray Facility and Yeshvir Chaudhary, Zahra Homan, Ruth Capriano-Hall and other technical staff in the Applied Chemistry laboratories for training and technical assistance, as well as Mike Allan in the School of Civil, Environment and Chemical Engineering.

I owe many thanks to colleagues in the Food Science laboratory for Omar Masaud Al-Mrhag,Vinita Chaudhary, Thi Ngog Diep Duong, Paul George, Anastasia Fitria Devi, Sobhan Savadkoohi, Sarim Khem, Natasha Yang , Vilia Darma Paramita, Lita Katopo, Dr Enamul Haque, Jasmeet Kaur, Carine Semasaka, Nashi Khalid Al-Qahtani, Oliver Buddvick, Addion Nizori, Helen Tuhumury, Wenywati Chietra, Yunnita Francisca, Sana Subzwari, William Sullivan, Anusha Jayathilake, Nirasha Lakmini Horana Pathirage, Bo Wang, and Yakindra Timilsena for their ongoing support friendship and encouragement. This Thesis would not have been completed in a timely manner without them. I also wish to thank Cambodian graduate, Nuth Monyrath and all Thai graduates in particular Borisut Padungpokkasoon, Wudhichart Sawangphol and Boonlom Thavornyutikarn who have delivered their sense of humour, help, in a welcoming academic and social atmosphere. It was a pleasure joining with all of you.

Above all, I am deeply indebted to my greatest King Rama V and King Bhumibol Adulyadej of Thailand who are respected and revered by many Thais for their felt love. I furthermore would like to offer my special thanks to my parents and my younger sister for their continuing immense love, patience and moral support in every step of my PhD study and career. Finally, I would like to say that the time I spend in Australia so far has given me great experiences and opportunities to achieve a meaning of life. I love all the memories that I will take with me from my time in Melbourne, Australia.

RMIT UNIVERSITY

SGR-80

School of Graduate Research
Thesis with Publications declaration

Instructions to candidates:

1. Many HDR candidates produce publications during their candidature at RMIT. In order to have a summary record of the number and type of publications associated with your thesis you are required to complete this form.
2. The format of a thesis with publications is outlined in section 2.1.1.2 of the HDR Submission and examination procedure . Candidates who have not published during their candidature are not regarded as submitting in 'thesis with publications' mode.
3. Candidates who have published should complete section 1.
4. If your thesis contains sole-authored published work, please complete section 2,
   and/or,
   If your thesis contains co-authored published work, please complete section 3 and attach a statement for **each** publication that clarifies your contribution to the work. This may be in the form of a description of your precise contributions to the published work and/or a statement of your percent contribution. This statement must be signed by all authors. If signatures from all the authors cannot be obtained, the statement detailing your contribution to the published work must be signed by your Senior /Joint senior supervisor.

Section 1: Candidate name and details

Student ID: Title: Mr

Family Name: Panyoyai Given name(s): Naksit

School: Science

Program name: PhD (Food Science) Program code: DR232

Thesis/project title: Fundamental studies of vitamin diffusional mobility in high-solid hydrocolloid

Section 2: Candidate declaration – sole author

This thesis contains **only sole-authored** work, some of which has been published and/or prepared for publication under sole authorship. The bibliographical details of the work and where it appears in the thesis are attached.

☐ Statement/s attached.

Candidate signature: ..... Date: / /

Section 3: Candidate declaration – co-author

This thesis contains published work and/or work prepared for publication, some of which has been **co-authored**. The bibliographical details of the work, where it appears in the thesis, and what contribution I made to the publication/s are explained in the attached statements. I have the permission of all co-authors to include this work in my thesis.

☑ Statement/s attached.

Candidate signature: ..... Date: 06/01/2016

PUBLICATIONS AND PRESENTATIONS

A list of the included publications

Panyoyai, N., Bannikova, A., Small D. M., & Kasapis, S. (2016). Diffusion kinetics of ascorbic acid in a glassy matrix of high-methoxy pectin with polydextrose. *Food Hydrocolloids, 53,* 293-302. *(IF 4.09)*

(This published paper is presented as Chapter 3 in this Thesis.)

Panyoyai, N., Bannikova, A., Small D. M., & Kasapis, S. (2015). Controlled release of thiamin in a glassy κ-carrageenan/glucose syrup matrix. *Carbohydrate Polymers, 115,* 723-731. *(IF 4.07)*

(This published paper is presented as Chapter 4 in this Thesis.)

Panyoyai, N., Bannikova, A., Small D. M., Shanks, R. A., & Kasapis, S. (2016). Diffusion of nicotinic acid in spray-dried capsules of whey protein isolate. *Food Hydrocolloids, 52,* 811-819. *(IF 4.09)*

(This published paper is presented as Chapter 5 in this Thesis.)

A list of the oral presentations

Naksit Panyoyai*, Darryl M. Small, Anna Bannikova, & Stefan Kasapis (2015). Controlled release of thiamin in a glassy κ-carrageenan/glucose syrup matrix, presented at the 18th Gums & Stabilisers for the Food Industry Conference, Hydrocolloid Functionality for Affordable and Sustainable Global Food Solutions, (23rd-26th June 2015), Glyndwr University, Wrexham, UK.

Naksit Panyoyai*, Darryl M. Small, Anna Bannikova, & Stefan Kasapis (2014). Ascorbic acid diffusion kinetics in the vicinity of the glass transition temperature of a high-solid matrix, presented at the 12th International Hydrocolloids Conference, Natural Hydrocolloids: A Key to Human Health, (5-9th May 2014), Taipei, Taiwan.

Naksit Panyoyai*, Darryl M. Small, Anna Bannikova, & Stefan Kasapis (2015). Controlled release of thiamin in a glassy κ-carrageenan/glucose syrup matrix presented at AIFST Food Science Summer School 2015, (28-30th January 2015), RMIT University, Melbourne, Victoria, Australia.

Naksit Panyoyai*, Darryl M. Small, Anna Bannikova, Robert A. Shanks & Stefan Kasapis (2016). Diffusion of nicotinic acid in spray-dried capsules of whey protein isolate presented at AIFST Food Science Summer School 2016, (27-29th January 2016), Charles Sturt University, Wagga Wagga, New South Wales, Australia.

Naksit Panyoyai* (2014). Glassy-to-rubbery biopolymeric materials: delivery matrices for food applications, presented at 3MT competition, (13th June 2014), School of Applied Sciences, Melbourne, Victoria, Australia.

A list of the poster presentations

Naksit Panyoyai*, Darryl M. Small, Anna Bannikova, & Stefan Kasapis (2016). Controlled release of water soluble vitamins in high-solid hydrocolloid matrices at the16th Food Colloids Conference, (10-13th April 2016), Hotel de Wageningsche Berg Generaal Foulkesweg, Wageningen,
The Netherlands.

Naksit Panyoyai*, Darryl M. Small, Anna Bannikova, & Stefan Kasapis (2014). Diffusion kinetics of ascorbic acid in high-solid polysaccharide matrix undergoing glass transition phenomena, presented at 47th Annual AIFST convention, Food-The Final Frontier, (22-25th June 2014), Melbourne Convention and Exhibition, Melbourne, Victoria, Australia.

Naksit Panyoyai*, Darryl M. Small, Anna Bannikova, & Stefan Kasapis (2014). Diffusion kinetics of ascorbic acid in high-solid polysaccharide matrix undergoing glass transition phenomena, presented at Higher Degree Research Student Conference, Today is innovation; tomorrow is success, (17th October 2013), RMIT University, Melbourne, Victoria, Australia.

Naksit Panyoyai*, Darryl M. Small, Anna Bannikova, & Stefan Kasapis (2013). Diffusion kinetics of ascorbic acid in high-solid polysaccharide matrix undergoing glass transition phenomena, presented at Annual Research Day, (14th June 2013), School of Applied Sciences, Melbourne, Victoria, Australia.

TABLE OF CONTENTS

LIST OF FIGURES

LIST OF TABLES

LIST OF ABBREVIATIONS

ABVR	Alizarin Brilliant Violet R
ACT	Australian Capital Territory
*p*NPG	α-D-glucopyranoside
α-La	alpha lactalbumin
AMMRF	Australian Microscopic and Microstructure Research Facility
AAS	Atomic Absorption Spectrometer
BSE	Backscattered Electron
β-Lg	beta lacto globulin
BSA	Blood Serum Albumin
CAS	Chemical Abstracts Service
DE	Degree of methyl Esterification, Dextrose equivalent
DNPH	Dinitophenylhydrazine
DP	Degree of Polymerisation
DSC	Differential Scanning Calorimeter
DMSO	Dimethyl sulfoxide
DMA	Dynamic Mechanical Analyser
DMTA	Dynamic Mechanical Thermal Analyser
FAAS	Flame Atomic Absorption Spectroscopy
FRAP	Fluorescence Recovery After Photobleaching
FTIR	Fourier Transform Infrared Spectrometer
GRAS	Generally Recognised As Safe
HM	High Methoxyl-esterified Pectin
HMP	High-Methoxy Pectin
Ig	Immunoglobulins
JECFA	The Joint FAC/WHO Expert Committee on Food Additives
LVR	Linear Viscoelastic Region
LALLS	Low Angle Laser Light Scattering
LM	Low Methoxyl-esterified Pectin
M	Magnification
MDSC	Modulated Differential Scanning Calorimeter
NMR	Nuclear Magnetic Resonance Spectroscopy
pH	The Power of Hydrogen
RMIT	Royal Melbourne Institute of Technology
SEM	Scanning Electron Microscope
SE	Secondary Electron

LIST OF ABBREVIATIONS (CONT.)

SPV	Sulfo-Phospho-Vanillin
NIST	The National Institute of Standards and Technology
TTS	Time Temperature Superposition
TEM	Transmission Electron Microscope
TN	Total Nitrogen Content
UV/Vis	Ultraviolet/Visible
vs	Versus
WAXD	Wide Angle X-ray Diffraction
WLF	Williams-Landel-Ferry
XRD	X-ray Diffraction

LIST OF UNITS AND SYMBOLS

T	Absolute temperature
A	Absorbance
Ea	Activation energy
A	Alpha
Å	Angstrom
ω	Angular frequency
M_∞	Amount of bioactive compound release at infinite time
M_t	Amount of bioactive compound release at any time
M_i	Amount of bioactive compound release at intial
A	Arrhenius equation constant
b*	Blue-Yellow axis
cPS	Centipoise
cS	Centistokes
cfu/g	Colony forming unit per gram
G^*	Complex modulus
C	Concentration of bioactive compound
k	Constant characteristic of the bioactive compound-polymer system
ξ	Coupling parameter
β	Decoupling parameter
°	Degree
°C	Degree Celsius
°C/min	Degree Celsius per min
n	Diffusion exponent characteristic of the release mechanism
X	Distance
G'	Elastic/storage modulus
H	Enthalpy
f, u_f	Free volume
u_{fg}	Free volume at and below T_g
u_T	Free volume component increasing with temperature
T_g	Glass transition temperature
g	Gram
g/ml	Gram per millilitre
C_p	Heat Capacity
ΔH_f	Heat flow
Hz	Hertz
hr	Hour

LIST OF UNITS AND SYMBOLS (CONT.)

J/g	Joule per gram
κ	Kappa
K	Kelvin
kDa	Kilo Dalton
kPa	Kilo Pascal
kV	Kilo Volt
kW	Kilo Watt
L*	Lightness
l	Litre
G''	Loss/viscous modulus
a_T	Logarithmic shift factor
Ka	Mass transfer coefficient
MPa	Mega Pascal
X	Magnification
λ_{max}	Maximum wavelength
T_m	Melting temperature
m/s	Metre per second
m^3/hr	Metre volume per hour
μm	Micro metre
mA	Milli Ampere
mm	Milli metre
mM	Milli Molar
ml	Millitre
ml/hr	Millitre per hour
ml/min	Millitre per minute
min	Minute
M	Molar
g/mol	Molar mass
Mn, MW	Molecular weight
nm	Nano metre
N	Normal
u_0	Occupied volume
ppm	Part per Million
R	Radius of sphere or cylinder
Pa.s	Pascal second
a*	Red-green axis

LIST OF UNITS AND SYMBOLS (CONT.)

cm^{-1}	Per centimeter
Tan δ	Phase angle
ωa_T	Reduced frequency of oscillation
G_p'	Reduced shear elastic modulus
G_p''	Reduced shear loss modulus
Rad/s	Revolution per second
T_r	Rubbery state temperature
η	Steady shear viscosity
V	Specific volume
R^2	The coefficient of determination
α_L	Thermal expansion coefficient of above T_g
α_θ	Thermal expansion coefficient of below T_g
α_f	Thermal expansion coefficient of free volume
L	Thickness of flat matrix of length of cylinder
t	Time
u	Total volume per unit mass
2θ	Two theta
R	Universal gas constant
W/g	Watt per gram
w/w	Weight by weight
B	WLF equation constant

EXPLANATORY NOTES

These notes shortly describe the viewpoints adopted during the writing of this Thesis. They explain to the expression of word spelling, science units and the referencing of scientific literary texts:

(i) British spellings are in common use in the context than the American format. The example includes vocabulary ending with –ise (rather than –ize) and some terminology. In addition, a lengthy name or expression is repeated, chemical symbols of elements have been used instead the full name (e.g. free volume as f)

(ii) In expressing results, SI units have generally been used whether possible throughout this Thesis, Symbols of Units used have followed the recent reccommodations of The National Institute of Standards and Technology (NIST).

(ii) The format, citation and the list of reference and information sources have followed the current guidelines to authors for *Food Hydrocolloids* (published by Elsevier).

(iv) The brief of high-solid hydrocolloid matrix and reagent preparations, including experimental protocols is overview in Chapter 2. Further specific details of materials, calibration of methods and experimental parameters are emphasised in each experimental chapter (Chapter 3-6) of this Thesis.

SUMMARY

Physical principles underlying the delivery of biofunctionality in neutraceuticals and functional foods have found a wide interest in the area of food science and technology. However, studies on the controlled release of bioactive compounds throughout hydrocolloids systems often appear to follow the complicated patterns. In an endeavour to understand the fundamentals of release mechanisms of bioactive compounds in high-solid systems, this study deals with the diffusion kinetics of water and lipid soluble vitamins in relation to the physics of matrices with glasslike consistency where the molecular behaviour of biomacromolecules is characterised as temperature dependent according to state transitions. This work sought to further advance the understanding in this field by utilising micro- and modulated differential scanning calorimetry, small-deformation rheological techniques, wide-angle X-ray scattering, Fourier transform infrared spectroscopy, particle size analysis and scanning electron microscopy to characterise encapsulants and bioactive compounds within the composite materials. The release kinetics of a series of vitamins was monitored as a function of environmental temperature and time using external methods of visible spectrophotometry and dye-binding assays.

The first system to be investigated was high-methoxy pectin in the presence of polydextrose as cosolute and incorporated ascorbic acid. Physicochemical and structural characterisation of the high-solid systems demonstrated that the mechanism of free volume governs stress relaxation phenomena of the polymeric system through the process of vitrification yielding the mechanical T_g. It was shown that the diffusion kinetics of ascorbic acid from the concentrated matrix to the organic solvent exhibits freedom in mobility which is strongly temperature dependent in the glass transition region. The results demonstrated that utilisation of the concept of diffusion coefficient sheds further

light into the relationship between free volume of the polymeric system and diffusion coefficient of the micronutrient.

The second experimental chapter is devoted to the κ-carrageenan and glucose syrup matrix in which thiamin has been entrapped. Similar to the previous chapter, relationships between rheological properties of the polysaccharide/cosolute system and vitamin mobility were observed via the combined theoretical framework of the free volume and the explanation of the reaction rate. Results obtained theoretically and experimentally confirm that mass mobility of the micronutrient is controlled by the relaxation phenomena of the high-solid carrier.

The next piece of work utilised spray-drying technique to develop whey protein microcapsules containing nicotinic acid. UV/Vis spectroscopy, the newly introduced concept of spectroscopic shift factor and the König reaction were employed to elucidate the rate of vitamin transport through the polymeric matrix as a function of a broad time and temperature spectrum. The modified Arrhenius equation was applied and found to demonstrate that the kinetics of nicotinic acid mobility were distinct from the structural relaxation of the polymeric segments. As before, a relationship between fractional free volume of the whey protein network and diffusion coefficient of the nicotinic acid was established within the observation temperature range.

The last experimental phase of the work presented in this Thesis explored the diffusion patterns of the lipid-soluble vitamin tocopheryl acetate from spray-dried capsules prepared from waxy maize starch. Here, changes in viscoelastic properties of spherical microcapsules were found to reflect the extent of vitamin diffusion. Mathematical modelling tailored on the dependence of nutrient diffusion from the free volume of biopolymer matrix demonstrated that an understanding of the glass transition provides a valuable new window for the encapsulation processes and physical release of micronutrients.

Thus, the present study is particularly important in developing the innovative advance of characterising the mobility of bioactive compounds in relation to the T_g. It was found that the glassy state of the developed amorphous composite materials limits the large-scale motion of the polymeric matrix resulting in slow vitamin diffusion. Non-Fickian kinetics confirmed the finding rationalising the diffusion mechanism of vitamins from the core to the outer layer of polymeric matrix. It can now be further clarified that large-scale vibrational motions of polymer chains are in concordant with effective diffusion coefficients of the vitamins. The current research elucidates the significance of the transition from the glassy to rubbery region in controlling the diffusion of bioactive compounds for hydrocolloid matrices. This will form a foundation for studies of a wider range of bioactive materials and for the design of further specific controlled release systems for industrial exploitation.

CHAPTER 1

INTRODUCTION

ABSTRACT

Globally, foods with positive health benefits have been introduced to consumers, who increasingly expect to acquire good health and wellbeing via functional food products. In terms of designing novel products, such expectations can be met by understanding the physicochemical properties of the biopolymer matrix aimming control the kinetics of diffusional mobility of bioactive compounds added to these products. The food scientist has to deal with condensed or low moisture material that has been observed in starch-based polymers, their hydrolysates, other polysaccharides as well as proteins. The interplay between structural development and diffusional mobility occurring in high-solid mixtures of biopolymers in the presence of bioactive compounds is poorly understood at a fundamental level. This Thesis will deal comprehensively with the structure-function relationships that control physical stability and the kinetics of delivery of compounds with a nutraceutical property. This research scope has largely been scant in the food science area and yet provides significant points for food product innovation and commercial exploitation.

In the following section, the relevant scientific literature on four keywords of this Thesis: food polymers, vitamins, glass transition and release kinetics are critically reviewed. The chapter covers theories behind the glass transition as well as their significance, definition and mathematical modelling. In the kinetics release section, background on the mechanism and mathematical approaches used to model the rates of transport is provided. In the last section, current knowledge is summarised on the basis of an extensive review related to the release kinetics of vitamins incorporated in food hydrocolloid systems encompassing the glass transition.

1.1 FOOD POLYMERS

Biopolymers originate from living organisms and these are of interest for food applications as well as pharmaceutical and cosmetic industries. The biopolymers convey various functional roles in food matrices and these include water binding, solubility, viscosity, emulsification, gel formation and nutrient delivery. Polysaccharides and proteins are the two large groups of food polymers which can be dissolved in water as the primary solvent and plasticiser (Tolstoguzov, 2008). This topic provides an overview of five food polymers, pectin, carrageenan, polydextrose, whey protein and starches particularly their structural features as well as physicochemical and functional properties.

1.1.1 Pectin

Pectins are one of the common food hydrocolloids having a complex polysaccharide structure and found in the plant cell walls, including fruits and vegetables (Willats, Knox, & Mikkelsen, 2006). They are anionic biopolymers consisting of linearly connected α(1-4) D-galacturonic acid residues including a proportion of the carboxyl groups esterified by a methyl group, as shown in Fig. 1.1 (Iijima, Nakamura, Hatakeyama, & Hetakeyama, 2000; Kasapis, 2006a). It is known from the literature that the degree of methyl esterification (DE) is the proportion of methyl esterified galacturonic groups to total galacturonic acid groups. Depending on the DE, pectins are widely classified into two categories comprising high methyl-esterified (HM) pectins for DE equal to or greater than 50%, and low methyl-esterified (LM) pectins for DE lower than 50% (Fu & Rao, 2001; Thakur, Singh, & Handa, 1997).

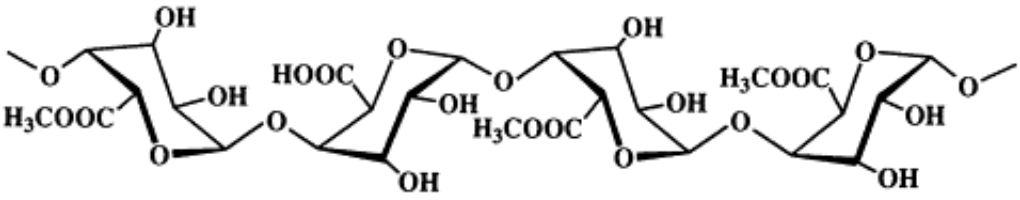

Fig. 1.1 Chemical structure of a representative section of the pectin polysaccharide chain (Iijima, Nakamura, Hatakeyama, & Hetakeyama, 2000)

Gel formation is the most important functional property of pectin. Factors that influence the functionality of pectins include the differences in their composition, solubility, presence of solid and cosolute, DE, pH and temperature (Gnanasambandam & Proctor, 1999). High-methoxy pectin can form gels in acidic conditions (pH 2.5-3.8) and reduced water activity in the presence of sugar between 55 to 70%. The stable gel is obtained from both hydrogen bonds and hydrophobic forces. In contrast, gel formation of low-methoxy pectin takes place over a broad spectrum of pH with or without the incorporation of sugar. The junction zones of the gel network called the “egg box model” are formed by calcium links between two carboxyl groups of two distinct chains in close proximity (Iijima, Nakamura, Hatakeyama, & Hetakeyama, 2000; Sila et al, 2009).

Pectins have always been a natural constituent of human foods. At present, citrus peel and apple pomace are the primary sources of commercially available pectins. The Joint FAO/WHO Expert Committee on Food Additives (JECFA) regards pectin as a safe food ingredient without limits on acceptable daily intake (Thakur, Singh, & Handa, 1997). Pectin is considered as dietary fiber because it affects important gastrointestinal and systemic body processes (Brownlee, 2011). In food industry, pectins have been widely known as gelling, thickening and stabilising agents for a large number of years, and they are utilised in the creation of desired textures of a wide range of foodstuffs, particularly jams, marmalades, gummy confections, jellies (van Buggenhout, Sila, Deuvetter, van

Loey, & Hendrickx, 2009; Chinachoti, 1995). Typically, only 0.2-0.4% of pectin is needed to achieve an acceptable firmness (Evageliou, Richardson, & Morris, 1999; May, 1990). It was shown that the rheological T_g of pectin and cosolute mixtures at a total level of solid of 81% (1% of citrus peel pectin with DE 92, 40% sucrose and 40% glucose syrup) was -12°C. This system demonstrated viscoelastic behavior with the values of G' being above 10^9 Pa in the glassy state (Kasapis, Al-Alawi, Guizani, Khan, & Mitchell, 2000).

1.1.2 Carrageenan

Carrageenan is an important food hydrocolloid extracted from red seaweed of the class Rhodophyceae. Structurally, it is an anionic linear sulfated polysaccharides consisting of D-galactopyranose residues connected by regularly alternating α-(1→3) and β-(1→4) bonds (Hilliou, Wilhelm, Yamanoi, & Gonçalves, 2009; Nickerson & Paulson, 2005). Carrageenans are classified into three types and these are designed as lamda, iota and kappa carrageenan. κ-Carrageenan is an essential gelling polysaccharide harvested primarily from *Eucheuma cottonii* in the Philippines and Indonesia. The idealised chemical structure of κ-carrageenan is 3-linked β-D-galactopyranosyl 4-sulfate alternating with 4-linked 3,6-anhydro-α-D-galactopyranose (Fig. 1.2) that imparts gelation properties (Distantina, Wiratni, Fahrurrozi, & Rochmadi, 2011; Jiang, Guo, & Tian, 2005).

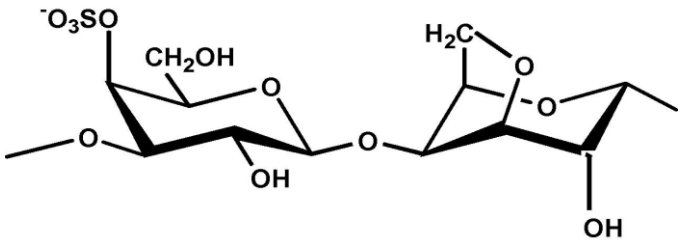

Fig. 1.2 The repeating disaccharide that occurs in κ-carrageenan (Abad, Saiki, Kudo, Muroya, & Katsumura & de la Rosa, 2007)

κ-Carrageenan forms gels via a cationic gelation method together with a cold-set mechanism. Following heating to 60°C to solubilise the carrageenan (<1%) and potassium salt in water, the helical molecules will join together from disordered sequences during cooling (40-50°C) involving the gel-inducing K^+ ions. The selected ions are used to aid helix formation and support the aggregation linkage between the helices of junction zones (Hilliou, Wilhelm, Yamanoi, & Gonçalves, 2009). This so-called domain model is achieved by three-dimensional structures resulting in a characteristically firm and brittle gel via the network formation process. The gels of κ-carrageenan are thermo-reversible and stable at room temperature. However, systems of κ-carrageenan (0.5%) in the presence of potassium salt (0.2%) will lose their viscosity and gel strength at low pH (<4.5) due to autohydrolysis as carrageenan in the acid form is cleaved at the 3,6-anhydrogalactose linkage. In practice, carrageenan should be introduced at the last stage in acidic systems to circumvent extreme acid degradation (Burey, Bhandari, Howes, & Gidley, 2008; Imeson, 2000). It was revealed that high-solid systems (70-85% total solids) comprising 1% κ-carrageenan and 84% glucose syrup as cosolute in the presence of K^+ ions (20 mM) were able to form a gel at high temperature (80°C) and exhibit amorphicity with a T_g value of -30°C (Kasapis, Al-Marhoobi, & Giannouli, 1999).

κ-Carrageenan has found broad application in the food formulation because of its GRAS status, biodegradability, high water holding capacity and ability to form gels. For gelation and syneresis control, typical concentrations of 0.5-3% of κ-carrageenan are utilised in water dessert gels, canned meat, puddings, pie fillings and cold-prepared custard (Chinachoti, 1995; Burey, Bhandari, Howes, & Gidley, 2008). Amounts of 0.01-0.02% of κ-carrageenan are added in ice cream and ice milk formulations to control meltdown and preserve whey systems. Carrageenan can also be used as a food thickener

and stabiliser in chocolate milk to maintain creaminess and so that cocoa particles remain in suspension (Imeson, 2000; Prakash, Huppertz, Karrchuk, & Deeth, 2010).

1.1.3 Polydextrose

Polydextrose is a vastly branched low-molecular weight of glucose polymer consisting random glycosidic bonds (Stowell, 2009). The following glycosidic bonds with the anomeric carbon of glucose are exists: α and β (1-2), (1-3), (1-4) and (1-6), with (1-6) bonds being dominant (Fig. 1.3). The average degree of polymerisation (DP) of polydextrose is approximately 10 with a broad range of molecular weight between 162 and 18,000 Da (Radosta, Boczek, & Grossklaus, 1992; Riberio, Zimeri, Yildiz, & Kokini, 2003).

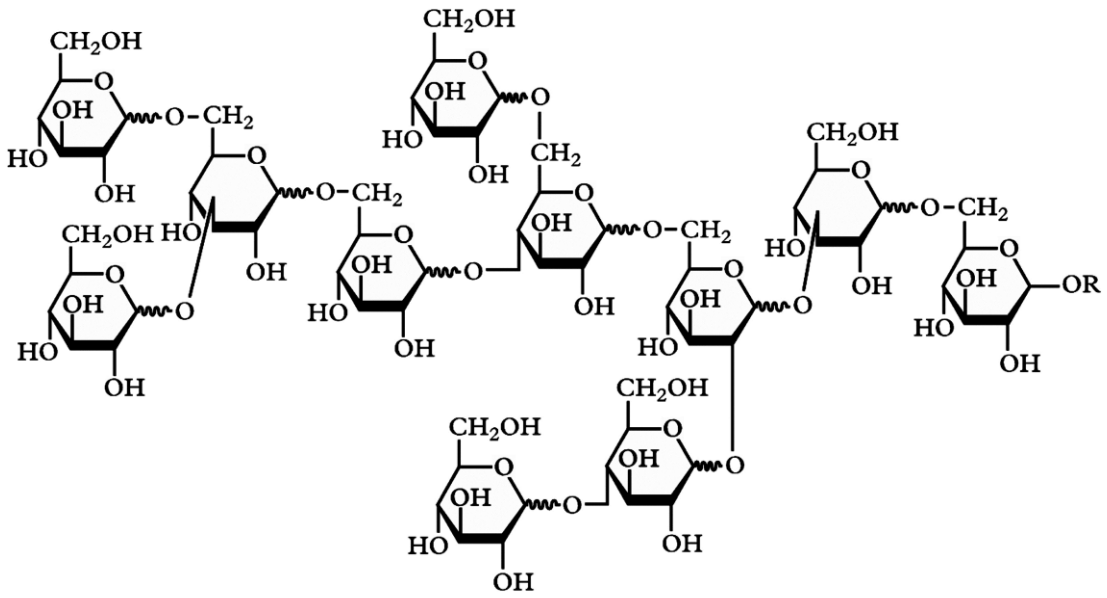

Fig. 1.3 Chemical structure of polydextrose. The subunit R can be either hydrogen, sorbital, sorbital bridges, or more polydextrose (Stowell, 2009)

Polydextrose has specific physicochemical characteristics and is available in several forms: amorphous powder, granulates and solution. Polydextrose is a highly-soluble polymer of glucose allowing solutions to be made with more than 80% (w/v) concentration at 25°C in water, but it is hardly solubilised in ethanol and no solubility in glycerol or propylene glycol. It is relatively stable against hydrolysis in acidic conditions (as low as pH 3) and high temperature. The T_g of polydextrose falls with a rise in moisture resulting from the plasticising effect of water in food polymer systems (Stowell, 2009; Riberio, Zimeri, Yildiz, & Kokini, 2003).

Polydextrose is safe for human consumption without showing any reproductive toxicity, carcinogenesis, mutagenicity, genotoxicity or laxative problems. In 1987, JECFA reviewed the safety of polydextrose and stated that it can be incorporated to food formulations at the amount of requirement to obtain the optimum functionality (Burdock & Flamm, 1999; Craig, Holden, Troup, Auerbach, & Frier, 1998; Jie et al, 2000). Polydextrose is categorised as both a resistant polysaccharide and resistant oligosaccharide (commonly known as non-digestible oligosaccharides). In many countries, polydextrose is widely accepted as a dietary fibre, however, a few countries narrowly define fibre as a material from an intrinsic plant source. Since polydextrose has a low digestibility, it can be utilised to replace highly glycaemic carbohydrate ingredient and lower the total glycaemic index of food (Stowell, 2009). Polydextrose is now well documented as a prebiotic by enhancing growth of both *Bifidobacteria* and *Lactobacilli* in the human colon. It has been reported to enhance fecal mass, soften stools and decrease transit time (Gibson & Roberfroid, 1995; Raninen, Lappi, Mykkänen, & Poutanen, 2011).

Polydextrose is alternatively employed in many food formulations as a functional carbohydrate. The desire to reduce the amount of calories in food products had led to the utilisation of polydextrose as a sugar or fat replacement (Auerbach, Craig, Howlett, & Hayes, 2007: Hicsasmaz, Yazgan, Bozoglu, & Kantnas, 2003; Míčková, Čopìková, &

Synytsya, 2007). Polydextrose can produce body and texture in confectionery products when used in combination with sucrose or glucose syrup facilitating the manufacture of hard and chewy confectionary products (Dodson & Pepper, 1985). It is also used to prevent sugar or polyol crystallisation in hard candies. Polydextrose was designed to balance and lower the level of sweetness in food products showing also oral health benefits being non-cariogenic (Burdock & Flamm, 1999). Polydextrose plays a protective role in structure and stability of frozen foods. Thus, the replacement of sugar or polyol with polydextrose raises the composite T_g of foods, and disrupts sugar recrystallisation in frozen dairy desserts and starch retrogradation in frozen dough and surimi (Kovačevič, Mastanjevič, & Kordič, 2011: Stowell, 2009).

1.1.4 Whey proteins

Whey proteins are one of the groups of milk proteins and these have been studied extensively in the contexts of milk chemistry, functionality and applications (Creamer & MacGibbon, 1996). Whey proteins are recognised for their excellent nutritional value and GRAS status, finding wide application in the food industry as gelling agents, texturiser, emulsifiers, thickener and foaming agents (Bryant & McClements, 1998). The dairy proteins are used as egg protein replacements in confectionery and bakery goods, milk replacers in ice cream and fat replacers in low-fat dairy products (de Wit, 1998; Etzel, 2004). The proteins have a high biological value and can be utilised in sports nutrition, infant foods, breakfast cereals, snacks and energy nutrition bars. Four proteins predominant in whey are β-lactoglobulin (β-Lg, 50%), α-lactalbumin (α-La, 20%), bovine serum albumin (BSA, 10%) and immonoglobulins (Ig, 10%) (Fox, 2001).

β-Lg is the fraction present in the largest proportion in whey protein and has been of particular interest in food science and nutrition. It is a globular protein and a rich source

of cysteine which stimulates glutathione synthesis resulting in protection against intestinal tumors in rats (McIntosh, Regester, Lelue, Royle, & Smithers, 1995). The tertiary structure of β-Lg is shown in Fig. 1.4 and includes an α-helix that is located in parallel to three-strand β-barrels. The thiol can catalyse the disulfide centre where the reactions to heat-induced protein denaturation occur. Denaturation of whey protein isolate (15% w/w) in the presence of glucose syrup (65 %w/w) and 10 mM $CaCl_2$ at 85°C resulted in a coherent network formation with a reduction of whey protein aggregates. The viscoelastic and amorphous matrix in sugar environment exhibited a vitrification phenomena near the subzero temperature pinpointing T_g at 2°C (George, Lundin, & Kasapis, 2013)

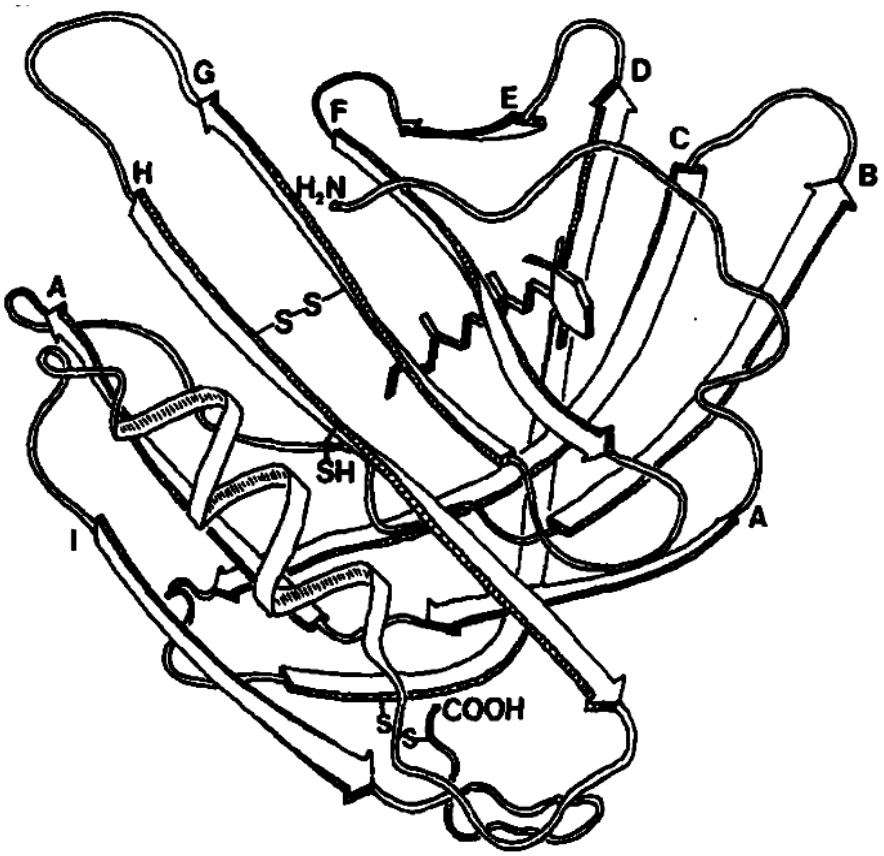

Fig. 1.4 Chemical structure of β-lactoglobulin. The arrows indicate the strand of β-sheet (Papiz et al, 1986)

Protein gelation relates to the agglomeration of denatured proteins with a certain level of order and a continuous structure formation. The two step process, agglomeration and denaturation, can be partially or totally enhanced by changes in the physical or chemical environment, as summarised in Table 1.1. In addition, protein gel formation is a complicated process which involves intrinsic and extrinsic interactions in the protein molecule, a list of which are presented in Table 1.2.

Table 1.1 Physical and chemical factors influence on the protein gelation (Boye, Alli, Ismail, Gibbs, & Konishi, 1995; Clark, Kavanagh, & Ross-Murphy, 2001; Devi, Liu, Hemar, Buckow, & Kasapis, 2013; Josh, 1993; Totosaus, Montejano, Salazar, & Guerrero, 2002)

Classification	Factor	Process
Chemical	Ions	Following salt addition and initial thermal treatment, electrostatic repulsion or charges are protected, producing a gel. Disruption of secondary arrangement initiates a hydrophobic interaction.
	Urea	Urea encourages intermolecular thiol-disulfide oxidation of thiol groups, leading to a network formation.
	Acids	Slow pH reduction lets denaturation to produce aggregations or clusters. These fractions can be regarded as the gel's building blocks.
	Enzymes	Enzyme catalyses cross-linking between glutamine fractions to form a gel network.
	Lactose	Lactose replaces expelled water molecules in exposed hydrophobic pockets, resulting in a softer protein aggregation.
Physical	Heat	Heat can partially unfold native protein to produce a structure. Ordered protein matrix, by aggregation of the molecules.
	High pressure	Pressure (200-600 MPa) enhances hydrophobic interactions and disulfide bonds between protein molecules, resulting in a rearrangement of the gel structure

Table 1.2 Interactions involved in protein gel formation (adapted from Totosaus, Montejano, Salazar, & Guerrero, 2002)

Classification	Factor	Description
Intrinsic	Electrostatic interactions	They alter the net charge of the protein chain via the repulsive and attractive ion forces.
	Disulfide bonds and thiol-disulfide interactions	They relate to the capability of proteins to increase the molecular weight and the length of polypeptide chain.
	Molecular weight	Polypeptide critical molecular weight (~23,000 Da) supports individual gel networks
	Amino acid composition	A coagulant-type gel is form when the content of hydrophobic residues is lower than 31.5% whereas the higher percentage forms a translucent gel.
	Hydrophobicity	Play a role in protein organisation by arrangement themselves in the interior of the protein molecule in aqueous medium.
Extrinsic	Protein concentration	The cross-linking protein molecules for gelation are proportional to the high protein concentration.
	pH	Greater electrostatic repulsion, as a result of greater net charges between protein molecules, can inhibit gel formation.
	Ionic strength	It influences the swelling, solubility and absorption pf protein molecules.
	Temperature	The gelling temperature is high; the denaturation occurs at higher rate than the aggregation.
	Pressure	It modifies the native volume of protein by affecting the balance between stabilising and destabilising interactions within the protein sequence and with water.
	Type of salts	Divalent cations (Ca^{2+}, Mg^{2+}, Br^{2+}) at low concentration (10-20 mM) form a protein matrix.

Whey protein gelation is important for the general application of these proteins as gelling and thickening agents in foods. This is based on the unfolding and aggregation of protein molecules in aqueous solution. Physical interactions between the constituting protein molecules including hydrophobic, electrostatic interactions and hydrogen bonds are the primary molecular forces in a protein network, and these are accompanied by chemical interactions through disulfide bonds (Bryant & McClements, 1998; van Vliet, Lakemond, & Visschers, 2004).

1.1.5 Starch

Starch is one of the agro-products from cereal crops grown in temperate countries and being used for human consumption. Starch obtained, particularly is a nutritional source of carbohydrate, which also promotes greater to the texture and viscosity of conventional processed foods. The food industry generally uses starch as a viscosity modifier, glazing agent, colloidal stabiliser, as well as gelling, bulking and water retention agent (Ellis et al, 1998; Singh, Singh, Kaur, Sodhi, & Gill, 2003). The starch granule has a unique architecture with a wide variety of sizes ranging from 3 to over 100 μm. For example, native maize starch granules are irregular and polygonal shapes with an average diameter of 10 μm (Chung & Lai, 2006).

Starch consists of two biopolymers of D-glucose molecules, namely: a linear fraction, amylose (MW 10^5-10^6) and its branched counterpart, amylopectin (MW 10^7-10^9), as shown in Fig. 1.5. Amylose has a DP of 1,000-10,000 glucose units with the linear structure being made up of glucopyranose units connected through α-D(1-4) glycosidic linkages (Singh, Singh, Kaur, Sodhi, & Gill, 2003). A recognised property of amylose is its unstable nature at high temperatures (110-160°C). Conversely, amylopectin is a much larger material with the DP exceeding one million and being stable at high temperatures.

Approximately 5% of glucose units are linked by α(1-6) bonds within amylopectin molecules resulting in a highly branched, tree-like structure and a complex architecture. Amylopectin associates exclusively in semi-crystalline structures within lamellae of native starch granules because the chains are packed into a crystalline lattice. In contrast, amylose primarily represents the amorphous region of the lamellae (Copeland, Blazek, Salman, & Tang, 2009; Zobel, 1988).

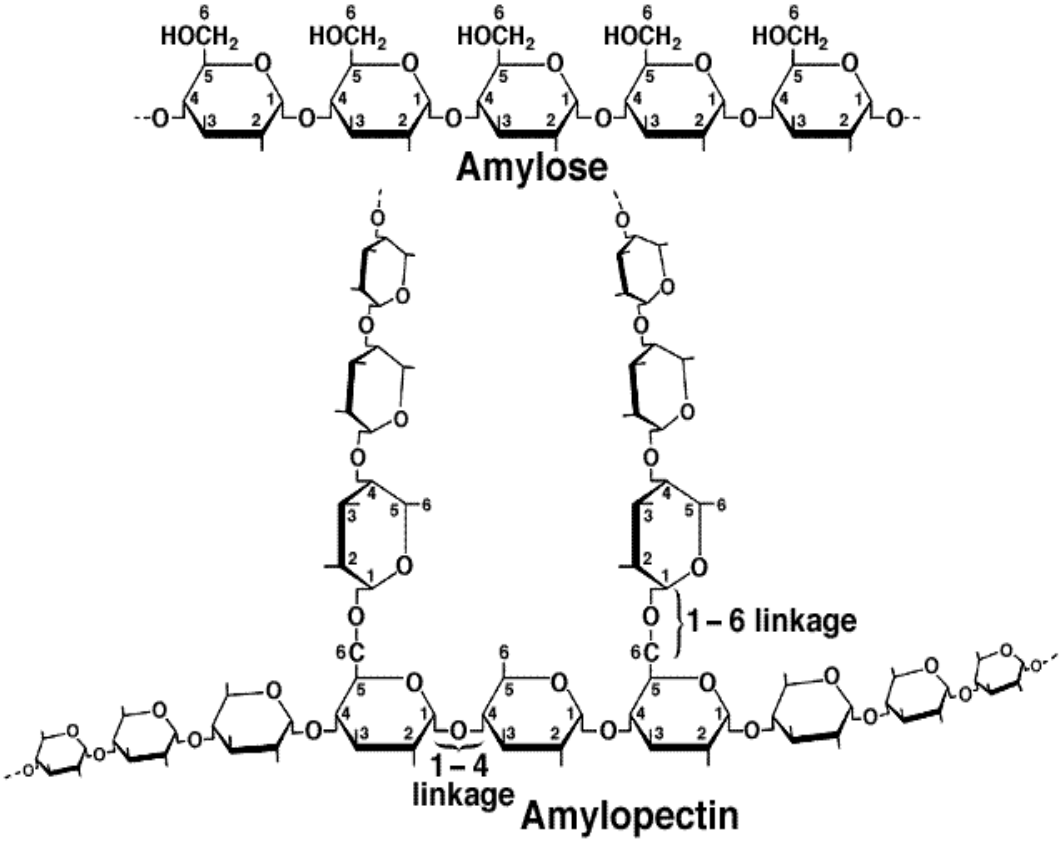

Fig. 1.5 Chemical structure of amylose with α-D(1-4) and amylopectin with branch points at the 1,6-position (Moore, Clark,. & Vodopich, 1998)

It is known that starch undergoes gelatinisation as a result of heating. Sufficient amounts of water are essential to complete the gelatinisation and reduce or eliminate the degree of crystallinity in starch granules. Gelatinisation occurs initially in the amorphous region due to weakened hydrogen bonding in these areas (Singh, Singh, Kaur, Sodhi, &

Gill, 2003). Subjecting the aqueous suspension of native starch granules to 40-50°C results in water hydration and swelling of the materials. In the case of wheat starch granules, low molecular weight, short, linear polyglucans leach from the granules at the beginning of the heating routine, i.e. around 59°C, whereas higher-molecular weight and more branched segments leach later at higher temperatures, i.e. at 66°C (Ellis et al, 1998). At this stage, collapse of crystalline or structural organisation within the starch granules leads to irreversible disruption by uncoiling and non contact of the double helices.

The gelatinisation of starch has many food industrial applications relating to the production of a desirable texture, viscosity and consistency of the end products, including bakery products, sauces, soups, and snack foods (Olkku & Rha, 1978). During aging, gelatinised starch undergoes retrogradation by changing from the disaggregated state to more ordered structure or semi-crystalline aggregates that are distinct from the native granules. This phenomenon takes place easily during storage of heat-treated foods that are rich in starch and has a considerable effect on the texture, stability, quality and biofunctionality along with the shelf life (Fu, Wang, Li, Zhou, & Adhikari, 2013). The thermodynamic transitions of gelatinisation and retrogradation are a qualitative index of crystallinity and can be analysed by differential scanning calorimetry via the enthalpy loss of the crystalline order during gelatinisation and reordering during cooling (Singh, Singh, Kaur, Sodhi, & Gill, 2003).

In some conditions, native starch has limitations for food applications because of low shear and thermal resistance, and excessively high viscosity. Starch modification via physical and chemical treatments alters the polymer architecture resulting in an enhancement of starch functional characteristics for specific usage, as presented in Table 1.3.

Table 1.3 Some properties and applications of modified starch (Singh, Kaur, & McCarthy, 2007)

Type	Property	Application
Pregelatinisation	Cold water dispersibility	Useful in instant convenient foods
Partial acid or enzymatic hydrolysis	Reduced molecular weight polymers and viscosity, increased retrogradation and setback	Confectionery products and food coating
Oxidation/bleaching	High clarity, low viscosity, and low temperature stability	Utilised in batters and breading for coating many bakery goods, in confectionery as binders and film forming agent, in dairy as texturisers
Pyroconversion (dextrinisation)	Low to high solubility depending on the process, low viscosity, high reducing sugar content	Used as coating agents for wide range of foods, excellent film forming capability and as fat replacer in dairy products
Esterification	Lower gelatinisation temperature and retrogradation, reduce occurrence to form gels and higher paste clarity	Used in chilled and frozen foods, emulsion stabilisers and for encapsulation
Cross-linking	Increase stability of granules in high temperature, high shear and low pH environment	Used as viscosity and texture modifiers in soups, sauces, bakery and dairy goods

1.2 VITAMINS

Vitamins are organic bioactive compounds designated as vital nutrients because they are indispensable in very small amounts in food. Vitamins are classed as micronutrients that humans need via the regular diet (Leśková, Kubíková, Kováčiková, Košická, Porubská, & Holčíková, 2006). This section provides information on some water soluble vitamins (ascorbic acid, thiamin and nicotinic acid) and a lipid soluble vitamin (tocopherol) used as small molecules in the studies of diffusional mobility reported in this Thesis.

1.2.1 Sources, roles, deficiency and requirements

Vitamins are essential nutrients that are required in maintaining health, wellbeing and cannot be synthesised in the human body. Foods from animals and plants are the primary sources of vitamins for daily consumption and even though vitamins are not a direct source of energy, in a number of cases, their function relates to energy metabolism. They have specific functions to catalyse numerous biochemical reactions, promote growth and reproduction, and prevent disease (Lukaski, 2004). Therefore, vitamin requirements have been a standard for formulation and labeling in foods and supplements. Main sources, role and deficiency of vitamins that have been utilised in this study are presented in Table 1.4.

Table 1.4 Sources, role and deficiency of some vitamins (adapted from Ball, 2006; Bui, Small, & Coad, 2013; Eitenmiller, Ye, & Landen, 2008; FAO/WHO, 2004; Lukaski, 2004 ; Ottaway, 1993; Walter, 1994)

Vitamin	Main source	Role	Deficiency
Thiamin (vitamin B1)	**Animal products:** -Offal (liver, kidneys, heart) -Fish, lean pork **Plant products:** -Rice, cereals, wheat bran, oat meal, whole grain cereals, cereal germs - Nuts, pulses, legumes, pistachios - Fortified breakfast cereals, some types of bread and Asian noodles **Other:** -Brewer's yeast, vegemite -Fortified baking flour	-Co-enzyme functions in metabolism of branched-chain amino acids, lipids and carbohydrates -Proper function of the nervous system and muscles and cardiovascular system	-Beri-Beri, -Fatigue -Weight loss -Muscle cramps -Weakness -Neurotic pain -Paralysis -Decreased endurance

Table 1.4 Sources, role and deficiency of some vitamins (cont.)

Vitamin	Main source	Role	Deficiency
Ascorbic acid (vitamin C)	**Animal products:** -Milk, liver (cattle), kidney **Plant products:** -Fruits (especially citrus fruits, guavas, kiwis, strawberries, blackcurrants) -Vegetables (leafy greens, peppers, tomatoes, lettuce, broccoli, sprouts)	-Synthesis of collagen, metabolism of iron, copper, carnitine, tyrosine) -Free radical scavenger -Stimulates the body's immune system -Strengthen blood vessel walls, healthy gum -Antioxidant	-Scurvy hypovitaminosis (fatigue, loss of appetite and weight, lowered immunity to infections) -Muscle weakness, bleeding gums, easy bruising
Niacin (vitamin B3)	**Animal products:** -Offal (liver, kidneys, heart) -Milk, fish, pork, beef, eggs **Plant products:** -Cereals, nuts, pulses, beans -Fruits (avocados, figs, dates, prunes)	- The energy supply to all metabolic reactions in the body - Normal growth -Healthy digestive tract and nervous system - Electron transport system	-Pellagra with "three Ds" namely Diarrhoea, Dermatitis and Dementia
Tocopherols (vitamin E)	**Animal products:** -Milk, butter, eggs, fish oils -Fats of meat, poultry **Plant products:** -Vegetable oils (wheat germ, sunflower, safflower, canola, olive, cottonseed, soybean), cereal germs, almond, hazelnuts -Vegetables (spinach, lettuce, cabbage)	-Biological antioxidant for lipids, proteins and DNA -Assists fertility -Reducing muscle damage - Enhancing recovery from exercise -Antioxidant	-Red blood cell destruction -Long-term impact includes muscle and connective tissue diseases -Protein and energy malnutrition -Low birth weight babies

Some of the human vitamin recommendations as reported by the Department of Health and Aging, National Health and Medical Research Council, Australia Government of Australia and New Zealand are shown in Table 1.5.

Table 1.5 Reference values for selected vitamins in Australia and New Zealand (2005)

Age group & gender		Ascorbic acid mg/day		Thiamin mg/day		Niacin[c] mg/day (niacin equivalents)		α-tocopherols mg/day (α-tocopherol[d] equivalents)	
		AI	UL	AI	UL	AI	UL	AI	UL
Infants[a]	0-6 mo.	25	BM	0.2	NP	2	BM	4	BM
	7-12 mo.	30	B/F	0.3	NP	4	B/F	5	B/F
		RDI	UL[b]	UL	UL	UL	UL	UL	UL
Children	1-3 yr	35	NP	0.5	NP	6	10	5	70
	4-8 yr	35	NP	0.6	NP	8	15	6	100
Boys	9-13 yr	40	NP	0.9	NP	12	20	9	180
	14-18 yr	40	NP	1.2	NP	16	30	10	250
Girls	9-13 yr	40	NP	0.9	NP	12	20	8	180
	14-18 yr	40	NP	1.1	NP	14	30	8	250
Men	19-30 yr	45	NP	1.2	NP	16	35	10	300
	31-50 yr	45	NP	1.2	NP	16	35	10	300
	51-70 yr	45	NP	1.2	NP	16	35	10	300
	>70 yr	45	NP	1.2	NP	16	35	10	300
Women	19-30 yr	45	NP	1.1	NP	14	35	7	300
	31-50 yr	45	NP	1.1	NP	14	35	7	300
	51-70 yr	45	NP	1.1	NP	14	35	7	300
	>70 yr	45	NP	1.1	NP	14	35	7	300

Abbreviations: AI, adequate intake; BM, amount normally obtained from breast milk; B/F, content in breast milk and food; RDI, recommended dietary intake; NP, not possible to set may be insufficient evidence or no clear level for adverse effects; UL, Upper level of Intake

Note:

[a] All infant AIs are based on milk levels in healthy female and average volumes

[b] Not possible to determine UL for ascorbic acid from the available data, but 1,000 mg/day would be an advisable limit

[c] The UL for niacin is based on nicotinic acid. For supplemental nicotinamide, the UL is 900 mg/day for both female (not pregnant) and male, and 150, 250, 500 and 750 mg/day for 1-3 yr-olds, for 4-8 yr-olds, for 9-13 yr-olds and for 14-18 yr-olds, respectively. There is no standard UL for infancy (because their intake comes from breast milk, formula or foods) or pregnancy and lactation

[d] One α-tocopherol equivalent is proportionate to 1 mg RRRα-(or d-α-) tocopherol, 2 mg β-tocopherol, 10 mg γ tocopherol or 3 mg α-tocotrienol. The relevant value for synthetic all-rac-α-tocopherols (*dl*-α-tocopherol) is 14 mg

1.2.2 Structure, physical characteristics and stability

Each vitamin has its own distinctive structural features which relate to chemical and physical functions and stability. For example, the chemical structure of tocopherol consists of various methylated phenols that are highly non-polar dissolved in an oil-based medium. The free hydroxyl site in the tocopherol's aromatic ring plays important role in its antioxidant properties (Fig. 1.6). Ascorbic acid has stronger antioxidant properties and higher polarity than tocopherol because of the two free hydroxyl groups that are readily oxidised by free radicals.

In contrast, nicotinic acid and thiamin hydrochloride have no antioxidant capacity but they are more acidic than ascorbic acid. Both thiamin and niacin are catagorised as B-group vitamins but the former is sensitive to alkaline conditions whilst the latter is chemically stable in a broad range of pH conditions. Niacin is considered as the most stable vitamin and the physical characteristics as well as stability of the four vitamins are summarised in Table 1.6.

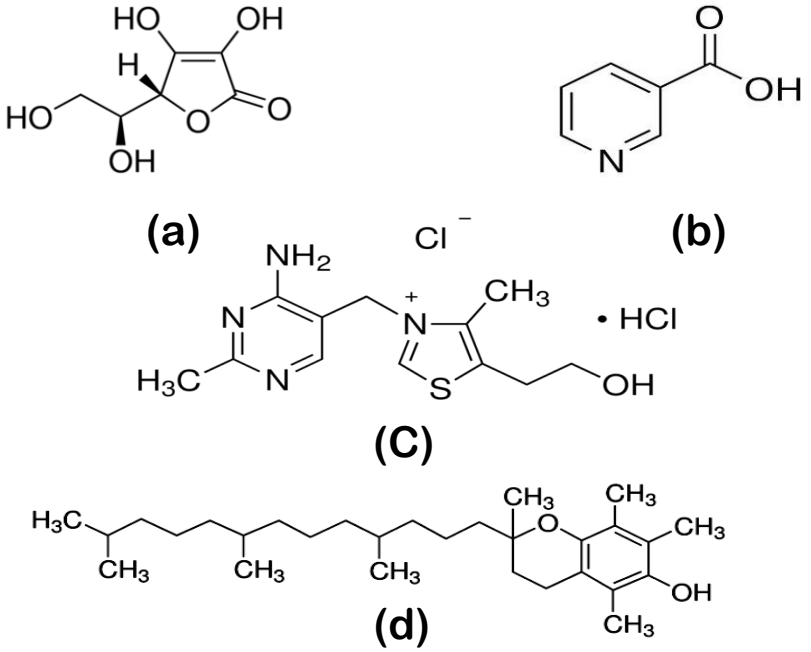

Fig. 1.6 Chemical structure of (a) L-ascorbic acid, (b) nicotinic acid, (c) thiamin hydrochloride, and (d) tocopherol (Sigma-Aldrich, 2014)

Table 1.6 Physical characteristics and stability of selected vitamins (adapted from Ball, 2006; Bui, Small, & Coad, 2013; Eitenmiller, Ye, & Landen, 2008; & Ottaway, 1993; Teleki, Hitzfeld, & Eggersdorfer, 2013)

Vitamin	Physical characteristic	Stability
Ascorbic acid	**Appearance** -White crystals **Solubility** -Soluble in water (33 g/ml at 25°C) -Less soluble in 95% ethanol (3.3 g/100 ml) and absolute ethanol (2 g/100 ml at 25°C)	**Sensitive to:** - Aqueous model systems at room temperature in the pH range of 5-7 - The presence of Cu (II) and Fe (III) due to metal-catalysed oxidation - Light (both sunlight and fluorescent light) - Oxygen, humidity, bases **Stable in the presence of:** -Weak acid (pH 3-4.5) at 20°C
Thiamin	**Appearance** -White or almost white crystals **Solubility** -Thiamin hydrochloride is soluble in water (1 g/ml at 25°C) -Thiamin mononitrate is slightly soluble in water (0.027 g/ml at 25°C) -Soluble in glycerol and diethylene glycol	**Sensitive to:** **-** Sulfites and destructive minerals (Cu, Fe, and Hg) -Oxidants, heat, humidity, bases and radiation **Stable in the presence of:** - Acids (pH 2-4.5) - Oxygen in the absence of light *the most heat labile of the B vitamins
Nicotinic acid	**Appearance** -White crystals -Odour free **Solubility** -Soluble in alkali -Sparing soluble in water, ethanol, methanol, acetone, dimethylsulfoxide	**Stable in the presence of:** - Oxygen, light, heat, acids, bases and oxidants **Sensitive to:** -Reducing agents and UV light * the most stable of the B vitamins
Tocopherols	**Appearance** -Liquid -Colour to pale yellow viscous oils -Nearly odourless **Solubility** -Soluble in most organic solvents (ethanol, acetone, chloroform, either) and vegetable oils	**Stable in the presence of:** -Acids and reducing agents **Sensitive to:** -Oxidants, light , heat , bases and destructive minerals (Cu, Fe, Ca and Mg), lipoxidase -Free radicals in the fat initiate auto-oxidation

Most vitamins are unstable in foods. Based upon the information in Table 1.6, loss of vitamins depends on the specific parameters during food processing and storage conditions, causing vitamin degradation, with the extent and rate of losses influenced by particular conditions of temperature, pH, oxygen, light, moisture, minerals, enzyme and length of exposure. Hence, the stability of vitamins in food products could be preserved by controlling chemical and physical properties (e.g. moisture content, water activity and T_g) particularly in reduced moisture food systems (Zhou & Roos, 2012a,b). In the non-equilibrium and low moisture systems, dynamic changes in glass-like viscosity systems may be influenced by the kinetic mobility of vitamins that affects T_g, which is now to be described and reviewed (Maltini, Torregiani, Venir, & Bertolo, 2003).

1.3 GLASS TRANSITIONS

Understanding the molecular dynamics in food matrix is one of the most critical aspects in food science and utilises an approach adapted from synthetic polymer research. This segment provides an overview of glass transitions, concepts of the free volume theory and network T_g for high-solid biopolymers matrices, along with their measurement and analysis.

1.3.1 Definition

Glass transition is the terminology describing a phenomena observed when a glass is heated until the material behaves like as a supercooled melt (Le Meste, Champion, Roudaut, Blond, & Simatos, 2002). The process is a second order thermodynamic process in which the glass encounters an alteration in state rather than in phase. The nature of a second order time-temperature dependent transition is based on monitoring changes within a certain temperature range. Apart from a second-order thermal transition, this

phenomenon is also described as a kinetic and relaxation transition (Rahman, 2006 & 2010).

In the amorphous state, materials are characterised as having a random and disordered molecular structure. Rapid reduction of a liquid's temperature to well below the equilibrium melting temperature without crystallisation preserves molecular disorder and allows freezing of the particles to their irregular positions for the formation of an amorphous material. This supercooled melt is in non-crystalline condition, which is detected between the glass transition and the melting point. (Champion, Le Meste, & Simatos, 2000; Roos, 2010).

Materials are solid-like, rigid, brittle and fragile without fluidity in the glassy state. The commonly available glass is non crystalline with a regular arrangement but retains the disorder nature of the liquid state. This common material thus has lost its capability to move in a short timeframe so that glass itself can be used as a container for liquid instead of itself taking the shape of its container. Accordingly, other glassy materials also behave effectively as a solid, which can support its own weight against movement as a result of gravity. Supercooling a low molecular weight material will result in a process of viscosity increase in excess of 10^{13} Pas (Noel, Ring, & Whittam, 1990; Rahman, 2006 & 2010).

As mentioned, glass transition is a reversible phenomenon over a relatively narrow or broad temperature range depending on a molecular weight of the constituents of the matrix. In cooling to temperatures below T_g, the amorphous material behaves as a solid that possesses a transparent arrangement typical of the glassy material. In this, molecules are relatively immobile, and molecular motions are constrained to rotations and vibrations, thus behaving in the same way as a solid material. As the temperature rises above T_g, the glassy material demonstrates a soft or rubbery structure and an increasing molecular mobility. The thermal transition between the liquid and solid-like conditions of amorphous

materials is very important due to their influence on food processing and food stability (Bell & Hageman, 1994; Buera et al, 2011; Roos, 2010).

Clearly, the molecular arrangement of amorphous systems is different from the crystalline state. In the latter, the molecules are packed in a regular lattice and they posses a lengthy molecular order within the matrices. In the amorphous system, a single molecule is also compact as for the crystalline solid with a similar gap to the nearest molecule. However, the arrangement in the amorphous material is totally lacking long-range order and the crystaline characteristic. Such material can possess high-intensity of α-regions, which are surrounded by low-density of β-regions (Liu, Bhandari, & Zhou, 2006; Rahman, 2010).

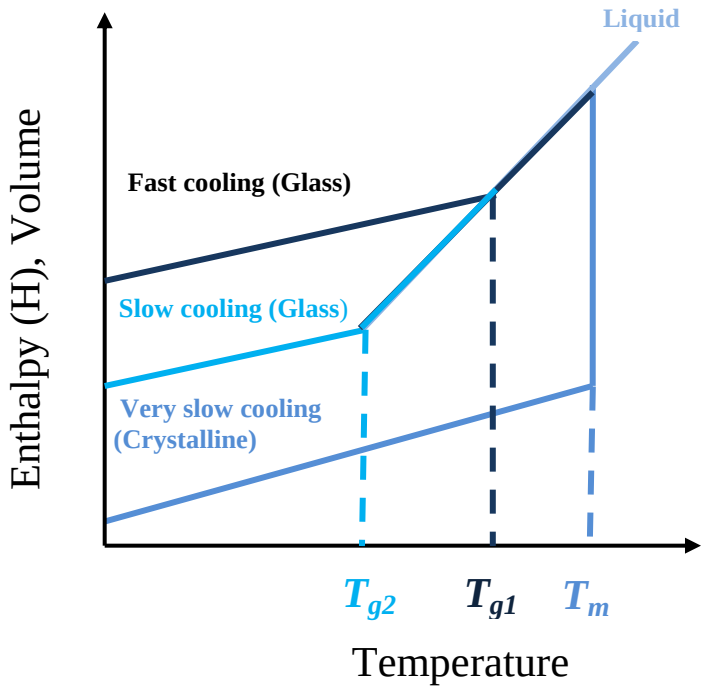

Fig. 1.7 Diagram of the changes in enthalpy and volume with temperature showing $T_{g1,}$ T_{g2} and T_m with various cooling rates (Hancock & Zografi, 1997; Noel, Ring, & Whittam, 1990)

Differences between amorphous solid and crystalline material structures can be depicted in the disparity of volume or enthalpy with temperature. Fig. 1.7 displays the enthalpy (H) and specific volume (V) of a solid material as a function of temperature. For crystalline materials, change in enthalpy and volume with respect to a very low temperature is negligible. In crystal construction, H and V exhibit a thermal discontinuity of the first-order order transition to the liquid phase at the melting temperature (T_m). Application of rapid cooling may cause the values of H and V to decrease along the equilibrium line of liquid beyond T_m into a supercooled liquid area. Further cooling produces a change in gradient at a specific temperature known as the T_g (Hancock & Zografi, 1997).

1.3.2 The concept of free volume

The concept of macromolecular free volume as a traditional glass transition theory is developed for the understanding of rubbery to glass transition. The approach is popular for elaborating the thermal and mechanical transitions correctly in synthetic polymers, biopolymers, and low molecular weight organic and inorganic materials. Such approach is applicable in diverse products, including plastic, cosmetic, drug, and food. Accordingly, this technique has been proposed as being universally applicable to glass forming systems where the differences in the free volume are not influenced by the material's chemical features (Kasapis, 2008b).

The mathematical model of free volume effect in concentrated liquids is based on the work by Doolittle and Doolittle (1957). They observed that the viscosity variation of straight chain polymer of n-alkanes over a wide temperature range could be described by the simple Andrade equation (1930) as follows:

$$\eta = Aexp\left(\frac{B}{T}\right) \tag{1.1}$$

where, η is the shear viscosity, T is temperature in Kelvin and A,B are constants for non-associated compounds.

Based on this, they advanced an alternative equation to offer a good representation of data that was used as a foundation for the development of a glass-transition related theory (Angell, 1988; Berry & Fox, 1968).

$$\eta = Aexp\left(\frac{u_o}{u_f}\right) \tag{1.2}$$

The concept of free volume (u_f), which shows the disparity between the total (u) and the occupied (u_o) volumes of a polymer molecule, is used to construct Equation (1.2). The u_o is the specific volume to which a polymer will condense without encoutering a phase alteration during cooling to subzero temperatures (Ward & Hadley, 1993).

Ferry (1980) explained that the holes between long chain segments of polymers are the space required for their stretching that accounts for the free volume (u_f). Combining this to the area taken by the polymer contours' Van der Waals radii and the thermal pulsations of each residue (u_o, the occupied volume), the total specific volume per unit mass of a material (u) can be determined.

At the point of T_g, the thermal expansion coefficient of free volume (α_f) experiences a discontinuity as seen in an alteration in slope of total volume's line as the temperature increases (Fig. 1.8, Kasapis, 2008b & 2009a).

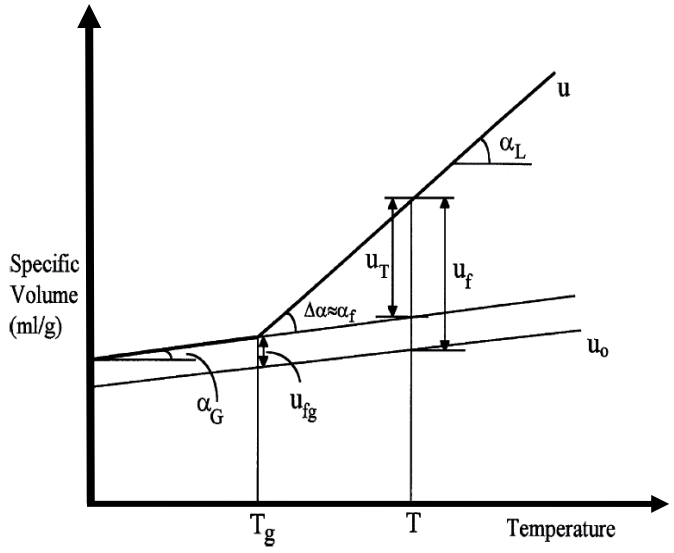

Fig. 1.8 Schematic diagram of free volume theory (Kasapis, 2008b)

In the case that the occupied volume u_o is assumed to be a constant portion of the total volume below T_g, then a straight line can be plotted nearly parallel to the total specific volume (u) beneath T_g, with the disparity being a small constant portion of u. Beyond T_g, the expansion of u_o does not agree with the overall expansion, generating an increasing disparity in volume that is defined as u_f or free volume. At and beneath T_g, there is a particular small portion of of free volume u_{fg} that is considered to be constant (Fig.1.8).

The variation between the expansivity above T_g (α_L) and that below T_g (α_G) produces a free volume component rising with temperature (u_T) as depicted in Equation (1.3), where T is the observation temperature.

$$u_T = (\alpha_L - \alpha_G)(T - T_g) \tag{1.3}$$

Equation (1.4) illustrated the total free volume as a function of temperature. The disparity ($\Delta\alpha$) between α_L and α_G is expressed as α_f, or the free volume's thermal expansion coefficient.

$$u_f = u_{fg} + u_T \; or \; u_f = u_{fg} + (\alpha_L - \alpha_G)(T - T_g) \tag{1.4}$$

The thermal expansion coefficient (α_f in deg^{-1}) of the total free volume (u_f or f) thus generally can be calculated the reference temperature, T_o, in Equation (1.5) (Slade & Levine, 1991).

$$f = f_o + \alpha_f (T - T_o) \tag{1.5}$$

The fractional increase in free volume (f), i.e. the dimensionless ratio of u_f/u, is calculated by determining the shift factor (a_T), using Equation (1.2), that links two sets of experimental temperature data (Hutchinson, 1995):

$$\log a_T = \frac{B}{2.303}\left(\frac{1}{f} - \frac{1}{f_o}\right) \tag{1.6}$$

Combining the above equation with the fractional free volume in Equation (1.5) gives (Arridge, 1975):

$$\log a_T = -\frac{(B/2.303 f_o)(T - T_o)}{(f_o/\alpha_f) + T - T_o} \tag{1.7}$$

In the form of C^o_1 = B/2.303f_o and $C^o_2 = f_o/\alpha_\beta$ this is the final equation developed by Williams, Landel and Ferry (WLF) (1955) to predict the temperature reliance of viscoelasticity in the glass transition region.

The WLF model can be recast as follows (van der Put, 2010):

$$\log a_T = C_1^o (T - T_o)/(T_\infty - T) \tag{1.8}$$

where the temperature T_∞ is equal to $T_o - C^o_2$

The WLF theory is not applicable at temperatures below T_g or above T_g+100°C where the temperature dependent relaxation process is controlled by specific chemical features (Roudaut, Simatos, Champion, Contreras-Lopez, & Le Meste, 2004). Thus, the WLF equation is incapable of following the process of viscoelasticity at the lower temperature range of the glassy regime and the rubbery plateau. Mechanical characteristics in these regimes are better explained by the modified Arrhenius equation (Kasapis, 2000).

$$\log a_T = \frac{E_a}{2.303\mathrm{R}}\left(\frac{1}{T} - \frac{1}{T_o}\right) \quad (1.9)$$

This conveys the thought of activation energy (E_a) for a slow motion of macromolecules in the glassy state, which is not dependant to temperature. Furthermore, the boundary between free volume phenomena on the glass transition domain and the energetic hurdle to movement in the glassy state serves as a theoretical basis for the estimation of the rheological/mechanical T_g of amorphous biopolymers (Kasapis, 2008a). Currently, the significance of glass transition effect for the better understanding of the structural properties of high-solid biomaterials have become extensively investigated in three categories of high-solid preparations, particularly, polysaccharides, starch and starch hydrolysates, and a range of proteins (Kasapis, 2009b).

1.3.3 Measurements and analysis of a glass transition

Measuring the T_g in food systems can be performed by many experimental techniques. Thermal and mechanical methods are classical routines that elucidate the molecular dynamics in regards to the glass transition of food systems.

1.3.3.1 The calorimetric T_g

Differential scanning calorimetry (DSC) is a common thermal analysis for the determination of T_g in food materials. The DSC measurements detect changes in thermodynamic characteristics particularly heat capacity, enthalpy and volume (Liu, Bandari, & Zhou, 2006). When a sample is heated above T_g, the transition appears as a change in enthalpy and volume, and this can be measured as the empirical DSC T_g or the calorimetric T_g (Kasapis, Al-Marhoobi, & Mitchell, 2003). Due to the manifestation of the glass transition over a broad temperature range, the various points on DSC thermograms may be reported as onset (T_{gi}), midpoint or peak (T_{gp}) and endset (T_{ge}) temperatures of the

phenomena observed (Fig. 1.9). It has been recommended that at least two parameters be reported, for example the onset or midpoint and the area of the glass transition (Champion, Le Meste, & Simatos, 2000). The experimental parameters used should always be reported in detailed together with the temperature values, including heating and cooling rate, sample size and annealing conditions. However, calorimetric measurements have some disadvantages in regards to sample size and shape as well as control of moisture content. For products containing starch or flour, DSC is not sensitive to notice the glass transition because of the minute change in specific heat capacity (Rahman, 2006).

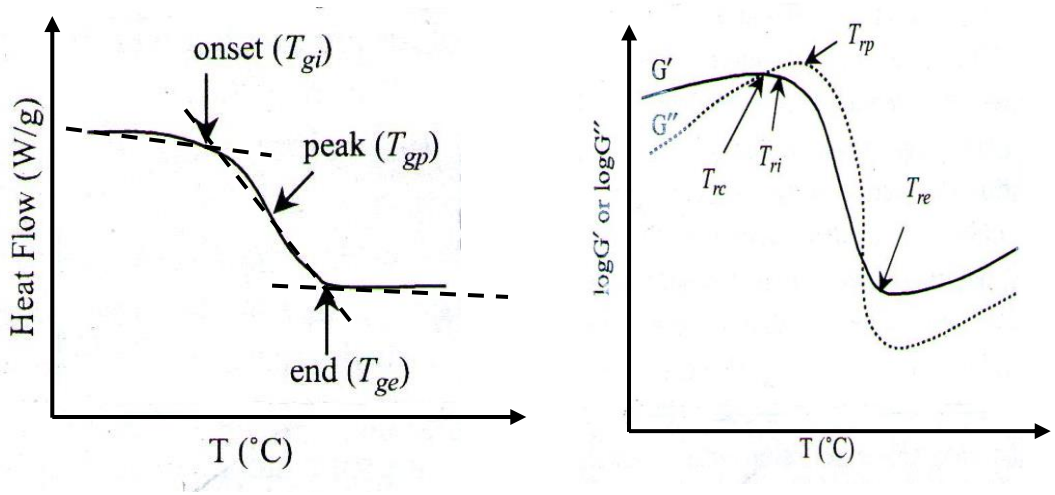

Fig. 1.9 Typical DSC thermogram (right) and the plot of log G' or log G'' for the glass transition phenomenon (left) (Rahman, 2006)

1.3.3.2 The rheological T_g

Rheological or mechanical T_g is used to rationalise the mechanical properties of biopolymers during vitrification. The mechanical pattern in the form of small deformation dynamic oscillation and shear relaxation during a glass transition has been the technique of choice to provide estimates of T_g in matrices of single or mixed macromolecules in the presence of cosolutes (Kasapis & Mitchell, 2001). In dynamic oscillation techniques, mechanical properties, i.e. storage modulus (G') and loss modulus (G''), are investigated as

a function of temperature at a constant frequency of measurements. T_g determined by DSC and T_r from rheological techniques of measurements should not be considered as fully equivalent. Mechanical T_r is higher than DSC T_g due to the ability of the sample to retain its form (Shalaev & Kanev, 1994). In general, it could be recommended to present the T_r as an intersection between G' and G'' (T_{rc}), whereas in DSC measurements the onset (T_{gi}), midpoint or peak (T_{gp}) and endset (T_{ge}) are the parameters which describe T_g.

Amorphous materials exhibit many primary relaxations subjected to an external small deformation dynamic oscillation. The main relaxation related to the rheological glass transition between the glass transition and glassy state is called α-relaxation (Kasapis, Al-Marhoobi, & Sworn, 2001). Such relaxation can be observed as a dramatic decrease in modulus for both storage and to some extent loss modulus with increasing temperature. The frequency or temperature of the α-relaxation is generally obtained from the ratio of G'' to G', or known as the loss factor (tan δ). The maximum of the tan δ value is a more appropriate approach for the determination of the T_g with physical significance than from DSC analyses (Champion, Le Meste, & Simatos, 2000; Liu, Bandari, & Zhou; 2006; Roos, 2010).

1.3.4 The master curve of amorphous biopolymers

The viscoelastic spectrum of the master curve for high-solid biopolymers is categorised into four temperature regions as described by Kasapis (2004 & 2009a) and shown in Fig. 1.10.

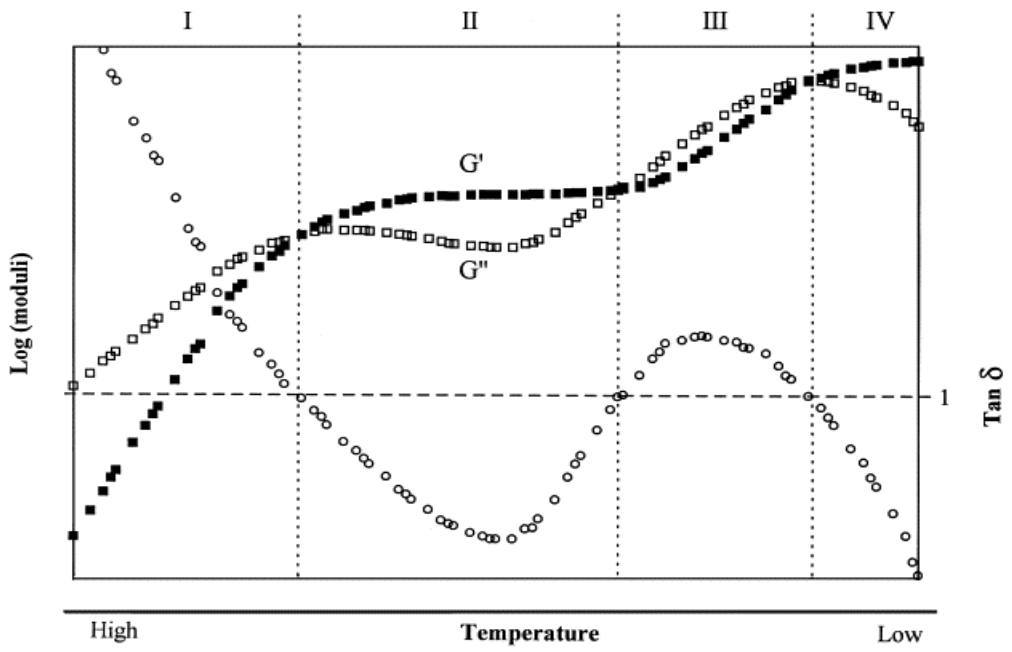

Fig. 1.10 Master curve for the dynamic mechanical oscillation describing the relaxation, rubbery, glass transition, and glassy states with decreasing temperature (Kasapis, 2009a)

In region I or the relaxation zone, very high experimental temperatures prmote complete energy dissipation and polymer chain relaxation resulting in negligible values of storage modulus in shear. Rapid cooling the high-solid biopolymers accelerates an increase in both G' and G'' (terminal zone: part I), respectively, and ultimately the viscoelastic parameters enters the plateau zone, where the values of tan δ is approximately 1. In dilute protein or polysaccharide solutions and condensed peparations of cosolute the molecular flow is predominant which corresponds with $G'' > G'$.

In region II or the rubbery zone, the elastic component remains unchanged while the viscous counterpart goes through a minimum due to more polymeric segments of the network structure supporting the applied stress. Flow is not observed in this region as for the relaxation time zone. Samples of rubbery gels at room temperature produce elastic networks of stable physical associations, as indicated by the greater values of G' compared to G''.

Region III refers to the glass transition region where the long-range movement of the polymer main chain is restricted because of elasticity, however, local relaxation events that deplete energy can occur. In the absence of crystallisation, cooling of rubbery food stuffs ushers in this region where the liquid-like behaviour again becomes dominant ($G'' > G'$).

In region IV or glassy state, the storage modulus cross over the viscous counterpart for a third time (tan $\delta = 1$) at the end of temperature of measurement. Thus the system comes into the glassy zone where the rates of chemical and enzymatic reactions as well as microbial growth decelerate substantially.

1.3.5 The network T_g

High-solid foods comprised primarily of mixtures of protein, starch, as well as non-starch polysaccharides are (e.g. carrageenan, pectin) in the presence of cosolutes. Confectionery products may be considered as an example and gelatin has been the most frequently used structuring agent in these products for almost a century. However the ingredient has been increasingly causing concern for consumers and producers in relation to the need to circumvent its use in the diet, reflecting certain health issues or perceptions, including the bovine spongiform encephalopathy (mad cow disease), vegetarianism and religious dietary guidelines and restrictions (e.g. Muslim and Hindu). For these reasons, there is a motivation to understand the behaviour of polysaccharides combined with high amounts of sugar or sugar replacers as cosolute since this class of biopolymers may be used as vegetarian substitutes for gelatin (Kasapis, 2008b).

In systems of biopolymer/cosolute with pertinence to confectionery goods, formulations include gelling polysaccharides at levels less than 2% with high sugar concentrations of up to 90% (Kasapis, 2012). Many high sugar confectionery products

contain 10-25% moisture providing prolonged shelf life of such products. High sugar confectionery products contain gelling biopolymers where the scientific approach underlying the behaviour of food polymers is particularly relevant (Kasapis, Mitchell, Abeysekera, & MacNaughtan, 2004). Partial replacement of sugar with high molecular weight carbohydrates that are considered to be dietary fibre (e.g. pectins or polydextrose) can create formulations with a low glycaemic index, which is in the consumers interest hence increase greatly market value. Furthermore, fundamental understanding on the structure and functionality of food hydrocolloids acting as potential sugar analogues has a profound effect on consumer acceptance and food palatability (Fumani, 2011).

Research in the multifarious state transitions of biological glasses and food-related applications has been originated from the sophisticated synthetic-polymer methodology and includes the theoretical concept of the network glass transition temperature. This has been fostered using dynamic mechanical techniques and a combined framework of the WLF/free volume theory and the modified Arrhenius equation (Kasapis, 2004; Kasapis, 2006b). Biological molecules are complex blends of biopolymers, small polyhydric compounds (e.g. sugars and glucose syrup) and water as solvent, thus, requiring critical consideration when evaluating their mechanical characteristics (Kasapis, Al-Marhoobi, & Mitchell, 2003). Small deformation dynamic shear oscillation has been the technique of choice in the characterisation of the rheological T_g (Kasapis & Mitchell, 2001).

The approach of small deformation dynamic oscillation is carried out to study the vitrification properties of biopolymer structure. In doing so, mechanical spectra of complex modulus have been obtained at specific temperature intervals (3-5 degree) and superimposed along of the log frequency axis. This is the time-temperature superposition (TTS) principle, which utilises lateral shifts of isothermal oscillatory frequency data to generate logarithmic shift factors (log a_T) in order to produce a typical master curve of viscoelasticity (Nickerson, Paulson, & Speers, 2004). As discussed, four zones of

viscoelastic behavior are generated from the master curve, and then the combined framework of WLF and modified Arrhenius equations (or the Andrade equation) are used to indicate the rheological/network T_g. The network T_g is defined as the combination od two different process, i.e. free volume phenomena in the glass transition zone and the projections of the reaction-rate in the glassy condition (Kasapis & Mitchell, 2001).

The rheological properties of high-solid biopolymers (73-99%) have been examined with a view to evaluate whether the network-forming capability of macromolecules had an effect on the network T_g. Thus, structural properties of high-solid systems (more than 78% (w/w) solid content) comprising high-methoxy pectin with cosolute were monitored at subzero temperatures. Experimental observations reveal that systems formed a rubbery structure which was readily transformed into a glassy consistency. That was further confirmed with theoretical modelling based on the TTS principle (Al-Ruqaie, Kasapis, & Abeysakera, 1997).

Furthermore, the rheological T_g was higher due to the addition of small quantities of gelling biopolymer (less than 2% in the formulation) to glucose syrup within the total solid content between 73% and 85%. For example, the presence of 1% pectin enhanced the gelation, formation of a hydrated network, and acceleration of vitrification in the system (Al-Amri, Al-Adawi, Al-Marhoobi, & Kasapis, 2005; Kasapis, 2008b). Addition of 0.7% κ-carrageenan to a system of 93% solids also increased the values of T_g, which were dictated by the biopolymer in the mixture. Therefore, a high level of cosolute in the polysaccharide network reduces the ability for progression of intermolecular forces and a three-dimensional structure formation (Deszczynski, Kasapis, MacNaughton, & Mitchell, 2002). This further confirms that the network formation in condensed sugar/biopolymer systems, as followed by the determination of rheological T_g, is a macromolecular process based on the interactions between the polysaccharides and sugar.

Apart from glassy carbohydrate matrices, proteins are of interest in relation to structure and network formation (Kasapis, 2001a,b). This relates, for example, to condensed whey protein systems (80% w/w total solids), which were under pressurisation at 600 MPa, at 22°C for 15 min. This process of compression retarded the movement of polypeptide chains in addition to dehydration resulting in the formation of pressured-treated networks in the native arrangement when compared to the conventional thermal treatment at 85°C for 20 min which, however, exhibited glassy consistency (Dissanayake, Kasapis, Chaudhary, Adhikari, Palmer, & Meurer, 2012).

Literature reveals that there is a range of factors which affect the network T_g, including the level of total solids, complexity of gelling polysaccharide/cosolute systems, molecular weight of biopolymers and the presence of plasticisers, as well as the application of pressure and temperature. The summary of T_g estimates from a literature review on high-solid food polymer systems is presented in Table 1.7.

Table 1.7 Literature values for the network T_g for various high-solid foodpolymer matrices

Matrix	**Total solids (%)**	**Network T_g (°C)**	**Calorimetric T_g (°C)**	**Reference**
25% gelatin+30% sucrose +15% glucose syrup (1) M_n [a] = 29,200 Da (2) M_n = 39,800 Da (3) M_n = 55,800 Da (4) M_n = 68,000 Da	80	 -25 -22 -15 -2	 -	Kasapis, Al-Marhoobi & Mitchell (2003)
1.5% agarose + 7% gelatin+ 66.5% glucose syrup[b]	75	-38	-	Sharma et al, (2011)
(1) 0.5% κ-carrageenan + 79.5% glucose syrup (2) 80% glucose syrup	80	-34 -46	-46 -46	Jiang & Kasapis (2011)

Table 1.7 Literature values for the network T_g for various high-solid food polymer matrices (cont.)

Matrix	Total solids (%)	Network T_g (°C)	Calorimetric T_g (°C)	Reference
(1) 2% high-methoxy pectin +[c] 78% glucose syrup	80	-34	-48	Almrhag et al, 2012a
(2) 2% high-methoxy pectin + 78% polydextrose		-22	-42	
(1) 1.5% agarose+ 78.5% polydextrose	80	-27	-43	Almrhag et al, 2012b, 2013
(2) 15% gelatin 65% polydextrose		-22	-45	
(3) 80% polydextrose		-30	-45	
1.5% agarose +7.5% gelatin+ 71.5% polydextrose	80.5	-23	-45	Almrhag et al, 2012c
(1) 1% deacylated gellan + 79% polydextrose	80	-28	-45	Chaudhary et al, 2013a
(2) 80% polydextrose		-30	-45	
(1) 2% deacylated gellan + 85% polydextrose	85	-14	-38	Chaudhary et al, 2013b
(2) 85% polydextrose		-20	-38	
Whey protein isolate				Dissanayake et al,2012
(1) atmospheric conditions	80	-10	-	
(2) pressurised		-12	-	
Immunoglobulins				George et al, 2013a
(1) atmospheric conditions	80	-23	-	
(2) pressurised		-26		
15% whey protein isolate+ 65% glucose syrup	80	+1	-47	George et al, 2013b
Bovine serum albumin				Savadkoohi et al, 2014
(1) atmospheric conditions	80	12	-	
(2) pressurised		-53	-	

Note:

[a] M_n is the molecular weight of gelatin.

[b] Glucose syrup had DE 42.

[c] High-methoxy pectin had DE 70.3%, 81.1% galacturonate, 92.0% polysaccharide content.

[d] High-pressure at 600 MPa for 15 min

[e] The ratio of whey protein isolate and lactose was 4:1

1.4 RELEASE KINETICS

Development of controlled release systems enables food scientists to encapsulate, protect and release bioactive compounds including flavor, antioxidants or micronutrients for particular purposes (Jones & MacClements, 2010). To understand the release characteristics, this review provides the mechanism of kinetic release in regards to the glass transition, mathematical modelling of diffusion, and prevalent rate law. Last, the applications of high-solid food systems regarding stability, delivery and controlled release for functional food applications are discussed.

1.4.1 The mechanism of release in relation to a glass transition

Bioactive compounds can be loaded into polymer matrices using two different methods which are post loading and *in situ* loading. In the post loading technique, a bio-matrix is formed followed by absorption of the bioactive compound to the matrix. For *in situ* loading, a bioactive compound is introduced to a biopolymer matrix at the commencement of the sample preparation stage, and the matrix subsequently forms a network

The release mechanism is governed by the composition of the matrix, the type of polymer and bioactive compound, preparation techniques, environmental conditions of bioactive compound release as well as geometry (size and shape). One or more of the following physical and chemical phenomena might be involved in the bioactive compound release kinetics. However, these events concern only the bioactive compound diffusion in the model system, not within the living entities. Release will take place as follows (Siepmann & Siepmann, 2008):

(i) Wetting of the matrix surface with the release medium (water or solvents).

(ii) Penetration of the release medium into the matrix (e.g. via holes and/or through uninterrupted polymeric networks).

(iii) Phase transitions of polymers (e.g. glassy-to-rubbery transition).

(iv) Bioactive compound dissolution and convection that drives the compound release because of the considerable hydrostatic pressure generated within the matrix.

(v) Diffusion of the bioactive compound out of the delivery device controlled by time-and/or position dependent diffusion coefficients.

(vi) Diffusion of bioactive compounds through the unstirred liquid layer surrounding the matrix.

It is known that the mechanism of bioactive compound release is related to a state-transition from the glass to rubbery condition in high-solid biopolymer matrices. In the glassy state, bioactive molecules remain immobile, while under the conditions of the rubbery state the bioactive molecules rapidly diffuse to the surrounding phase through a layer of polymer. In this process, released bioactive compound molecules come in contact with the external layer of the matrix. With time, the following two phenomena take place: there is a decrease in concentration gradient of the bioactive molecule (the driving force of diffusion) and also release rate due to the relatively long distance of bioactive compound transport from interior to the exterior of the matrix (Zarzycki, Modrzejewska, & Nawrotek, 2010).

1.4.2 Theoretical modelling of diffusion kinetics

For a biopolymer model in which the bioactive compound is homogeneously spread throughout the polymeric matrix, unsteady-state solute (bioactive) compound diffusion in a slap-shaped matrix (one-dimension) can be explained by Fick's second law (Favre & Girard, 2001; Busk & Labuza, 1979):

$$\frac{\partial C}{\partial t} = D\frac{\partial^2 C}{\partial X^2} \tag{1.8}$$

where, C is the level of solute's variation in the flat sample, t is release time, X is the distance, D is the diffusion coefficient (assumed to be constant at equilibrium).

Equation (1.8) can be integrated under the above hypothesis/limitations to plot the relative solute mass release vs the square root of time:

$$\frac{M_t}{M_\alpha} = f(\sqrt{t}) \tag{1.9}$$

where, M_t is the quantity of solute discharged at any time, M_α is the initial solute loading in the biopolymer matrix.

Various diffusion mathematical concepts have been constructed to describe aspects of kinetic release applied to food and drug delivery designs (Bayarri, Rivas, Costell, & Durán, 2001; Lesmes & McClements, 2009; Pothakamury & Barbosa Cánovas, 1995; Ritger & Peppas, 1987; Siepmann & Siepmann, 2008a,b; Vergnaud, 1991). Some of these theoretical approaches are shown in Table 1.8.

In this Thesis, the diffusion study has been carried out under conditions whereby when the high-solid biopolymer matrix undergoes a glass-to-rubbery transition. As discussed, the polymer chains in the rubbery region are more mobile than those in the the glassy zone, thus, facilitating the bioactive compounds to be released from the matrix rapidly. According to Equation (1.10), a linear relationship is obtained for the first part of the curve (typically for $M_t/M_\alpha \leq 0.5$ in a thin polymer film). The power n is determined from the gradient of the diffusion fraction vs time in *ln-ln* plot. Precision values of around 5% are reported to be achievable with experimental data based on this strategy (Favre & Girard, 2001). When n is equal to 0.5 the compound is said to diffuse with simple Fickian diffusion whereas if the value is in the range of 0.5 and 1.0, Non-Fickian or anomalous

transport is obtained (Mártinez-Ruvalcuba, Sánchez-Díaz, Becerra, Cruz-Barba, & González-Álvarez, 2009).

Table 1.8 Theoretical modelling to describe the aspects of diffusion in food and pharmaceutical systems

Model	Term and limitation	Equation
$\frac{M_t}{M_\infty} = k_a t^n$	k_a and n are the system constant parameters depending on the polymer-penetrant-bioactive compound interactions	(1.10)
$\frac{M_t}{M_\infty} = 1 - \sum_{n=o}^{\infty} \frac{8}{(2n+1)^2\pi^2} \exp\left[\frac{-D_{eff}(2n+1)^2\pi^2 t}{L^2}\right]$	Flat infinite matrices dissolved in an infinite well-agitated medium	(1.11)
$\frac{M_t}{M_\infty} = \frac{4}{L}\left(\frac{D_{eff}\, t}{\pi}\right)^{0.5}$	Short time diffusion studied in the flat infinite source and $M_t/M_\infty < 0.6$	(1.12)
$\frac{M_t}{M_\infty} = 1 - \sum_{n=o}^{\infty} \frac{6}{(n)^2\pi^2} \exp\left[\frac{-D_{eff}(n)^2\pi^2 t}{R^2}\right]$	Finite spherical source and well-mixed infinite sink	(1.13)
$\frac{M_t}{M_\infty} = 4\left(\frac{D_{eff}\, t}{\pi}\right)^{0.5}\left(\frac{1}{R} + \frac{1}{2L}\right)$	Short time diffusion studied in the cylindrical probe and $M_t/M_\infty < 0.5$	(1.14)

Note:

D_{eff} is the effective diffusion coefficient of the bioactive component through the boundary

K_a is the mass transfer coefficient

M_t is the quantity of bioactive compound diffused during t (time)

M_∞ is the quantity of bioactive compound diffused at infinite time (partially equivalent to the initial bioactive addition)

L is the thickness of the flat matrix or length of cylinder

R is the radius of the sphere or cylinder

Fundamental reaction rates have been used to describe the diffusion rate of bioactive compounds in model systems. Thus, the literature so far describes the diffusion or gain of chemical compounds (e.g. vitamins, minerals, and antioxidants) in regards to zero, first or higher kinetic reactions (Corradini & Peleg, 2006; Labuza, 1984; Labuza & Riboh, 1982; van Boekel, 2008), which are given by the following equation:

$$\frac{dC(t)}{dt} = k(T)C(t)^m \tag{1.15}$$

where *C(t)* is the temporary concentration of the bioactive compound, *k(T)* is the pseudo rate constant, which is temperature dependent, or slope of the curve within the appropriate extent of the reaction vs time, and *m* is the power that specifics the reaction order (a curve-fitting parameter).

Equation (1.15) can also be advanced in the following form:

$$\frac{dC(t)}{d(t)^m} = k(T)dt \tag{1.16}$$

For isothermal predicaments (*T* = constant), both sides of the equation can be combined to construct the recognizable function:

For zero order reaction (*m*=0):

$$C(t) = C_o + k(T) \tag{1.17}$$

and for first order reaction (m=1) :

$$C\,(t) = C_o \exp[+k(T)t] \tag{1.18}$$

or

$$ln\frac{C(t)}{C_0} = +kt \tag{1.19}$$

For zero order reactions, the plot of the extent of reaction (y-axis) against time (x-axis) is linear in Cartesian coordinates. For a first-order reaction, it is a straight line on a semilog plot of the extent of reaction vs time. It is possible to determine other orders if the

mechanism is known and the experimental procedure is very precise (Labuza, 1984). Generally, effects of factors including viscosity of the reacting phase and changes in concentration are impossible to determine in a dynamic food system and are included in the magnitude of the measured rate constant (Labuza & Riboh, 1982).

The prevailing effect of food temperature in relation to the reaction rate has been considered as the critical factor affecting food stability and food quality. One of the most refereed models in this respect is that of Arrhenius in which the temperature effect is incorporated into an exponential theoretical model. The Arrhenius law was derived from thermodynamic laws of statistical mechanical properties. This relation is the most widely used and has shown to be very useful in chemical kinetics. The model relates the reaction rate constant (k) to temperature (K), as follows (Sablani, Dalta, Rahman, Qaboos, & Majumdar, 2006):

$$k = Aexp\left(\frac{-E_a}{RT}\right) \tag{1.20}$$

where k is the experimental observation at different temperatures, A is the Arrhenius equation constant or pre-exponential factor, E_a is the energy of activation (or extra energy) required to initiate a reaction, R is the universal gas constant (1.9872 cal/(mol K) or 8.3144 J/(mol K), T is the absolute temperature in Kelvin.

This equation points out that a graph of $ln\ k$ vs the inverse of absolute temperature gives a linear line which its gradient is the activation energy over the gas constant (R) (Labuza & Riboh, 1982). The linearised form is given thus:

$$\ln k = ln\ k_o - \frac{E_a}{RT} \tag{1.21}$$

The activation energy can be described as the minimum energy hurdle that molecules need to overcome with increasing temperature for the reaction to occur. The physical meaning of A in Equation (1.20) is that it refers to the rate constant at which all

molecules posses sufficient energy to react (van Boekel, 2008). The value of E_a is a certain value of the temperature sensitivity of the particular reaction, i.e. the E_a rates should increase with an increase in temperature.

The activation energy of a chemical reaction can be resolved by calculating the rate constant at two different temperatures:

$$\ln\left(\frac{k}{k_{ref}}\right) = \frac{E_a}{R}\left(\frac{1}{T} - \frac{1}{T_{ref}}\right) \tag{1.22}$$

To predict the influence of temperature on the reaction rate for a particular isothermal decay, values of k are evaluated at different temperatures, and $ln\ k$ is constructed vs $((1/T)-(1/T_{ref}))$. A linear line is obtained with a gradient of $-E_a/R$ on a semilog graph, and then the activation energy is calculated (Sablani, Dalta, Rahman, Qaboos, & Majumdar, 2006).

1.4.3 Applications of high-solid matrices on stability, delivery and controlled release for functional foods

Functional foods are foods or ingredients that serve special physiological benefits apart from their nutritional aspect (International Life Sciences Institute, 1999). Regardsless of their definition, these products have found wide interest in commercial, academic and government sectors (Jones & Jew, 2007). In order to respond to consumer demand for healthful foods, design of new and reformulation of existing food products are the key roles to enhance nutrition and obtain desirable health effects (Turgeon & Rioux, 2011). In this regard, incorporating bioactive components into food systems is crucial for the delivery of bioactive nutrients and functional food components (Day, Seymour, Pitts, Konczak, & Lundin, 2009).

It is known that the stability and shelf life of food matrices can be affected during prolonged storage. The concept of T_g from state diagrams represents a design of change in the consistency of the matrices as a function of increasing level of total solids that makes it relevant in shelf-life investigations (Salbani, Kasapis, & Rahman, 2007). Products become self-stable when stored below T_g due to a reduction in microbial growth and rates of chemical reactions. Therefore, the concept of glass transition is significant in controlling the molecular mobility and decelerating chemical reactions (Karel, Anglea, Buera, Karmas, Levi, & Roos, 1994; Roos, 1995). The stability of micronutrients (in particular vitamins) in low moisture polymer matrices was analysed depended on the glass transition concept, and it was found that factors including the types of cosolute in the matrix, water content and temperature affect the T_g and are crucial in food stability (Rahman, 2006).

Storage of foods below T_g or increasing T_g in novel formulations of food enhances storage stability by retaining the unfrozen part (e.g. unfrozen water) in the glassy consistency. The solvent in the concentrated phase gets kinetically immobilised and hence does not involve in chemical reactions, thereby enhancing the stability of unfrozen foods. In this matter, polysaccharides (carrageenan and dextran) have been used in frozen dessert products to delay growth of ice crystals in stabilised ice cream and increase the viscosity of the unfrozen part (Golf, 1992 &1994).

Microencapsulation is the creation of high-solid glassy matrices with a stable medium and controlled release of bioactive ingredients. The barrier capsule is created to avoid chemical and biological reactions. To control the stability, several principles can be utilised including viscosity and T_g in the entrapped amorphous phase leading to a reduction in the effective diffusivity of water and bioactive compounds (Labuza & Hyman, 1998). In the food industry, such technique is employed to maximize the retention of bioactivity from constituents throughout processing and storage of the formulated products (Wilson & Shah, 2007). Microencapsulation can be used to prevent degradation

and protect against oxidation of nutrients (vitamins and specific fatty acids) (Ottley, 2000; Shen, Apriani, Weerakody, Sanguansri, & Augustin, 2011). Table 1.9 shows a mini literature review on the applications of spray drying and freeze drying in vitamin encapsulation.

Microencapsulation is the most familiar controlled-release technique in the food industry to deliver the desired bioactive components (vitamins, minerals, amino acids) to the target site of the body (Wilson & Shah, 2007). Controlled-release could be described as a delivery method by which one or more active components are made available at a desired site at a particular rate (Pothakamury & Barbosa-Cánovas, 1995). The advantage of controlled release is that it occurs over prolonged periods of time at specific rates from the high-solid food matrices. Ingredients should be released from coated particles, capsules, tablets or gel-like substances, liquified in the appropriate amount of digester (for example water), and consequently absorbed in the human body (Parada & Aguilera, 2007). Once the component has been released, the proportion that has been absorbed and actually reached the systemic circulation represents its bioavilability. Some components will pass through the digestive tract without being digested, absorbed and are then eliminated. To meet the bioavailability requirements, bioactive compounds should be studied both *in vitro* and within the human body (Granado-Lorencio, Donoso-Novarro, Sánchez-Siles, Blanco-Navarro, & Pérez-Sacristán, 2011; Turgeon & Rioux, 2011). Table 1.9 shows a mini literature review on the applications of spray drying and freeze drying in vitamin encapsulation.

Table 1.9 Compilation of information on vitamin encapsulation

Vitamin	Loading technique	Carrier	Total solids (%)	Calorimetic T_g	Reference
Ascorbic acid	Spray dried capsules	Purple sweet potato flour+maltodextrin	89.0	10-29 [a]	Ahmed, Akter, Lee, & Eun (2010)
Ascorbic acid	Spray dried capsules	Gum arabic+ maltodextrin	90.0	39-62 [a]	Righetto & Netto (2006)
Ascorbic acid	Spray dried capsules	Modified starches (maize, potato, rice)	97.9-98.5	85-125 [b]	Palma-Rodriguez et al (2013)
Ascorbic acid	Spray dried capsules	Milk solid+ wheat flour	80.7-95.2	3.6-27 [a]	Sablani, Al-Belushi, Al-Marhubi, & Al-Marhubi, (2007)
Ascorbic acid Thiamin	Freeze dried capsules	Lactose, trehalose	97.5-98.0	99-106 [b]	Zhou & Roos (2012a)
α-tocopherol	Freeze dried capsules	Lactose, trehalose milk protein isolate soy protein isolate	96.3-96.5	101-116 [b]	Zhou & Roos (2012b)
Thiamin	Freeze dried capsules	Polyvinyl pyrolidones (PVP)	82.3-96.3	51-104 [b]	Bell & White (2012)

Note:

[a] Midpoint temperature

[b] Onset temperature

Design of food-grade delivery systems has found wide application in the food industry, which can draw extensively from the medical field (Lesmes & McClements, 2009; van de Velde & Kiekens, 2002). Such systems have been selected to facilitate the introduction of active components in foods including bioactive lipids, vitamins, minerals, enzymes, peptides and dietary fibre (Jones & McClements, 2010). For example, encapsulation is the approach of choice to deliver the functionality of active ingredients in complex food matrices utilising carbohydrates, lipids, biopolymer complexes and surfactants (Ubbink, Burbidge, & Mezzenga, 2008). The functionality of encapsulated systems is governed by the wall material that can reduce molecular mobility and rates of reactions. It should be mentioned that absorption of water in the system leads to a plasticisation effect and additional free volume resulting in a changing diffusion front during ingredient release (Ubbink & Krüger, 2006).

Colloidal matrices used in the food industry are produced from either globular proteins alone or protein/polysaccharide mixture. The common food-grade polysaccharides for assembling biopolymer colloid particles are pectin, carrageenan, chitosan, xanthan gum, methyl cellulose, inulin and alginate (Jones & McClements, 2010). In a gel or solid emulsion, the dispersed phase is in mesoscale and is created artificially via food processing (van der Sman & van der Goot, 2009). The structure of an elastic and chewable product that provides oral indulgence owning to its rubbery texture and sweet taste is highly important for young consumers (Day, Seymour, Pitts, Konczak, & Lundin, 2009). The interest in this type of functional food technology includes the development of a hydrocolloid cellular solid as a food ingredient carrier. Production of a dried, chewable and textured product with a low moisture content, in order to limit undesirable chemical reactions, inhibit microbial growth and preserve bioactive compounds is highly desirable (Nussinovitch, 2005; Schmidl, 1993).

1.5 SUMMARY OF CURRENT KNOWLEDGE

Based on the aspects reviewed in this chapter, we feel it is a tendency that the concept of glass transition is relevant to a variety of amorphous food polymers particularly in high-solid concentrations. It has been recognised that the slow motion of molecules in the glassy state of biological molecules is a crucial consideration for the delivery of bioactive compounds. This physical delivery approach is the basis of systematic understanding of hydrocolloids as bioactive compound carriers in the development of food-grade controlled release systems. Fundamental research in addressing the concept of network T_g as a molecular factor in high-solid hydrocolloid matrices produces a series of fundamental values for vitamin diffusion control. This can lead to micronutrient stability required in a variety of food formulations with industrial interest.

1.6 RATIONALE FOR THE RESEARCH

This PhD research impacts the field on fundamental and technological grounds in the following issues:

1.6.1 The Asia-Pacific Vitamins (Nutraceuticals) market is forecast to increase 7% in the period 2014 to 2019 with the driving factors being consumer awareness of their health and nutrition including the rise in purchasing power for functional products (Research & Markets 2015). Therefore, fundamental research is an initial and potential stage to develop novel food products containing health-promoting ingredients.

1.6.2 Delivery of vitamins and other nutraceuticals in processed and functional foods should be based on structural design, process optimisation and bio-functionality (McClements, Decker, Park, & Weiss, 2009). Using food architecture rationalised from biopolymer science has the potential to achieve encapsulation, protection, biological function and controlled release.

1.6.3 Based upon the recent literature it can be proposed that molecular dynamics of biopolymers at the vicinity of the mechanical T_g may explain diffusional control in substrate/enzyme interactions (Chaudhary, Small, Shanks, & Kasapis, 2014) and limit mobility of bioactive compounds (Jiang & Kasapis, 2011). It is challenging to broaden this into the physical release of vitamin in condensed food systems, which might become commercially available in the form of viscoelastic gels, tablets and microcapsules.

1.6.4 It is critical to implement the concept of controlled release in micronutrient delivery and bridge the gap between vitamin diffusional kinetics and macromolecular dynamics of common food polymers in condensed systems. Understanding the molecular structure-function relationship will elucidate the influence of hydrocolloids on control of nutrient diffusion for enhanced biofunctionality.

1.6.5 Biomacromolecules have structural complexity and specific free volume that lie beyond synthetic polymer considerations. This research in this field has to take into account the specific nature of the biomaterials, the quantity and kind of organic solvent and cosolute, and the effect of thermal processing to generate embodiments, which are edible and acceptable to consume.

1.7 RESEARCH HYPOTHESIS AND PRIMARY RESEARCH QUESTIONS

This research has been based upon the hypothesis that there might be *a quantitative relationship between fraction free volume of high-solid hydrocolloid matrices undergoing glassy dynamics and vitamin diffusional mobility, i.e. a means of physical delivery control of bioactivity via* T_g.

There are four research questions developed for this fundamental research.

(i) What are viscoelastic characteristics and T_g of high-solid hydrocolloid matrices undergoing a rubber-to-glass transition?

(ii) What are the diffusional patterns for vitamins entrapped in high-solid hydrocolloid matrices?

(iii) How does the release mechanism describe vitamin diffusion for those entrapped in high-solid hydrocolloid matrices?

(iv) How does the free volume theory explain diffusivity of vitamins in relation to glassy dynamics of high-solid hydrocolloid matrices?

1.8 RESEARCH OBJECTIVES

To answer the above research questions, the following operational objectives have been underlined according to the research plan and methodology:

(i) Investigate the viscoelasticity of high-solid hydrocolloid matrices as a function of temperature (frequency) and predict the T_g using a synthetic polymer approach

(ii) Probe the diffusion kinetics of vitamins on time and temperature using the chemical reaction pathway

(iii) Implement the concept of shift factors and empirical models to examine molecular mobility

(iv) Relate the diffusion coefficients of vitamins to the fractional free volume of biopolymer matrices as a function of temperature

(v) Investigate whether there is a qualitative relationship in the interplay between vitamin diffusional mobility and fractional free volume

1.9 BROAD RESEARCH PLAN

According to this framework of experimental Chapters 3-6, four essential bioactive compounds (ascorbic acid, thiamin, nicotinic acid and tocopheryl acetate) and four different high-solid hydrocolloid systems were utilised to underpin the hypotheses of this work. The hydrocolloids studies comprised two common polysaccharides for the food and drug industries (high-methoxy pectin and κ-carrageenan), as well as whey protein isolate and modified waxy maize starch commonly used in microencapsulation. In each case, the experimental approach in Chapter 2 involved preparation and chracterisation of the structural, rheological, thermal, FTIR, X-ray diffraction and microscopy characteristics of the high-solid carbohydrate and protein systems in the form of hydrocolloid gels and spray-dried microcapsules. In addition, vitrification phenomena in high-solid macromolecules and diffusion kinetics of vitamins have been investigated using theoretical modelling based on the glass transition concept and the projections of the reaction rate. In Chapter 7, vitamin mobility in condensed hydrocolloid systems was elucidated via diffusion kinetics that unveil a congruent picture in the development of fractional free volume in polymer matrices and diffusional mobility of microconstituent in the blend.

CHAPTER 2

MATERIALS AND METHODS

ABSTRACT

This chapter describes materials (food biopolymers, vitamins, solvents, and reagents), methods, instrumentation and equipment used in this research. In addition, the theories behind the analytical methods have been overviewed in this part of the Thesis. Theoretical and practical approaches for the measurements of T_g by calorimetric and rheological methods are provided. Experimental procedures that have been utilised in this study to analyse physical and chemical characteristics of biopolymers and their mixtures are also introduced and those include Fourier transform infrared spectroscopy, wide-angle X-ray diffraction, SEM, particle size measurements and UV/Vis spectroscopy. Among the experimental protocols overviewed in this chapter are molecular dynamics of biopolymers, structural characterisation of vitamin carriers, and kinetic studies of vitamin diffusion.

2.1 PRINCIPLES

This part provides an overview focusing on the evaluation of macromolecular properties and glass transition of high-solid biopolymer matrices. The spectrophotometry is used to investigate the release kinetics of bioactive compounds. Some analytical routines are introduced in order to characterise the release systems.

2.1.1 Food rheology

The technical term rheology involves the study of deformation and flow behaviour of matter having properties in those of between solids and fluids (viscoelastic materials). Furthermore, rheology defines the relationships between the force or stress and the deformation of materials (Barbosa-Cánovas, Kokini, Ma, & Ibarz, 1996; Tabilo-Munizaga, & Barbosa-Cánovas, 2005). In the food industry, the principal aims of rheology are to determine the ingredient functionality in product development, evaluate food texture and collate this with the sensory evaluation, as well as design the process engineering in order to control product quality and shelf life (Fischer & Windhab, 2011).

According to Gunasekaran & Mehmet Ak (2000), small deformation dynamic oscillation can be applied to a material to characterise the viscoelasity of biopolymers and food products in relation to time, temperature, strain or frequency. These tests are non-destructive due to application of relatively small amplitudes. Complex modulus (G^*) is the total resistance of a material to oscillatory shear, and the modulus is composed of two parameters, G' and G'' where the equation, $G^* = (G'^2 + G''^2)^{1/2}$. Elastic or storage modulus (G') shows the strength of the network while the viscous or loss modulus (G'') is a measurement of flow behaviour. Moreover, phase angle (tan δ) is the level of viscoelasticity of the material expressed as $\tan \delta = (G'' / G')$. A high value of tan δ means

that the sample is more viscous or liquid-like whereas low value of tan δ indicates that the sample is more elastic or solid-like. Table 2.1 summarises the various rheological parameters described here.

Table 2.1 Standard rheological parameters of small deformation dynamic oscillation

Parameter	Definition	Symbol	Units
Shear storage modulus	Scope of elasticity of material	G'	*Pa*
Shear loss modulus	The capability of the material to dissipate energy or flow behaviour	G''	*Pa*
Complex modulus	The total resistance of sample to oscillatory shear	G^*	*Pa*
Phase angle	Degree of viscoelasticity	tan δ	-

The viscoelastic properties of food systems can be analysed using consecutive relations which are obtained with dynamic rheological tests, namely strain sweep, temperature sweep, time sweep, and frequency sweep (Brummer, 2006).

Strain sweep is employed to determine the linear viscoelastic region (LVR) of a material by increasing the amplitude of oscillation at a constant frequency and temperature thus observing the magnitude of phase lag and amplitude variation. The drastic changes in values of rheological properties (G' or G'') are the limit of the LVR. Within this LVR, the stress and strain elements are linearly related and property of the sample is entirely described by a lone function of time. The samples are assumed to be stable before carrying a strain sweep otherwise it is needed to subject a sample to a time sweep prior to determination of LVR. This test is very useful to study the stability of physical gels.

Frequency sweep is used to provide viscoelastic properties as a function of frequency at a fixed strain and temperature. The data obtained from the test can categorise the nature and behaviour of biopolymers and food products into four groups (Fig. 2.1): a dilute solution, an entangled solution, a weak gel or a strong gel. Furthermore, the test is

used in time-temperature superposition to gauge long term properties of samples beyond a wide range of reasonable experimental time.

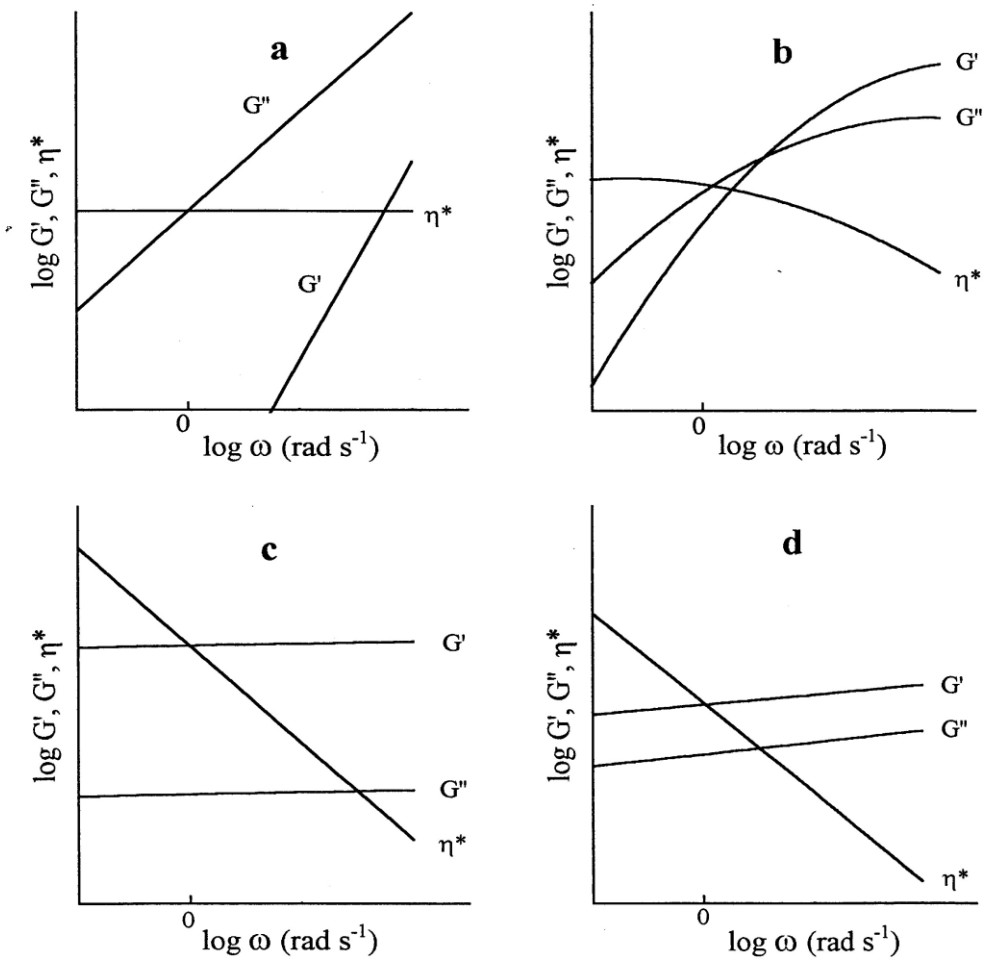

Fig. 2.1 The four classifications of mechanical spectra in low-solid food materials: (a) dilute solution, (b) entangled solution, (c) strong gel and (d) weak gel (Richardson & Kasapis, 1998).

Temperature sweep or temperature ramp is a measurement of G' and G'' as a function of experimental temperature at a constant frequency and strain. Such text is very useful to study gel formation.

Time sweep is analysed after temperature ramp where both moduli have shown a considerable increase as a function of time at a certain strain, frequency and temperature until equilibrium is more or less achieved. The importance of time sweep is to determine

the sample changes over a certain period. This test is very useful to study the development of physical gels.

Rheometer is used to perform the rheological measurements, including the viscoelasticity of biopolymers, particularly intermolecular network formation (Fig. 2.2, left). AR-G2 (Advanced rheometer generation 2) is commonly used to refer to advanced rheometer generation 2 which was the first patented instrument to use magnetic trust bearing technology for nano-torque control.

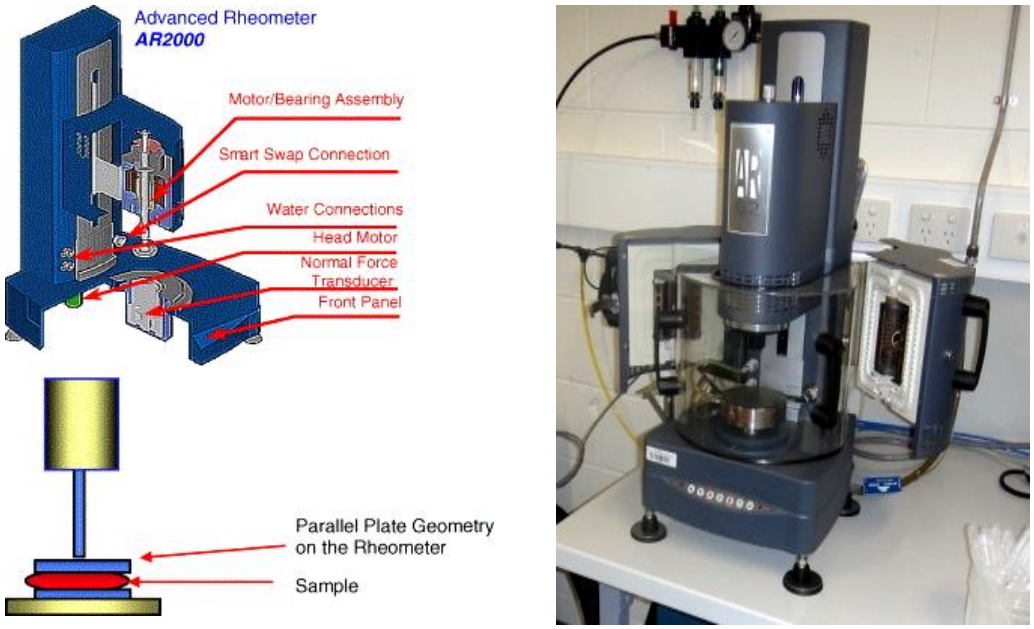

Fig. 2.2 Controlled stress rheometer with parallel plate geometry (AR 2000, left) (Rudraraju & Wyandt, 2005) and Advanced Rheometer Generation 2 (AR-G2, right)

The advanced rheometer used in the current study (Fig. 2.2, right) can measure various mechanical properties of the biomaterial, including direct controlled stress, strain or convection/radiant heating concept. Furthermore, the instrument features Smart Swamp^{TM} Geometrics that detects and stores geometry information automatically. The AR-G2 is also equipped with a parallel Peltier plate that provides precise control over a wide range of temperatures (TA Instruments, 2013a).

2.1.2 Differential scanning calorimetry

Thermal analysis techniques have been used extensively in food research, providing qualitative and quantitative information on the thermodynamic properties of food systems. Differential scanning calorimetry (DSC) pertains to the thermal analysis of materials by measuring a change of temperature and enthalpy associated with kinetic reactions during heating or cooling. Standard DSC measurements provide information as a function of temperature and time relating to heat absorption or emission of materials, and example include crystallisation and/or melting. The most typical application of conventional DSC is probably the detection of glass transition phenomena and $T_{g.}$ However, the DSC has a limitation to determine the T_g when the presence of the enthalpic relaxation overlaps the glass transition zone (Artiaga, López-Beceiro, Tarrío-Saavedra, Gracia-Fernández, Naya, & Mier, 2011).

2.1.2.1 Micro differential scanning calorimetry

For the thermal profile analysis, micro-calorimetry provides a high sensitivity in revealing the thermal events of solid samples or diluted solutions. Enhancements in the sensitivity and functions of commercially available micro-DSC have made this as a useful tool in providing quantitative and qualitative information on the thermodynamic properties of foods and their components. These are associated with endothermic and exothermic processes in heat capacity, e.g. thermal stability of protein, protein denaturation in aqueous solution and thermodynamic measurements of unfolding of compact globular proteins (Raemy & Lambelet, 1991).

The micro DSC VII (SETARAM, Fig. 2.3, top) provides high sensitivity of thermal events in between 0 and 90°C. The DSC consists of a measurement calorimetric block made up of a gold plate metal cylinder with high thermal conductivity (Fig. 2.3,

down left). This chamber provides for homogeneous temperature control and the two hollows are machined into the block to take the closed vessels (Fig. 2.3, down right). The measurement vessel takes the solid or liquid sample to be analysed whereas the reference vessel contains an inert material (e.g. distilled water) to compensate the thermal effect linked to the heating or cooling of the sample. The vessel is especially designed for measuring protein denaturation, gelification and phase transitions. Each vessel is surrounded by a plane-surface detector with very high sensitivity providing a thermal link with the calorimetric block. These transducers are good thermal conductors collecting the temperature in the vessels identical to that in the calorimetric block and the electrical signal is proportion to the heat transfer between the sample vessel and the calorimetric block (SETARAM, 2014).

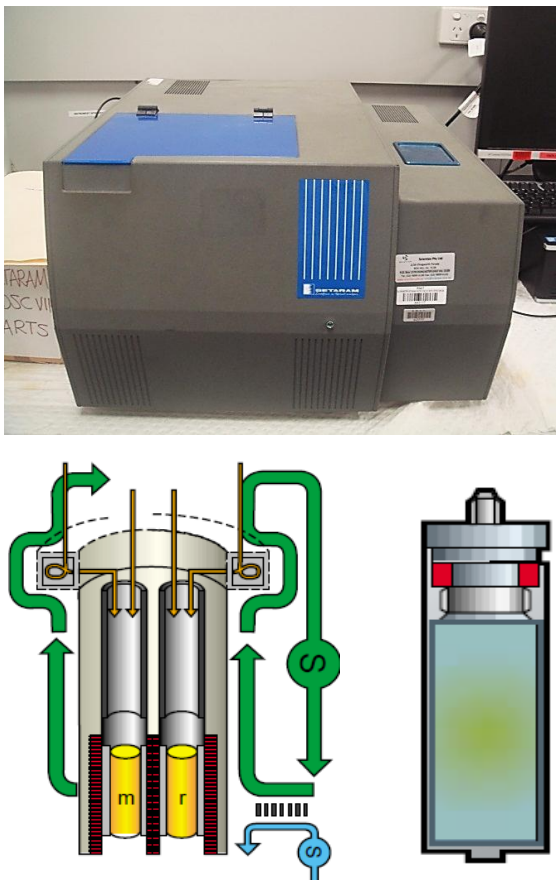

Fig. 2.3 Micro-DSC VII SETARAM (top), schematic diagram of micro-DSC (lower, left) and the closed batch vessel (lower, right)

2.1.2.2 Modulated differential scanning calorimetry

Modulated differential scanning calorimetry (MDSC) is an advanced DSC designed to overcome limitations of conventional DSC thus providing new insights into the properties of materials e.g. identification of thermal events. MDSC administers two simultaneous heating rates, the traditional linear and a sinusoidal heating rates of the material-experiment (Verdonck, Schaap, & Thomas, 1999). The average heating rate generates information on total heat flow and a sinusoidal heating rate produces heat capacity information from the change of heat flow along with the temperature ramp and kinetic component as shown in the Equation (2.1) (Gill, Sauerbrunn, & Reading, 1993).

$$\frac{\mathrm{d}Q}{\mathrm{d}t} = -\frac{\mathrm{d}T}{\mathrm{d}t}\left[C_p + f'(t,T)\right] + f(t,T) \qquad (2.1)$$

where: dQ/dt is heat flow generated by the sample, dT/dt is heating rate, C_p is the heat capacity of sample, t is time, T is temperature, $f'(t,T)$ is the thermodynamic heat flow element and $f(t,T)$ is kinetically-limited heat flow. For MDSC, total heat flow is derived from the average values for the reversing heat flow signal using a Fourier transformation analysis and the non-reversing counterpart which is the arithemetic disparity between the total heat flow and the heat capacity signal.

The Q2000 (TA Instruments) is a modulated DSC with high performance in baseline stability, sensitivity and resolution (Fig. 2.4). The features of Q2000 include both Advanced Tzero™ and Modulated DSC™ technologies to record broad thermal events in a wide range of temperature (-90-200°C). The modulated DSC has the 50-position intelligent auto-samples, auto schedule tests and digital mass flow controllers. (TA Instruments, 2013b).

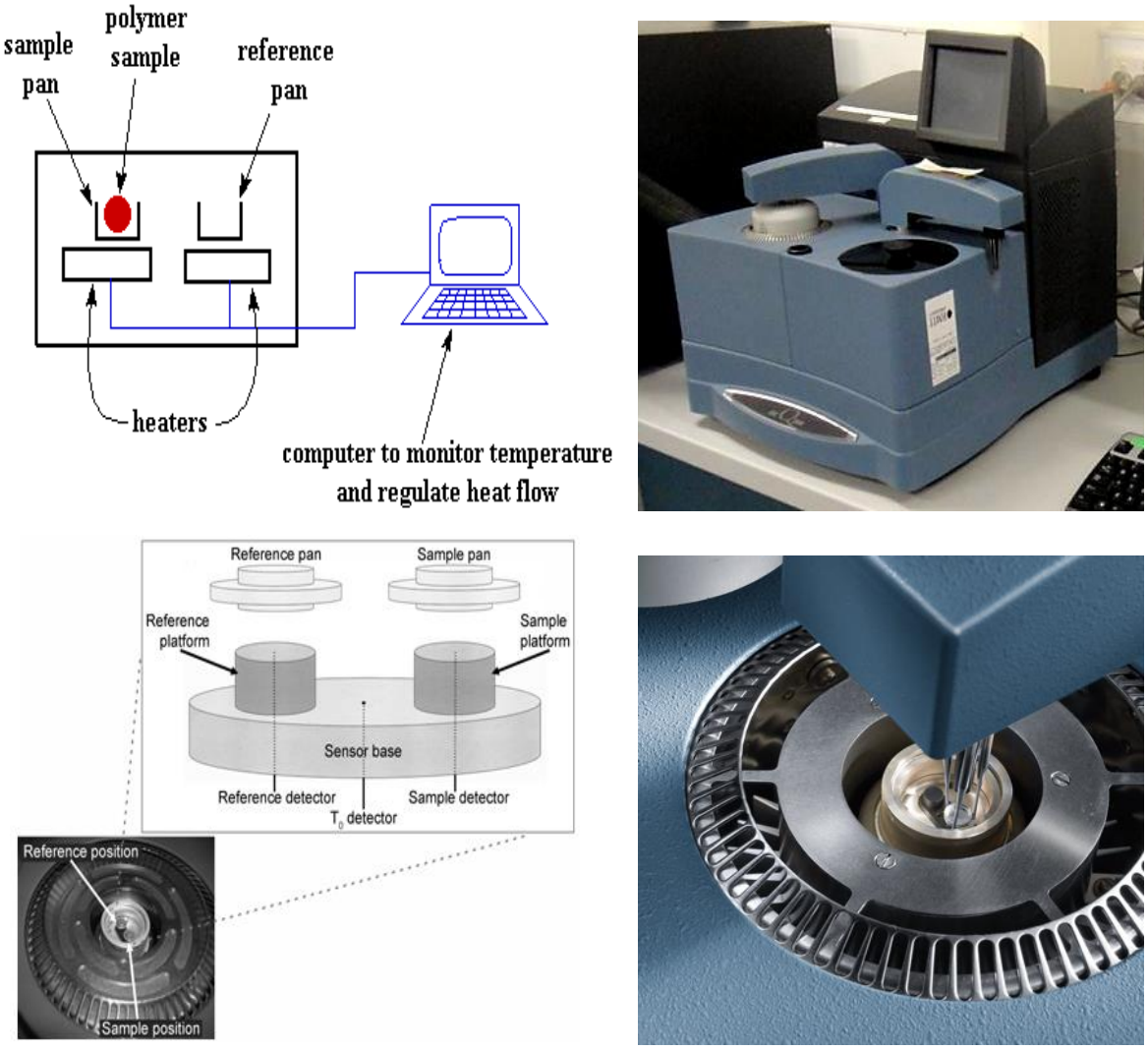

Fig. 2.4 Schematic diagram of DSC (left) (Polymer Science Learning Centre, 2013) and MDSC Q 2000 (right)

2.1.3 Dynamic mechanical analysis

Dynamic mechanical analysis (DMA) and dynamic mechanical thermal analysis (DMTA) are similar techniques in which a small deformation is administered on a sample in a cyclic mode. This analysis is primarily utilised to characterise thermomechanical properties with variation in temperature, time, frequency, stress, strain or multi parameters.

DMA performs oscillatory measurements at a set of frequencies and reports changes in temperature and transition in materials. The sample can be tested on a controlled stress or a controlled strain manner. For powder samples, a novel material pocket has been designed to fix samples that cannot support their own weight. A force motor generates the sinusoidal signal which is conveyed to the sample via a drift shaft. The two moduli can report the small deformation with an in-phase element, the storage modulus or the elastic behaviour and an out of phase element, the loss modulus. As shown in Fig. 2.5, the ratio of the loss to the storage modulus is defined as the tan δ or a measurement of the extent to which a material dissipates or absorbs energy under a cyclic load (Perkin-Elmer, 2013a).

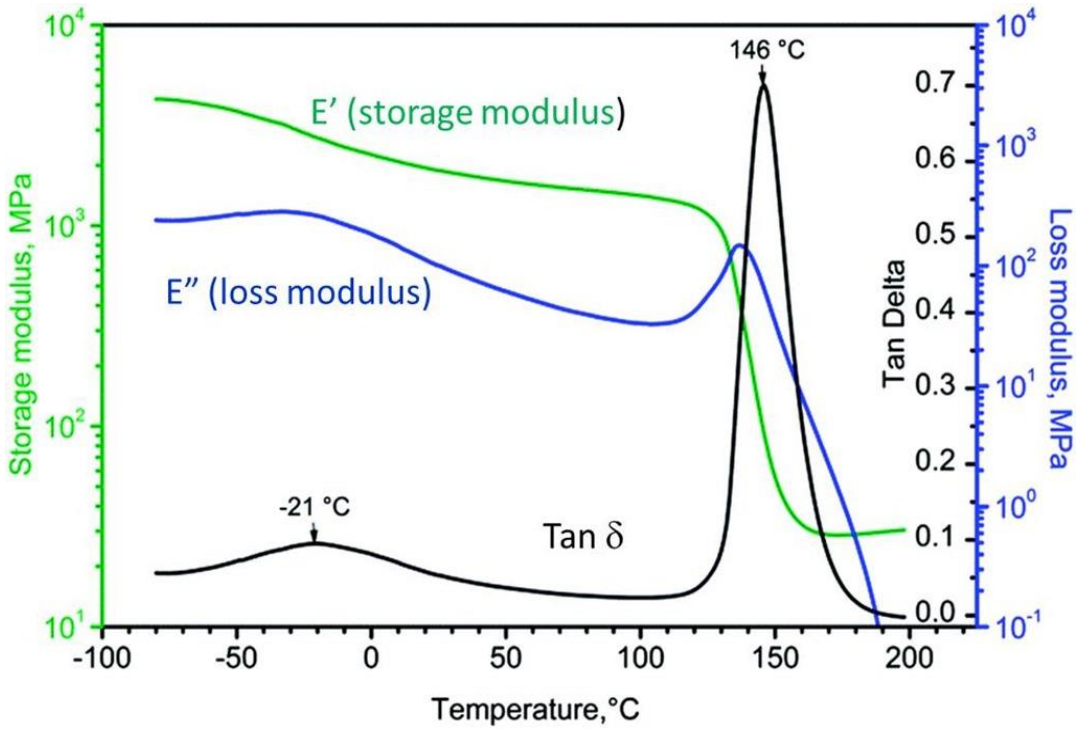

Fig. 2.5 A typical DMA curve recording a tan δ or mechanical T_g (Gotro, 2016).

The DMA 8000 dynamic mechanical analyser has been described as a flexible and cost-effective instrument (Fig. 2.6). The DMA measures the viscoelastic parameters which include storage modulus (*E′*), loss modulus (*E″)* and tan delta (δ) of high-solid materials as a function of a period (sinusoidal) deformation. The T_g is determined by a concurrent peak in the tan delta or a peak in the log of storage modulus (*E′*) scanned as a function of temperature against a Linear Variable Differential Transformer (LVDT) at a specific frequency of oscillation and the clamp type used (Perkin-Elmer, 2013a).

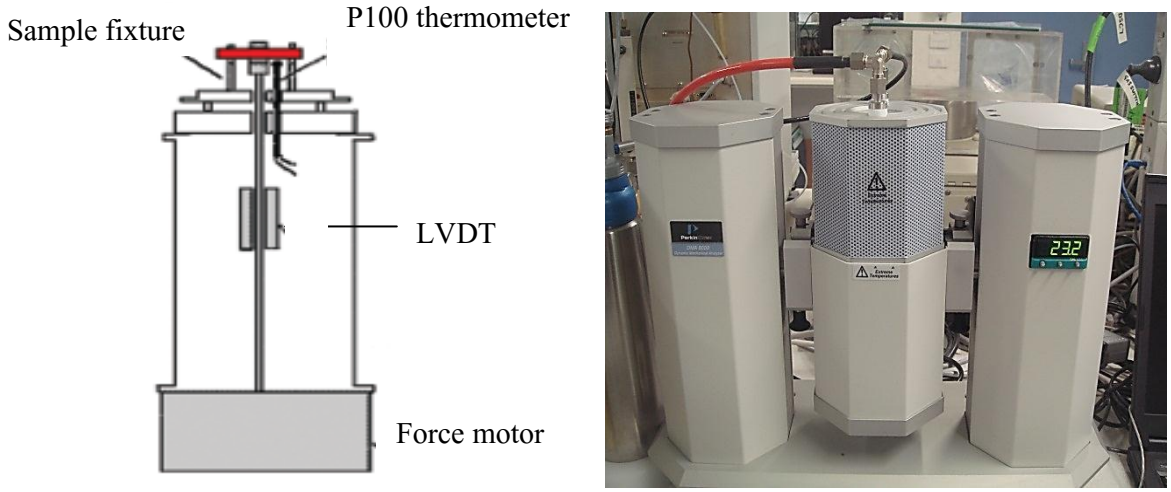

Fig. 2.6 Schematic diagram of the DMA 8000 analytic train (left) and the DMA 8000 (right)

2.1.4 Fourier transform infrared spectroscopy

Fourier transform infrared spectroscopy technology is another quality control tool available to food researchers. The method is convenient, rapid and accurate to characterise the structure and functional groups in biomaterials (van de Voort, 1992).

FTIR is the commonly abbreviation for Fourier transform infrared spectroscopy, which is derived from a mathematical exercise displayed by Jean Fourier. An infrared spectrum can be considered as a fingerprint of a material with the absorption peaks which reflect the vibrational frequencies between the bonds of the atoms creating the material.

The current technology of such technique can identify many types of material and the size of each of the peaks in the spectrum implies the quantity of component present (Thermo Nicolet, 2001). Accordingly, this analytical approach is a versatile tool in food, chemistry and pharmacy which provide the evidences of vibration of atoms of compound.

Fig. 2.7 depicts the FTIR instrument employed in this study, i.e. FTIR Spectrum 100. It consists of an infrared light source, a fixed mirror, a sliding mirror, beam splitter and a detector (Fig. 2.7). A beam exuded by the infrared light is divided into two via the beam splitter and the half of each signal will be reverted to both sliding and fixed mirrors. The light beams return to the splitter at which point they are recombined to produce either constructive or destructive interference. Afterwards, the signal is captured by the detector to compile an interferogram which is then transferred into spectra of the source, with and without sample absorption. The proportion of the both spectra (i.e. former to the latter) is interpreted as the FTIR transmission spectrum of the samples (Dole, Patel, Sawant, & Shedpure, 2011).

The FTIR Spectrum 100 is supplied with a MIRacle^{TM} ZnSe Single reflection ATR plate. Spectra were recorded in absorbance mode within the wavelength vicinity of 4000-600 cm^{-1} with a specific resolution of 4 cm^{-1} (Fig. 2.7). This was calibrated against the background spectrum of distilled water (i.e. solvent) at ambient temperature (Perkin-Elmer, 2013b).

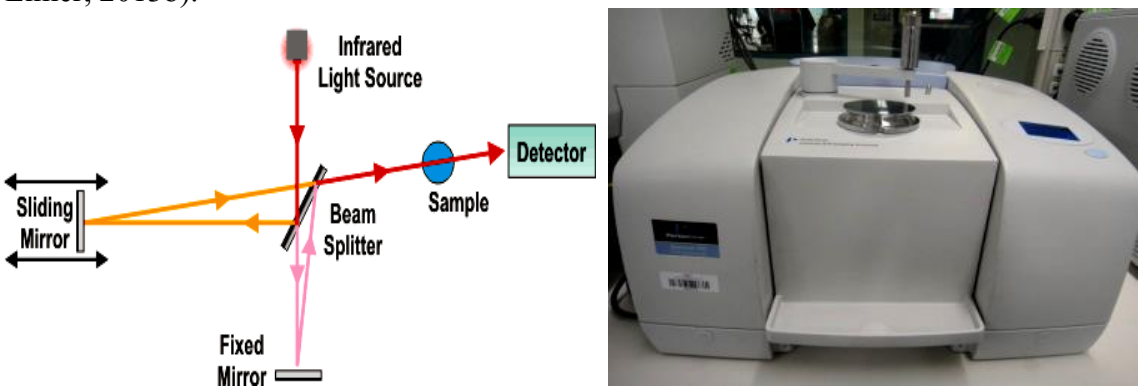

Fig. 2.7 Schematic diagram of FTIR (left) (ETS Laboratories®, 2013) and FTIR Spectrum 100 (right)

2.1.5 X-ray diffraction

X-ray diffraction (XRD) is a method which is generally carried out to determine the chemical structure of crystalline substance, loss of crystallinity, and the presence of repeating structure of atoms or molecules. XRD is non destructive analysis requiring s very small sample sizes and quantity. The technique has applications in material science pharmaceutical and food science to correlate physical appearance with chemical motions.

XRD can describe the differences between amorphous and crystalline material. In crystal structure, the atoms are arranged systematically while the atoms in amorphous material are randomly aggregated. When an X-ray beam attacks atoms in a non-crystalline material, the electrons around the atoms start to oscillate with the same level frequency of the beam, and the oscillation occurs in all directions. This results in destructive interference and no energy leaving the material. In contrast, the atoms in crystalline structures oscillate in a limited direction resulting in constructive interference. Based on the comparison of peaks in X-ray graphs, amorphous substances usually create broad bands while crystalline materials show distinctive, sharp peaks (Duvvuri, Ko, Krommenhoek, & Sanchez, 2013; Jenkins & Snyder, 1996).

Fig. 2.8 demonstrates the x-ray diffraction process as well as the wide angle X-ray diffractometer (WAXD) utilised in this study. Inside the X-ray tube, a current is transferred between an anode and a cathode. The number of electrons exuded from the cathode and moved towards the anode rises with increasing current. A range of high voltages from 15 to 60 kV is applied to accelerate the electrons, so that these bombard, the anode generating the X-ray radiation which passes filters to limit their direction of travel. They are piled up through the application of collimators in the vacuum tube before reading the sample material. When the diffraction is detected, the signal will be recorded and transformed into a count rate. The result is plotted in the form of the diffraction intensity

against the angle (2θ) of x-rays' incidence. Finally, a database is used to determine the crystalline structure of the substance by comparing the peaks in the diffractogram (Duvvuri, Ko, Krommenhoek, & Sanchez, 2013).

This advanced diffractometer is supplied with Cu-Ka (1.54 Å) radiation and employs 40 mA current and 40 kV accelerating voltage. Sample in powder form were located on a sample holder and scanned steadily to acquire diffractograms within a 2θ range of 5° and 90° at an interval of 1°. The Bruker Advanced X-ray Solutions software, DIFFRAC^{plus}c Evaluation (Eva), enables users to schedule the tests automatically at off work time (BRUKER AXS, 2013).

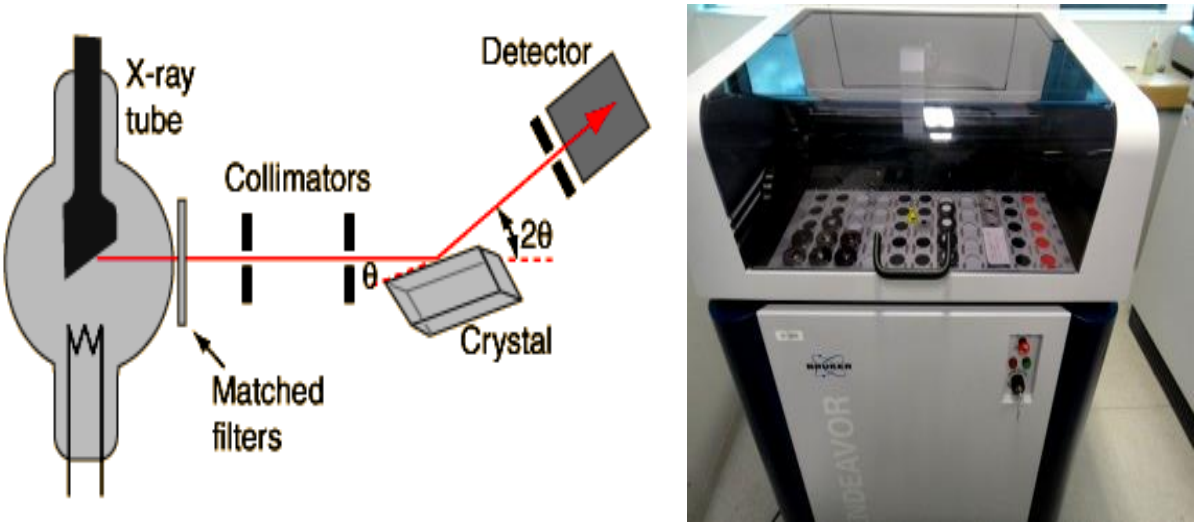

Fig. 2.8 Schematic diagram of XRD (left) (HyperPhysics, 2013) and BRUKER AXS D4. Diffractometer (right)

2.1.6 Scanning electron microscopy

Scanning electron microscopy (SEM) is a versatile technique to examine the nature of a wide range of materials. The SEM is popular choice for food researchers to visualise the surface feature of specimens with a higher resolution limit (around 1 nm) compared to

the traditional light microscopy (around 0.2 μm) (Fazaeli, Tahmasebi, & Djomeh, 2012; Kaláb, Allan-Wojtas, & Shera Miller, 1995).

In SEM systems, the specimen is typically dried and layered with a thin sheet of gold to provide electric conductivity. The source of illumination is usually generated by passing an electric current from an electron source located at the top of a column. A voltage (300-40kV) accelerates the electron beam down towards the specimen to decrease spot size. The electrons are focused in an electron microscope by two electromagnetic lens. The condenser lens collimates the electron beam thenthe focusing lens objects on the specimen to producea clear image. The beam passes across the specimen in a series of parallel lines without any interactions and energy transfer between electrons and matter. These are put together a two dimensional image is obtained form the photographic record. The secondary electron (SE) and backscattered electron (BSE) are the two signals usually used to produce SEM images (Royal Society of Chemistry, 2013a).

The Philips XL30 SEM scanning electron microscope (XL32) is a conventional SEM equipped with secondary electron and backscatter electron detectors and an energy dispersive X-ray analysis system. The key instrument features are fully monitored stage facilitating systematic searching of specimens, which is capable of recording and returning the feature of interest. A rapid production stereopairs permits performance of on-screen measurements and a Glaten XuM nano-CT system facilitates the 2D and 3D-images of the surface structure of gold-coated objects in the SEM at a high resolution (Natural History Museum UK, 2013).

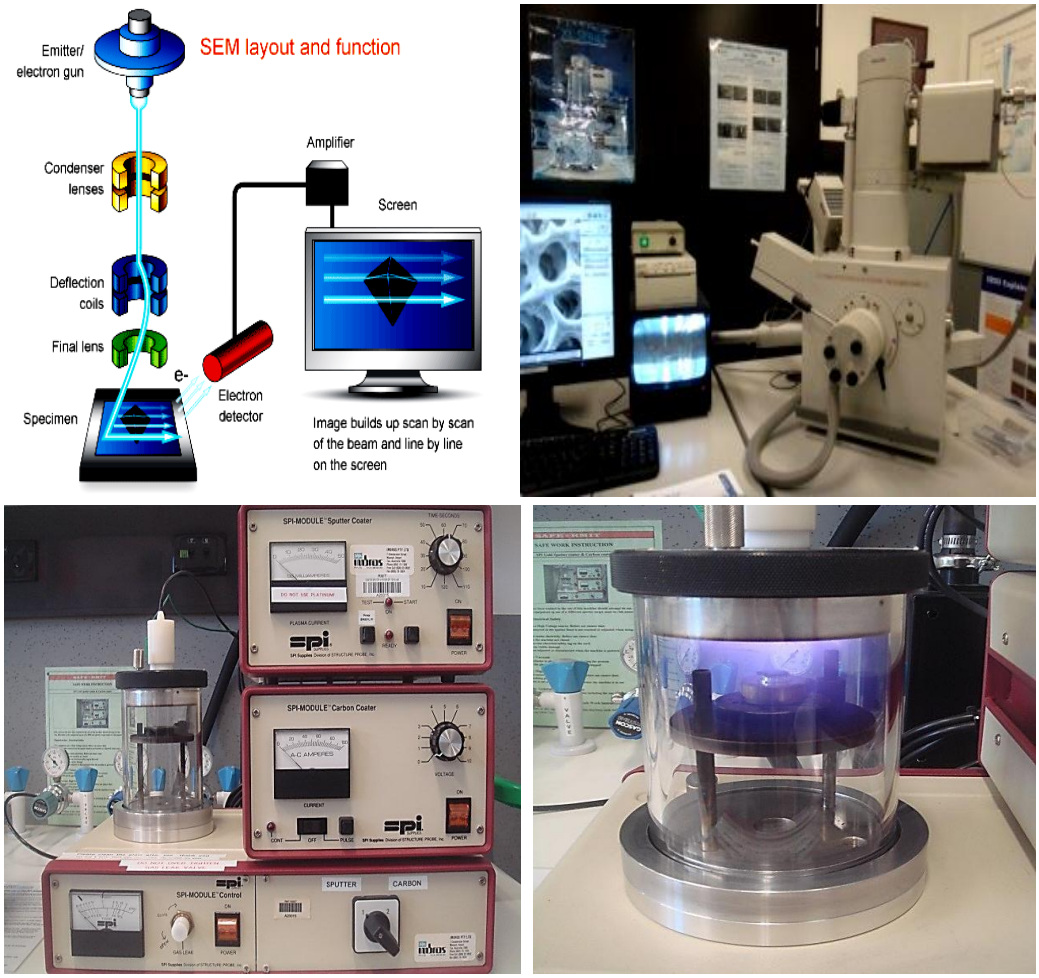

Fig. 2.9 Schematic diagram of SEM (upper left) (AMMRF, 2013), Philips XL30 SEM (upper right) and SPI Gold Sputter Coater (lower)

2.1.7 Ultraviolet/Visible spectroscopy

UV/Vis spectroscopy is a technique that analyses the molecular absorption of ultraviolet light (190-400 nm) and in the visible zone (400-700 nm) of the electromagnetic area. The transition of atomic and molecular electrons can cause the absorption of particular samples in solution.

In a conventional spectrophotometer, the electromagnetic radiation is passed through a lens and then the sample which is placed in a small square-section cell (or cuvette). The whole UV/Vis radiation is scanned over a short period (30 s). The same radiation is also simultaneously traversed a reference cell consisting of solvent alone.

Afterwards, photocells detect the radiation signal and the absorption is recorded by subtracting the intensity of the reference cell from the intensity of the sample cell. In the ultraviolet range, the deuterium discharge lamp is used as the light source while a tungsten filament can cover the visible range. Using both lamps can complete the whole part of the spectrum used for UV/Vis spectroscopy. Detection of the radiation passing through both cells can be achieved by using a grating and diode array to convert photons of radiation into tiny electrical currents (Royal Society of Chemistry, 2013b).

A UV/Vis spectrophotometer model of LAMBDA 35 manufactured by Perkin-Elmer is employed in this study (Fig. 2.10). It can be operated with double beam for the wide wavelength range of 190-1100 nm. The bandwidth of the wavelength can be varied within 0.5-4.0 nm. The UV WinLab™ software enables users to simplify analysis and report generation through a step-by-step process (Perkin-Elmer, 2013c).

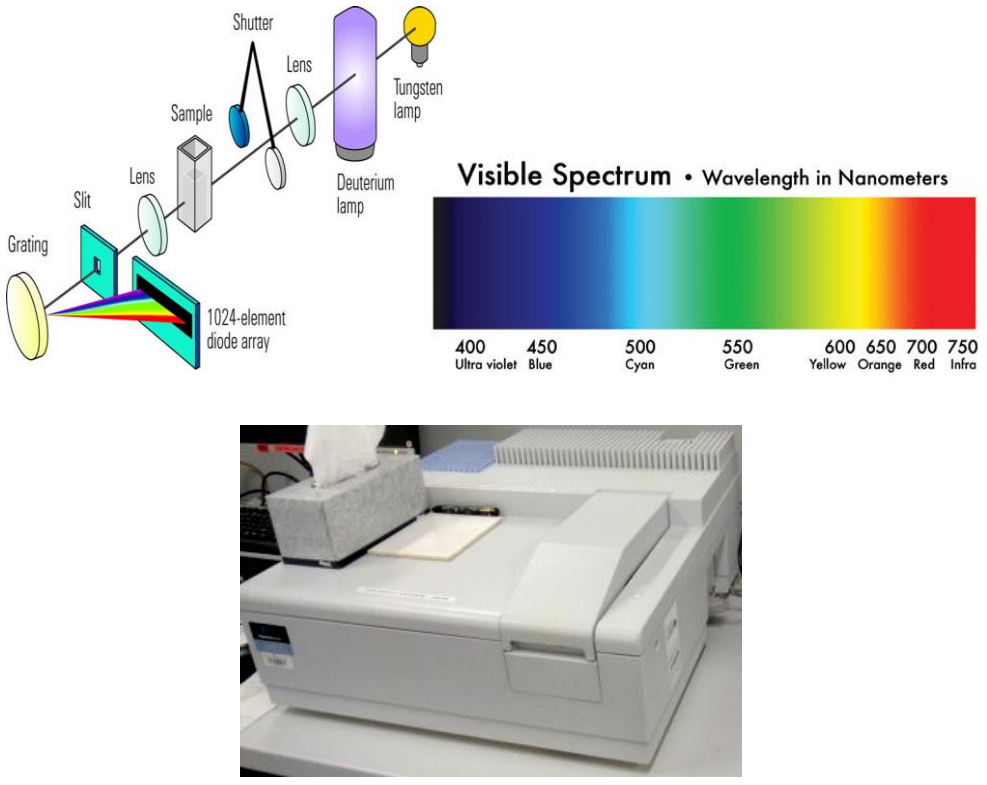

Fig. 2.10 Schematic diagram of UV/Vis spectroscopy, visible spectrum (top) (Agilent Technologies, 2013a) and LAMBDA 35 UV/Vis spectrophotometer (lower)

2.1.8 Atomic absorption spectroscopy

Flame atomic absorption spectroscopy (FAAS) is an analytical method frequently employed in food analytical laboratories for trace element determinations. The main advantages of the so-called furnace-in-flame approach are the versatility and low cost operation (Bings, Bogaerts, & Broekaert, 2010).

Flame atomic absorption is based on the fact that an atom in the vapour state will absorb light of certain frequencies as a specific characteristic. A hollow cathode lamp is basically a glass lamp with a metal cathode inside. When the lamp is heated there is emission of radiation of a certain wavelength and these are unique characteristics of the cathode materials. Sample solution nebulised and transferred into a flame of around two thousand degrees, which atomises the sample so that the gaseous atoms are generated and passed through the length path of the spectrometer. If those atoms are potassium, they will absorb those lines at 769.9 nm using an air-propane flame. The decreasing intensity of the light results from the atoms absorbing light which can relate that decrease in intensity to concentration. The radiation flux of a blank (i.e. solvent alone) and a sample in the atomiser is determined using a light-sensitive detector, and the ratio between the two absorbances is used to calculate analyte level or mass using the Beer-Lambert equation (Hind, 2011).

The VARIAN AA 280FS atomic absorption spectrometer (Fig. 2.11) is an external PC-controlled flame atomic absorption spectrometer supporting multi-element flame determinations. The instrument has a double-beam design to ensure a stable baseline and is suitable for manual flame analyses and vapour generation using the VGA 77 vapour generation accessory with Spectra AA base and PRO software (Agilent Technologies, 2013b).

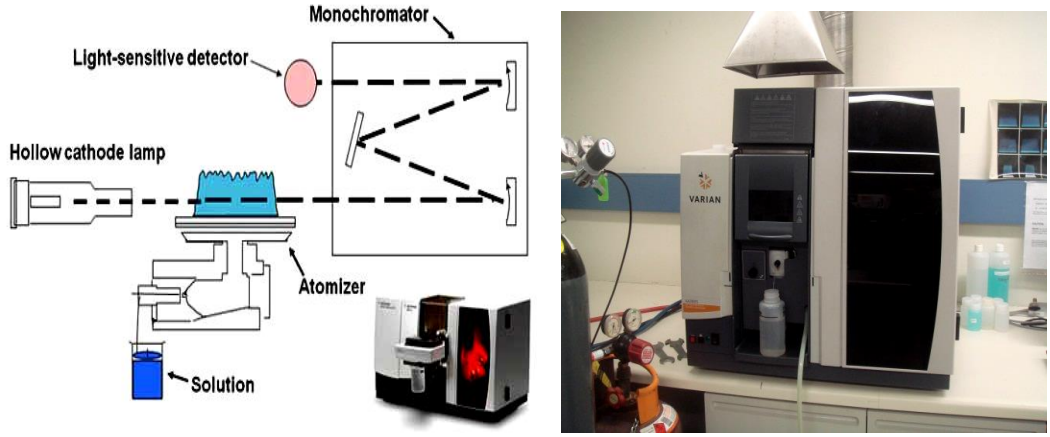

Fig. 2.11 Schematic diagram of AAS (left) (Hind, 2011) and VARIAN AA 280FS AAS (right)

2.1.9 Particle size analysis

Particle size measurements are important in food science due to the high correlation between the properties of materials and their particle size. To determine particle size distribution, the laser diffraction or more specific technique called Low Angle Laser Light Scattering (LALLS) has been recognised as the standard procedure for the characterisation of systems, quality control and product optimisation (Rawle, 2014; Stojanovic & Markovic, 2012).

The principle of light scattering to measure the particle size developed by Malvern Instruments Ltd, UK, is a special sampling device. In this there is an arrangement whereby a dispersed sample is passed through a measurement zone and a laser beam passes through it. A laser beam is a coherent-intense light and a He-Ne is the most common source of the light, providing the best stability and a signal with low noise. The light intensity of the laser beam is scattered by the particles within the sample and over a wide range of angles so that series of receiver lens or semicircular diodes are used detector to collect the high intensity light. Curve-fitting software converts the light intensity distribution into a series of empirical particle size distribution functions.

A particle size analyser developed by Malvern, i.e. Mastersizer 3000, can measure the particle size of suspensions, emulsions and dry powders with a fast and accurate method (Fig. 2.12). The instrument has a wide measuring capacity over the nanometer to millimeter (0.01-3500 μm) particle size range. This analysis reports the results in a short period of time (less than 10 s) with accuracy higher than 1% and precision less than 0.5% variation (Malvern, 2014).

Fig. 2.12 Schematic diagram of laser diffraction particle size analysis (left) (Spray Analysis and Research services, 2014) and the Mastersizer 3000 (right)

2.2.11 Spray dryer

Spray drying is one of the encapsulation techniques that has vast applications in the food industry and the advantages of the technique include relatively low cost, simplicity and flexibility. There are three steps involved in the encapsulation and protection of a range of micronutrients, polyphenols and flavours, namely: (i) forming the coating around the bioactive compounds; (ii) avoiding the loss of bioactivity of core materials and (iii) minimising the contamination of undesired impurities (Fang & Bhandari, 2010).

For encapsultaion, the shell material is hydrated first, then the core material is homogenised with the shell solution (Fig. 2.13). The mixture is introduced into a spray dryer and atomised with a nozzle jet in a heated air stream, after which water is vaporised

by the hot air that comes into contact with the solid particles inside a drying chamber. The encapsulated products are finally collected after they fall to a collection vessel at the base of the cyclone powder collector. The exhaust vapour is blown by exhaust fan to the outside atmosphere or fume/dust extractor (Armfield Group, 2014; Teleki, Hitzfeld, & Eggersdorfer, 2013).

Lab Plant SD Basic FT30MKIII spray dryer is a unit designed for producing a dry fine powder (Fig. 2.13). The operation mode is downward with co-current air flow and drying air throughflow of 70 m^3/hr. The dryer specification is a heater capacity 3 kW, jet size 0.5 mm, air inlet temperature up to 200°C and maximum product flow rate 150 ml/hr. The spray dryer is described as producing a fine food powder for various applications including beverages, milk, cereals, plant and vegetable extracts (Armfield Group, 2014).

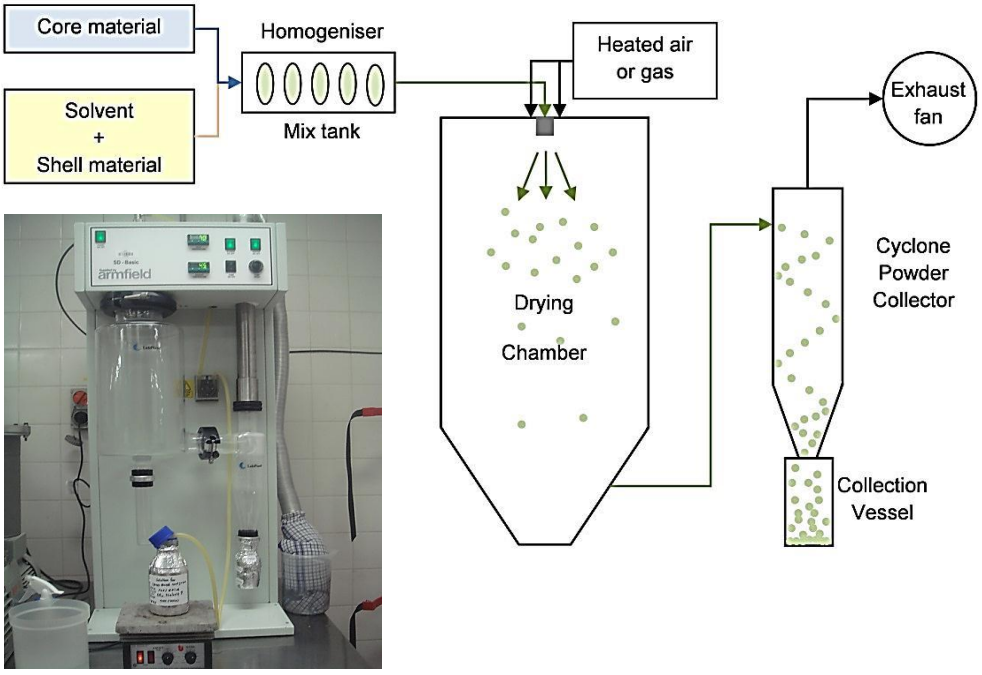

Fig. 2.13 A Lab Plant SD Basic FT30MKIII spray dryer (Armfield Group, 2014, left) and schematic illustration of a spray drying process (Chávarri, Marañón, & Villarán, 2012, right)

The detail of major analytical instrument used in this study is listed in Table 2.2, and other equipment is detailed in Table 2.3

Table 2.2 List of analytical instrument

Instrument	Trade Name	Manufacturer
Rheometer	ARG-2	TA Instruments (New Castle, DE, USA)
Dynamic mechanical analyser	DMA8000	Perkin Elmer (MA, USA)
Micro differential scanning calorimeter	Micro-DSC-III calorimeter	SETARAM (Caluire, France)
Differential scanning calorimeter	MDSC Q2000	TA Instruments (New Castle, DE, USA)
FTIR spectrometer	FTIR Spectroscopy-spectrum 100	Perkin-Elmer (Norwalk, USA)
X-ray diffractometer	BRUKER AXS D4	Bruker AXS Corporation (Madison, USA)
UV/Visible spectrophotometer	LAMDA 35	Perkin-Elmer (Norwalk, USA)
Scanning electron microscope	Philips XL30 SEM	FEI company (Sussex, England).
SPI Gold Sputter Coater	SPI-MODULD™ Sputter coater	IMBROS Pty. Ltd. (Hobart, Australia)
Optical microscope	Nikon H550s	Nikon (Japan)
Atomic absorption spectrometer	VARIAN AA 280FS	Agilent Technologies (California, USA)
Particle size analyser	Masteriser 3000	Malvern Instruments Ltd. (Worcestershire, UK)
Refractometer	ABBE	Erma Inc. (Tokyo, Japan)
pH meter	LabCHEM-pH	TPS (Springwood, QLU, Australia)
Colour meter	CR-400B	Minolta Camera Co. Ltd. (Osaga, Japan)
Water activity meter	Novasia ms1	Novasina AG (Lachen, Switzerland)
Moisture analyser	Ohaus MB45	Ohaus Europe GmbH (Greifensee,Switzerland)
Tzero® DSC Sample Encapsulation Press	Tzero® DSC Press	TA Instruments (New Castle, DE, USA)
Analytical balance (DSC lid-pan weighting)	Metter AE2000	Metter Instrument AG (Greifensee-Zurich, Switzerland)
Analytical balance	ADGR-202	A&D Company Limited (Japan)
Digital Thermocuple (-50) -150°C	HANNA	HANNA Instruments Inc. (Woonsocleet, USA)

Table 2.3 List of equipment

Equipment	Trade Name	Manufacturer
Muffle furnace	Techtrader	Techtrader Pty. Ltd. (Australia)
Spray drier	LabPlantSD Basic FT30MKIII	Keison Products (England)
Freeze drier	FDB 5503	Operon (Gimpo City, South Korea)
Air blast freezer	Batehilt	Barker & Taylor Pty. Ltd. (Canterbury, Australia)
Fridge freezer	ARB	ARB Corporation Ltd. (China)
Lab Freezer	Thermoline Scientific	Thermoline Scientific Instruments Pty. Ltd. (Australia)
Refrigerator	Kelvinator	Australia
Incubator	Qualtex Solidstate	Watson Victor, Ltd. (Australia & New Zealand)
Water bath (thermostatically controlled)	Thermoline Scientific	Thermoline Scientific Instruments Pty. Ltd. (Australia)
Magnetic hot plate	Industrial Equipment & Control	Industrial Equipment & Control Pty. Ltd. (Australia)

2.2 MATERIALS

The summary of chemical reagents and materials used in this study including supplier information is listed in Tables 2.4-2.7.

Table 2.4 List of vitamins

Vitamin	Formula	Molecular mass (g/mol)	Assay (%)	CAS Number	Supplier
L-ascorbic acid	$C_6H_8O_6$	176.12	≥99.0	50-81-7	Sigma-Aldrich, Australia
Thiamin hydrochloride	$C_{12}H_{17}ClN_4OS$ .HCl	337.27	≥99.0	67-03-8	Sigma -Aldrich, Australia
Nicotinic acid	$C_6H_5NO_2$	123.11	≥99.5	59-67-6	Sigma-Aldrich, Australia
DL-α tocopheryl acetate	$C_{31}H_{52}O_3$	472.74	≥96.0	7695-92-2	Sigma-Aldrich, Australia

Table 2.5 List of food polymers

Food polymer	Specification	CAS Number	Supplier
High-methoxy pectin (from citrus peel)	-polysaccharide content 93.3% (dry basis) -galacturonate 86.3% (dry basis) -DE 55-65 -light brown powder	9000-69-5	Sigma-Aldrich, Australia
κ-carrageenan	-extracted from *Euchema cottonii* type III -white to yellow-tan powder	11114-20-8	Sigma-Aldrich, USA
Whey protein isolate	-protein (TN × 6.38) 91.3% -fat 0.7% -ash 3.8% -lactose 0.44%. - moisture content 3.5% -pH 6.3 for 10% (w/w) solution -bulk density 0.45 g/ml -aerobic plate count 9,900 cfu/g	9013-90-5	MG Nutritionals, Murray Goulburn Co-operative Co. Ltd., Australia
Polydextrose (Sta-Lite III)	- purity 90% - moisture content 4%	68424-04-4	Tate & Lyle, USA
Modified waxy maize starch-Capsule®	-starch 91% -moisture content 7.85% -0.5% protein -<0.3% ash -0.15% fat	-	National Starch & Chemical Pty. Ltd., Bangkok, Thailand.

Table 2.6 List of solvents

Solvent	Formula	Molecular mass	Purity (%)	CAS Number	Supplier
Ethanol	CH_3CH_2OH	46.07	≥99.5	64-17-5	Sigma-Aldrich, Australia
Ethylene glycol	$(HOCH_2CH_2)_2O$	106.12	≥99.0	111-46-6	Sigma-Aldrich, Australia
Dimethyl sulfoxide	C_2H_6OS	78.13	≥99.5	67-68-5	Sigma-Aldrich, Australia

Table 2.7 List of reagents and other materials

Reagent/material	Formula	Molecular mass	Purity (%)	CAS Number	Supplier
2,4-Dinitrophenyl hydrazine	$(O_2N)_2C_6H_3N$-HNH_2	198.14	97.0	119-26-6	Sigma-Aldrich, Australia
Alizarin Brilliant Violet R	$H_{15}NNaO_6S$	432.40	98.0	4430-18-6	Jacquard, USA
Vanillin	4-$(HO)C_6H_3$-3-$(OCH_3)CHO$	152.5	99.0	121-33-5	Sigma-Aldrich, Australia
Barium chloride	$BaCl_2$	208.32	99.9	10361-37-2	Unilab, Ajax Finechem, Australia
Potassium bromide	KBr	119.00	≥99.0	7758-02-3	BDH, Chemicals Pty. Ltd., Australia
Cyanogen bromide	CBrN	105.92	>97.0	506-68-3	Sigma-Aldrich, Australia
Potassium chloride	KCl	74.55	≥99.0	7447-40-7	Unilab, Ajax Finechem, Australia
Sodium dihydrogen phosphate monohydrate	Na $H_2PO_4.H_2O$	137.99	≥98.0	10049-21-5	Sigma-Aldrich, Australia
Potassium dihydrogen phosphate	KH_2PO_4	136.09	≥98.0	7778-77-0	BDH Chemicals Pty. Ltd., England
Calcium chloride	$CaCl_2$	110.98	>97.0	10043-52-4	Unilab, Ajax Finechem, Australia
Magnesium chloride	MgCl2	95.21	>97.0	7786-30-3	Merck, Germany
Sodium chloride	NaCl	58.44	>99.5	7647-14-5	Merck, Pty. Ltd. ,Australia
Silver nitrate	AgNO3	169.87	>99.0	7761-88-8	Sigma-Aldrich, Australia
Meta-phosphoric acid	HPO3	79.98	33.5-36.5	37267-86-0	BDH, Chemicals Pty. Ltd., Australia
Sulfanilic acid	C6H7NO3S	173.19	≥99.0	121-57-3	Sigma-Aldrich, Australia

Table 2.7 List of reagent and other materials (cont.)

Reagent/material	Formula	Molecular mass	Purity (%)	CAS Number	Supplier
Sulfuric acid	H_2SO_4	98.08	95.0-98.0	7664-93-9	Sigma-Aldrich, Australia
Nitric acid	HNO_3	63.01	≥90.0	7697-37-2	Sigma-Aldrich, Australia
Hydrochloric acid	HCl	36.46	37.0	7647-01-0	Sigma-Aldrich, Australia
Phosphoric acid	H_3PO_4	98.0	85	7664-38-2	Sigma-Aldrich, Australia
Ammonium hydroxide	H_5NO	35.05	28-30	1336-21-6	Sigma-Aldrich, Australia
Sodium hydroxide	NaOH	40.00	≥97.0	1310-73-2	Sigma-Aldrich, Australia
Ammonia solution	NH_3	17.03	25	67-56-1	BDH, Chemicals Pty. Ltd., Australia
Thiourea	$NH_2C_SNH_2$	76.12	≥99.0	62-56-6	Sigma-Aldrich, Australia
Sodium hypochlorite solution	NaClO	74.44	10-15	7681-52-9	Sigma-Aldrich, Australia
Chloroform	$CHCl_3$	119.38	≥99.0	67-66-3	Sigma-Aldrich, Australia
Glucose syrup	-	-	-	8029-43-4	Edlyn Foods Pty. Ltd., Australia
Amberlite® IR-120 resin, hydrogen form	-	-	-	39389-20-3	Supelco, USA

Table 2.7 List of reagent and other materials (cont.)

Reagent/material	Formula	Molecular mass	Purity (%)	CAS Number	Supplier
Silicone Oil	$[-Si(CH_3)_2O-]n$	-	-	63148-62-9	BDH, Chemicals Pty. Ltd., Australia
Cellulose tubing for dialysis	-	-	-	-	Sigma, Germany
Millipore water	H_2O	18.02	-	-	Millipore Pty. Ltd., Australia

2.3 SAMPLE AND REAGENT PREPARATION

2.3.1 High-solid polysaccharide/cosolute matrices

Composite matrices of pectin/polydextrose and κ-carrageenan/glucose syrup were prepared at 80 and 85% (w/w) total solids, respectively. In doing so, pectin powder or κ-carrageenan in potassium form (7.8% w/w) were dissolved in Millipore water at 90°C with constant stirring on a hot plate, and then the temperature was reduced to approximately 70°C. Known amounts of cosolutes were solubilised separately in water and carefully mixed with the polymer solutions at the same temperature. The final levels of solids were adjusted with the addition of the known amount of ascorbic acid or thiamin solutions at 30°C. The pH of the former was fixed to 3.0 using 0.2 M HCl solution and for the latter to 4.5 using 50 mM potassium dihydrogen phosphate buffer solution in order to produce the required gelling conditions for experimentations and maintain the bioavailability of vitamins. Samples were kept overnight at 4°C to facilitate equilibration.

2.3.2 Spray dried microcapsules

Wall materials (whey protein or modified waxy maize starch) were dispersed in Millipore water. The starch solution was heated at 70°C for 15 min, and then both biopolymer solutions were stored in a refrigerator overnight. Premix-vitamin solution was prepared as follows: (i) nicotinic acid was hydrated in a phosphate buffer solution at pH 6.5; and (ii) tocopheryl acetate was dissolved in absolute ethanol treated with homogenisation. The feed solutions were steadily mixed with a magnetic bar throughout the dehydration process, which was facillitated by a spray dryer. Working operating conditions were set at: diameter of a nozzle (0.5 mm), liquid flow 8.5 ml/min for nicotinic acid/whey protein solutions and 7.5 ml/min for tocopheryl acetate/maize starch, a controlled air pressure of 250 kPa, inlet and outlet air temperatures were 120 and 75°C, respectively. The powder was collected in amber bottles and then chilled for 16±2 h in a refrigerator before analysis.

2.3.3 Reagent preparations

2.3.3.1 DNPH solution

This was dissolved by heating of 2 g DNPH dissolved in 100 ml 0.5 N sulfuric acid and filtered before use, to give a final concentration of 2% DNPH (Rajan, 2011).

2.3.3.2 ABVR solution

ABVR (0.2 g) was dissolved in 100 ml Millipore water in a volumetric flask (0.2% ABVR) (Prasad, Rajasree, Khan, & Narayana Reddy, 1997).

2.3.3.3 Cyanogen bromide solution

Cyanogen bromide (10 g) was added to 80 m1 of warm water (40°C) in a large flask. The solution was shacken until it was fully dissolved, cooled, diluted to 100 ml and stored in a refrigerator **(**Deutsch, 1984).

2.3.3.4 SPV solution

Vanillin (3 g) was dissolved in 0.5 g Millipore water and diluted to a mark in a 2 l beaker using concentrated phosphoric acid and mixing vigorously. SPV reagent was stored in a refrigerator for up to one month (Paramita, Bannikova, & Kasapis, 2015).

2.3.3.5 Bromine solution

Addition of 30 ml of 5.25% sodium hypochlorite to a solution of 5.07 g of potassium bromide in 42 ml of 1 N hydrochloric acid and 28 ml Millipore water was used to prepare an aqueous solution of bromine of 3.4 g/100 ml. The procedure was performed in a working fume hood to minimise exposure to poisonous chlorine gas and bromine vapor. The resultant solution was not stored but rater prepared freashly as required.

Three equations of the halogen displacement reactions were used, as follows (Hiegel, Abdala, Vincent Burke, & Beard, 1987).

$$NaClO\ (aq) + 2HCl\ (aq) \longrightarrow Cl_2\ (g) + NaCl\ (aq) + H_2O\ (l) \quad (2.2)$$

$$Cl_2\ (g) + 2KBr\ (aq) \longrightarrow 2KCl\ (aq) + Br_2\ (aq) \quad (2.3)$$

$$2KBr\ (aq) + NaClO\ (aq) + 2HCl\ (aq) \longrightarrow Br_2\ (aq) + 2KCl\ (aq) + NaCl\ (aq) + H_2O\ (l) \quad (2.4)$$

2.3.3.6 Sulphanilic acid solution

Ammonium solution was added dropwise to a mixture of 20 g sulfanilic acid and 120 ml Millipore water until sulfanilic acid was dissolved. Then the pH was optimised to 4.5 with a solution hydrochloric acid and water (1+1) and the resultant the solution was diluted to 200 ml **(**Deutsch, 1984).

2.3.3.7 Sodium dihydrogen phosphate buffer solution

Sodium dihydrogen phosphate monohydrate (13.80 g) was dissolved in 900 ml of Millipore water. The pH was adjusted using a 400 g/l solution of sodium hydroxide. The final preparation was diluted to 1000 ml with Millipore water (European Pharmacopoeia, 2013).

2.3.3.8 Potassium dihydrogen phosphate buffer solution

Potassium dihydrogen phosphate (6.80 g) was dissolved in 1l of Millipore water. The pH of 0.05 M phosphate buffer solution is 4.5 (European Pharmacopoeia, 2013).

2.4 EXPERIMENTAL METHODS

2.4.1 Molecular dynamics of biopolymers

For 80% (w/w) total solids pectin/polydextrose and 85% (w/w) total solids κ-carrageenan/glucose syrup mixtures were evaluated molecular dynamics of composite gel matrices using thermal and rheological measurements. For MDSC analyses, a weighted amount of samples (10 mg) was sealed in an aluminium pan and then subjected to a reverse scan by cooling from 20 to -90°C and heating to the initial temperature at a controlled ramp rate of 1 °C/min. A difference in heat flow signals (W/g) of sample pan and an empty pan was reported including a mid-point T_g.

Small deformation dynamic oscillation in shear was used to develop the viscoelastic components (G' and G'') of the gel network as a function of time and frequency of oscillation. Experiments were performed on a rheometer and samples were placed on the preheated plate at a temperature of 70-80°C. A geometry of 5 mm diameter was applied within the experimental temperature scope. Molten preparations were cooled beyond sub-zero temperatures at 1°C/min with a fixed frequency of 1 rad/s and strains of 0.01% (pectin/polydextrose matrix) or 0.1% (carrageenan/glucose syrup matrix) that was recorded within the LVR region. The rheological T_g was derived from the TTS principle and WLF/modified Arrhenius equations.

Effect of spray drying on a molecular structure of protein and starch micro capsules was evaluated by DSC. A resuspended solution made up at 10% (w/w) total solids of microcapsules was heated from 20 to 85°C with a ramp rate of 1°C/min and then maintained at the highest temperature for 20 min. The initial, mid and end-point temperatures and enthalpy changes of endotherms (J/g) were calculated in order to probe protein denaturation and a starch gelatinisation.

DMA measurements of protein and starch microcapsules were carried out to obtain a sinusoidal force resulting from a small deformation as a function of temperature. Viscoelasticity, force and the phase shift were performed in tension or compression mode at a scan rate of 2°C/min in the range of -100 to 140° C. The measured parameters were collected at a frequency and a strain of 1 Hz and 0.025%, respectively.

2.4.2 Dynamic vitamin release studies

For studies of vitamin release, temperatures were carfully controlled. Preweighed sample of gel matrices and microcapsules as well as the organic solvents were equilibrated in either the thermostatted waterbath or the freezer. A known amount of a high-solid gel or microcapsule with vitamin was transferred to a beaker and rounded with aluminium foil to avoid an exposure to light. Following equilibration for 30 min (in the waterbath) or overnight (in the freezer), the solvents in test tubes and samples were incubated at the observation temperature of interest. The solvent portion was poured swiftly to the beakers then the beakers were promptly closed with parafilm sheet to prevent solvent evaporation and returned to the observation temperature for immediate sampling of an aliquot thus setting the initial time of the experiment. Subsequently aliquots were taken, as follows: (i) ascorbic acid within 60 min for the temperature range of -30 to 20°C; (ii) thiamin within 90 min for the temperature range of -22 to 22°C; (iii) nicotinic acid within 60 min for the

temperature range of 15 to 90°C; and (iv) tocopheryl acetate within 30 min for the temperature range of -30 to 70°C.

Vitamin release from the high-solid matrices to the respective solvents was recorded in the form of absorbance using colorimetric methods and the spectrophotometer. The methods were based on reactions between ascorbic acid and 2,4 DNPH in ethanol (λ_{max}= 521 nm), formation of a coloured thiamin/ABVR complex in ethylene glycol (λ_{max}= 575 nm), the König reaction of nicotinic acid, cyanogen bromide and sulfanilic acid in DMSO (λ_{max}= 450 nm), and the reaction between tocopheryl acetate and SPV reagent in ethanol (λ_{max}= 525 nm) as shown in Fig. 2.14. A Calibration curves were constructed by dissolving vitamin in the appropriate solvents at particular concentrations and the same assay was applied for absorbance measurement as for the diffusion studies.

2.4.3 High-solid matrices structural analysis

Structural analysis of high-solid gels and spray dried powder was performed by a series of techniques including FTIR spectroscopy, SEM and WAXD. FTIR spectroscopy was employed to pinpoint molecular interactions and chemical functional groups by scanning within the wavenumber range of 4000-650 cm^{-1}. The crystalline and amorphous structure was examined using a diffractometer between 5° and 90° (2θ) at ambient temperature. Morphology of gold coated samples was observed by SEM in high-vacuum mode at different magnifications. For microcapsules, physicochemical measurements of particle size distribution, moisture content, water activity and colour profiles were also determined.

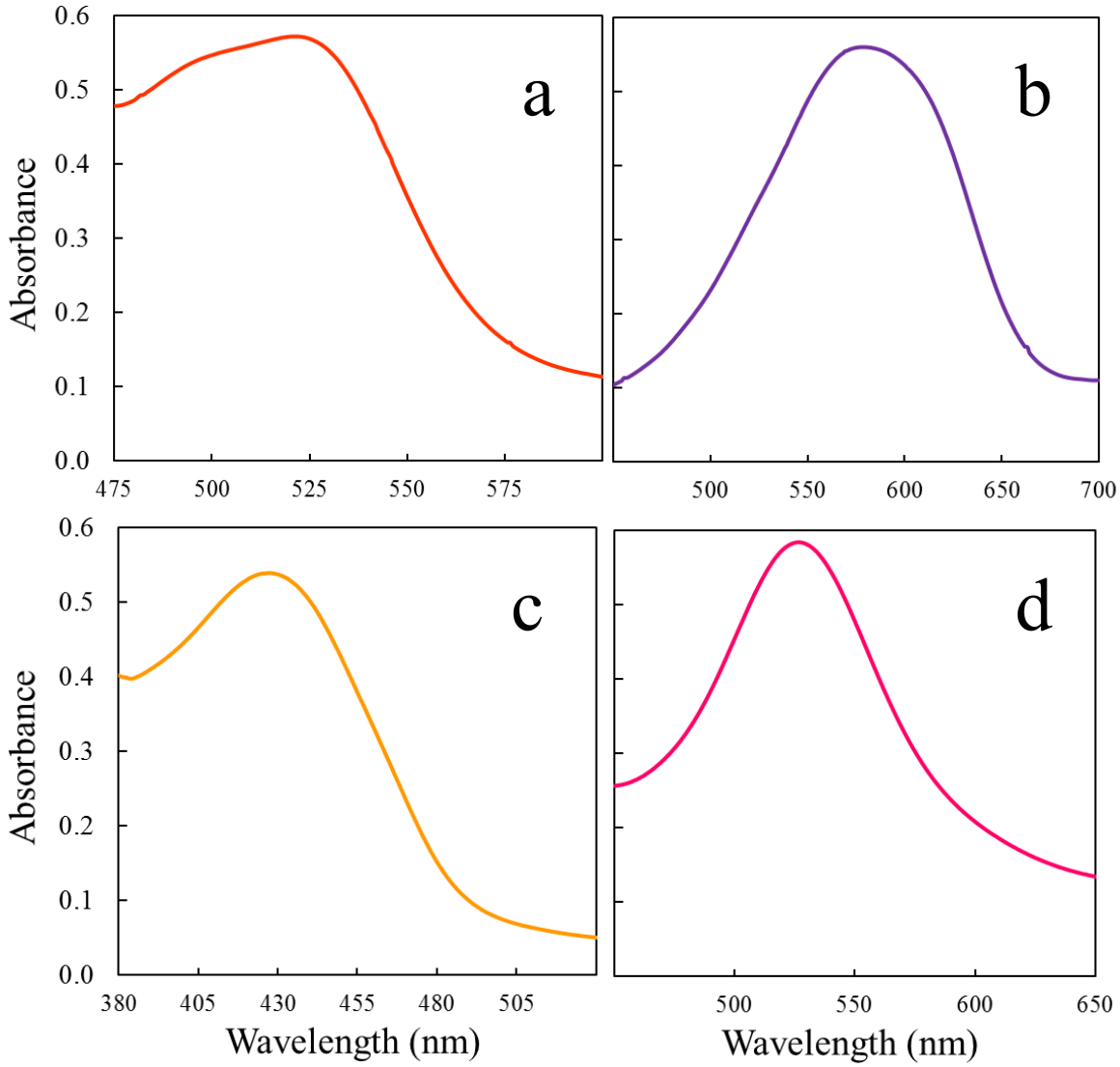

Fig. 2.14 Visible absorbance spectra of vitamin analysed with dye-binding assay based on (a) the chemical reactions between ascorbic acid and 2,4 DNPH in ethanol (λ_{max}= 521 nm), (b) formation of a coloured ion-pair complex between thiamin and ABVR in ethylene glycol (λ_{max}= 575 nm), (c) the König reaction of nicotinic acid, cyanogen bromide and sulfanilic acid in DMSO (λ_{max}= 450 nm), and (d) the reaction between tocopheryl acetate and SPV reagent in ethanol (λ_{max}= 525 nm)

CHAPTER 3

DIFFUSION KINETICS OF ASCORBIC ACID IN A GLASSY MATRIX OF HIGH-METHOXY PECTIN WITH POLYDEXTROSE

Panyoyai, N., Bannikova, A., Small D. M., & Kasapis, S. (2016). Diffusion kinetics of ascorbic acid in a glassy matrix of high-methoxy pectin with polydextrose. *Food Hydrocolloids, 53,* 293-302. *(IF 4.09)*

School of Science

Chapter Declaration for Thesis with Publications

Chapter 3 is presented by the following paper:

[Diffusion kinetics of ascorbic acid in a glassy matrix of high-methoxy pectin with polydextrose]

[Naksit Panyoyai, Anna Bannikova, Darryl M. Small, & Stefan Kasapis]

[Food Hydrocolloids]

[53, 293-302]

[2016]

Declaration by candidate

I declare that I wrote the initial draft of this manuscript, and my overall contribution to this paper is detailed below:

Nature of contribution	**Extend of contribution (%)**
(1) Performed all experiments (2) Collected and calculated all of the data (3) Interpreated the results including a repetition (4) Implemented the mathematical models and plotted graphs	70

The following co-authors contributed to the work. The undersigned declare that the contributions of the candidate and co-authors are correctly attributed below.

Author	**Nature of contribution**	**Extent of contribution (%)**	**Signature**
Anna Bannikova	(1) Designed the experiments (2) Assisted to carry out the thermal and rheological measurements (3) Partially interpreated the results (4) Edited the first draft	5	
Darryl M. Small	(1) Designed the vitamin analysis (2) Commented on the second draft	5	
Stefan Kasapis	(1) Supervised the project (2) Edited the final draft (3) Approved the manuscript	20	

Candidate's Signature date		**Date** 14/01/2016
Primary Supervisor's Signature		**Date** 18/01/2016

Food Hydrocolloids 53 (2016) 293–302

Contents lists available at ScienceDirect

Food Hydrocolloids

journal homepage: www.elsevier.com/locate/foodhyd

Diffusion kinetics of ascorbic acid in a glassy matrix of high-methoxy pectin with polydextrose

Naksit Panyoyai, Anna Bannikova, Darryl M. Small, Stefan Kasapis*

School of Applied Sciences, RMIT University, City Campus, Melbourne, Vic 3001, Australia

ARTICLE INFO

Article history:
Received 27 May 2014
Accepted 15 July 2014
Available online 22 July 2014

Keywords:
High-methoxy pectin
Polydextrose
Ascorbic acid
Glass transition temperature
Diffusion kinetics

ABSTRACT

The relative mobility of ascorbic acid incorporated in a condensed matrix of high-methoxy pectin (HMP) and polydextrose is reported. Physicochemical and structural characterisation of the high-solid systems utilised modulated differential scanning calorimetry, small deformation dynamic oscillation in shear, scanning electron microscopy, Fourier transform infrared spectroscopy and wide angle X-ray diffraction. Theoretical modeling of the thermomechanical measurements demonstrated that the mechanism of free volume governs stress relaxation phenomena of the polymeric system through the process of vitrification yielding the mechanical glass transition temperature. Combination of UV-vis spectrophotometry and a vitamin-dye binding method was employed to follow for 60 min the diffusion process of ascorbic acid from the concentrated HMP/polydextrose matrix to the absolute ethanol phase throughout the temperature range of −30 to 20 °C. A relatively low estimate of activation energy for the diffusion of vitamin C reflects its freedom of mobility and high free volume, as compared to the relaxation of the polymeric system that exhibits strong temperature dependence in the glass transition region. Utilisation of the concept of diffusion coefficient sheds further light into the relationship between free volume of the polymeric system and diffusional mobility of the micronutrient.

1. Introduction

Glass transition describes the passage from a hard and brittle material to a melt during heating or the reverse transformation to a supercooled liquid upon rapid cooling (Le Meste, Champion, Roudaut, Blond, & Simatos, 2002). Under these conditions, molecules are unable to rearrange themselves into a crystalline form but become "frozen" with very high viscosity that limits molecular mobility (Nelson & Labuza, 1994; Rahman, 2010). The concept of glass transition temperature (T_g) has been proposed to control the rates of chemical, enzymatic and biological processes below which these are thought to proceed extremely slowly hence providing an index of quality assessment (Liu, Bhandari, & Zhou, 2006).

Differential scanning calorimetry (DSC) has been used extensively in the past to monitor the enthalpic relaxation of a wide range of small-molecule biomaterials (Liu, Yu, Liu, Chen, & Li, 2009). More recently, mechanical spectroscopy has been used to assess the vitrification properties of hydrocolloid networks in the presence of high levels of co-solute (Ferry, 1980; Kasapis, 2004). The concept of "network T_g" has been introduced to describe the viscoelastic properties of these systems from the rubbery to the glassy state as a function of temperature and time of observation (Kasapis, 2006).

The desire to improve the stability and quality of processed foods, where chemical reaction pathways and enzymatic processes are critical considerations, initiated studies in the molecular dynamics of bioactive compounds at the vicinity of T_g (Bell & Hageman, 1994; Liu et al., 2006). Caffeine has been incorporated in condensed carbohydrate matrices to examine their stability and controlled release in relation to the vitrification properties of the matrix (Jiang & Kasapis, 2011). Work has been extended to encompass the activity of an enzyme, α-D-glucosidase, on the substrate, 4-nitrophenyl α-D-glucopyranoside (pNPG), while embedded in a glassy carbohydrate matrix (Chaudhary, Small, & Kasapis, 2013). Both investigations demonstrated that the free volume of the condensed matrix is a determining parameter of biofunctionality in these innovative mixtures.

It has long been known that ascorbic acid has a protective role as an antioxidant in various foods and dietary supplements. However, it is unstable in air, light, oxygen, moisture, basic pH conditions, and high temperature being easily degradable from the biologically

* Corresponding author. Tel.: +61 3 992 55244; fax: +61 3 992 55241.
E-mail addresses: stefan.kasapis@rmit.edu.au, stefankasapis@hotmail.com (S. Kasapis).

http://dx.doi.org/10.1016/j.foodhyd.2014.07.016
0268-005X/

active substance (L-ascorbic acid and dehydroascorbic acid) to 2,3-diketogulonic acid, which has no biological activity in the human body (Ottaway, 1993). The biological activity of vitamin C is preserved to a good extent when delivered within a polymeric matrix using, for example, spray drying techniques (Desai & Park, 2005; Velikov & Pelan, 2008; Wijaya, Small, & Bui, 2011).

The present investigation attempts to provide fundamental understanding on the kinetics of diffusional mobility of vitamin C in condensed matrices of high-methoxy pectin and polydextrose. HMP is a major polysaccharide for industrial application, with polydextrose being a relatively low molecular weight and glycemic content material. The latter facilitates engineering of high solid matrices and polysaccharide network formation. In this investigation, therefore, HMP contributes structure to the mixture and polydextrose is the polydisperse, hence non-crystalline co-solute that is effectively free of caloric content. Theoretical concepts from synthetic polymer and drug delivery science are employed to ascertain the molecular processes controlling the mobility of the bioactive compound at the vicinity of the glass transition temperature.

2. Materials and methods

2.1. Materials

2.1.1. Polydextrose

The material used was a product from Tate and Lyte (IL, USA). The purity of the powder was 90% with 4% moisture content and has passed the microbiological testing under the food grade standards.

2.1.2. High-methoxy pectin (HMP)

The citrus pectin was purchased from Sigma–Aldrich Co (Sydney, Australia). The content of polysaccharide was 93.3% on dry weight basis of which 86.3% is galacturonate with a degree of methyl esterification (DE) of 60–65%. Chromatographic analysis carried out by the supplier, produced a number average molecular weight (M_n) for the material of 154 kDa.

2.1.3. Ascorbic acid

L-ascorbic acid [$C_6H_8O_6$, molecular weight of 176.12 g/mol] was obtained from Sigma–Aldrich Co, as above. The material was in the form of white crystal with an analytical grade of more than 99% purity.

2.1.4. Absolute ethanol

It was purchased as an analytical grade reagent (assay 99.5%) from Sigma–Aldrich Co. Absolute ethanol is widely used as a solvent in organic chemistry, since it is less harmful than other organic solvents to dissolve ascorbic acid (Shalmashi & Eliassi, 2008). The freezing point of absolute ethanol can be as low as −110.5 °C (Mellan, 1977), which facilitates its utilization in the current experimental temperature range of −30 to 20 °C.

2.1.5. Ascorbic acid analytical reagents

2,4-dinitrophenylhydrazine (2,4-DNPH), thiourea, sodium hypochlorite solution, hydrochloric acid and sulfuric acid were supplied from Sigma–Aldrich Co, while metaphosphoric acid and potassium bromide were obtained from BDH Chemicals (Poole, England). All reagents were used without further purification. A saturated solution of bromine water was prepared using the halogen displacement reactions method by mixing 5.25% sodium hypochlorite to a solution of potassium bromide in 1 N hydrochloric acid and Millipore water (Hiegel, Abdala,Vincent & Beard, 1987).

2.2. Sample preparation

The polysaccharide solution was prepared by dissolving the powder in Millipore water at 90 °C with constant stirring on a hot plate, and then the temperature was dropped to 75 °C. Polydextrose powder was dissolved separately in water and added to the polymer solution at the same temperature. At that stage, the total level of solids was higher than the required final concentration but that was adjusted with the addition of the ascorbic acid solution at 30 °C to yield the experimental concentration of 2% (w/w) high-methoxy pectin with 77.6% (w/w) polydextrose and 0.4% (w/w) ascorbic acid. The pH of the system was also adjusted to 3.0 using 0.2 M HCl solution to create the required gelling conditions for experimentation and maintain the bioavailability of ascorbic acid. Care was taken to dissolve the ascorbic acid in Millipore water in an amber glass bottle. Beakers with final preparations were wrapped in aluminium foil, and the top was sealed with a stretchable laboratory film to prevent exposure to light. The above tertiary sample was used for the study of the diffusional mobility of vitamin C in the glass transition region. Other samples made in a similar manner for the remaining experimentation included single systems of 80% polydextrose, and mixtures of 2% HMP with 78% polydextrose or 2% HMP with 76% polydextrose and 2% vitamin C (w/w).

2.3. Experimental analysis

2.3.1. Modulated differential scanning calorimetry

Thermal measurements were performed using Q 2000 (TA instruments, New Castle, DE), which includes a refrigerated cooling system (RCS 90) to achieve temperatures down to −90 °C. Nitrogen was used to purge the DSC cell at the flow rate of 50 mL/min. Calibration of the heat flow signal was performed with a traceable indium standard (ΔH_f = 28.3 J/g) and for the heat capacity we used a sapphire standard. Samples were loaded in hermetic aluminium pans and an empty pan served as a reference. Ten milligrams of our material was sealed in the pan and cooled from 20 to −90 °C at the ramp rate of 1 °C/min followed by heating to 20 °C at the same scan rate. Modulated amplitude of 0.53 °C for every 40 s was applied throughout, and all measurements were performed in triplicate yielding effectively overlapping traces.

2.3.2. Rheological analysis

Small deformation dynamic oscillation in shear was used to provide readings of the elastic (G'; storage modulus) and viscous (G'', loss modulus) components of the network. These two parameters are part of the complex shear modulus ($G^* = G' + iG''$), and variations of the relative liquid-like and solid-like structure of the material with time and temperature can be further assessed with the tan δ (G''/G'). Measurements were executed on AR-G2 (TA instruments, New Castle, DE), a controlled strain rheometer with magnetic thrust bearing technology.

Samples of high-methoxy pectin and polydextrose with a total solids content of 80% (w/w) were loaded on the preheated Peltier plate at 70 °C. The exposed edge of the plate was covered with silicone oil from BDH (50 cS) to minimize moisture loss, and a measuring geometry of 10 mm diameter was used within the experimental temperature range. Molten preparations of pectin and polydextrose were cooled from 70 to −60 °C at 1 °C/min with a frequency of 1 rad/s and a strain of 0.01% that was within the linear viscoelastic region of our material. Frequency sweeps were performed at temperature intervals of 4 °C within the range of 0.1–100 rad/s.

2.3.3. Fourier transform infrared spectroscopy

Readings were obtained from a Perkin Elmer Spectrum 100 using ZnSe single reflection ATR plate (Perkin Elmer, Norwalk, CT). Samples of high-methoxy pectin, polydextrose, ascorbic acid and their combinations were analysed to identify the nature of molecular interactions between the three constituents. Absorbance spectra were recorded continuously within the range of 600–4000 cm^{-1} at an average scan number of 8 and a resolution of 4 cm^{-1}. Each measurement was performed in triplicate.

2.3.4. Wide angle X-ray diffraction

Diffractograms were obtained using a D8 Advanced Bruker AXS (Karlsruhe, Germany) attached with Cu-Kα radiation (1.54 Å) source. Freeze dried samples of high-methoxy pectin, polydextrose, ascorbic acid crystals and their combinations were scanned under accelerating voltage and current of 40 kV and 40 mA, respectively. Raw data were obtained within a 2θ range of 5° and 90° and analysed using, DIFFRAC^{plus} Evaluation (Eva), version 10.0 revision 1, which is a Bruker Advanced X-ray Solutions software. Measurements were performed in triplicate.

2.3.5. Scanning electron microscopy

Micrographs of single preparations of high-methoxy pectin, polydextrose and ascorbic acid, and mixtures thereof were obtained using Philips XL30 SEM (Sussex, England). Freeze dried samples were attached to sample holders followed by gold plating. A high vacuum mode and an accelerating voltage of 20 kV were used to produce microscopic images of single and mixed preparations in these conductive samples, thus assisting in the characterisation of network morphology.

2.3.6. Kinetic study of diffusional mobility

Four grams of our preparation with 0.4% (w/w) vitamin C were transferred into twelve 25 mL beakers (overall thirty six replicates per experimental temperature) wrapped with aluminium foil to prevent exposure to light. The thickness and diameter of the sample in the beaker were 5 and 25 mm, respectively. Care was taken to obtain a smooth surface without any bubble formation following sample transfer to the beaker. These materials and separate 4 mL of absolute ethanol in test tubes were kept overnight at the experimental temperature of interest for equilibration. Following this, the ethanol portion was poured swiftly to the beakers as a separate phase on top of the sample; ethanol is immiscible in the HMP/polydextrose system. The beakers were promptly sealed with a stretchable laboratory film to prevent solvent evaporation and returned to the measuring temperature for immediate removal of an aliquot thus setting the zero time of experimentation. Subsequent aliquots were obtained up to 60 min at intervals of 5 min for each experimental temperature, i.e. 20, 15, 10, 5, 0,−5,−10,−15,−20,−25 and −30 °C.

Diffusion of ascorbic acid from the high-solid matrix to absolute ethanol was determined colourimetrically in the form of absorbance using 2,4 dinitrophenylhydrazine method and a Lambda 35 UV-vis spectrophotometer (Perkin Elmer, MA, Singapore). For this, 1 mL of ascorbic-acid containing absolute ethanol was taken from the aliquot and a few drops of 5% metaphosphoric acid were added to optimise the acidic conditions to a pH value of 3.5. Then, 1 mL bromine water was added in order to oxidise the ascorbic acid to its dehydro form. A few drops of 10% thiourea were added to remove the excess of bromine and stabilise the oxidised ascorbic acid, thus converting the yellow bromine water into a colourless solution. One millilitre of 1% 2,4-DNPH solution was added with continuous stirring and the ensuing reaction was completed by incubating the samples at 37 °C for 3 h in a thermostatic water bath (Thermoline, Australia). Preparations were cooled in an ice bath followed by treatment with 2 mL of 85% sulfuric acid to generate orange-red colour for further analysis.

The resultant orange-red ozazone solution was poured into 1 cm glass cell to read the maximum absorbance ($\lambda_{max} = 521$ nm); colour intensity remains constant within 5 h of measurement at ambient temperature. High-methoxy pectin/polydextrose preparations at 80% (w/w) solids without ascorbic acid served as the control. A calibration curve was constructed from an absolute ethanol solution containing ascorbic acid concentrations of 0.0005–0.003% by taking the corresponding λ_{max} readings. Experiments were carried out in three replicates, and average values are reported.

3. Results and discussion

3.1. Estimation of the calorimetric glass transition temperature for single and mixed high-methoxy pectin/polydextrose systems

Molecular rearrangements in high-solid systems undergoing a glass transition can be monitored with differential scanning calorimetry, a technique that measures energy inputs into a substance as a function of temperature to provide its heat flow characteristics (Champion, Le Meste, & Simatos, 2000). The glass transition region of the material can be demarcated by the onset (T_{gi}), mid-point (T_{gp}) and endset (T_{ge}) temperatures of the sigmoidal change in heat capacity. In the present study, we hydrated single polydextrose systems, and mixtures of high-methoxy pectin and polydextrose with or without ascorbic acid to a total solid content of 80%, with the HMP concentration being fixed at 2%.

Fig. 1 reproduces thermograms obtained for our condensed systems at a relatively low scan rate of 1 °C/min. Continuous and sigmoidal variation in the signal of heat flow yields a relatively broad transition that is considered as a pseudo-equilibrium relaxation response to the changing calorimetric regime (Almrhag, George, Bannikova, Katopo, & Kasapis, 2012). The mid-point T_g of the single polydextrose, HMP/polydextrose with 2 and 0.4% or without ascorbic acid was calculated to be at −44.8, −42.9, −43.5 and −43.8 °C, respectively. At this fixed moisture content of 20%, ice formation was avoided, and the reversible concept of vitrification could be identified as the governing molecular mechanism. Clearly, there was no significance change in the glass transition patterns of

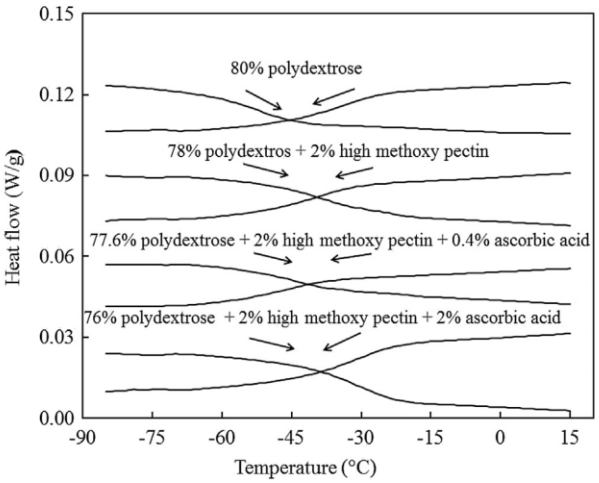

Fig. 1. Variation of heat flow as a function of temperature for 76% polydextrose plus 2% high-methoxy pectin with 2% ascorbic acid, 77.6% polydextrose plus 2% high-methoxy pectin with 0.4% ascorbic acid, 78% polydextrose with 2% high-methoxy pectin, and 80% polydextrose alone obtained using MDSC at a scan rate of 1 °C/min.

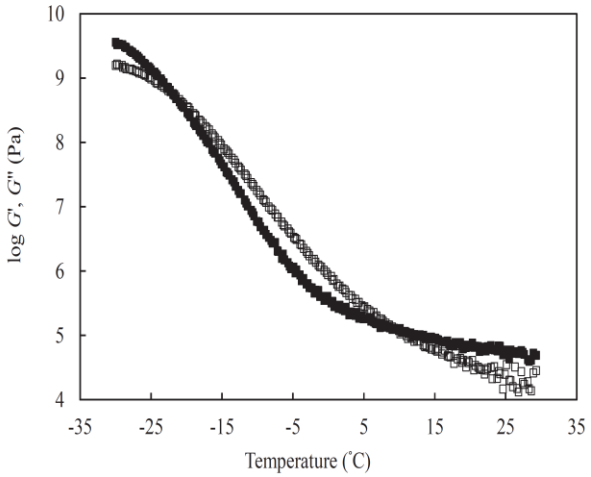

Fig. 2. Cooling profiles of storage (G', ■) and loss (G'', □) modulus as a function of temperature for 78% polydextrose with 2% high-methoxy pectin (0.2 M HCl, pH 3) scanned at a rate of 1 °C/min, frequency of 1 rad/s and strain of 0.01%.

the single, binary and tertiary systems of this investigation. A similar conclusion regarding the calorimetric glass transition temperature was reached when 0.4% caffeine was added to high-solid carbohydrate mixtures (Kasapis & Shrinivas, 2010).

3.2. Viscoelastic behaviour of high-methoxy pectin/polydextrose matrices as high level of solids

Calorimetric measurements in the preceding paragraph established a baseline of glass transition behaviour in preparations of this investigation. This section takes the work forward by employing mechanical measurements that focus on the macromolecular properties, i.e. network characteristics of high-methoxy pectin/polydextrose mixtures. Fig. 2 reproduces the variation in storage (G') and loss (G'') moduli for the condensed material, which shapes up three thermal regions, i.e. rubbery plateau, glass transition region and glassy state during cooling. Modulus values increase almost six orders of magnitude from about 10^4 Pa in the rubbery plateau to $10^{9.5}$ Pa at the end of the glassy state. The viscous component predominates between 10 and −20 °C, which is one of the fingerprints of the glass transition region in amorphous polymer mechanics.

Further resolution of the time and temperature contributions to the linear viscoelasticity of the 2% HMP/78% polydextrose mixture can be achieved using the time–temperature superposition principle (TTS). The approach produces a set of shift factors (a_T) from the horizontal superposition of isothermal mechanical data to obtain a single master curve of viscoelasticity, and an example of its implementation is as follows (Nickerson, Paulson & Speer, 2004): Measurements of G' and G'' were taken within the frequency range of 0.1–100 rad/s at regular temperature intervals of 4 °C, as shown in Fig. 3(a and b). Mechanical spectra of both storage and loss modulus have been relatively flat at the low range of temperatures (e.g. −30 °C in the glassy state), whereas a steep rise in viscoelasticity with increasing frequency is observed in the glass transition region (e.g. −2 °C).

These were superposed horizontally by choosing an arbitrary reference temperature within the glass transition region ($T_o = -15$ °C) to yield a composite (master) curve of viscoelasticity in Fig. 4a. For both normalized moduli (G'_p and G''_p), a ten-decade window of reduced frequency from 10^{-6} to 10^4 rad/s was obtained. The entirety of the glass transition region is recorded at normalised frequencies between 10^{-4} and 10^2 rad/s where the values of G''_p exceed those of G'_p. This master curve obtained here is the time (or frequency) analogue of the temperature profile discussed in the master curve in Fig. 2.

To impart physical significance to the mechanical data in the glassy state and rubbery plateau of the high solid preparations in Fig. 4a, we opted to utilise the predictions of the Arrhenius rate law. This advocates that the reaction rate is proportional to exp (E_a/RT), with E_a being the activation energy of a molecular process, and is expressed as follows (Chaudhary et al., 2013):

$$\log a_T = \frac{E_a}{2.303R}\left(\frac{1}{T} - \frac{1}{T_o}\right) \quad (1)$$

where, R is the universal gas constant. As illustrated in Fig. 4b for the factor a_T, this type of analysis produces a straight line with the linear gradient reflecting constant activation energies of 189 and 203 kJ/mol for the rubbery and glassy state, respectively. It confirms that relaxation processes are heavily controlled by specific physicochemical processes leading to molecular mobility from one conformational state to another.

We also found that within the glass transition region, progress in viscoelasticity is not compliant with the predictions of the reaction rate theory but, instead, it can be modeled by the framework

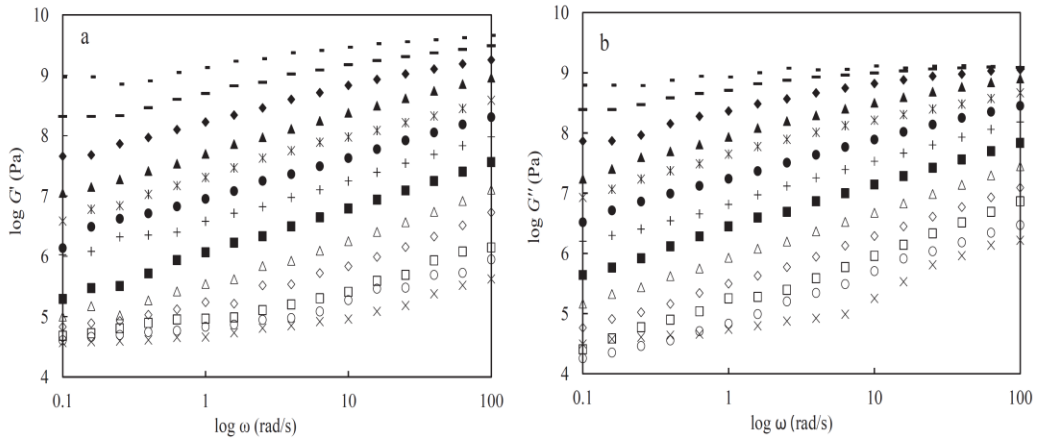

Fig. 3. Frequency variation of G' (a) and G'' (b) for 78% polydextrose with 2% high-methoxy pectin (0.2 M HCl, pH 3). The bottom curve was taken at 22 °C (×), other curves successively upwards: 18 (○), 14 (□), 10 (◊), 2 (Δ), −2 (■), −6 (+), −10 (●), −14 (*), −18 (▲), −22 (◆), −26 (−) and −30 (-) °C.

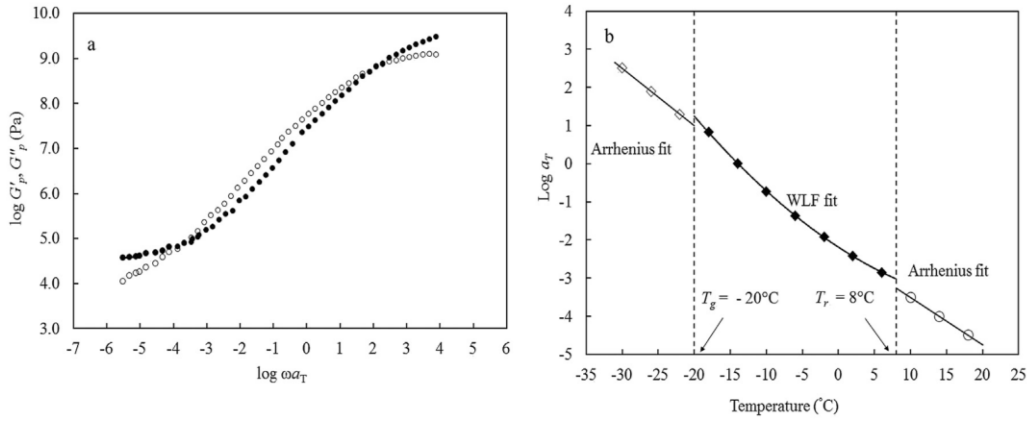

Fig. 4. (a) Master curve of reduced shear modulus (G'_p, ●; G''_p, ○) for 78% polydextrose with 2% high-methoxy pectin (0.2 M HCl, pH 3) as a function of reduced frequency of oscillation (ωa_T) based on the frequency sweeps of the previous figure and utilising a reference temperature of −15 °C, and (b) logarithmic shift factors a_T as a function of temperature for this sample within the rubbery plateau (○), glass transition region (◆) and glassy state (◊), with the solid lines reflecting the WLF and modified Arrhenius fits of the shift factors, and dash lines pinpointing the T_g and T_r predictions.

of free volume. This predicts that free volume collapses from about 30% in the rubbery plateau to 3% in the glassy state thus making it the overriding process of molecular dynamics in the glass transition region. Williams, Landel and Ferry have innovated with the following mathematical expression to describe this (van der Put, 2010):

$$\log a_T = \log[G'(T)/G'(T_o)] = -\frac{(B/2.303f_o)(T - T_o)}{\left(f_o/\alpha_f\right) + T - T_o} \quad (2)$$

where, f_o is the fractional increase in free volume at T_o (or f_g at T_g), α_f is the thermal expansion coefficient, and B is usually set to one.

The conjunction of the free volume and modified Arrhenius predictions for the shift factors generated by the horizontal superposition of our mechanical data can be considered as the mechanical or network glass transition temperature, $T_g = -20$ °C (Fig. 4b). Parameters of this framework of thought include the fractional free volume at T_o ($f_o = 0.044$) and T_g ($f_g = 0.040$), the thermal expansion coefficient, $\alpha_f = 8 \times 10^{-4}$ deg^{-1}, and the temperature of the rubbery plateau ($T_r = 8$ °C) that bears an f_o value of 0.061. Estimates are in accordance to experience (Almrhag et al., 2012), indicating the influence of HMP network on the mechanical manifestation of vitrification, as compared with the predictions of the calorimetric T_g in Fig. 1.

3.3. Molecular interactions leading to tangible evidence of network morphology in HMP/polydextrose systems

Fourier transform infrared spectroscopy (FTIR) was used to examine the nature of molecular forces in single systems and mixtures of this investigation. Fig. 5a illustrates a variety of molecular events that correspond to specific chemical linkages including O–H stretching vibrations at 3681–2900 cm^{-1}, and esterified (COO–R) along with non-esterified (COO$^-$) carbonyl groups at 1576–1500 cm^{-1} (Monsoor, Kalapathy, & Proctor, 2001). Polydextrose, as a highly branched glucose polymer, produces reference peaks of C–O–C glycosidic linkages (1180–927 cm^{-1}), C–O stretching and bending at 1493–1173 cm^{-1}, C=O stretching of aldehyde at 1621 cm^{-1}, and C–H stretching along with O–H stretching vibrations at 3652–2843 cm^{-1} (Míčková, Čopìková, & Synytsya, 2007). These profiles indicate that addition of ascorbic acid to concentrated high-methoxy pectin/polydextrose systems did not lead to the development of covalent interactions thus

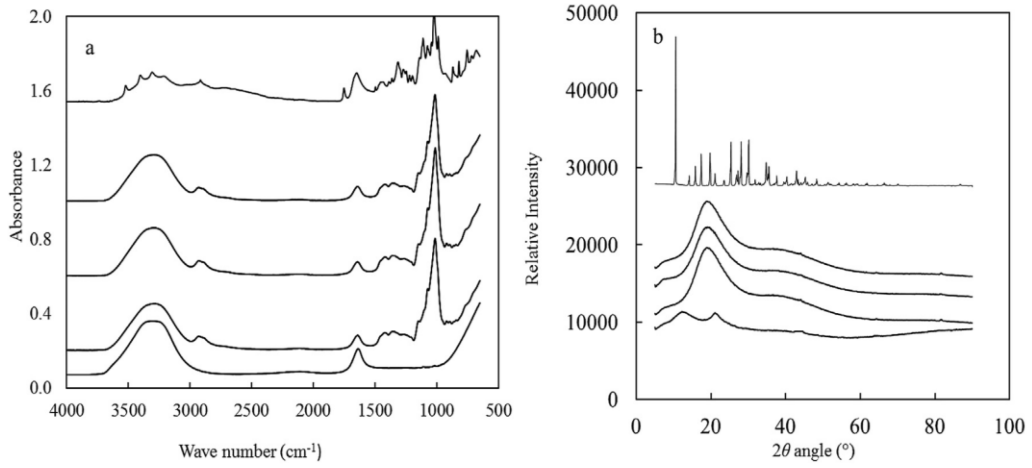

Fig. 5. (a) FTIR spectra and (b) X-ray diffractograms for 2% high-methoxy pectin with 0% and 78% polydextrose in mixture, an 80% single polydextrose preparation, 2% high-methoxy pectin plus 76% polydextrose with 2% ascorbic acid in a mixture, and ascorbic acid arranged successively upwards.

leaving unaffected the physical and conformation properties of the macromolecules.

FTIR studies were complemented with wide angle X-ray diffraction (WAXD) to obtain an overall picture of the physical property in these preparations. The diffractograms in Fig. 5b reproduce two relatively sharp peaks at 13 and 21°, as the scattering angle reflects the processing conditions of freeze drying used in preparing the high-methoxy pectin. The matching X-ray diffraction pattern is characteristic of a randomly ordered polygalacturonic acid sequence (Georget, Cairns, Smith, & Waldron, 1999). At the top of the figure, the crystalline nature of ascorbic acid is evident by exhibiting multiple sharp peaks varying from 5° to 60° (Devi & Kakati, 2013). In contrast, single polydextrose and high-methoxy pectin/polydextrose mixtures, with and without ascorbic acid, record single fingerprints of broad peaks at 22° with a shouldering until 50°, an outcome that strongly argues for amorphicity in the macromolecular architecture of these materials. Therefore, the hydration of ascorbic acid and its mixture with pectin in the presence of high levels of polydextrose have considerably diminished the ordered/crystalline nature of these materials in single aqueous preparations.

Scanning electron microscopy was employed to obtain tangible evidence of the network morphology in these systems following elucidation of their physicochemical properties from FTIR and X-ray studies. Freeze drying of aqueous HMP systems in Fig. 6a yields an arrangement of individual pectin fibres, since in the low solid environment the polysaccharide is unable to form a cohesive network. In contrast, addition of high levels of co-solute transforms preparations into sheet-like featureless fields (Fig. 6b and c). This amorphous pictogram does not change in the presence of hydrated vitamin C in the mixture (Fig. 6d), which is distinct from the conventional crystal structure of the micronutrient in Fig. 6e. Overall, microscopy images further confirm the amorphous nature of high-solid tertiary mixtures in accordance with earlier thermomechanical, infrared and X-ray evidence, which is an encouraging result for the application of the glass transition theory.

3.4. Diffusion kinetics of ascorbic acid in the high-solid carbohydrate matrix recorded with UV-vis spectroscopy

Glassy carbohydrate matrices are increasingly used as molecular vehicles for the delivery of bioactive compounds and micronutrients, a subject of interest in functional food and nutraceutical

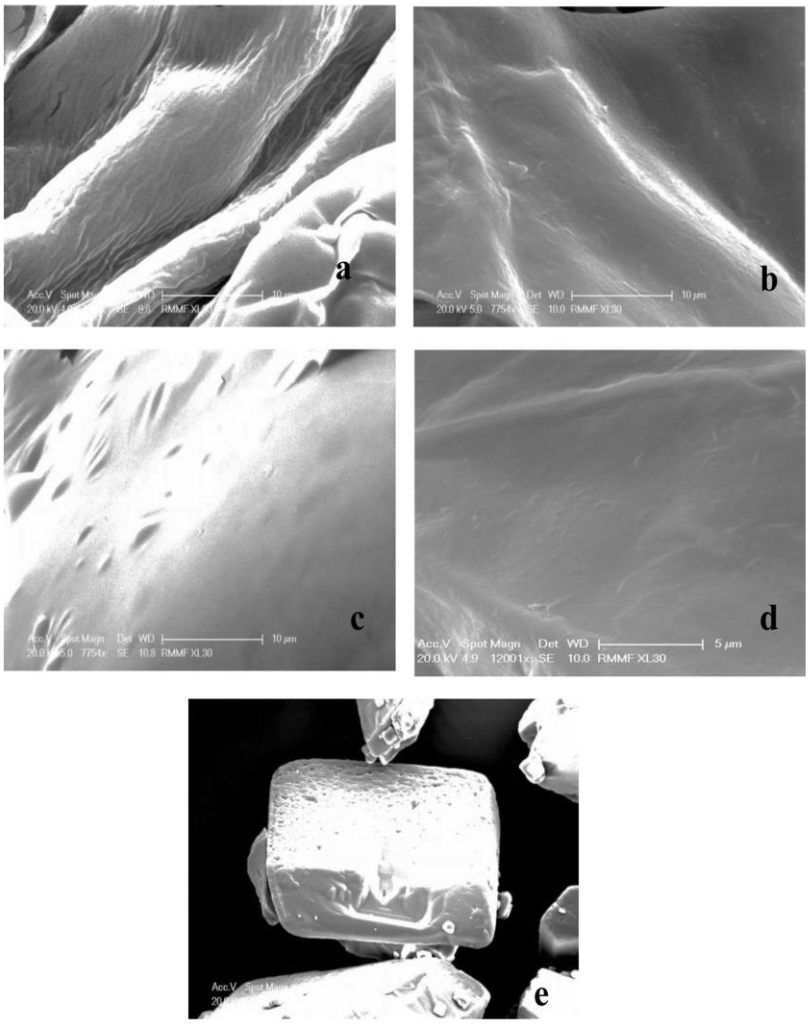

Fig. 6. Conventional SEM micrographs for (a) 2% high-methoxy pectin, (b) 80% polydextrose, (c) a binary mixture of 2% high-methoxy pectin with 78% polydextrose, and (d) a tertiary mixture of 2% high-methoxy pectin plus 77.6% polydextrose with 0.4% ascorbic acid, and (e) ascorbic acid crystals.

industries (Day, Saymour, Pitts, Konczak & Lundin, 2009; Kasapis, 2008). The present work pursues fundamental understanding in this area of innovative product development by examining the kinetics of diffusional mobility of vitamin C entrapped in the high-methoxy pectin/polydextrose matrix. The vitamin is, of course, commercially available in fortified formulas and supplemented foods thus providing a quality index for the retention of other nutrients in food matrices (Sablani, Al-Belushi, Al-Marhubi, & Al-Belushi, 2007; Zhou & Roos, 2012).

Diffusion patterns of ascorbic acid were monitored using UV-vis spectroscopy, which provides a sensitive method of quantitative analysis. The method is based on the oxidation of ascorbic acid to dehydroascorbic acid and subsequent transformation to diketogulonic acid, which is coupled with 2,4-dinitrophenylhydrazine (2,4-DNPH). Under carefully controlled conditions, this produces stable red-coloured osazones (in fact, a bis-hydrazone) with the detected absorption being within the range of 500–550 nm (Al-Ani, Opera, Al-bahri & Al-Rahbi, 2007; Bell, 2006). Our results document that instrumental readings at the absorption maximum ($\lambda_{max} = 521$ nm at 20 °C) have an excellent linear relationship ($R^2 = 0.999$) with ascorbic acid concentration in absolute ethanol within the experimental range of 0–0.25 A, hence following the Beer–Lambert law (data not shown).

Experimental materials were based on a formulation of 80% high-methoxy pectin/polydextrose including 0.4% vitamin C. Observations were carried out for 240 min, but maximum release of the micronutrient was observed within 60 min, which is discussed presently. An extensive temperature range of −30–20 °C was probed in Fig. 7a to cover the entirety of the rubber-to-glass transition, as monitored using rheology in Fig. 2. Smooth absorbance curves are illustrated reaching a plateau once the timescale of observation exceeds 30 min. Raising the temperature from subzero to ambient doubles the intensity of ascorbic acid absorbance at the end of the experimental routine. Results were replotted as a function of temperature for selected recording times in Fig. 7b to highlight the reduction in molecular mobility of vitamin C in the vicinity of the mechanical glass transition temperature ($T_g = -20$ °C), whereas increasing absorbance readings are noted in the temperatures (e.g. 15 °C) of the rubbery plateau.

3.5. Theoretical modeling of ascorbic-acid release based on the free volume theory and the concept of effective diffusion coefficient

To address in a quantitative manner the issue of the glassy matrix controlling the mobility of the bioactive compound, we considered the first part of the spectrum in Fig. 7a that exhibits an acceptable linearity within the first 30 min of observation. This section of the spectrum corresponds to a zero-order reaction, with the gradient being constant at $k = dx/dt$. For each experimental temperature, the spectroscopic shift factor ($\log k_o/k$) was developed, with k_o being the rate constant at the reference temperature of −15 °C. Plotting the spectroscopic shift factors against experimental temperature within the range of −30–20 °C affords in Fig. 8 a direct comparison between release kinetics of vitamin C and molecular relaxation of the polymeric matrix.

A high quality linear fit ($R^2 = 0.997$) follows the progression of diffusion kinetics of the micronutrient based on the reaction rate theory discussed earlier in the form of the modified Arrhenius Equation (1). It returns a constant activation energy of 7.60 kJ/mol, which is a low estimate in comparison with the corresponding E_a value of around 200 kJ/mol for the high-methoxy pectin/polydextrose matrix. This outcome indicates that although the diffusion of vitamin C is controlled by the specific physicochemical features

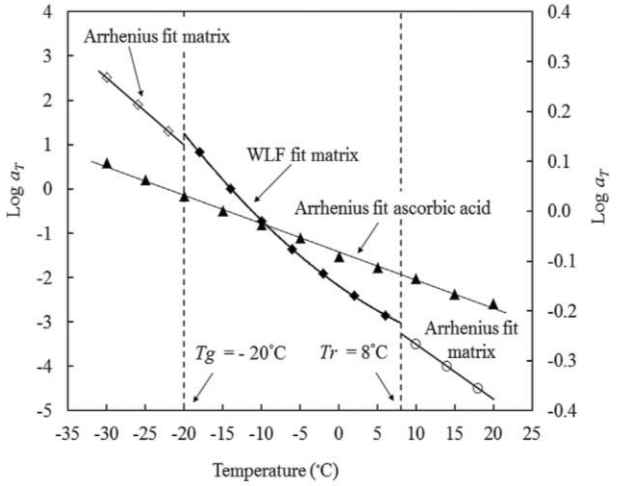

Fig. 8. Logarithmic shift factors a_T as a function of temperature within the glassy state (◊), glass transition region (◆) and the rubbery state (○) for 78% polydextrose plus 2% high-methoxy pectin matrix (left *y*-axis), and for kinetic data of 0.4% ascorbic acid diffused from the carbohydrate matrix to absolute ethanol (▲, right *y*-axis). The reference temperature for both systems is −15 °C, and the dash lines pinpoint the network T_g and the rubbery state temperature, T_r, predictions.

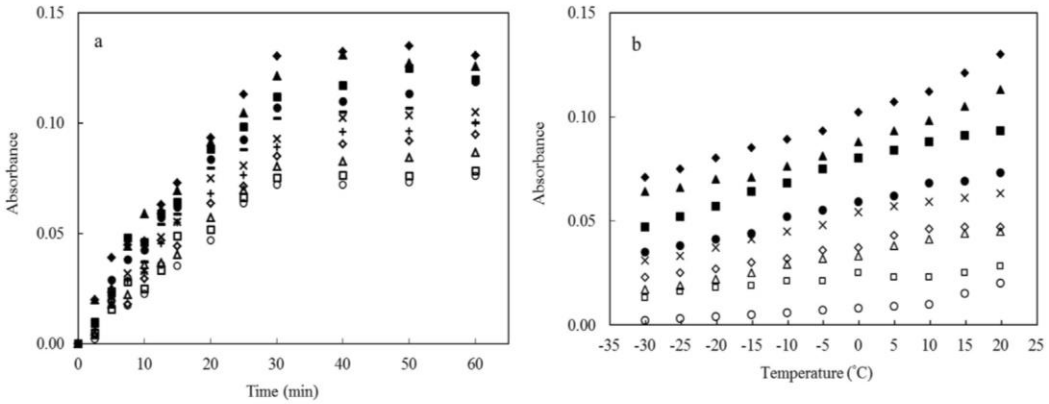

Fig. 7. Absorbance of 0.4% ascorbic acid diffused from 77.6% polydextrose with 2% high-methoxy pectin (0.2 M HCl, pH 3) to absolute ethanol: (a) as a function of time of observation (1 h) at −30 (○), −25 (□), −20 (Δ), −15 (◊), −10 (+), −5 (×), 0 (-), 5 (●), 10 (■), 15 (▲) and 20 (◆) °C, and (b) as a function of experimental temperature for the period of 2 (○), 5 (□), 7 (Δ), 10 (◊), 12 (×), 15 (●), 20 (■), 25 (▲) and 30 (◆) min, obtained at 521 nm.

of the polymeric matrix, its free volume is considerably higher than for the high-methoxy pectin, and is congruent with observations on caffeine (Jiang & Kasapis, 2011; Kasapis & Shrinivas, 2010).

In order to relate the physics of free volume to a mechanistic model that describes the release of a bioactive compound from a high-solid carbohydrate matrix, we employed the concept of Fickian diffusion (Crank, 1975). The idea of molecular diffusivity becomes workable over a wide range of experimental conditions with the introduction of an empirical power law model, as follows (Peppas, 1985; Singh & Chauham, 2009):

$$\frac{M_t}{M_\infty} = kt^n \tag{3}$$

where, M_t/M_∞ is the fractional release of a bioactive compound at experimental time (t) and infinite time (∞), k is a constant characteristic of the bioactive compound-polymer system, and n is a diffusion exponent characteristic of the release mechanism (Meinders & Vliet, 2009).

Using the absorbance values (M_t) from Fig. 7a and the equilibrium state reached after 60 min (M_∞), the values of the diffusion exponent and gel characteristic constant within the fifty-degree experimental temperature range were evaluated from the gradient and the intercept of the plot ln (M_t/M_∞) *versus* ln t (s) in Fig. 9. These are summarized in Table 1, and the variation in n values, within the range of 0.79–0.98 (Ritger & Peppas, 1987a), indicates an anomalous transport for the micronutrient release from the core to the surface of the polymeric matrix.

The general applicability of the Fickian model to the molecular dynamics of our tertiary system encourages us to delve deeper into the major driving force behind experimental observations. In particular, the anomalous mode of transport discussed in the preceding paragraph confirms that the diffusion process has occurred through the molecular sieve of the polymeric network, which reduces gradually the diffusion rate of mobile micromolecules. This process of unsteady state diffusion is described by Fick's second law, and provided the said diffusion takes place in one dimension, it can be described by the following mathematical expression (Baker, 1987; Busk & Labuza, 1979):

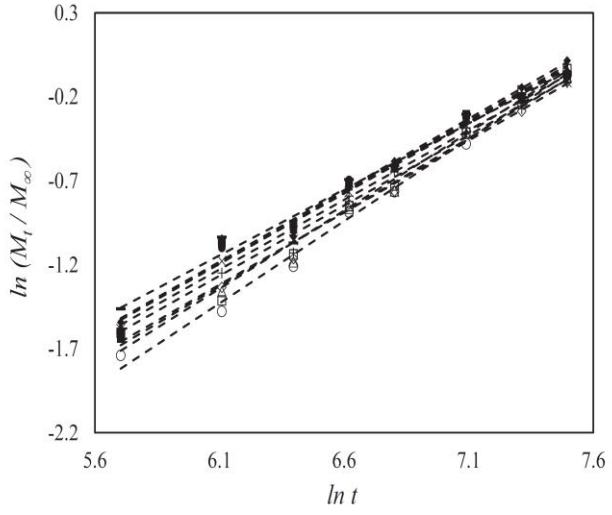

Fig. 9. Plot of ln (M_t/M_∞) *versus* ln t to evaluate the diffusion exponent, n, and gel characteristic constant, k, for the condensed matrix of high-methoxy pectin plus polydextrose at −30 (○), −25 (□), −20 (Δ), −15 (◊), −10 (+), −5 (×), 0 (-), 5 (●), 10 (■), 15 (▲) and 20 (◆) °C within 30 min arranged successfully upwards; calculated values of n and k are presented in Table 1.

Table 1
Diffusion exponent (n) and gel characteristic constant (k) for the release of ascorbic acid from the condensed high-methoxy pectin with polydextrose system of this investigation.

Temperature (°C)	Diffusion exponent (n)	Gel characteristic constant ($k \times 10^2$)
−30	0.98	16.46
−25	0.93	11.48
−20	0.88	8.24
−15	0.86	7.02
−10	0.84	5.86
−5	0.83	5.40
0	0.79	3.78
5	0.83	5.23
10	0.84	5.76
15	0.84	5.72
20	0.85	5.90

$$\frac{\partial C}{\partial t} = D\frac{\partial^2 C}{x^2} \tag{4}$$

where, C is the concentration of diffusant, t is the time of diffusion, D is the diffusion coefficient, and x is the distance travelled.

The concept of diffusion coefficient is based on the assumption that release kinetics are carried out in the absence of a significant change in the morphological characteristics of the polymeric carrier, i.e. the time–independent permeability of the matrix for the bioactive compound is maintained (Siepmann & Siepmann, 2008). This, however, does not preclude certain heterogeneity in the junction-zone forming network of high-methoxy pectin in the presence of polydextrose that has resulted in the anomalous pattern of diffusion of vitamin C discussed earlier. The other condition of compliance for Fick's second law to be operational is met here, since the ascorbic acid release has taken place in one dimension within the matrix's geometry, which is considered to be a finite slab with negligible edge effects. Theoretical Equation (4) of Fick's second law is solved as follows (Ritger & Peppas, 1987b):

$$\frac{M_t}{M_\infty} = 1 - \sum_{n=0}^{\infty} \frac{8}{(2n+1)^2\pi^2} \exp\left[\frac{-D_{eff}(2n+1)^2\pi^2 t}{L^2}\right] \tag{5}$$

where, M_t and M_∞ denote the absolute accumulative amounts of compound release at time (t) and infinity (∞), n is a dummy variable in the algorithmic solution, D_{eff} is the effective diffusion coefficient of the compound within the matrix, and L is the slab's thickness.

In practice, a simplified assumption is made that only the first term in the series Equation (5) is significant, which discards the remaining terms to allow the following linear solution:

$$\ln\left(\frac{M_\infty - M_t}{M_\infty - M_i}\right) = \ln\frac{8}{\pi^2} - \frac{D_{eff}\pi^2 t}{4L^2} \tag{6}$$

where, M_i is the original absorbance reading in Fig. 7a for each experimental temperature.

Application of Equation (6) to the absorbance data of vitamin C generates Fig. 10, where the effective diffusion coefficient of the micronutrient within the condensed HMP/polydextrose matrix is given as a function of the experimental temperatures of observation. Values of D_{eff} show a dramatic drop at subzero temperatures with a minimum of 7.90×10^{-8} m^2/s at −30 °C, which corresponds to the glassy consistency of the matrix. They level off on the opposite end of the temperature range with a maximum of 9.7×10^{-8} m^2/s at 15 °C in the rubbery plateau. The figure also

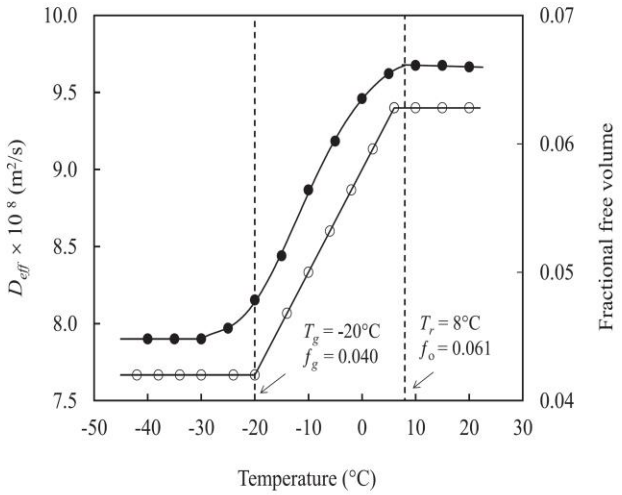

Fig. 10. Effective diffusion coefficient (D_{eff}) of 0.4% ascorbic acid from 77.6% polydextrose with 2% high-methoxy pectin (0.2 M HCl, pH 3) to absolute ethanol as a function of experimental temperature within 30 min (●, left *y*-axis), and fractional free volume (f_o) of the high-solid matrix in the rubber to glass transformation (○, right *y*-axis).

reproduces the estimates of fractional free volume for the HMP/polydextrose mixture in this study. These vary from a maximum of about 0.061 in the rubbery state temperature to a minimum of 0.040 in the glass transition temperature.

It appears that holes between packing irregularities of long chain segments is sufficient large to allow diffusion of ascorbic acid in the malleable consistency of the HMP/polydextrose rubber. In contrast, reduction in free space within the brittle and hard texture of the glassy state drops considerably the rate of diffusional mobility of ascorbic acid. Introduction of the Fickian diffusion model in this work confirms the postulate of the mechanical glass transition temperature as a critical parameter in the diffusional mobility of bioactive compounds within glassy hydrocolloid matrices. Indeed, the agreement between free volume patterns of the matrix and diffusional mobility of the chemical compound within the temperature range of this investigation is quite remarkable.

4. Conclusions

Whilst it has been long known that bioactive compounds can be preserved within a high-solid environment, the precise nature of the effect of processing time and temperature on bioactivity is not entirely understood. Mathematical modeling based on high-utility empirical relations in combination with theoretical schools of thought has considerable potential for innovative product development. To understand the molecular interactions of vitamin C in a high-methoxy pectin/polydextrose system, we utilised the combined framework of free volume theory with the concept of effective diffusion coefficient. Our modeling has taken into account the amorphous nature of the polymeric matrix, which is cable of forming a cohesive three dimensional network, its geometry and the direction of diffusion pathways for the bioactive compound within the surrounding solid-like environment. Improved understanding of the underlying molecular process was achieved by relating the network glass transition temperature to release patterns of the vitamin within the structured matrix. This free-volume driven effect is further modeled with a diffusion mechanism for delivery of the bioactive compound. Thus, the work offered insights both into the physics and the rate of bioactive-compound transport within the glassy network.

Acknowledgements

Thai Government Scholarship awarded to Naksit Panyoyai by the Cooperation Office in The Civil Service Commission of the Thai Government is duly acknowledged.

References

Al-Ani, M., Opara, L. U., Al-Bahri, D., & Al-Rahbi, N. (2007). Spectrophotometric quantification of ascorbic acid contents of fruit and vegetables using 2,4-dinitrophenylhydrazine method. *Journal of Food, Agriculture & Environment, 5*, 165–168.

Almrhag, O., George, P., Bannikova, A., Katopo, L., & Kasapis, S. (2012). Networks of polysaccharides with hydrophilic and hydrophobic characteristics in the presence of co-solute. *International Journal of Biological Macromolecules, 51*, 138–145.

Baker, R. W. (1987). *Controlled release of biological active agents*. NY: John Wiley & Sons.

Bell, G. F. M. (2006). *Vitamins in food: Analysis, bioavailability, and stability*. Boca Raton, FL: Taylor & Francis Group, CRC Press.

Bell, L. N., & Hageman, M. J. (1994). Differentiating between the effects of water activity and glass transition dependent mobility on a solid state chemical reaction: aspartame degradation. *Journal of Agricultural and Food Chemistry, 42*, 2398–2401.

Busk, G. C., Jr., & Labuza, T. P. (1979). A dye diffusion technique to evaluate gel properties. *Journal of Food Science, 44*, 1369–1372.

Champion, D., Le Meste, M., & Simatos, D. (2000). Towards an improved understanding of 515 glass transition and relaxations in foods: molecular mobility in the glass transition range. *Trends in Food Science & Technology, 11*, 41–55.

Chaudhary, V., Small, D. M., & Kasapis, S. (2013). Effect of a glassy gellan/polydextrose matrix on the activity of α-D-glucosidase. *Carbohydrate Polymers, 95*, 389–396.

Crank, J. (1975). *The mathematic of diffusion*. NY: Oxford university press, Inc.

Day, L., Seymour, R. B., Pitts, K. F., Konczak, I., & Lundin, L. (2009). Incorporation of functional ingredients into foods. *Trends in Food Science & Technology, 20*, 388–395.

Desai, K. G. H., & Park, H. J. (2005). Encapsulation of vitamin C in tripolyphosphate cross-linked chitosan microspheres by spray drying. *Journal of Microencapsulation, 22*, 179–192.

Devi, N., & Kakati, D. K. (2013). Smart porous microparticles based on gelatin/sodium alginate polyelectrolyte complex. *Journal of Food Engineering, 117*, 193–204.

Ferry, J. D. (1980). Dependence of viscoelastic behavior on temperature and pressure. In *Viscoelasttic properties of polymers*. NY: John Wiley.

Georget, D. M. R., Cairns, P., Smith, A. C., & Waldron, K. W. (1999). Crystallinity of lyophilized carrot cell wall components. *International Journal of Biological Macromolecules, 26*, 325–331.

Hiegel, G. A., Abdala, M. H., Vincent Burke, S., & Beard, D. P. (1987). Methods for preparing aqueous solutions of chlorine and bromine for halogen displacement reactions. *Journal of Chemical Education, 64*, 156.

Jiang, B., & Kasapis, S. (2011). Kinetics of a bioactive compound (caffeine) mobility at the vicinity of the mechanical glass transition temperature induced by gelling polysaccharide. *Journal of Agricultural and Food Chemistry, 59*, 11825–11832.

Kasapis, S. (2004). Definition of a mechanical glass transition temperature for dehydrated foods. *Journal of Agricultural and Food Chemistry, 52*, 2262–2268.

Kasapis, S. (2006). Definition and applications of the network glass transition temperature. *Food Hydrocolloids, 20*, 218–228.

Kasapis, S. (2008). Recent advances and future challenges in the explanation and exploitation of the network glass transition of high sugar/biopolymer mixtures. *Critical Reviews in Food Science and Nutrition, 48*, 185–203.

Kasapis, S., & Shrinivas, P. (2010). Combined use of thermomechanics and UV spectroscopy to rationalize the kinetics of bioactive compound (caffeine) mobility in a high solids matrix. *Journal of Agricultural and Food Chemistry, 58*, 3825–3832.

Le Meste, M., Champion, D., Roudaut, G., Blond, G., & Simatos, D. (2002). Glass transition and food technology: a critical appraisal. *Journal of Food Science, 67*, 2444–2458.

Liu, Y., Bhandari, B., & Zhou, W. (2006). Glass transition and enthalpy relaxation of amorphous food saccharides: a review. *Journal of Agricultural and Food Chemistry, 54*, 5701–5717.

Liu, P., Yu, L., Liu, H., Chen, L., & Li, L. (2009). Glass transition temperature of starch studied by a high-speed DSC. *Carbohydrate Polymers, 77*, 250–253.

Meinders, M. B. J., & Vliet, T. V. (2009). Modeling water sorption dynamics of cellular solid food systems using free volume theory. *Food Hydrocolloids, 23*, 2234–2242.

Mellan, I. (1977). *Industrial solvents handbook* (2nd ed.). Noyes Data Corporation.

Míčková, K., Čopìková, J., & Synytsya, A. (2007). Determination of polydextrose as a fat replacer in butter. *Czech Journal of Food Science, 25*, 25–31.

Monsoor, M. A., Kalapathy, U., & Proctor, A. (2001). Improved method for determination of pectin degree of esterification by diffuse reflectance Fourier transform infrared spectroscopy. *Journal of Agricultural and Food Chemistry, 49*, 2756–2760.

Nelson, K. A., & Labuza, T. P. (1994). Water activity and food polymer sciences: implications of state on Arrhenius and WLF models in predicting shelf life. *Journal of Food Engineering, 22*, 271–289.
Nickerson, M. T., Paulson, A. T., & Speers, R. A. (2004). A time-temperature rheological approach for examining food polymer gelation. *Trends in Food Science & Technology, 15*, 569–574.
Ottaway, P. B. (1993). *The technology of vitamins in food*. London: Chapman and Hall.
Peppas, N. A. (1985). Analysis of Fickian and non-Fickian drug release from polymers. *Pharmaceutica Acta Helvetiae, 60*, 110–111.
van der Put, T. A. C. M. (2010). Theoretical derivation of the WLF-and annealing equations. *Journal of Non-Crystalline Solid, 356*, 394–399.
Rahman, M. S. (2010). Food stability determination by macro-micro region concept in the state diagram and by defining a critical temperature. *Journal of Food Engineering, 99*, 402–416.
Ritger, P. L., & Peppas, N. A. (1987a). A simple equation for description of solute release I. Fickian and non-Fickian release from non-swellable devices in the form of slabs, spheres, cylinders or discs. *Journal of Controlled Release, 5*, 23–36.
Ritger, P. L., & Peppas, N. A. (1987b). A simple equation for description of solute release II. Fickian and anomalous release from swellable device. *Journal of Controlled Release, 5*, 37–42.
Sablani, S. S., Al-Belushi, K., Al-Marhubi, I., & Al-Belushi, R. (2007). Evaluating stability of vitamin in fortified formula using water activity and glass transition. *International Journal of Food Properties, 10*, 61–71.
Shalmashi, A., & Eliassi, A. (2008). Solubility of L-(+)-ascorbic acid in water, ethanol, methanol, propan-2-ol, acetone, acetonitrile, ethyl acetate and tetrahydrofuran from (293–323) K. *Journal of Chemical Engineering Data, 53*, 1332–1334.
Siepmann, J., & Siepmann, F. (2008). Mathematical modeling of drug delivery. *International Journal of Pharmaceutics, 364*, 328–343.
Singh, B., & Chauham, N. (2009). Modification of psyllium polysaccharides for use in oral insulin delivery. *Food Hydrocolloids, 23*, 928–935.
Velikov, K. P., & Pelan, E. (2008). Colloidal delivery systems for micronutrients and nutraceuticals. *Soft Matter, 4*, 1964–1980.
Wijaya, M., Small, D. M., & Bui, L. (2011). *Microencapsulation of ascorbic acid for enhanced long-term retention during storage*. Technical report number DSTO-TR-2504. Fishermans Bend, Victoria, Australia: Division, Defence Science and Technology Organisation.
Zhou, Y., & Roos, Y. H. (2012). Stability and plasticizing and crystallization effects of vitamins in amorphous sugar systems. *Journal of Agricultural and Food Chemistry, 60*, 1075–1083.

CHAPTER 4

CONTROLLED RELEASE OF THIAMIN IN A GLASSY κ-CARRAGEENAN/GLUCOSE SYRUP MATRIX

Panyoyai, N., Bannikova, A., Small D. M., & Kasapis, S. (2015). Controlled release of thiamin in a glassy κ-carrageenan/glucose syrup matrix. *Carbohydrate Polymers, 115,* 723-731. *(IF 4.07)*

School of Science

Chapter Declaration for Thesis with Publications

Chapter 4 is presented by the following paper:

[Controlled release of thiamin in a glassy κ-carrageenan/glucose syrup matrix]
[Naksit Panyoyai, Anna Bannikova, Darryl M. Small, & Stefan Kasapis]
[Carbohydrate Polymers]
[115, 723-731]
[2015]

Declaration by candidate

I declare that I wrote the initial draft of this manuscript, and my overall contribution to this paper is detailed below:

Nature of contribution	**Extend of contribution (%)**
(1) Performed all experiments (2) Collected and calculated all of the data (3) Interpreated the results including a repetition (4) Implemented the mathematical models and plotted graphs	70

The following co-authors contributed to the work. The undersigned declare that the contributions of the candidate and co-authors are correctly attributed below.

Author	**Nature of contribution**	**Extent of contribution (%)**	**Signature**
Anna Bannikova	(1) Partially interpreated the results (2) Edited the first draft	5	
Darryl M. Small	(1) Designed the vitamin analysis (2) Commented on the second draft	5	
Stefan Kasapis	(1) Supervised the project (2) Designed the experiment (3) Partially interpreated the results (4) Edited the final draft (5) Approved the revised manuscript	20	

Candidate's Signature date		**Date** 14/01/2016
Primary Supervisor's Signature		**Date** 18/01/2016

Carbohydrate Polymers 115 (2015) 723–731

Contents lists available at ScienceDirect

Carbohydrate Polymers

journal homepage: www.elsevier.com/locate/carbpol

Controlled release of thiamin in a glassy κ-carrageenan/glucose syrup matrix

Naksit Panyoyai, Anna Bannikova, Darryl M. Small, Stefan Kasapis*

School of Applied Sciences, RMIT University, City Campus, Melbourne 3001, VIC, Australia

ARTICLE INFO

Article history:
Received 4 June 2014
Received in revised form 11 July 2014
Accepted 30 July 2014
Available online 12 August 2014

Keywords:
κ-Carrageenan
Glucose syrup
Thiamin
Glass transition temperature
Diffusion kinetics

ABSTRACT

The work dealt with the diffusional mobility of thiamin embedded in a high-solid matrix of κ-carrageenan with glucose syrup. It utilized thermomechanical analysis in the form of modulated differential scanning calorimetry and small-deformation dynamic oscillation in shear, Fourier transform infrared spectroscopy, wide angle X-ray diffraction, scanning electron microscopy and UV–vis spectrophotometry. The structural properties of the matrix were assessed in a temperature induced rubber-to-glass transformation. A thiamin-dye binding assay was employed to monitor the diffusion process of the vitamin from the high-solid preparation to ethylene glycol. The relationship between mechanical properties of the carbohydrate matrix and vitamin mobility was assessed *via* the application of the combined framework of the free volume theory and the predictions of the reaction rate theory. Results argue that the transport of the micronutrient is governed by the structural relaxation of the high-solid matrix. These were further treated with the concept of Fickian diffusion coefficient to provide the rate of the bioactive compound mobility within the present experimental settings.

1. Introduction

Thiamin (vitamin B1) is the first member of a wide group of B complex vitamins. Staple foods like cereals, grains and rice as well as the various forms of dietary supplements (capsules, tablets, powder and gels) are vehicles for thiamin fortification (Bui, Small, & Coad, 2013). The consistency and retention of thiamin in these materials have been evaluated in relation to temperature, pH, water activity and added counterion (Bell & White, 2000; Bui & Small, 2007; Zhou & Roos, 2012). A recent approach in examining the stability of micronutrients in systems of industrial interest has been focusing on the phenomenon of glass transition that allows modeling of the time–temperature function during processing and subsequent storage (Leśková et al., 2006; Rahman, 2006). This is based on the expectation that in the glassy state various diffusion processes, and rates of physicochemical, enzymatic and biological reactions become extremely slow thus facilitating the preservation of nutrients in foodstuffs (Roos, 1995, 2003, 2010).

Thermoanalytical methods including modulated differential scanning calorimetry (MDSC) and dynamic mechanical analysis (DMA) have become useful techniques in the determination of the glass transition temperature of condensed systems (Gunasekaran & Ak, 2000). Further work using small-deformation dynamic oscillation in shear offered an avenue to define a mechanical or network glass transition temperature with physical significance in biopolymer/co-solute preparations (Kasapis, 2006). It utilized the concept of free volume to follow the relaxation kinetics within the glass transition region as a function of solids content, polymer molecular weight and extent of counterion or thermally induced network formation in biomaterials (Kasapis, 2001, 2008; Kasapis, Mitchell, Abeysekera, & MacNaughtan, 2004).

κ-Carrageenan is the collective name of a family of sulphated galactans comprising an alternating α(1-3)-D-galactose-4-sulphate and β(1-4)-3,6-anhydro-D-galactose (Morris & Chivers, 1983; Michel, Mestdagh & Axelos, 1997). The marine-based polysaccharide is extracted from red algae (*Eucheuma cottonii*) and is used extensively in the food industry as a gelling, thickening, stabilizing and water holding agent, diffusion controller, and texture enhancer (Campo, Kawano, da Silva & Carvalho, 2009; Michel et al., 1997). The rapid gelation of κ-carrageenan involves coil-to-helix transformation and aggregation of the ordered molecules with alkali metal ions (particularly those of potassium), sugars and polyols (Hermansson, Eriksson & Jordansson, 1991; Nishinari & Watase, 1992; Nishinari, Watase, Williams & Phillips, 1990). Recently, the effect of network formation in a high-solid system of κ-carrageenan

* Corresponding author. Tel.: +61 3 992 55244; fax: +61 3 992 55241.
E-mail addresses: stefan.kasapis@rmit.edu.au, stefankasapis@hotmail.com (S. Kasapis).

http://dx.doi.org/10.1016/j.carbpol.2014.07.060
0144-8617/

and glucose syrup on the preservation and diffusion of caffeine as a typical psychoactive stimulant and diuretic in humans has been examined (Jiang & Kasapis, 2011).

Various micronutrients and antioxidants have been widely incorporated in delivery vehicles in the form of capsules, tablets or colloidal gels, which has generated great interest in fundamental approaches that build a foundation for the design and fabrication of food-grade systems targeting specific applications (Fisher & Windhab, 2011; Lesmes & McClements, 2009; Pothakamury & Barbosa-Cánovas, 1995). The current investigation aims to provide basic understanding on the physical mechanisms and transport rates of thiamin entrapped in a condensed matrix of κ-carrageenan/glucose syrup undergoing thermally induced vitrification.

2. Materials and methods

2.1. Materials

Glucose syrup, as the co-solute of this investigation, is a product of Edlyn Foods Pty Ltd (Sydney, Australia) with a dextrose equivalent (DE) value of about 42. The total level of solids in the stock solution is 81% (w/w), and percentages in the preparations of this investigation refer to dry solids. This is a non-crystalline material that converts from a viscous solution at ambient temperature to a rigid and transparent glass at subzero temperatures.

κ-Carrageenan, as the structuring agent of this investigation, is supplied by Sigma-Aldrich Pty Ltd (Sydney, Australia). The polysaccharide is extracted from *E. cottonii* type III and used as the basic material for further purification prior to our experimentation.

Thiamin. The vitamin in its hydrochloride form ($C_{12}H_{17}ClN_4OS{\cdot}HCl$ with a molecular weight of 337.27 g/mol) was obtained from Sigma-Aldrich Pty Ltd (Sydney, Australia). The material was in the form of small white crystals with an analytical grade of more than 99% purity.

Ethylene glycol was purchased at a spectrophotometric grade (purity of about 99.9%) from Sigma-Aldrich Pty Ltd (Sydney, Australia). It is commonly used as an antifreeze fluid for the preservation of biological tissues and organs. Our eye observations and calorimetric analysis at a scan rate of 0.1 °C/min showed that the freezing point of ethylene glycol was below −30 °C. This property facilitates its utilization as a stable liquid phase in the current experimental temperature range of −22 to 26 °C.

Thiamin hydrochloride analytical reagents. The acid dye, Alizarin Brilliant Violet R, was purchased from Jacquard (Healdsburg, USA) in the form of a violet powder. Chloroform was obtained from Sigma-Aldrich Pty Ltd (Sydney, Australia) and potassium dihydrogen phosphate, for the preparation of the phosphate buffer at pH 4.5, was purchased from BDH Chemicals Pty Ltd (Poole, England). Reagents were used without further purification and Millipore type II water was the diluent in all experiments.

2.2. The potassium form of κ-carrageenan

The material of this investigation was converted in the potassium form by ion exchange, as described by Evageliou, Kasapis, and Hember (1998). In doing so, an Amberlite IR-120 exchanging resin from Supelco (Bellefonte, Pennsylvania, USA) was used. Two hundred grams of the resin was first eluted with 0.1 M HCL to bring it to the hydrogen form until the eluent was at pH 1, and then with a solution of 2 M KCl to bring it to the potassium form. The resin was rinsed with millipore water to remove the excess of salt until there was no precipitation in the washings with 0.1 M silver nitrate, and was heated up to 90 °C with Millipore water.

Table 1
Cation and sulphate contents of the potassium κ-carrageenan, as compared to its commercial counterpart.

Ions	Commercial κ-carrageenan (% w/w)	Potassium κ-carrageenan (% w/w)
Potassium	6.5	7.8
Calcium	2.8	0.3
Sodium	0.7	0.1
Magnesium	0.2	0.02
Sulphate	17.8	17.5

Five grams of κ-carrageenan were transferred in a conical flask and dissolved with 1 L of Millipore water followed by heating to 90 °C on a hot plate with stirring. The hot resin was introduced into the polysaccharide flask and stirred for 30 min. κ-Carrageenan in the potassium form was separated from the resin, dialyzed against Millipore water for 24 h at 25 °C and freeze-dried using an Operon freeze dryer (Gimpo, Seoul, Korea).

The purity of the ion exchanged material was analyzed with an atomic absorption spectrometer (Agilent, Santa Clara, California, USA). K^+, Na^+ and Mg^{2+} were identified using an air-acetylene flame whereas Ca^{2+} was determined with a nitrous oxide-acetylene flame. Calibration curves were constructed for each cation, with the absorbance readings versus cation concentration in ppm being expressed finally in percentages (w/w). The amount of sulfate was evaluated gravimetrically (Chan, Mirhosseini, Taip, Ling, & Tan, 2013). The method is based on sulfate hydrolysis with 1 M HCl and reaction of the sulfate groups with barium chloride leading to the formation of a white precipitate of barium sulfate. The sulfate content was calculated by multiplying the weight of barium sulfate with a conversion factor (0.4116) and expressing in percentages (w/w). All measurements were performed in triplicate and results are presented in Table 1.

2.3. Sample preparation

In general, samples were prepared at 85% (w/w) total solids. In doing so, κ-carrageenan in the potassium form was dispersed in Millipore water at 90 °C with constant stirring for 10 min and then the temperature was reduced to 70 °C. Appropriate amounts of glucose syrup were dissolved separately and added carefully to the polymer solution at the same temperature. The total level of solids was higher than the required final concentration but that was adjusted with the addition of thiamin hydrochloride, in a potassium dihydrogen phosphate buffer (50 mM, pH 4.5), to the viscous carbohydrate preparation at 30 °C to yield the experimental concentration of 1% thiamin with 2% κ-carrageenan and 82% glucose syrup (w/w).

The above conditions encourage smooth network formation and prevention of thiamin degradation (Imeson, 2000; Pachapurkar & Bell, 2005). Care was taken to dissolve the thiamin in the potassium dihydrogen phosphate buffer using an amber glass bottle. Beakers with final preparations were wrapped in aluminum foil and the top was sealed with a stretchable film to prevent exposure to light. Samples were kept overnight at 4 °C to allow sample equilibration and used subsequently to study the controlled release of thiamin in the polymeric matrix. Other samples without thiamin were made in a similar manner to analyze the structural properties of the matrix including single systems of 85% glucose syrup, and 83% glucose syrup with 2% κ-carrageenan (w/w).

2.4. Structural studies

2.4.1. Modulated differential scanning calorimetry

Measurements were performed using Q 2000 (TA Instruments, New Castle, DE). The instrument interfaced a refrigerated

cooling system (RCS 90) to achieve temperatures down to −90 °C, and nitrogen was the purging gas at a flow rate of 50 mL/min. Heat flow signals were calibrated using a traceable indium standard (ΔH_f = 28.3 J/g) and the heat capacity with a sapphire standard. About 10 mg of sample were hermetically sealed and analyzed by cooling from 20 to −90 °C at the scan rate of 1 °C/min followed by heating to 20 °C at the same rate. Measurements were performed at modulation amplitude of ±0.53 °C for each period of 40 s, and an empty pan served as a reference. Duplicates of the thermograms were recorded yielding effectively overlapping traces.

2.4.2. Small-deformation rheology

Mechanical properties were studied as a function of temperature and angular frequency with small-deformation dynamic-oscillation measurements in shear. This type of mechanical analysis provides readings of the elastic (storage modulus, G') and viscous (loss modulus, G'') components of the network, with variations of the relative liquid-like and solid-like structure of the material being assessed with the damping factor ($\tan\delta = G''/G'$).

Low amplitude oscillatory measurements were executed using AR-G2, a controlled strain rheometer with a magnetic thrust bearing technology (TA Instruments, New Castle, DE). Samples were placed on a preheated Peltier plate supporting a parallel-plate measuring geometry (10 mm diameter) at 80 °C and exposed edges were covered with silicone oil (50 cS) to minimize moisture loss. High-solid preparations were cooled to −25 °C with an environmental test chamber (ETC) at 1 °C/min using a frequency of 1 rad/s and 0.1% strain that was within the linear viscoelastic region of our materials. That allowed recording of the rubbery plateau, glass transition region and glassy state as a function of temperature. Further, mechanical spectra were recorded from 0.1 to 100 rad/s at temperature intervals of 4° upon subsequent heating.

Fourier transform infrared spectroscopy. Data for single, binary and tertiary samples were obtained with a Perkin Elmer Spectrum 100 using MIRacle^{TM} ZnSe single reflection ATR plate (Perkin Elmer, Norwalk, CT). The absorbance spectra were recorded within the range of 600 to 4000 cm^{-1} at an average scan number of 8 and a resolution of 4 cm^{-1}. That was normalized against the background spectrum of Millipore water at ambient temperature, and each measurement was performed in triplicate.

Wide angle X-ray diffraction. Measurements were carried out using a D8 Advanced Bruker AXS (Karlsruhe, Germany) attached with Cu-*K*α radiation source (l = 1.54 Å). Diffractograms of freeze-dried samples of κ-carrageenan, glucose syrup, thiamin hydrochloride and their combinations were obtained at 25 °C using an accelerating voltage and current of 40 kV and 40 mA, respectively. Raw data were obtained within a 2θ range of 5° and 90° in the measuring interval of 0.1° and analyzed using DIFFRAC^{plus} Evaluation (Eva), version 10.0 revision 1, which is a Bruker Advanced X-ray Solutions software. As before, experimentation was performed in triplicate.

Scanning electron microscopy. Philips XL30 SEM (Edwards High Vacuum, Sussex, England) was used to investigate the network morphology and phase topology of single preparations and mixtures of our materials. Freeze dried preparations were attached to sample holders followed by gold plating. A high-vacuum mode at an accelerating voltage of 5 and 10 kV, spot size from 4.3 to 5 and observing distance between 9.7 and 12.5 mm were used to obtain micrographs.

2.5. Control release kinetics

Four grams of the high-solid κ-carrageenan/glucose syrup preparation with thiamin hydrochloride were transferred into twelve 25 mL beakers (overall thirty six replicates per experimental temperature) and wrapped with aluminum foil to avoid exposure

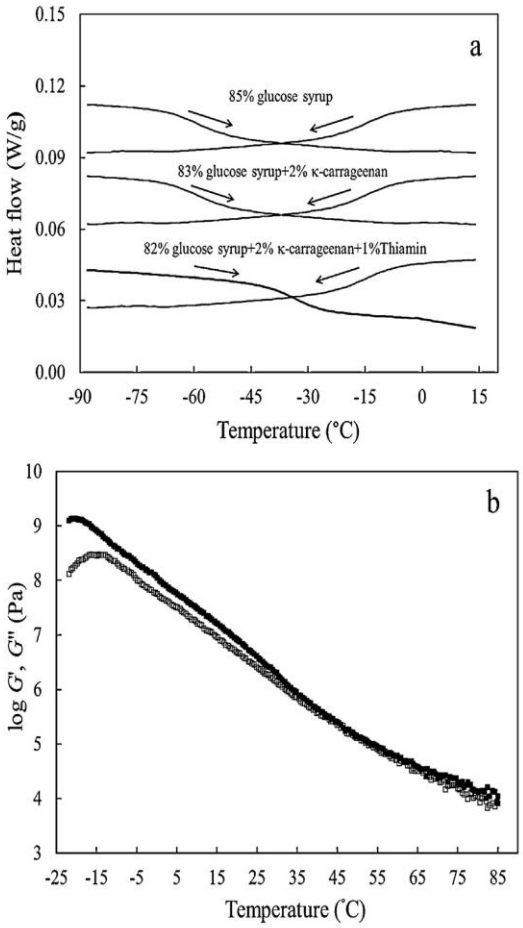

Fig. 1. (a) Variation of heat flow as a function of temperature for 82% glucose syrup plus 2% potassium κ-carrageenan with 1% thiamin hydrochloride (50 mM K^+; pH 4.5), 83% glucose syrup with 2% potassium κ-carrageenan, and 85% glucose syrup alone obtained using MDSC at a scan rate of 1 °C/min; (b) cooling profiles of storage (G', ■) and loss (G'', □) modulus as a function of temperature for 82% glucose syrup plus 2% potassium κ-carrageenan with 1% thiamin hydrochloride (50 mM K^+; pH 4.5) scanned at a rate of 1 °C/min, frequency of 1 rad/s and strain of 0.01%.

to light. The thickness and diameter of the sample in the beaker were 5 and 25 mm, respectively. Care was taken to obtain a smooth surface without any bubble formation following sample transfer to the beaker. These materials and 4 mL of ethylene glycol in test tubes were kept overnight at the experimental temperature of interest for equilibration. After that, ethylene glycol was transferred swiftly to the beakers as a separate phase on top of the sample; ethylene glycol is insoluble in the κ-carrageenan/glucose syrup system. Beakers were promptly sealed with stretchable film to prevent solvent evaporation and returned to the required temperature for immediate removal of an aliquot thus setting the zero time of the experimentation. Subsequent aliquots were obtained within 2 h at intervals of one to twenty minutes for the experimental temperature range of −22 to 26 °C every 4 °C.

Vitamin diffusion from the high-solid matrix to ethylene glycol was estimated in the form of absorbance using a dye-binding assay and a Lamda 35 UV–vis spectrophotometer (Perkin Elmer, Singapore). This is based on the formation of a colored ion-pair complex between thiamin hydrochloride and Alizarin brilliant violet *R* (modified assay from Prasad, Rajasree, Khan & Reddy, 1997). In doing so, 1 mL ethylene glycol containing diffused thiamin was mixed with 2 mL of 50 mM potassium dihydrogen phosphate buffer

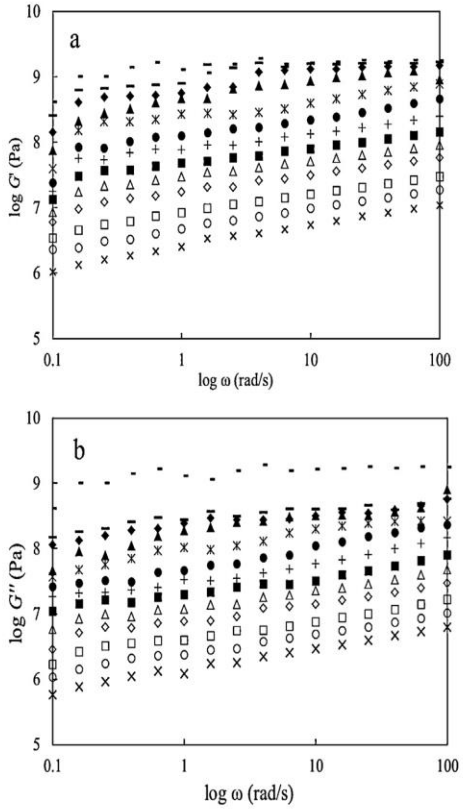

Fig. 2. Frequency variation of G' (a) and G'' (b) for 82% glucose syrup plus 2% potassium κ-carrageenan with 1% thiamin hydrochloride (50 mM K^+; pH 4.5). The bottom curve was taken at 26 °C (×), other curves successively upward were taken at 22 (○), 18 (□), 14 (◊), 10 (Δ), 6 (■), 2 (+), −2 (●), −6 (·), −10 (▲), −14 (♦), −18 (−) and −22 (–) °C.

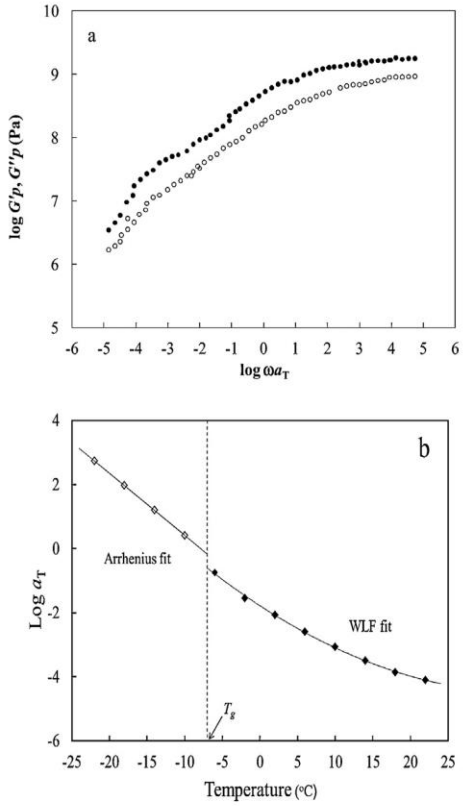

Fig. 3. (a) Master curve of reduced shear modulus (G_p', ●; G_p'', ○) for 82% glucose syrup with 2% potassium κ-carrageenan (50 mM K^+; pH 4.5) plus 1% thiamin hydrochloride as a function of reduced frequency of oscillation (ωa_T) based on the frequency sweeps in Fig. 2 and utilizing a reference temperature of −6 °C, and (b) logarithmic shift factors a_T as a function of temperature for this sample within the glass transition region (closed symbols) and glassy state (open symbols), with the solid line reflecting the WLF and modified Arrhenius fits of the shift factors, and the dash line pinpointing the prediction of network T_g.

to bring the solution to pH 4.5 and prevent vitamin degradation. Then, the preparation was transferred into a 100 mL separating funnel and mixed with 10 mL chloroform, 2 mL of 0.2% Alizarin brilliant violet *R* and Millipore water to a total of 20 mL. The separator was shaken for 2 min and set aside at ambient temperature for 10 min to yield a two-layer liquid mixture.

Some of the bottom layer of blue chloroform was removed into 1 cm glass cell and maximum absorbance was measured at λ_{max} = 575 nm; color intensity remains constant within 4 h of observation at ambient temperature. A calibration curve was constructed by dissolving thiamin hydrochloride in ethylene glycol at concentrations ranging from 0.0001 to 0.006% and applying the same assay for absorbance measurements as for the diffusion studies. Tests were carried out in triplicate and average values are reported.

3. Results and discussion

3.1. Single and mixed κ-carrageenan/glucose syrup/thiamin systems examined calorimetrically

MDSC is a common technique to investigate changes in heat capacity with temperature leading to mechanical, enthalpic and dielectric transformations. In the present study, addition of high levels of glucose syrup prevents ice formation at subzero temperatures, thus allowing observation of molecular relaxations in supersaturated matrices of κ-carrageenan/glucose syrup/thiamin, κ-carrageenan/glucose syrup and glucose syrup alone, with the total solids content for all preparations being fixed at 85% (w/w). Direct measurements of heat capacity at modulated regime were performed in heating and cooling cycles at the relatively low scan rate of 1 °C/min.

Fig. 1a reveals a decrease in the total heat capacity of samples during cooling due to reduction in thermal motion and molecular mobility. The calorimetric glass transition temperature can be pinpointed empirically at the middle of the thermogram. This mid-point T_g for the single glucose syrup and a binary mixture of κ-carrageenan/glucose syrup was recorded to be approximately −37 °C. Addition of thiamin shifted the T_g estimate to a slightly higher temperature of −35 °C. It appears, therefore, that the presence of small amounts of κ-carrageenan and thiamin hydrochloride has no significant effect on the characteristics of the glucose-syrup thermogram. Similar reports on the DSC readings for high-solid carbohydrate preparations were obtained by Kumagai, MacNaughtan, Farhat, and Mitchell (2002) and Jiang and Kasapis (2011). This outcome argues that calorimetric spectra are mainly dominated by the enthalpic relaxation of small molecule co-solute, with the addition of threshold gel concentrations of polymeric materials acting merely as a cross-contaminant in the system (Chaudhary, Small, & Kasapis, 2013).

3.2. Rheological examination of vitrification in high-solid preparations

The calorimetric glass transition temperature describes micromolecular aspects of high-solid preparations, which are complemented by small-deformation oscillatory measurements

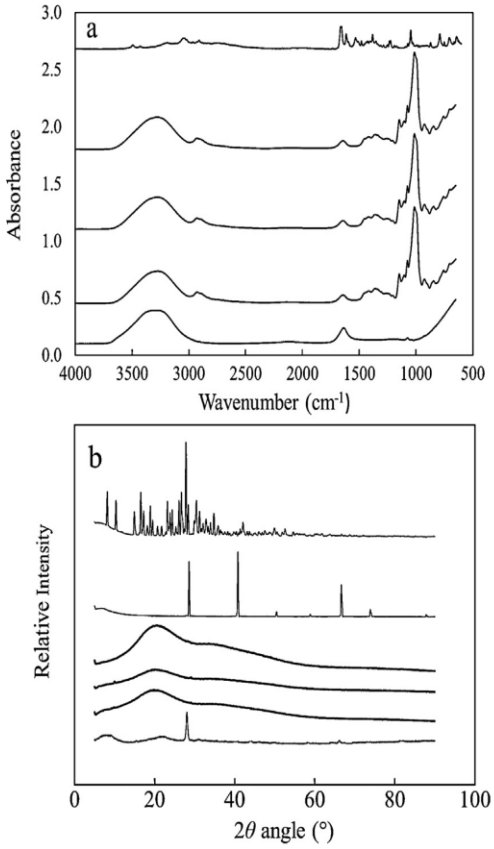

Fig. 4. (a) FTIR spectra and (b) X-ray diffractograms of 2% potassium κ-carrageenan with 0% or 83% glucose syrup, an 85% glucose syrup preparation, 2% potassium κ-carrageenan plus 82% glucose syrup with 1% thiamine hydrochloride, potassium dihydrogen phosphate (for X-ray diffractograms only), and thiamine hydrochloride arranged successively upwards.

identifying macromolecular features of glass transition phenomena. This section examines the viscoelastic nature of 2% κ-carrageenan (50 mM K^+) with 82% glucose syrup and 1% thiamin hydrochloride over a temperature range and scan rate that are comparable to the calorimetric routine in the preceding section and results are reproduced in Fig. 1b. Similar viscoelasticity has been obtained for the system of 2% κ-carrageenan (50 mM K^+) with 83% glucose syrup but is not shown here.

Storage (G') and loss (G'') modulus values cover five-and-a-half orders of magnitude from $10^{3.8}$ to $10^{9.2}$ Pa within the experimental temperature range (Fig. 1b). At the high temperature end, e.g. at 80 °C, the low and relatively flat mechanical traces indicate the consistency of a rubbery plateau. This is followed by the glass transition region (e.g. at 45 °C) where the gap between the two moduli is reduced. Further cooling of the system leads gradually to the glassy state where the modulus values diverge from each other culminating in a sharp drop in the viscous response at the low end of the cooling run, i.e. at temperatures below −10 °C. Throughout the rubber-to-glass transformation, storage modulus remains above the liquid-like counterpart indicating the formation of a coherent network in the presence of 2% κ-carrageenan and 50 mM K^+ counterions (Iijima, Hatakeyama, Takahashi, & Hatakeyama, 2007; Loret, Ribelles, & Lundin, 2009). This κ-carrageenan/glucose syrup network yields a rapid manifestation of the mechanical vitrification, as compared to the calorimetric T_g of about −37 °C in Fig. 1a.

Next, we used the time–temperature superposition (TTS) principle to advance the discussion from the empirical state in Fig. 1b to an understanding that disentangles the temperature and time contributions in glass transition behavior (Nickerson & Paulson, 2005). In doing so, shear modulus measurements were taken within the frequency range of 0.1 to 100 rad/s in fixed intervals of 4 °C covering a temperature range of 26 to −22 °C (Fig. 2a and b). Clearly, mechanical spectra remain relatively flat in the glassy state (e.g. at −18 °C) while exhibiting a steep rise in the glass transition region with increasing oscillatory frequency (e.g. at 22 °C).

Mechanical spectra were superposed horizontally by selecting arbitrarily a reference temperature within the glass transition region (T_o = −6 °C). The technique is based on the premise that moduli recorded at any temperature are equivalent to those at T_o provided that the frequency, ω, is multiplied by a shift factor, a_T. Values of factor a_T were calculated using proprietary software (Orchestrator from TA Instruments) and confirmed manually by performing least square calculations of the horizontal displacement in shear-modulus data required for the construction of the viscoelastic master curves. Fig. 3a illustrates the master or composite curve obtained over a frequency window of ten decades from 10^{-5} to 10^5 rad/s, with the values of G'_p exceeding those of G''_p, as observed in the temperature analog of Fig. 1b.

Generated shift factors were modeled by utilizing the modified Arrhenius equation, which advocates that molecular processes are proportional to (E_a/RT), with E_a being the activation energy of molecular reorientation from one conformational state to another and R being the universal gas constant (Kasapis, 2001):

$$\log\ a_T = \frac{E_a}{2.303R}\left(\frac{1}{T} - \frac{1}{T_o}\right) \tag{1}$$

The approach follows well the temperature dependence of factor, a_T, at temperatures below −10 °C in Fig. 3b to generate a linear gradient with an activation energy value of about 180 kJ/mol that reflects the specific physicochemical fingerprints of this system.

We found that at temperatures higher than −10 °C in Fig. 3b, progress in viscoelasticity is better described by the concept of free volume, which in rheological terms can be given by the mathematical framework of Williams, Landel and Ferry (WLF equation in Ferry, 1980):

$$\log a_T = -\frac{C_1^0(T - T_0)}{C_2^0 + T - T_o} = -\frac{\left(B/2.303f_o\right)(T - T_o)}{\left(f_o/\alpha_f\right) + T - T_o} \tag{2}$$

where C_1^0 and C_2^0 are the WLF constants at T_o, f_o is the fractional free volume (the ratio of free to total volume per gram of material), α_f is the thermal expansion coefficient, and B is usually taken as one for simplicity.

Utilization of the WLF equation yields good fits for the temperature dependence of molecular processes at the upper range of experimental temperatures. It also pinpoints, in conjunction with the modified Arrhenius equation, the network glass transition temperature at −7 °C in Fig. 3b, as the threshold of the free volume and reaction rate theories; detailed discussion of the scientific basis for the derivation of a glass transition temperature with physical significance can be found in Kasapis (2008). WLF modeling produces values of C_1^0 (11.20), C_2^0 (50°), α_f (7.6×10^{-4} deg^{-1}) and f_g (0.038 at T_g), which are congruent with earlier estimates for amorphous synthetic polymers and bioglasses (Kasapis, 2008).

3.3. Molecular morphology of condensed carbohydrate/thiamin matrices

Thermomechanical work in the preceding sections was augmented with physicochemical and microscopy studies. FTIR was utilized first to identify potential interactions between the three constituents of these preparations. Fig. 4a illustrates spectra for κ-carrageenan indicating a broad —OH stretching absorption band at wavenumbers between 3650 and 3100 cm^{-1}. Glucose syrup, on

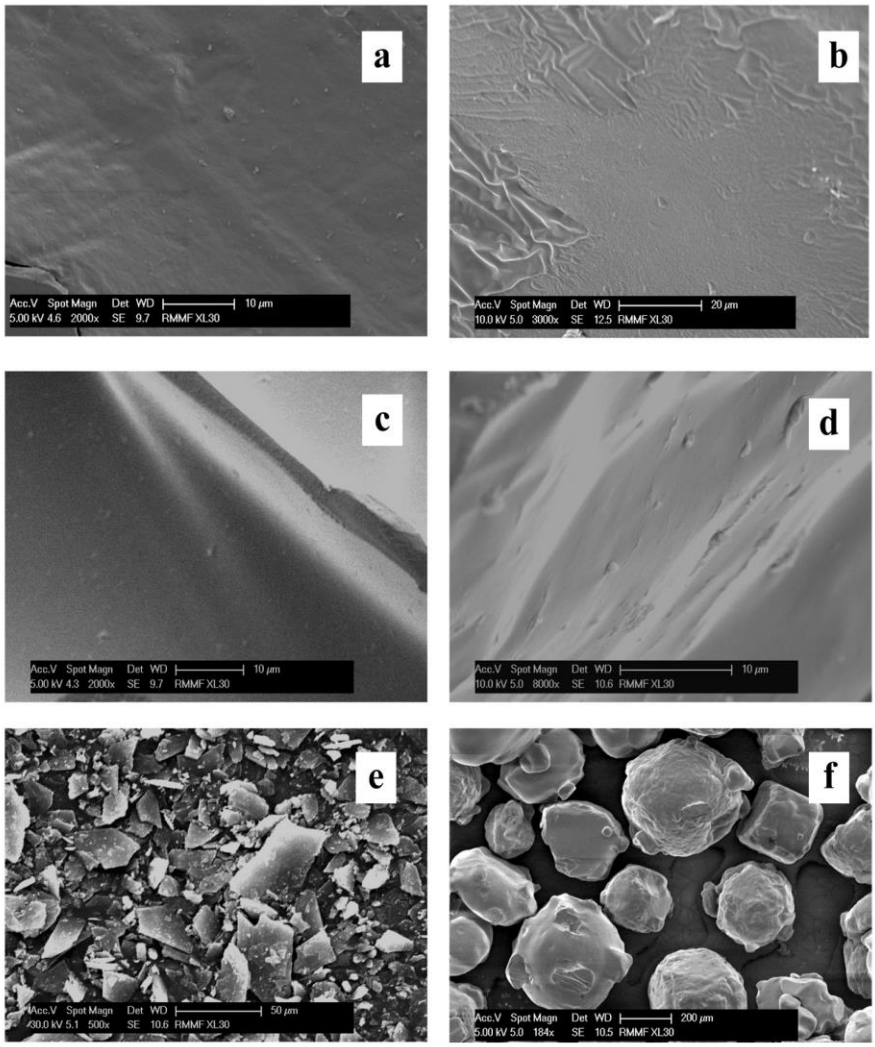

Fig. 5. SEM micrographs of (a) 2% potassium κ-carrageenan, (b) a binary mixture of 2% potassium κ-carrageenan with 83% glucose syrup, (c) 85% glucose syrup, (d) 2% potassium κ-carrageenan plus 82% glucose syrup with 1% thiamine hydrochloride, (e) thiamin hydrochloride crystals, and (f) potassium dihydrogen phosphate crystals.

the other hand, produces peaks of C—H stretching along with a major OH-group at 3645 to 2845 cm^{-1}, C=O stretching vibrations of aldehyde at 1624 cm^{-1}, C—O stretching and bending at 1493 to 1173 cm^{-1} and the C—O—C glycosidic linkage at 1172 to 875 cm^{-1} (Almrhag et al., 2012). Clearly, molecular FTIR spectra argue that the addition of thiamin does not affect the structural integrity and physical interactions within the high-solid κ-carrageenan/glucose syrup mixture.

FTIR studies were complemented with WAXD in an effort to observe possible alterations in the microsized order of the high-solid samples. Diffraction analysis in Fig. 4b indicates the specific site-binding of κ-carrageenan in the potassium form due to the cation exchange process implemented in this work. A typical non-crystalline aggregate supporting irregular junction zones is reflected in the diffractogram with one sharp peak ($2\theta = 28.06^{\circ}$), as reported by Martins et al. (2012). The thiamin and potassium dihydrogen sulphate crystals, positioned on the top of this presentation, exhibit multiple sharp peaks between 5 and 70°. In contrast, single glucose syrup and glucose syrup/κ-carrageenan systems, with or without thiamin, record a broad pattern centering at approximately 20° and shouldering at 35°, which is characteristic of the processing conditions used to manufacture the ingredients. The amorphous nature of the glucose-syrup containing samples is in agreement with the thermomechanical studies in Fig. 1a and b that detected vitrification phenomena in these systems.

Conventional scanning electron microscopy was used to obtain tangible evidence of the network characteristics in these systems. Lyophilized single preparations of κ-carrageenan, in the potassium form and in the presence of added 50 mM K^{+}, produce aqueous gels made of rather broad and loose aggregates (Fig. 5a). Polysaccharide preparations with co-solute in Fig. 5b and d exhibit an amorphous morphology, which is similar to the futureless background observed in Fig. 5c for single glucose–syrup fluids (Al-Amri, Al-Adawi, Al-Marhoobi, & Kasapis, 2005). Anhydrous thiamin and potassium dihydrogen sulphate crystals are also presented in Fig. 5e and f to make a contrast with the smooth three-dimensional structures in the hydrated preparations.

3.4. Experimental observations of thiamin's diffusional mobility in the high-solid carbohydrate matrix using UV–vis spectroscopy

Colloidal control release is a novel technique for the delivery of micronutrients (e.g. vitamins and minerals) in foods and nutraceuticals in relation to providing an overall quality index for the delivery of bioactivity in processed materials (Bell & White, 2000; Bui & Small, 2007; Bui et al., 2013; Zhou & Roos, 2012).

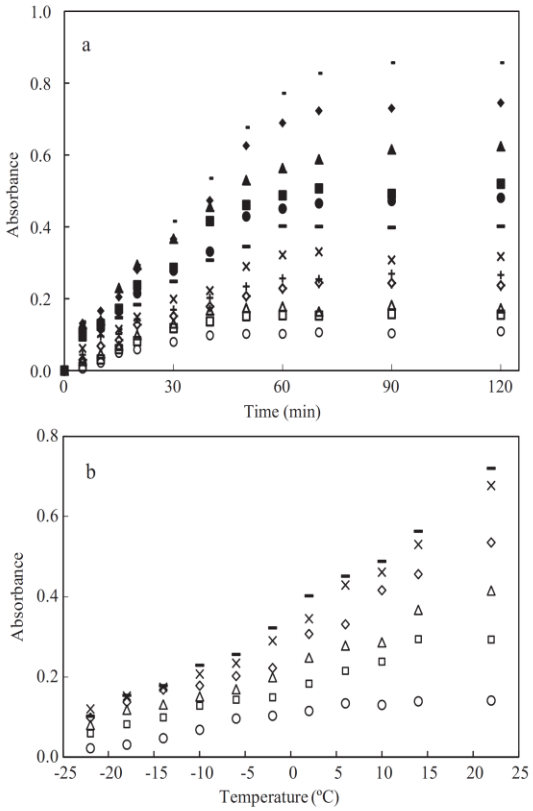

Fig. 6. Absorbance of 1% thiamin hydrochloride diffused from 82% glucose syrup with 2% potassium κ-carrageenan (50 mM K^+; pH 4.5) to ethylene glycol: (a) as a function of the time of observation at −22 (o), −18 (□), −14 (Δ), −10 (◊), −6 (+), −2 (×), 2 (−), 6 (●), 10 (■), 14 (▲), 18 (♦) and 22 (−) °C, and (b) as a function of experimental temperature for the periods of 10 (o), 20 (□), 30 (Δ), 40 (◊), 50 (×) and 60 (−) min, obtained at 578 nm.

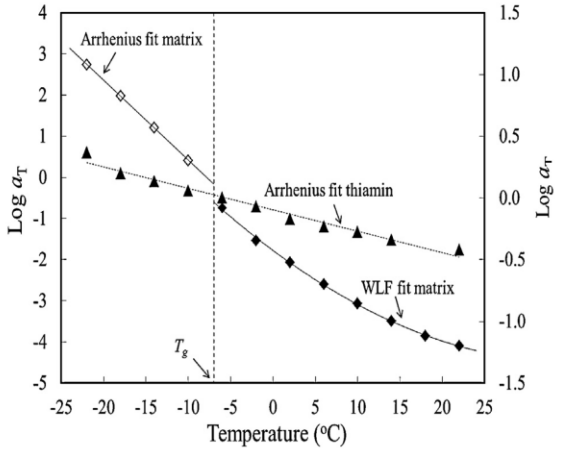

Fig. 7. Logarithmic shift factors, a_T, as a function of temperature within the glassy state (◊), and glass transition region (♦) for 82% glucose syrup plus 2% potassium κ-carrageenan with 1% thiamin (left *y*-axis), and for the kinetic data of 1% thiamin hydrochloride being diffused from the carbohydrate matrix to ethylene glycol (▲, right *y*-axis); reference temperature for both systems is −6 °C, with the dash line pinpointing the prediction of the network T_g.

It requires knowledge of the micronutrient's release kinetics in relation to the changing consistency of the high-solid structuring matrix in the time–temperature equivalence (Patel & Velikov, 2011; Pothakamury & Barbosa-Cánovas, 1995).

The present work elucidates the interplay between structural properties of a condensed matrix and diffusional mobility of an entrapped vitamin. Diffusion data, as a function of time and temperature of observation, were gathered with UV–vis spectroscopy, and the assay is based on the development of a colored ion-pair complex of thiamin hydrochloride and alizarin brilliant violet R in chloroform (Prasad et al., 1997). A bluish violet complex absorbed at λ_{max} of 578 nm yielding a highly linear relationship (R^2 = 0.9992) with the thiamin hydrochloride concentration in the ethylene glycol medium within the range of 0–0.74 Å (20 °C), which is in accordance with the Beer–Lambert law; calibration curve is not shown, but its equation of Absorbance = 121.340 × thiamin concentration (%) can be used for estimation of the vitamin amount released in the experimental time–temperature domain.

Observations on thiamin release from the κ-carrageenan/glucose syrup gel to ethylene glycol were carried out for 120 min within the temperature range of −22 to 22 °C, which according to Fig. 3b covers the glass transition region. It is evident in Fig. 6a that the absorbance of thiamin increases eight fold in this experimental timeframe but reaches an asymptotic equilibrium within the first 60 min of measurement. Increasing the temperature from subzero to ambient raises the intensity of micronutrient release, an outcome that argues for a considerable effect of the changing consistency in the polymeric matrix on the diffusion process. Fig. 6b illustrates these results by replotting them as a function of temperature for selected recording times. It is apparent that there is a slowdown in the rate of micronutrient mobility at subzero temperatures during the passage from the glass transition region to the glassy state, as argued from thermomechanical work in this system.

3.5. Modeling the kinetics of thiamin diffusion in the condensed carbohydrate matrix

Rationalization of the kinetic data describing thiamin's diffusional mobility was carried out by considering a linear relationship between absorbance and time of observation in the first 60 min in Fig. 6a. This section of the spectrum can be treated as a zero-order kinetic reaction with the gradient being constant at $k = dx/dt$. The recently introduced spectroscopic shift factor ($\log k_o/k$ in Jiang and Kasapis (2011)) was then utilized throughout the experimental temperature range, with k_o being the rate constant at the reference temperature of −6 °C. The outcome model is plotted in Fig. 7, where a direct comparison is afforded between kinetics of vitamin transport and relaxation of carbohydrate matrix.

The modified Arrhenius mathematical expression, i.e. Eq. (1) with two temperature terms provided a highly linear correlation (R^2 = 0.980) and a constant value of the activation energy (31.6 kJ/mol) for the diffusion of thiamin within the glassy matrix. In contrast, the activation energy of the carbohydrate matrix in this and earlier work is considerably higher, i.e. between 180 and 250 kJ/mol (Kasapis, 2001). This outcome argues that although the mobility of thiamin is restrained within the tertiary mixture, its mode of transport is distinct from the structural relaxation of the glassy matrix.

The next step of this work includes a correlation between the physics of the molecular processes taking place in Fig. 7 and the transport rate determining the diffusion of thiamin in the medium of this investigation. In doing so, we employed the concept of Fickian diffusion, which is based on the following power law equation (Pothakamury & Barbosa-Cánovas, 1995; Ritger & Peppas, 1987):

$$\frac{M_t}{M_\infty} = kt^n \tag{3}$$

where, M_t/M_∞ is the fractional release of a bioactive compound over the release time, t, k is a constant characteristic of the

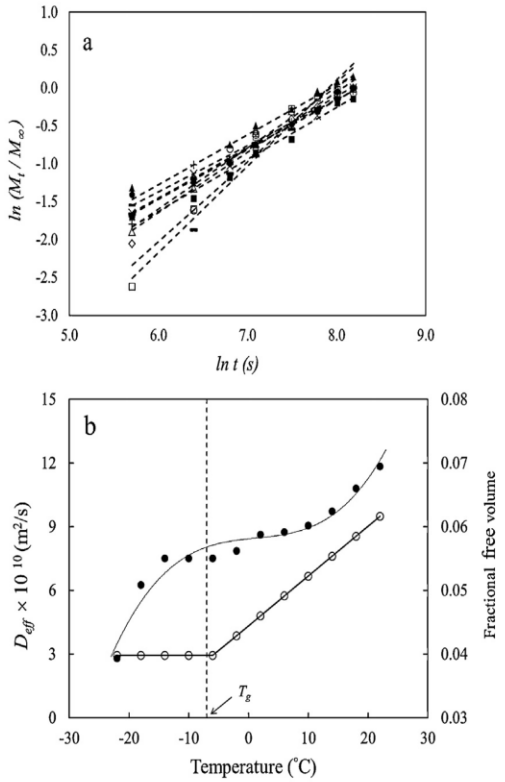

Fig. 8. (a) Plot of $\ln(M_t/M_\infty)$ versus $\ln t$ (s) to evaluate the diffusion exponent, n, and gel characteristic constant, k, for the high-solid matrix of potassium κ-carrageenan plus glucose syrup at −26 (o), −18 (□), −14 (Δ), −10 (◊), −6 (+), −2 (×), 2 (−), 6 (●), 10 (■), 14 (▲), and 22 (−) °C within an hour of observation arranged successfully upwards, and (b) effective diffusion coefficient of thiamin from the carbohydrate matrix to ethylene glycol as a function of temperature within an hour of observation (●, left y-axis), and fractional free volume of the high-solid matrix in the glass transition region and glassy state (o, right y-axis).

bioactive compound-polymer system, and n is the diffusion exponent for the release mechanism. Literature reports that normal Fickian diffusion is characterized by an n-value of 0.5, while Case II diffusion is defined by an n-value of 1.0, which makes the range of n-values between 0.5 and 1.0 the non-Fickian or anomalous diffusion.

Absorbance values within and at 60 min (M_t and M_∞, respectively) in Fig. 6a were used to produce the relevant parameters from the gradient and intercept of the plot $\ln M_t/M_\infty$ versus $\ln t$ (s) in Eq. (3). Thus, values of diffusion exponent and gel characteristic constant throughout the experimental temperature range were derived from Fig. 8a and are depicted in Table 2. Diffusion exponent estimates were found to lie between 0.61 and 0.87, hence arguing for an anomalous and rather rapid diffusion of the mainly hydrophilic thiamine molecule within the largely hydrophilic κ-carrageenan/glucose syrup matrix.

The above school of thought provides further insights in the form of a diffusion coefficient that can be identified in Fick's second law, as follows (Busk & Labuza, 1979):

$$\frac{\delta C}{\delta t} = D\frac{\delta^2 C}{x^2} \tag{4}$$

where C is the concentration of the diffusant molecule, t is the time of diffusion, D_{eff} is the effective diffusion coefficient, and x is the relative distance travelled.

Valid application of Fick's second law requires that the molecular sieve of the matrix maintains its physicochemical morphology

Table 2
Diffusion exponent (n) and gel characteristic constant (k) for the release of thiamin hydrochloride from the high-solid carbohydrate matrix.

Temperature (°C)	Diffusion exponent (n)	Gel characteristic constant (k) × 10^{-3}
−22	0.87	1.03
−18	0.86	0.98
−14	0.86	1.16
−10	0.80	1.64
−6	0.67	4.07
−2	0.65	4.52
2	0.64	4.86
6	0.61	6.53
10	0.69	5.34
14	0.66	3.59
22	0.83	0.93

throughout the diffusion process, which is the outcome argued in the spectroscopic observations in Fig. 4a and b. Further conditions of compliance require that the sample is a finite slab with negligible edge effects and the micronutrient release takes place in a single dimension within the geometry of the matrix. Under the above specified conditions, the theoretical Eq. (4) of Fick's second law can be solved in the form of a trigonometric series (Siepmann & Siepmann, 2008):

$$\frac{M_t}{M_\infty} = 1 - \sum_{n=0}^{\infty} \frac{8}{(2n+1)^2\pi^2} \quad \exp\left[\frac{-D_{\text{eff}}(2n+1)^2\pi^2 t}{L^2}\right] \tag{5}$$

where M_t and M_∞ denote the absolute accumulative amounts of compound release at time (t) and infinity (∞), n is a dummy variable in the algorithmic solution, D_{eff} is the effective diffusion coefficient of the compound within the matrix, and L is the slab's thickness.

Moisture transfer studies in breakfast cereals has shown that only the first term in this series equation is significant, which, in the absence of the higher terms, yields the following relationship (Tutuncu & Labuza, 1996):

$$\ln\left(\frac{M_\infty - M_t}{M_\infty - M_i}\right) = \ln\frac{8}{\pi^2} - \frac{D_{\text{eff}}\pi^2 t}{4L^2} \tag{6}$$

where M_i, M_t, and M_∞ denote the original absorbance reading in Fig. 6a for each experimental temperature, during experimentation and infinity/equilibrium, respectively, and L is the thickness of the slab.

Application of Eq. (6) to the absorbance data of thiamine release yields Fig. 8b, where the values of diffusion coefficient as a function of temperature are visualized. These show a considerable drop from about 12×10^{-10} m^2/s at 22 °C, i.e. within the glass transition region to 3×10^{-10} m^2/s at −22 °C, i.e. at the glassy state. Variation in the D_{eff} values follows closely progress in the fractional free volume of the carbohydrate supporting phase also plotted in Fig. 8b. Thus, the fractional free volume falls with controlled cooling from 0.062 to 0.039 at the mechanical glass transition temperature of −7 °C.

Clearly, the diffusional mobility of thiamin is controlled by the reduction in free space within the glassy state of the condensed matrix of κ-carrageenan with glucose syrup. Holes between packing irregularities of the carbohydrate gel allow diffusion of the micronutrient whose transport rate, as modeled by non-Fickian kinetics, can be related to the network glass transition temperature of the tertiary system. Estimates of thiamin's diffusion coefficient and polymeric free volume, reproduced in Fig. 8b, show a strong synchronization between physics and kinetic rate in the thermally induced process of vitrification.

4. Conclusions

It has long been known that bioactive compounds can be delivered in specific applications following preservation within systems of rubbery or glassy consistency. However, limited information is available on the effect of environmental conditions on the physics of vitrification in carbohydrate matrices, used as carriers of bioactivity, which determine the transport rates of diffusant molecules. The present work combines thermomechanical analysis and UV–vis spectroscopy to investigate the controlled release of thiamin embedded in a gelled κ-carrageenan/glucose syrup sample. Care was taken that the structural behavior of the constituents in the composite gel reflects the properties of single preparations thus being able to obtain the network glass transition of the mixture. The diffusion processes of the vitamin from the core to the surface of the carbohydrate matrix were followed using the spectroscopic shift factor, and were then modeled with the concept of non-Fickian kinetics. A similar pattern of behavior has been obtained for the diffusion of the hydrophilic molecule of Vitamin C in the congruent polarity of high-methoxy pectin with polydextrose being the supporting matrix (Panyoyai, Bannikova, Small, & Kasapis, 2014). In both cases, the diffusion rate of bioactive compound is moderated in accordance with the structural relaxation of the glassy matrix.

Acknowledgements

Scholarship awarded to Naksit Panyoyai by the Cooperation Office in The Civil Service Commission of the Thai Government is duly acknowledged.

References

Al-Amri, I. S., Al-Adawi, K. M., Al-Marhoobi, I. M., & Kasapis, S. (2005). Direct imaging of the changing polysaccharide network at high levels of co-solute. *Carbohydrate Polymers, 61*, 379–382.

Almrhag, O., George, P., Bannikova, A., Katopo, L., Chaudhary, D., & Kasapis, S. (2012). Analysis on the effectiveness of co-solute on the network integrity of high methoxy pectin. *Food Chemistry, 135*, 1455–1462.

Bell, L. N., & White, K. L. (2000). Thiamin stability in solids as affected by the glass transition. *Journal of Food Science, 65*, 498–501.

Bui, L. L. T., & Small, D. M. (2007). The influence of formulation and processing on stability of thiamin in three styles of Asian noodles. *Food Chemistry, 102*, 1394–1399.

Bui, L. T. T., Small, D. M., & Coad, R. (2013). The stability of water-soluble vitamins and issues in the fortification of foods. In V. R. Preedy, V. R. Srirajaskanthan, & V. B. Patel (Eds.), *Handbook of food fortification and health: From concepts to public health applications volume 1* (pp. 199–211). New York, NY: Humana Press, Springer.

Busk, J. R. G. C., & Labuza, T. P. (1979). A dye diffusion technique to evaluate gel properties. *Journal of Food Science, 44*, 1369–1372.

Campo, V. L., Kawano, D. F., da Silva, D. B., Jr., & Carvalho, I. (2009). Carrageenan: Biological, chemical modification and structural analysis—A review. *Carbohydrate Polymers, 77*, 167–180.

Chan, S. W., Mirhosseini, H., Taip, F. S., Ling, T. C., & Tan, C. P. (2013). Comparative study on the physicochemical properties of κ-carrageenan extracted from *Kappaphycus alvarezii* (doty) doty ex Silva in Tawau, Sabah, Malaysia and commercial κ-carrageenans. *Food Hydrocolloids, 30*, 581–588.

Chaudhary, V., Small, D. M., & Kasapis, S. (2013). Structural studies on matrices of deaclated gellan with polydextrose. *Food Chemistry, 137*, 37–44.

Evageliou, V., Kasapis, S., & Hember, M. W. N. (1998). Vitrification of κ-carrageenan in the presence of high levels of glucose syrup. *Polymer, 39*, 3909–3917.

Ferry, J. D. (1980). *Dependence of viscoelastic behavior on temperature and pressure, in viscoelastic properties of polymers*. New York, NY: John Wiley.

Fisher, P., & Windhab, E. J. (2011). Rheology of food materials. *Current Opinion in Colloid and Interface Science, 16*, 36–40.

Gunasekaran, S., & Ak, M. M. (2000). Dynamic oscillatory shear testing of foods-selected applications. *Trends in Food Science and Technology, 11*, 115–127.

Hermansson, A. M., Eriksson, E., & Jordansson, E. (1991). Effects of potassium, sodium and calcium on the microstructure and rheological behaviour of kappa-carrageenan gels. *Carbohydrate Polymers, 16*, 297–302.

Iijima, M., Hatakeyama, T., Takahashi, M., & Hatakeyama, H. (2007). Effect of thermal history on kappa-carrageenan hydrogelation by differential scanning calorimetry. *Thermochimica Acta, 452*, 53–58.

Imeson, A. P. (2000). Carrageenan. In G. O. Phillips, & P. A. Williams (Eds.), *Handbook of hydrocolloids*. Abington, MA: CRC Press.

Jiang, B., & Kasapis, S. (2011). Kinetics of a bioactive compound (caffeine) mobility at the vicinity of the mechanical glass transition temperature induced by gelling polysaccharide. *Journal of Agricultural and Food Chemistry, 59*, 11825–11832.

Kasapis, S., Mitchell, J., Abeysekera, R., & MacNaughtan, W. (2004). Rubber-to-glass transitions in high sugar/biopolymer mixtures. *Trends in Food Science and Technology, 15*, 298–304.

Kasapis, S. (2001). The use of Arrhenius and WLF kinetics to rationalise the rubber-to-glass transition in high sugar κ-carrageenan systems. *Food Hydrocolloids, 15*, 239–245.

Kasapis, S. (2006). Definition and applications of the network glass transition temperature. *Food Hydrocolloids, 20*, 218–228.

Kasapis, S. (2008). Recent advances and future challenges in the explanation and exploitation of the network glass transition of high sugar/biopolymer mixtures. *Critical Reviews in Food Science and Nutrition, 48*, 185–203.

Kumagai, H., MacNaughtan, W., Farhat, I. A., & Mitchell, J. R. (2002). The influence of carrageenan on molecular mobility in low moisture amorphous sugars. *Carbohydrate Polymers, 48*, 341–349.

Lešková, E., Kubíková, J., Kováčiková, E., Košická, M., Porubská, J., & Holčíková, K. (2006). Vitamin losses: Retention during heat treatment and continual changes expressed by mathematical models. *Journal of Food Composition and Analysis, 19*, 252–276.

Lesmes, U., & McClements, D. J. (2009). Structure-function relationships to guide rational design and fabrication of particulate food delivery systems. *Trends in Food Science and Technology, 20*, 448–457.

Loret, C., Ribelles, P., & Lundin, L. (2009). Mechanical properties of κ-carrageenan in high concentration of sugar solutions. *Food Hydrocolloids, 23*, 823–832.

Martins, J. T., Cerqueira, M. A., Bourbon, A., Pinheiro, A. G., Souza, B. W. S., & Vicente, A. A. (2012). Synergistic effects between κ-carrageenan and locust bean gum on physicochemical properties of edible films made thereof. *Food Hydrocolloids, 29*, 280–289.

Michel, A-S., Mestdagh, M. M., & Axelos, M. A. V. (1997). Physico-chemical properties of carrageenan gels in presence of various cations. *International Journal of Biological Macromolecules, 21*, 195–200.

Morris, V. J., & Chilvers, G. R. (1983). Rheological studies of specific cation forms of kappa carrageenan gels. *Carbohydrate Polymers, 3*, 129–141.

Nickerson, M. T., & Paulson, A. T. (2005). Time–temperature studies of κ-carrageenan gelation in the presence of high levels of co-solutes. *Carbohydrate Polymers, 61*(2005), 231–237.

Nishinari, K., & Watase, M. (1992). Effects of sugars and polyols on the gel–sol transition of kappa-carrageenan gels. *Thermochimica Acta, 206*, 149–162.

Nishinari, K., Watase, M., Williams, P. A., & Phillips, G. O. (1990). κ-Carrageenan gels: Effect of sucrose, glucose, urea and guadinine hydrochloride on the rheological and thermal properties. *Journal of Agricultural and Food Chemistry, 38*, 1188–1193.

Pachapurkar, D., & Bell, L. N. (2005). Kinetics of thiamin degradation in solutions under ambient storage conditions. *Journal of Food Science, 70*, C423–C426.

Panyoyai, N., Bannikova, A., Small, D. M., & Kasapis, S. (2014). Diffusion kinetics of ascorbic acid in a glassy matrix of high-methoxy pectin with polydextrose. *Food Hydrocolloids*, http://dx.doi.org/10.1016/j.foodhyd.2014.07.01 (in press)

Patel, A. R., & Velikov, K. P. (2011). Colloidal delivery system in foods: A general comparison with oral drug delivery. *LWT-Food Science and Technology, 44*, 1958–1964.

Prasad, P. S. S., Rajasree, K. P., Khan, K. A., & Reddy, M. N. (1997). Colorimetric determination of Thiamine hydrochloride using Alizarin brilliant violet R. *Indian Journal of Pharmaceutical Sciences, 59*, 194–196.

Pothakamury, U. R., & Barbosa-Cánovas, G. V. (1995). Fundamental aspects of controlled release in foods. *Trends in Food Science and Technology, 6*, 397–406.

Rahman, M. S. (2006). State diagram of foods: Its potential use in food processing and product stability. *Trends in Food Science and Technology, 17*, 129–141.

Ritger, P. L., & Peppas, N. A. (1987). A simple equation for description of solute release I. Fickian and non-Fickian release from non-swellable devices in the form of slabs, spheres, cylinders or discs. *Journal of Controlled Release, 5*, 23–36.

Roos, Y. H. (1995). Characterization of food polymer using state diagrams. *Journal of Food Engineering, 24*, 339–360.

Roos, Y. H. (2003). Thermal analysis, state transitions and food quality. *Journal of Thermal Analysis and Calorimetry, 71*, 197–203.

Roos, Y. H. (2010). Glass transition temperature and its relevance in food processing. *Annual Review of Food Science and Technology, 1*, 469–496.

Siepmann, J., & Siepmann, F. (2008). Mathematical modeling of drug delivery. *International Journal of Pharmaceutics, 364*, 328–343.

Tutuncu, M. A., & Labuza, T. P. (1996). Effect of geometry on the effective moisture transfer diffusion coefficient. *Journal of Food Engineering, 30*, 433–447.

Zhou, Y., & Roos, Y. H. (2012). Stability and plasticizing and crystallisation effects of vitamins in amorphous sugar systems. *Journal of Agricultural and Food Chemistry, 60*, 1075–1083.

CHAPTER 5

DIFFUSION OF NICOTINIC ACID IN SPRAY-DRIED CAPSULES OF WHEY PROTEIN ISOLATE

Panyoyai, N., Bannikova, A., Small D. M., Shanks, R. A., & Kasapis, S. (2016). Diffusion of nicotinic acid in spray-dried capsules of whey protein isolate. *Food Hydrocolloids, 52,* 811-819. *(IF 4.09)*

School of Science

Chapter Declaration for Thesis with Publications

Chapter 5 is presented by the following paper:

[Diffusion of nicotinic acid in spray-dried capsules of whey protein isolate]
[Naksit Panyoyai, Anna Bannikova, Darryl M. Small, Robert A. Shanks, & Stefan Kasapis]
[Food Hydrocolloids]
[52, 811-819]
[2016]

Declaration by candidate

I declare that I wrote the initial draft of this manuscript, and my overall contribution to this paper is detailed below:

Nature of contribution	**Extend of contribution (%)**
(1) Performed all experiments (2) Collected and calculated all of the data (3) Interpreated the results including a repetition (4) Implemented the mathematical models and plotted graphs	70

The following co-authors contributed to the work. The undersigned declare that the contributions of the candidate and co-authors are correctly attributed below.

Author	**Nature of contribution**	**Extent of contribution (%)**	**Signature**
Anna Bannikova	(1) Edited the first draft	5	
Darryl M. Small	(1) Designed the spray drying process and diffusion kinetics (2) Edited the second draft	5	
Robert A. Shanks	(1) Performed and interpreated the dynamic mechanical measurements (2) Edited the first draft	5	
Stefan Kasapis	(1) Supervised the project (2) Partially interpreated the results (3) Edited the final draft (4) Approved the revised manuscript	15	

Candidate's Signature		**Date** 14/01/2016
Primary Supervisor's Signature		**Date** 18/01/2016

Food Hydrocolloids 52 (2016) 811–819

Contents lists available at ScienceDirect

Food Hydrocolloids

journal homepage: www.elsevier.com/locate/foodhyd

Diffusion of nicotinic acid in spray-dried capsules of whey protein isolate

Naksit Panyoyai, Anna Bannikova, Darryl M. Small, Robert A. Shanks, Stefan Kasapis*

School of Applied Sciences, RMIT University, City Campus, Melbourne, Vic 3001, Australia

ARTICLE INFO

Article history:
Received 14 July 2015
Received in revised form
14 August 2015
Accepted 24 August 2015
Available online 28 August 2015

Keywords:
Whey protein isolate
Nicotinic acid
Mechanical glass transition temperature
Microencapsulation
Diffusion coefficient

ABSTRACT

Diffusion patterns of nicotinic acid were evaluated following its microencapsulation into a whey protein matrix through spray drying. Micro-differential scanning calorimetry, small-deformation rheological techniques, wide-angle X-ray scattering, Fourier transform infrared spectroscopy, particle size analysis and scanning electron microscopy were utilised to characterize encapsulant and bioactive compound in the composite material. UV–vis spectroscopy, the newly introduced concept of spectroscopic shift factor and the König reaction were also employed to elucidate the rate of vitamin transport throughout the polymeric matrix as a function of a broad time and temperature spectrum. Mechanical properties of the condensed matrix followed a progression that was described with the combined Williams-Landel-Ferry/free volume theory leading to the prediction of the mechanical glass transition temperature. Modified Arrhenius equation demonstrated that the kinetics of nicotinic-acid mobility were distinct from the structural relaxation of the polymeric segments. The former was further examined using the second law of Fickian diffusion. A direct relationship between fractional free volume of the whey protein network and diffusion coefficient of the nicotinic acid was established within the experimental temperature range.

1. Introduction

Whey protein is a by-product of the cheese or casein industry but finds increasing application in the development of added value food materials. It is mainly a mixture of β-lactoglobulin, α-lactalbumin, bovine serum albumin and immunoglobulins, with the isoelectric point being at pH ~5 (Evans, Zulewska, Newbold, Drake, & Barbano, 2010). Benefits of consuming whey protein focus on its natural origin being recognised as a safe food ingredient with superior nutritional value, bioactivity and techno-functionality (Yang, Liu, Ashton, Gorczyca, & Kasapis, 2013). Its globular protein structure is stabilised by interactions amongst adjacent peptide chains bringing together amino acid composition, net charge, hydrophobic/hydrophilic ratio and conformational rearrangements. Such molecular stabilisation is induced by a variety of environmental conditions including pH, temperature, pressure, enzyme or salt addition, and protein concentration or its interaction in mixture with polysaccharides (Liu & Zhong, 2013). In the last twenty years or so, attempts have been made to use whey protein in the controlled delivery of biologically active substances, hence serving as a robust bioactive carrier through informed manipulation of its structural functionality (Ju & Kilara, 1998).

Nicotinic acid, or pyridine-3-carboxylic acid, is also known as niacin or vitamin B_3 and produces aqueous alkaline solutions, which are highly stable to oxygen, heat and light. The potential benefits of the vitamin include human metabolic regulation and cell growth. For example, insufficient intake of nicotinic acid results in severe photosensitive dermatitis known clinically as pellagra (Bui, Small, & Coad, 2013). Fortification of processed foods with vitamins remains a subject of interest due to the persistent inadequate consumption of essential nutrients by a critical portion of the population (Gonçalves & da Piedade, 2012). Biopolymer based materials have been employed, using a variety of protocols, to deliver water or fat-soluble vitamin fortification (Chen, Remondetto, & Subirade, 2006). Advantages of using whey protein include the ability to control the release rate of small molecules with pH variation *via* the carboxylic and ammonium groups in polypeptide chains, which adjust their protons to acidic or neutral medium (Gunasekaran, Ko, & Xiao, 2007).

Condensed whey protein systems are mainly preparations that exceed fifty percent of solids on a dry matter basis (Abiad, Carvajal, & Campanella, 2009). Controlled heating through the denaturation

* Corresponding author.
E-mail address: stefan.kasapis@rmit.edu.au (S. Kasapis).

http://dx.doi.org/10.1016/j.foodhyd.2015.08.022
0268-005X/

temperature of the protein produces a three dimensional structure, which upon subsequent cooling exhibits properties of an amorphous matrix that undergoes a rubber-to-glass transition. Differential scanning calorimetry and dynamic mechanical analysis have been used extensively to pinpoint the glass transition temperature, T_g, in matrices of high-solid protein (García, Cova, Sandoval, Müller, & Carrasquel, 2012). This observation relates to the diminishing mobility of transverse string-like vibrations of polymer chains that can be displaced considerably in the presence of plasticizer, e.g. lactose. Values of T_g in relation to the storage temperature of food, nutraceutical and pharmaceutical applications are used as an index of quality control and stability against chemical, physical and biological degradation (Kalogeras, 2011).

This study aims to produce whey protein microcapsules *via* the method of spray drying in order to use them as encapsulating agents of nicotinic acid. The structural properties of the polymeric encapsulant are characterized to pursue fundamental understanding of release patterns observed for the microconstituent as a function of time and temperatures of observation. Both the physics of the polymer matrix and the rate of diffusional mobility of the vitamin are important factors for the elucidation of potential functionality in these mixtures.

2. Experimental protocol

2.1. Materials

2.1.1. Whey protein isolate

Work was carried out using a standard whey protein isolate (WPI) from MG Nutritionals, Murray Goulburn Co-operative Co Ltd, Vic, Australia. The composition of the WPI was reported by the supplier as 91.3% protein (TN × 6.38), 0.7% fat, 3.5% moisture, 3.8% ash and 0.44% lactose. pH of 10% (w/w) solution was 6.3, bulk density of the powder was 0.45 mg/mL, with a standard plate count producing 9900 cfu/g.

2.1.2. Nicotinic acid

That was supplied by Sigma–Aldrich Pty Ltd, Sydney, Australia [$C_6H_5NO_2$, molecular weight 123.11 g/mol]. It was in the form of a white powder, with its purity exceeding 99.5%. At concentration of 10 g/L, the vitamin produces aqueous solutions of pH 3.4 at ambient temperature.

2.1.3. Dimethyl sulfoxide

DMSO is an organic solvent widely used in cell cryo-protection and various medical treatments due to its low toxicity (Yu & Quinn, 1994). Its melting and boiling temperatures are 16 and 189 °C, respectively (Sigma–Aldrich, Material Safety Data Sheet). Nicotinic acid is more soluble in DMSO, as compared to ethanol and water over a wide range of temperatures (20–90 °C).

2.1.4. Chemical reagents

Cyanogen bromide, sulfanilic acid, ammonium hydroxide, hydrochloric acid, sodium dihydrogen phosphate monohydrate and sodium hydroxide were obtained from Sigma–Aldrich Co. These reagents were used without further purification and Millipore water type II was the diluent in all experiments.

2.2. Sample preparation

Whey protein dispersions with the addition of nicotinic acid in a phosphate buffer (100 mM, pH 6.5) were prepared by mixing the powders in Millipore water for 2 h and then stored at 4 °C overnight to achieve thorough hydration. Beakers containing these stock solutions of 9.5% w/w whey protein with 0.5% w/w nicotinic acid were wrapped in aluminium foil and the top was sealed with a stretchable film to prevent exposure to light. The dispersion was spray dried using a Lab Plant Spray Dryer SD Basic FT30MKIII (Keison products, Chelmsford, Essex, UK) with a 0.5 mm jet nozzle assembly, a peristaltic pump, a cyclone separator plus a hot air blower and exhaust blower to produce microcapsules.

Feed dispersions were continuously stirred using a magnetic stirrer prior to introduction to the drying chamber, where they were atomised by hot air from the blower at a flow rate of 8.5 mL/min and controlled air pressure of 250 kPa. Inlet and outlet temperatures were 120 and 75 °C, respectively. The spray-dried microcapsules were separated with a cyclone driven by the exhaust blower and collected in a receiving vessel. These were immediately sealed in amber glass bottles and stored at 4 °C for 16 h for further analysis.

2.3. Experimental analysis

2.3.1. Micro-differential scanning calorimetry

Measurements were performed using a Setaram Micro DSC VII (Setu-rau, Caluire, France), with the experimental and reference vessels being inserted into the furnace *via* two cylindrical cavities. Purging rate of nitrogen gas was 50 mL/min. Samples of whey protein with and without nicotinic acid (total solids of 10% w/w) at around 850 mg were accurately weighed into standard batch vessels and hermetically sealed. A vessel with Millipore water of equal weight was used as the reference. Samples were analysed by equilibrating at 20 °C as necessary, ramping the temperature to 85 °C at a rate of 1 °C/min and then cooling to 20 °C at the same scan rate. Triplicates were recorded yielding effectively overlapping thermograms. Analysis allowed recording of the temperature band and enthalpy change in sprayed dried materials, as compared to the largely native protein of the commercial sample, by resuspending microcapsules in Millipore water at the same level of solids, i.e. 10% (w/w).

2.3.2. Dynamic oscillation in-shear

A controlled strain rheometer ARG2 (TA Instruments, New Castle, DE) was used to examine the structure formation of whey protein samples and resuspended materials following spray drying at 10% (w/w) total solids content. Small deformation dynamic oscillation-in shear provides readings of the elastic (storage modulus, G') and viscous (loss modulus, G'') components of the network as a function of temperature using presently a parallel-plate geometry (40 mm diameter). Samples were introduced on a Peltier plate at 25 °C, with the outer edge being covered with silicone oil from BDH (50 cps) to minimise moisture loss. Gelation was induced by heating samples to 85 °C at a scan rate of 1 °C/min and holding there for 20 min. Constant angular frequency and strain at 1 Hz and 1%, respectively, were maintained during the thermal treatment. Duplicate experiments were recorded yielding consistent results.

2.3.3. Dynamic mechanical analysis in-tension

A Perkin–Elmer DMA 8000 (Waltham, MA, USA) was used to examine the mechanical behaviour of whey protein powders in-tension. Analysis was performed in a single cantilever mode at a heating rate of 2 °C/min from −100 °C to 140 °C, with liquid nitrogen as the coolant, at a frequency of 1 Hz and a strain of 0.5 μm. Tensile storage modulus (E'), loss modulus (E'') and tan δ values were recorded throughout, and the glass transition temperature was pinpointed from the maximum point in the loss tangent. Duplicate runs were obtained and low-variation averages are reported.

2.3.4. Wide-angle X-ray scattering

WAXS measurements were performed with a D4 Advanced Bruker AXS goniometer (Karlsruhe, Germany). Diffractograms were obtained within a 2θ range of 5–90° in the measuring interval of 0.1° using Cu–Kα radiation source (0.1–54 nm), tube voltage of 40 kV, tube current of 4 mA at a counting time of 1 s. Data were collected in triplicate at ambient temperature (22 °C) and analysed using DIFFRAC^{plus} Evaluation (Eva), version 10.0 revision 1, which is a Bruker Advanced X-ray Solutions software.

2.3.5. Fourier transform infrared spectroscopy

Micromolecular aspects of our materials were examined using FTIR with a Perkin–Elmer Spectrum 100 that includes a MIRacle™ ZnSe single reflection ATR plate (Perkin Elmer, Norwalk, CT), and ensured that sample loading was consistent throughout the various experimental runs. Absorbance spectra were recorded within the range of 1000–4000 cm^{-1} after background subtraction to eliminate extraneous artifacts. For each spectrum, an average of eight scans was calculated at a resolution of 4 cm^{-1}.

2.3.6. Conventional scanning electron microscopy

Micrographs of the specimens were obtained using a Philips XL30 SEM (Edwards High Vacuum, Sussex, England). Lyophilised and gold plated preparations were analysed under conditions of a high-vacuum mode at an accelerating voltage of 15 kV, spot size from 4.5 to 5 and observing distances of 10 mm. The protocol produced high quality images at magnification of 5000×.

2.3.7. Other physicochemical measurements

Size distribution of microparticles was determined with a laser light scattering method (Mastersizer 3000, Malvern Instruments, Worcestershire, UK). Encapsulation yield (microcapsule weight to initial weight of WPI plus vitamin) and encapsulation efficiency (weight of nicotinic acid in capsule to initial weight of the vitamin) were calculated using standard methodology (Deutsch, 1984; Shu, Yu, Zhao, & Liu, 2006). Moisture content, water activity and colour profiles of the microcapsules were also obtained and results are reproduced in Table 1.

2.3.8. Vitamin release procedure

Fifty mg of microcapsule were exactly weighed and transferred each into twelve 25 mL beakers wrapped with aluminium foil to avoid exposure to light. Each beaker represented a different time of measurement for every experimental temperature, and work was duplicated to require a total of twenty four beakers. These powders and equally twenty four beakers of 5 mL DMSO were incubated separately in a thermostatic water bath for 30 min at a particular temperature followed by a swift transfer of the organic solvent to the sample; DMSO does not mix with the whey protein matrices. Beakers were promptly sealed with stretchable film to prevent solvent evaporation and returned to the required temperature for immediate removal of an aliquot thus setting the zero time of experimentation. The release process was monitored within 5 min for a range of temperatures from 16 to 90 °C. Nicotinic acid solutions were separated from the whey protein microcapsules using a two-step procedure with Whatman No.4 and No.3 filter papers of 22 and 6 μm pore size, respectively. Filtrates were used to estimate the amount of vitamin released in DMSO.

Table 1
Physicochemical characteristics of whey protein microcapsules spray dried at 120 °C with and without nicotinic acid.

Samples	WPI	WPI + nicotinic acid
Encapsulation yield (%)	–	56.0 ± 2.7
Encapsulation efficiency (%)	–	95.2 ± 0.7
Moisture content (%) wet basis	9.4 ± 0.1	9.4 ± 0.1
Water activity	0.4	0.4
L* colour	96.9	97.3
a* colour	−0.5	−0.6
b* colour	4.9	4.5
Particle diameter (μm)	4.6 ± 0.1	5.2 ± 0.2

n = 3; L* = lightness axis (0 is black, 100 is white); a* = red – green axis ("+" values are red, "–" values are green, 0 is neutral); b* = blue–yellow axis ("+" values are yellow, "–" values are blue, 0 is neutral).

2.3.9. Nicotinic acid analysis

That was obtained in the form of absorbance using a colorimetric method and a Lamda 35 UV–vis spectrophotometer (Perkin Elmer, Singapore). It is based on the reaction amongst nicotinic acid, cyanogen bromide and sulfanilic acid (Deutsch, 1984). Accordingly, 50 μL of the filtrate were diluted with 4 mL Millipore water in a plastic tube, which was immediately swirled. Then, 0.5 mL of the diluted sample was mixed with 250 μL of 2% ammonium hydroxide and 2.5 mL of 10% cyanogen bromide solutions. That was held for 30 s and swirled. Following this, 1 mL of 10% sulfanilic acid solution was added to the tube and that was swirled again. The reaction was completed by the addition of 0.5 mL of Millipore water. Yellow colour was obtained and reached a maximum absorbance value within 1 min following the addition of sulfanilic acid to remain as such for 2 min.

Solutions were transferred into 1 cm cuvette to measure maximum absorbance at $\lambda_{max} = 450$ nm. Earlier, a calibration curve was plotted by diluting nicotinic acid in DMSO at a series of concentrations up to 0.5% (w/v), applying the protocol of the preceding paragraph and taking corresponding λ_{max} readings. Blank tests remained colourless, and work was carried out in triplicate yielding highly consistent average values.

3. Results and discussion

3.1. Thermomechanical profiles of whey protein – Nicotinic acid systems

The micromolecular technique of differential scanning calorimetry provides information on enthalpy changes that reflect conformational transitions in biomaterials. It is employed in Fig. 1 to depict thermograms of the commercial ("native") whey protein dispersion, and spray dried materials with or without nicotinic acid at two distinct inlet temperatures. Ten percent total solids of the

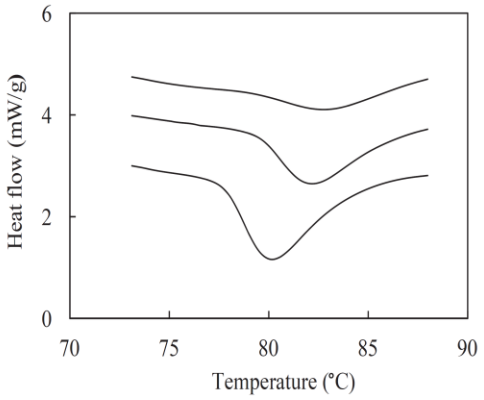

Fig. 1. Micro-DSC thermograms of 10% "native" whey protein, resuspended 9.5% whey protein plus 0.5% nicotinic acid being previously spray dried at 120 °C, and resuspended 10% whey protein being previously spray dried at 200 °C (thermograms arranged successively upwards; scan rate is 1 °C/min).

former create a broad endothermic transition with a midpoint at around 80 °C as a result of the polydisperse nature of the material and low cooperativity of the primarily negatively charged molecules at near neutral pH (Mimouni, Deeth, Whittaker, Gidley, & Bhandari, 2009). The presence of nicotinic acid at 0.5% produces effectively identical heat flow curves with those of the single whey protein preparations (data not shown here). In the slightly acidic aqueous media of this investigation, nicotinic acid is predominantly a non-zwitterion in a weak-acid and highly stable form (Abraham, & Acree, 2013), thus reducing the potential for strong intermolecular interactions with the protein.

In spray drying, the main operating parameter is temperature, which was fixed presently at 120 °C (inlet) and 75 °C (outlet). Fig. 1 demonstrates that spray drying at 120 °C preserves a considerable part of the native conformation of the macromolecule, which upon reconstitution and a subsequent heating scan with micro-DSC produces an endothermic event. This remains broad but is shifted 2 °C higher compared to the commercial whey protein dispersion. We also show the thermogram of a whey protein material that has been spray dried at the rather extreme temperature of 200 °C. This is also partially denatured during processing with a midpoint transition temperature of about 83 °C. Qualitative observations were firmed up by estimating enthalpy changes from the area under the peak of the thermal event. They were 0.55, 0.27 and 0.12 J/g for the commercial material and its spray dried counterparts at 120 and 200 °C, respectively. Within the temperature range of 120–200 °C, the degree of denaturation due to spray drying increases from about 50 to 80% in comparison to the purchased whey protein sample. It has been suggested in the literature that formation of agglomerates during spray drying creates a "protective crust" that prevents complete denaturation of the proteinaceous material (Anandharamakrishnan, Rielly, & Stapley, 2007).

Patterns of enthalpic relaxation were examined in relation to structure development in these systems using dynamic oscillation in-shear. As illustrated in Fig. 2, controlled heating followed by an isothermal run at 85 °C results in a sharp increase in the values of storage modulus for the commercial preparation of 10% whey protein. The heat induced structure formation is attributable to the denaturation of the globular protein (Bryant & McClements, 1998; Yoshii, Neoh, Furata, & Ohkawara, 2008), and produces similar values of rigidity in the presence of 0.5% nicotinic acid, i.e. ~ 0.45 kPa for the mature network at the end of the experimental routine.

It appears that the process of exposing hydrophobic groups to adjacent water molecules persists in samples that have been earlier spray dried at 120 °C leading to a network development, albeit, of reduced strength. Even weaker protein agglomerates, with the onset of three-dimensional structure formation being about 70 °C, are recorded for reconstituted materials that have been earlier spray dried at 200 °C due to rapid droplet drying. Overall, the macromolecular profiles of small-deformation rheology are consistent with the micromolecular events discussed earlier from differential scamming calorimetry.

3.2. Molecular fingerprints and phase morphology of whey protein – Nicotinic acid systems

Thermomechanical work has been complemented by a range of measurements using various physicochemical techniques. To start with, morphological characteristics were identified for vitamin containing microcapsules that have been spray dried at 120 °C (Table 1). Very acceptable encapsulation yield and efficiency were obtained for the polymeric and bioactive constituents of the composite capsule, considering the expected adhesion of agglomerated powders on the interior of the drying chamber (Adhikari, Howes, Bhandari, & Truong, 2001; Sablani, Kasapis, & Rahman, 2007). Encapsulated materials also have low levels of moisture content and water activity, an outcome that bodes well for the chemical and microbial stability of capsule containing formulations. Mean particle size is small and well controlled at about 5 μm influencing positively the sensory perception, for example, of fat replacement. Finally, the various colourimetric parameters indicate that the vitamin containing microparticles maintain a colour composition that is similar to the spray dried whey protein powder, i.e. appealing hues of bright white.

Molecular aspects of the structural morphology in whey protein powders and spray dried materials with or without added vitamin were considered next using XWAD. As depicted in Fig. 3, nicotinic acid is supplied in a crystalline form exhibiting multiple peaks between 15 and 42° at the top diffractogram. On the other hand, native whey protein powder is characterized by two broad peaks centered at 7.4 and 18.6°, with a further shouldering occurring above 30°, which is indicative of a largely amorphous material (Nakano et al., 2000). Spray drying of whey protein does not change this observation and, equally, addition of nicotinic acid maintains the amorphous profile of the spray dried matrix. Diffraction analysis of all whey protein samples in this study indicates a specific

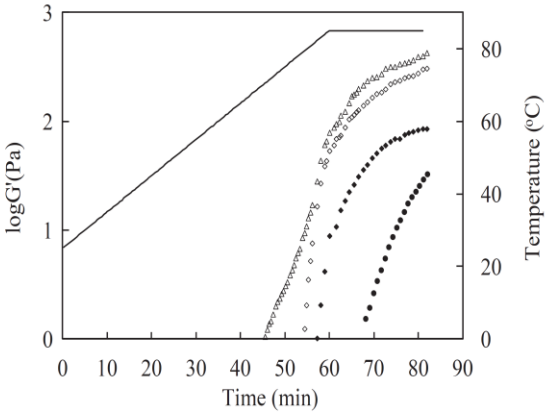

Fig. 2. Storage modulus variation of 10% "native" whey protein (◊), 9.5% whey protein plus 0.5% nicotinic acid (△), resuspended 9.5% whey protein plus 0.5% nicotinic acid being previously spray dried at 120 °C (◆), and resuspended 10% whey protein being previously spray dried at 200 °C (●) (frequency is 1 Hz and strain is 1%).

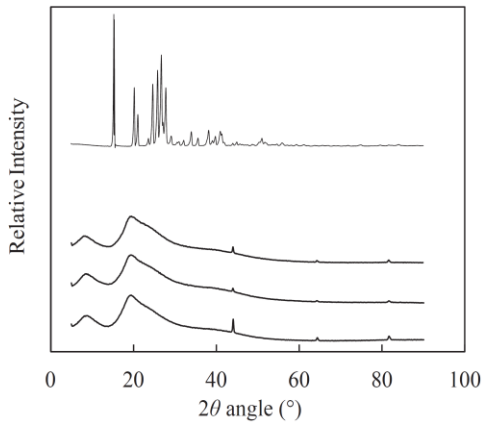

Fig. 3. X-ray diffractograms of whey protein powder as received by the supplier, spray dried whey protein at 120 °C, spray dried whey protein plus nicotinic acid (120 °C), and nicotinic acid crystals arranged successively upwards.

pattern for the calcium salt, which is naturally present in dairy materials, with a well defined peak at around 43° (Tien et al., 2000).

Possible intermolecular associations between the macro and micro-components of our materials were further considered using FTIR. In Fig. 4, prominent infrared spectra that are best positioned to identify the conformational characteristics of protein molecules are clearly visible. These refer to Amide I and II bands of the vibrational modes in the protein backbone. Collectively, they encompass molecular vibrations of the secondary conformation in β-lactoglobulin and α-lactalbumin, which are the two main molecular fractions of whey protein. Amide I band appears between 1620 and 1700 cm^{-1} being mainly attributable to stretching vibrations of the C═O group. Amide II absorption is within 1575 and 1480 cm^{-1} arising principally from N–H bending with a contribution from C–N stretching vibrations (Duongthingoc, George, Katopo, Gorczyca, & Kasapis, 2013). Spectra for the native whey protein, the spray dried counterparts and mixtures with nicotinic acid are according to experience. This outcome suggests that vitamin addition does not initiate considerable alteration of the secondary structure of the protein. Results are consistent with the discussion from thermomechanical and X-ray analyses in Figs. 1–3.

Finally, tangible evidence of the surface topology in single and mixed systems of whey protein/niacin was obtained using conventional scanning electron microscopy. In Fig. 5a, commercial whey protein powder has a spherical geometry with a wide particle-size distribution ranging between 30 and 50 μm. This contrasts strongly with the polymorphic surface of nicotinic acid in the crystalline form (Fig. 5b). Images obtained from spray-dried whey protein at 120 °C in Fig. 5c display a relatively homologous particle size distribution that does not exceed 5 μm (Table 1). It is evident that addition of nicotinic acid to the spray dried whey protein matrix also yields small-size particles (Fig. 5d), which maintain spheroidal characteristics as for the single polymer counterparts.

3.3. Profile of nicotinic acid release from whey protein microcapsules

Once fundamental aspects of the polymer-vitamin system have been explored using the preceding physicochemical protocol, we turned our attention to molecular relaxations that govern quality control parameters including texture and bioactivity in these systems (Gibbs, Kermasha, Alli, & Mulligan, 1999). As mentioned in some detail in Materials and Methods of this work, the König reaction allows formation of a pyridinium compound from niacin and cyanogen bromide, which undergoes rearrangements to couple with an aromatic amine (sulfanilic acid), hence producing coloured derivatives (Bell, 2006). A highly linear calibration curve ($R^2 = 0.996$) obeys the Beer–Lambert law up to 1.0 A to demonstrate the relationship between colour intensity and vitamin content. DMSO was used as the collection tank due to its high miscibility with nicotinic acid (Gonçalves & da Piedade, 2012), and lack of interaction with whey protein (Batista, Batista, Bolzani, Furlan, & Blanch, 2013; Heelan & Corrigan, 1998).

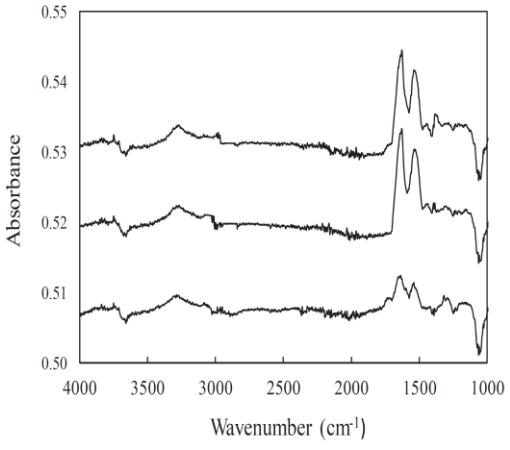

Fig. 4. FTIR spectra of whey protein powder as received by the supplier, spray dried whey protein at 120 °C, and spray dried whey protein plus nicotinic acid (120 °C) arranged successively upwards.

Fig. 6a illustrates diffusion patterns of the vitamin within the whey protein matrix as a function of the time of observation. These are affected considerably by the variation in experimental temperature from 16 to 90 °C. Release is rapid within 2 min of experimentation but approaches asymptotically equilibria at higher timeframes. Results have been replotted in Fig. 6b as a function of the broad temperature range employed presently to demonstrate maxima in absorbance as temperatures around 60 °C. Plotting focused on results in the first 2-min, since these produce overlapping traces at longer timescales of observation. As shown in Figs. 1 and 2, considerable denaturation of the globular molecule occurs at temperatures above 60 °C, which alters the macromolecular characteristics of the proteinaceous structure (Anandharamakrishnan, Rielly, & Stapley, 2008; Pelegrine & Gomes, 2012). The new state of network thermodynamics is reflected in a reduction in absorbance values between 60 and 90 °C, and implications of this observation on transport phenomena of the vitamin will be discussed and quantified in the following sections.

3.4. Free volume effects on the diffusional mobility of nicotinic acid in whey protein systems

The observed reduction in diffusional mobility of the vitamin by lowering the microcapsule temperature below 60 °C in Fig. 6b and the amorphous nature of the protein matrix, from X-ray diffractograms in Fig. 3, indicate that the concept of glass transition is operational under these conditions. This is reported in Fig. 7, which examines the temperature variation in tensile storage and loss modulus of a condensed whey-protein material (~91% w/w solids from data in Table 1) being spray dried at 120 °C. The ratio of E''/E' is known as tan δ (Panyoyai, Bannikova, Small, & Kasapis, 2015), and has also been plotted here. The tan δ peak is considered as an empirical index of convenience that identifies the mechanical T_g in relation to preservation and quality control of processed foodstuffs (Palzer, 2005; Relkin & Shukat, 2012; Renzetti, Voogt, Oliver, & Meinders, 2012). This appears to be at about 30 °C, and should be expected to influence the molecular mobility of nicotinic acid in the whey protein network.

Research in amorphous synthetic polymers commonly relates estimates of the glass transition temperature to the concept of free volume, which in rheological terms is described by the Williams, Landel and Ferry equation (Ferry, 1980):

$$\log a_T = -\frac{C_1^0(T - T_0)}{C_2^0 + T - T_o} = -\frac{(B/2.303f_o)(T - T_o)}{\left(f_o/\alpha_f\right) + T - T_o} \quad (1)$$

where, a_T is the shift factor of viscoelastic functions, C_1^0 and C_2^0 are the WLF constants at a reference temperature, T_o, f_o is the fractional free volume at T_o (the ratio of free to total volume of the macromolecule), α_f is the thermal expansion coefficient and B is usually set to one.

In calculating the fundamental parameters of the WLF equation, i.e. factor a_T and fractional free volume, we used the value of T_g from the tan δ data in Fig. 7 as the reference temperature; therefore f_o is

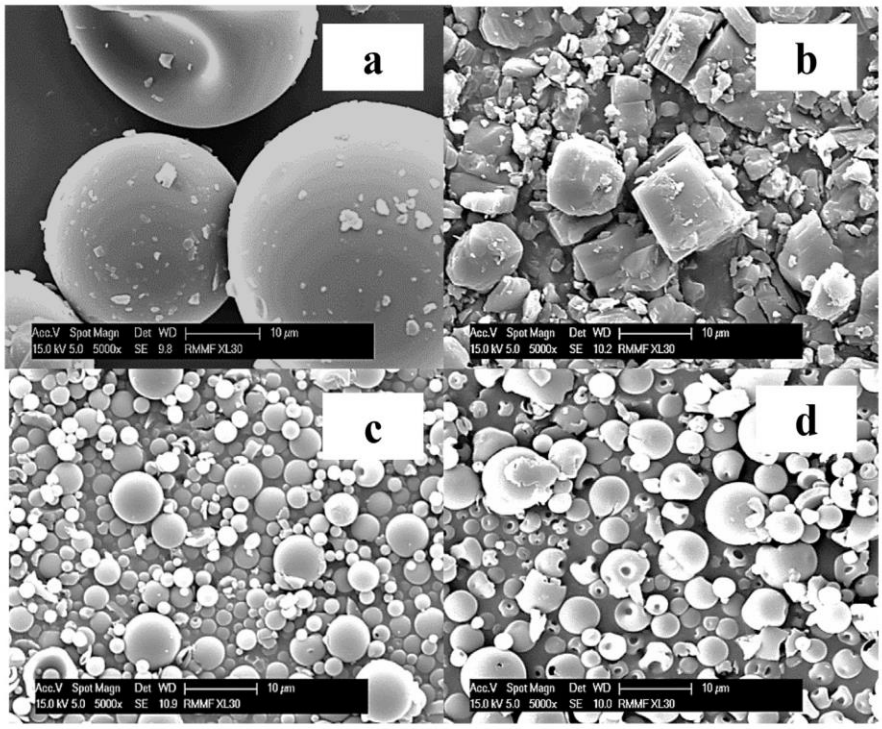

Fig. 5. Micrographs of (a) whey protein as received by the supplier, (b) nicotinic acid crystals, (c) spray dried whey protein at 120 °C, and (d) spray dried whey protein plus nicotinic acid (120 °C) at 5000× magnification.

now f_g. Further, C_1^0 and C_2^0 were 14.97 and 48.33 deg, respectively, from the literature for condensed whey protein systems (Dissanayake et al., 2012). Fig. 8 depicts a smooth and non-exponential relationship in the progression of viscoelastic functions with changing temperature, which is consistent with experience. It extends from 30 to 70 °C, i.e. within the temperature range where, according to results in Figs. 1 and 2, the energetic barrier to conformational rearrangement minimises changes in the thermodynamic nature of the whey protein structure. Remaining parameters of the WLF mathematical framework, i.e. f_g and α_f, are also calculated to be 0.029 and 6×10^{-4} deg^{-1}, respectively.

Regarding the diffusion of niacin within the matrix of spray dried whey protein, we considered a very acceptable linear relationship for the first seven readings of absorbance *versus* time in Fig. 6a. This section of the spectra can be treated as a zero-order kinetic reaction with the gradient being constant at $k = dx/dt$ (Jiang & Kasapis, 2011). A spectroscopic shift factor ($\log k_o/k$) is then advanced covering the experimental temperature range from 16 to 70 °C, where k_o is the rate constant at the reference temperature of 30 °C. Spectroscopic shift factors for the molecular transport of niacin as a function of experimental temperature are also plotted in Fig. 8, and modelled using a modified expression of the Arrhenius equation, which utilises a set of two experimental temperatures (Dissanayake et al., 2013; Jiang & Kasapis, 2011):

$$\log a_T = \left(\frac{k_o}{k}\right) = \frac{E_a}{R}\left(\frac{1}{T} - \frac{1}{T_o}\right) \quad (2)$$

where, E_a is the activation energy of molecular reorientation from one conformational state to another and R is the universal gas constant.

Progress in the spectroscopic shift factor with temperature is followed well by Equation (2) returning a highly linear correlation ($R^2 = 0.920$). Activation energy for the diffusional mobility of the vitamin was thus estimated to be 10.2 kJ/mol, with the corresponding parameter for the whey protein matrix at the glass transition temperature of 30 °C being 256.9 kJ/mol. Treatment of results in Fig. 8 argues that although the glassy consistency of the proteinaceous matrix controls transport patterns of the vitamin, structural relaxation of the two constituents leading to molecular mobility in the composite follows distinct kinetic rates.

3.5. Application of Fickian diffusion to the whey protein – Nicotinic acid system

The working protocol of free volume theory and reaction rate theory from Equations (1) and (2) unveil the molecular dynamics responsible for the diffusion of nicotinic acid within a whey protein matrix spray dried at 120 °C. Next, we addressed the rate of vitamin's diffusion in the polymeric medium of this investigation by considering the concept of Fickian release described by the following power law equation (Ritger & Peppas, 1987):

$$\frac{M_t}{M_\infty} = kt^n \quad (3)$$

where, M_t/M_∞ is the fractional release of a bioactive compound over the release time, t, k is a constant characteristic of the bioactive compound-polymer system, and n is the diffusion exponent for the release mechanism. It has been found experimentally that for spherical geometries, Fickian diffusion is characterised by an n-value of 0.43, Case II diffusion is defined by an n-value of 0.85 making the range of n-values between 0.43 and 0.85 anomalous transport, whereas diffusion rates yielding n-values below 0.43 describe a Less-Fickian regime (Ritger & Peppas, 1987):

Absorbance readings in Fig. 6a were used to produce the relevant parameters from the gradient and intercept of the plot $ln\ M_t/M_\infty$ *vs* $ln\ t$ (s) in Equation (3). These fits are shown in Fig. 9, which

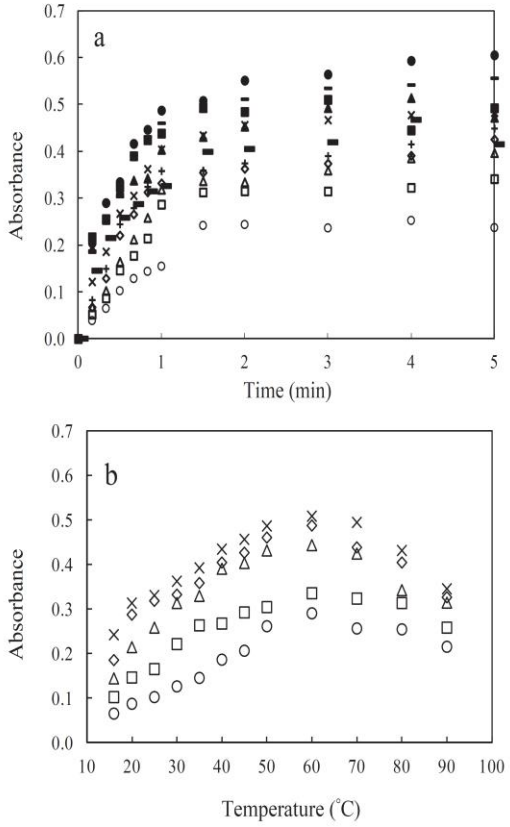

Fig. 6. Release of nicotinic acid from spray dried whey protein microcapsules to DMSO (a) as a function of time of observation at 16 (○), 20 (□), 25(△), 30 (◊), 35 (+), 40 (×), 50 (-), 60 (●), 70 (■), 80 (▲) and 90 (▪) °C, and (b) as a function of experimental temperature for the periods of 20 (○), 30 (□), 50 (△), 60 (◊) and 120 (×) s.

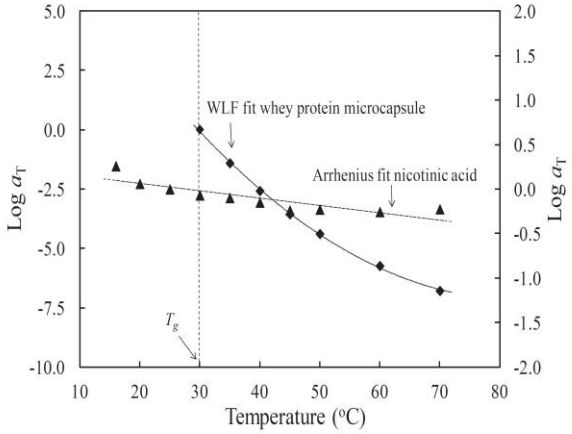

Fig. 8. Logarithmic shift factor, a_T, as a function of temperature for whey protein-nicotinic acid microcapsules (left y-axis, ◆), and nicotinic acid being diffused from the protein matrix to DMSO (right y-axis, ▲), with the arrow indicating the mechanical T_g.

allow estimation of the diffusion exponent and gel characteristic constant in our system. As reproduced in Table 2, *n*-values vary between 0.40 and 0.84 for the experimental temperature range of 16–90 °C. At temperatures below 60 °C where the polymer matrix of whey protein exhibits glassy consistency according to Figs. 7 and 8, molecular mobility is described by an anomalous transport. At temperatures between 60 and 90 °C, however, thermal denaturation recorded in Figs. 1 and 2 increases the density of cross-links in the whey protein network leading to Less-Fickian kinetics in vitamin diffusion.

Fick's second law can be further utilised to estimate the diffusion coefficient, *D*, of a small molecule within a solid-like macromolecular system. It describes the transport of such molecules from the core of the biopolymer matrix to the external collection tank due to a concentration-gradient differential. In this study, we considered spherical microcapsules and only diffusion in the radial direction yielding the following mathematical expression Meinders & van Vliet (2009):

$$\frac{\partial C}{\partial t} = \frac{1}{r^2}\frac{\partial}{\partial r} Dr^2 \frac{\partial C}{\partial r} \tag{4}$$

where, *C* is the concentration of the diffusant molecule in unit of mass per volume in relation to the radial position, *r*.

Equation (4) is a valid application of Fick's second law provided that the finite spherical source is a well-mixed infinite sink, i.e. all points of the polymeric matrix have consistent concentrations of the microconstituent, and particle edge effects are negligible.

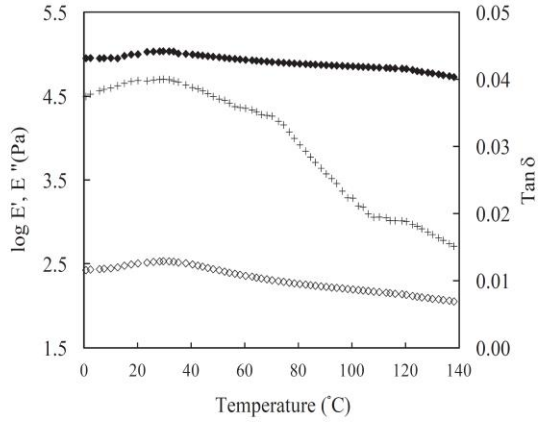

Fig. 7. Tensile storage modulus (*E'*; ◆), loss modulus (*E''*; ◇) and tan δ (+) as a function of temperature for spray dried whey protein plus nicotinic acid at 120 °C (scan rate is 2 °C/min; frequency is 1 Hz).

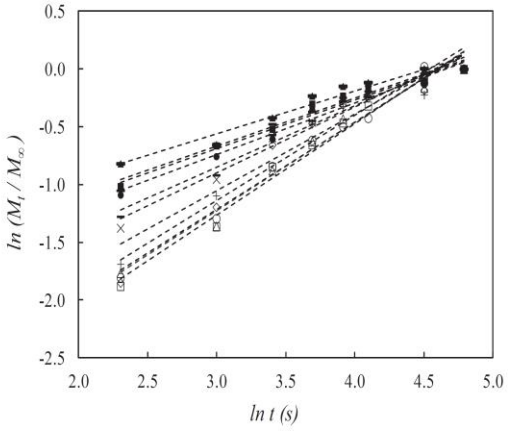

Fig. 9. Plot of $ln\ (M_t/M_\infty)$ *vs* $ln\ t$ (s) for spray dried whey protein plus nicotinic acid (120 °C) at 16 (○), 20 (□), 25 (△), 30 (◊), 35 (+), 40 (×), 50 (-), 60 (●), 70 (■), 80 (▲) and 90 (▪) °C arranged successfully upwards.

Table 2
Diffusion exponent (n) and gel characteristic constant (k) for the release of nicotinic acid from high-solid whey protein capsules.

Temperature (°C)	Diffusion exponent (n)	Gel characteristic constant (k) × 10^{-2}	Diffusion mechanism
16	0.84	2.33	Anomalous
20	0.83	2.18	Anomalous
25	0.83	2.27	Anomalous
30	0.84	1.64	Anomalous
35	0.84	2.53	Anomalous
40	0.68	5.20	Anomalous
45	0.64	6.24	Anomalous
50	0.52	9.94	Anomalous
60	0.49	11.70	Anomalous
70	0.42	15.43	Less-Fickian
80	0.42	17.25	Less-Fickian
90	0.40	6.87	Less-Fickian

Under the above specified conditions, Equation (4) of Fick's second law can be solved in the form of the relative mass change as a function of time Siepmann & Siepmann (2012):

$$\frac{M_t}{M_\infty} = 1 - \frac{6}{\pi^2}\sum_{n=1}^{\infty}\frac{1}{n^2}\exp\left[\frac{-D_{eff}n^2\pi^2 t}{R^2}\right] \quad (5)$$

where, M_t and M_∞ denote the absolute accumulative amounts of compound release at time (t) and infinity (∞), n is a dummy variable in the algorithmic solution, D_{eff} is the effective diffusion coefficient of the compound within the matrix, and R is the radius of spherical particle.

Earlier work in various biomaterials demonstrated that only the first term in this series equation is of consequence, which yields the following relationship (Garbado, Rech, & Ayub, 2011):

$$\ln\left(\frac{M_\infty - M_t}{M_\infty - M_i}\right) = \ln\frac{6}{\pi^2} - \frac{D_{eff}\pi^2 t}{R^2} \quad (6)$$

where, M_i, M_t, and M_∞ denote the absolute amounts of the diffusant compound released at times zero, during experimentation and infinity/equilibrium at each experimental temperature (Fig. 6a in our case), and R is the radius of microcapsules (2.6 μm in Table 1).

Fig. 10 depicts values of the effective diffusion coefficient for nicotinic acid as a function of experimental temperature in spray-dried whey protein microcapsules. These show a considerable decrease from 18.4 × 10^{-15} m^2/s at 60 °C to 8.5 × 10^{-15} m^2/s at the glass transition temperature (30 °C) of the system. Thereafter, i.e. at temperatures that lie within the solid-like glassy state, D_{eff} remains relatively constant at its minimum value. Variation in this essential parameter of the Fickian model follows closely progress in the fractional free volume of the whey protein matrix that is calculated from data in Fig. 8 and is also plotted in Fig. 10. Thus, values of fractional free volume drop rapidly in the glass transition region from 0.053 at 70 °C to a minimum within the glassy state, which is about 0.029 at 16 °C. Beyond 60 °C, i.e. at the point of thermodynamic discontinuity, due to the onset of protein denaturation with heating, values of D_{eff} also decrease to reflect the effect of thermal treatment on the formation of dense protein matrices leading to diminishing diffusional kinetics of the bioactive compound.

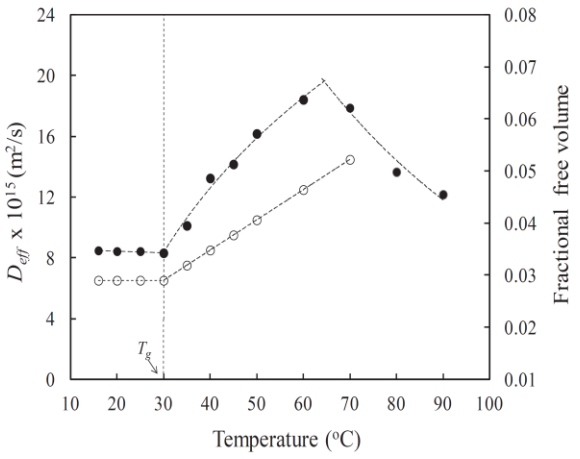

Fig. 10. Effective diffusion coefficient of nicotinic acid from spray dried whey protein (120 °C) to DMSO as a function of temperature (left y-axis, ●), and fractional free volume of the spray dried whey protein matrix (120 °C) (right y-axis, ○), with the arrow indicating the mechanical T_g.

4. Conclusions

This study developed a systematic protocol of experimentation and theory to rationalize the diffusional patterns of nicotinic acid in whey protein microcapsules. Outcomes should have generic interest in the structural relaxation of polymer-bioactive compound composites. Industrial application may emanate from the use of spray drying to achieve multiple droplet processing into high-solid systems with well characterized techno-functionality. It is thus documented that vitamin encapsulating protein matrices are amorphous in nature with a well defined mechanical glass transition temperature. The concept of free volume is operative in the viscoelastic functions of the glassy matrix whose relaxation is distinct from the diffusional mobility of the microconstituent. Temperature variability in the transfer of the vitamin was conveniently analysed with Fick's second law to unveil the effective diffusion coefficient. This is affected both by the extent of globular protein denaturation and the vitrification state of the polymeric network. Indeed, it is quite remarkable that a comprehensive relationship between free volume of the polymeric chain segments and diffusion rates of niacin in relation to experimental temperature is identified in Fig. 10 of the work.

Acknowledgements

Naksit Panyoyai would like to thank the Cooperation Office in The Civil Service Commission of the Thai Government for a scholarship award.

References

Abiad, M. G., Carvajal, M. T., & Campanella, O. H. (2009). A review on methods and theories to describe the glass transition phenomena: applications in food and pharmaceutical products. *Food Engineering Reviews, 1*, 105–132.
Abraham, M., & Acree, W. E., Jr. (2013). On the solubility of nicotinic acid and

isonicotinic acid in water and organic solvents. *The Journal of Chemical Thermodynamics, 61*, 74–78.
Adhikari, B., Howes, T., Bhandari, B. R., & Truong, V. (2001). Stickiness in foods: a review of mechanisms and test methods. *International Journal of Food Properties, 4*, 1–33.
Anandharamakrishnan, C., Rielly, C. D., & Stapley, A. G. F. (2007). Effects of process variables on the denaturation of whey proteins during spray drying. *Drying Technology, 25*, 799–807.
Anandharamakrishnan, C., Rielly, C. D., & Stapley, A. G. F. (2008). Loss of solubility of α-lactalbumin and β-lactoglobulin during the spray drying of whey proteins. *Lebensmittel-Wissenschaft & Technologie, 41*, 270–277.
Batista, A. N. L., Batista, J. M., Jr., Bolzani, V. S., Furlan, M., & Blanch, E. W. (2013). Selective DMSO-induced conformational changes in protein from Raman optical activity. *Physical Chemistry Chemical Physics, 15*, 20147–20152.
Bell, G. F. M. (2006). *Vitamin in foods: Analysis, bioavailability and stability* (pp. 373–374). Florida: CRC Press, Taylor & Francis Group, Boca Raton.
Bryant, C. M., & McClements, D. J. (1998). Molecular basis of protein functionality with special consideration of cold-set gels derived from heat-denatured whey. *Trends in Food Science & Technology, 9*, 143–151.
Bui, L. T. T., Small, D. M., & Coad, R. (2013). The stability of water-soluble vitamins and issues in the fortification of foods. In V. R. Preedy, V. R. Srirajaskanthan, & V. B. Patel (Eds.), *Handbook of food fortification and health: From concepts to public health applications* (Vol. 1, pp. 199–211). New York: Humana Press, Springer.
Chen, L., Remondetto, G. E., & Subirade, M. (2006). Food protein-based materials as nutraceutical delivery systems. *Trends in Food Science & Technology, 17*, 272–283.
Deutsch, M. J. (1984). Vitamins and other nutrients. In S. Williams (Ed.), *Official Methods of Analysis of The Association of Official Analysis Chemists* (pp. 841–842). Virginia: AOAC International.
Dissanayake, M., Kasapis, S., Chaudhary, V., Adhikari, B., Palmer, M., & Meurer, B. (2012). Unexpected high pressure effects on the structural properties of condensed whey protein systems. *Biopolymers, 97*, 963–973.
Dissanayake, M., Kasapis, S., George, P., Adhikari, B., Palmer, M., & Meurer, B. (2013). Hydrostatic pressure effects on the structure properties of condensed whey protein/lactose systems. *Food Hydrocolloids, 30*, 632–640.
Duongthingoc, D., George, P., Katopo, L., Gorczyca, E., & Kasapis, S. (2013). Effect of whey protein agglomeration on spray dried microcapsules containing *Saccharomyces boulardii*. *Food Chemistry, 141*, 1782–1788.
Evans, J., Zulewska, J., Newbold, M., Drake, M. A., & Barbano, D. M. (2010). Comparison of composition and sensory properties of 80% whey protein and milk serum protein concentrates. *Journal of Dairy Science, 93*, 1824–1843.
Ferry, J. D. (1980). Dependence of viscoelastic behavior on temperature and pressure. In *Viscoelastic properties of polymers*. New York: John Wiley.
Garbado, S., Rech, R., & Ayub, M. A. Z. (2011). Determination of lactose and ethanol diffusion coefficient in calcium alginate gel spheres: predicting values to be used in immobilized bioreactors. *Journal of Chemical & Engineering Data, 56*, 2305–2309.
García, L., Cova, A., Sandoval, A. J., Müller, A. J., & Carrasquel, L. M. (2012). Glass transition temperatures of cassava starch–whey protein concentrate systems at low and intermediate water content. *Carbohydrate Polymers, 87*, 1375–1382.
Gibbs, B. F., Kermasha, S., Alli, I., & Mulligan, C. N. (1999). Encapsulation in the food industry: a review. *International Journal of Food Science and Nutrition, 50*, 213–224.
Gonçalves, E. M., & da Piedade, M. E. M. (2012). Solubility of nicotinic acid in water, ethanol, acetone, diethyl ether, acetonitrile and dimethyl sulfoxide. *The Journal of Chemical Thermodynamics, 47*, 326–371.
Gunasekaran, S., Ko, S., & Xiao, L. (2007). Use of whey proteins for encapsulation and controlled delivery applications. *Journal of Food Engineering, 83*, 31–40.
Heelan, B. A., & Corrigan, O. I. (1998). Preparation and evaluation of microspheres prepared from whey protein isolate. *Journal of Microencapsulation, 15*, 93–105.
Jiang, B., & Kasapis, S. (2011). Kinetics of a bioactive-compound (caffeine) mobility at the vicinity of the mechanical glass transition temperature induced by gelling polysaccharide. *Journal of Agricultural and Food Chemistry, 59*, 11825–11832.
Ju, Z. Y., & Kilara, A. (1998). Gelation of pH-aggregate whey protein isolate solution induced by heat, protease, calcium salt, and acidulant. *Journal of Agricultural and Food Chemistry, 46*, 1830–1835.
Kalogeras, I. M. (2011). A novel approach for analyzing glass-transition temperature vs. composition patterns: application to pharmaceutical compound + polymer systems. *European Journal of Pharmaceutical Sciences, 42*, 470–483.
Liu, G., & Zhong, Q. (2013). Thermal aggregation properties of whey protein glycated with various saccharides. *Food Hydrocolloids, 32*, 87–96.
Meinders, M. B. J., & van Vliet, T. (2009). Modeling water sorption dynamics of cellular solid food systems using free volume theory. *Food Hydrocolloids, 23*, 2234–2242.
Mimouni, A., Deeth, H. C., Whittaker, A. K., Gidley, M. J., & Bhandari, B. R. (2009). Rehydration process of milk protein concentrate powder monitored by static light scattering. *Food Hydrocolloids, 23*, 1958–1965.
Nakano, T., Sugimoto, Y., Ibrahim, H. R., Toba, Y., Aoe, S., & Aoki, T. (2000). Preparation and characterization of milk calcium salts by using casein phosphopeptide. *Preparative Biochemistry and Biotechnology, 30*, 155–166.
Palzer, S. (2005). The effect of glass transition on the desired and undesired agglomeration of amorphous food powders. *Chemical Engineering Science, 60*, 3959–3968.
Panyoyai, N., Bannikova, A., Small, D. M., & Kasapis, S. (2015). Controlled release of thiamin in a glassy carrageenan/glucose syrup matrix. *Carbohydrate Polymers, 115*, 723–731.
Pelegrine, D. H. G., & Gomes, M. T. M. S. (2012). Analysis of whey protein solubility at high temperatures. *International Journal of Food Engineering, 8*. http://dx.doi.org/10.1515/1556-3758.1265. Article 23.
Relkin, P., & Shukat, R. (2012). Food protein aggregates as vitamin-matrix carriers: impact of processing conditions. *Food Chemistry, 134*, 2141–2148.
Renzetti, S., Voogt, J. A., Oliver, L., & Meinders, M. B. J. (2012). Water migration mechanisms in amorphous powder material and related agglomeration propensity. *Journal of Food Engineering, 110*, 160–168.
Ritger, P. L., & Peppas, N. A. (1987). A simple equation for description of solute release I. Fickian and non-Fickian release from non-swellable devices in the form of slabs, spheres, cylinders or discs. *Journal of Controlled Release, 5*, 23–36.
Sablani, S. S., Kasapis, S., & Rahman, M. S. (2007). Evaluating water activity and glass transition concepts for food stability. *Journal of Food Engineering, 78*, 266–271.
Shu, B., Yu, W., Zhao, Y., & Liu, X. (2006). Study on microencapsulation of lycopene by spray-drying. *Journal of Food Engineering, 76*, 664–669.
Siepmann, J., & Siepmann, F. (2012). Modeling of diffusion controlled drug delivery. *Journal of Controlled Release, 161*, 351–362.
Tien, C. L., Letendre, M., Ispas-Szabo, P., Mateescu, M. A., Delmas-Patterson, G., Yu, H.-L., et al. (2000). Development of biodegradable films from whey proteins by cross-linking and entrapment in cellulose. *Journal of Agricultural and Food Chemistry, 48*, 5566–5577.
Yang, N., Liu, Y., Ashton, J., Gorczyca, E., & Kasapis, S. (2013). Phase behavior and *in vitro* hydrolysis of wheat starch in mixture with whey protein. *Food Chemistry, 137*, 76–82.
Yoshii, H., Neoh, T. L., Furata, T., & Ohkawara, M. (2008). Encapsulation of proteins by spray drying and crystal transformation method. *Drying Technology, 26*, 1308–1312.
Yu, Z., & Quinn, P. J. (1994). Dimethyl sulfoxide: a review of its applications in cell biology. *Bioscience Report, 14*, 259–281.

CHAPTER 6

RELEASE OF TOCOPHERYL ACETATE IN RELATION TO FREE VOLUME OF STARCH MICROCAPSULES

ABSTRACT

The concept of glass transition for amorphous materials has been applied to predict the molecular mobility of food carbohydrates. To extend the important concept of nutrient delivery, spray-dried tocopheryl acetate microcapsules using modified waxy maize starch as encapsulating material were prepared to model the vitamin diffusion and macromolecular motion of starch governed by T_g. Thermal and rheological measurements including X-ray diffraction techniques were employed to propose amorphicity for the generated particles. Highly efficient micro particles were evaluated for the vitamin release rate as a function of time and temperature. Changes of high-solid viscoelasticity in spherical microcapsules have consequences for the levels of vitamin diffusion. Mathematical models based on T_g and free volume analysis tailored the dependence of nutrient diffusion in the vicinity of T_g, whereas the volume enlargement of the matrix with increasing temperature drives a higher release. This research suggested that an understanding of glass transition in high-solid amorphous carbohydrates offers a new window of encapsulation processes for the physical release of micronutrients.

Keywords: waxy maize starch, tocopheryl acetate, glass transition, diffusional mobility, spray dried microcapsules

6.1 INTRODUCTION

The release of bioactive compound has applications in a wide variety of foods, drugs and nutraceuticals aiming to deliver and adjust diffusion at a specific dosage form, including target and release conditions. To allow understanding and predicting the release profiles, numerous theories, mechanisms and mathematical models have been developed based on a combination of releasing factors involving bioactive compound concentration and solubility, physicochemical and geometry of delivery devices, temperatures and time of release (Panyoyai, Bannikova, Small, Shanks, & Kasapis, 2015). Bioactive compound diffusion out of the device is one kind of mass transport processes that could be simply quantified the diffusion coefficient based on Fick's laws of diffusion (Siepmann & Siepmann, 2008, 2012). In the unsteady state, Fick's 2^{nd} law relates the change in bioactive compound concentration as a function of time yielding diffusivity with respect to position of delivery device at a constant temperature.

Diffusion of bioactive compound in condensed biopolymer system is governed by glassy dynamics. Previous studies show the complexity of diffusion associated with thermodynamic and kinetics of polymeric materials (Panyoyai, Bannikova, Small, Shanks, & Kasapis, 2015; Paramita, Bannikova, & Kasapis, 2015). In a glassy state, the polymer has a less free volume due to a limitation of chain motion and entanglement in a non-thermodynamic equilibrium. Diffusion of bioactive compounds in this region is a slow kinetic and no time-dependent effect of biopolymer relaxation. Similar to a glassy material, rubbery biopolymers relax in a very short time as compare to the diffusion-time scale thus allow the bioactive compound to freely flow out the polymer matrix. In both cases, literature has suggested Fickian's concept is valid to explain the diffusion of fluid in glassy and rubbery state of porous foods (Takhar, 2008). However, Fick's law based models are not sufficient to describe the release in biopolymers near a glass transition

where the macromolecule dynamic is governed by viscoelastic relaxation. The contribution of time-dependent of viscoelastic property has been observed in the non-Fickian or anomalous diffusion (Kee, Liu, & Hinestroza, 2005).

Food polymer based microcapsules behave more like brittle solids in the glassy state, whereas in the melt exhibit liquid-like properties. Macromolecular kinetics during a glass transition has been widely explained with Williams-Landel-Ferry equation and free volume theory indicating a linear of free volume fraction of viscoelastic materials as a function of temperature above glass transition (Ubbink & Krüger, 2006). In contrast, in the classical reaction-rate theory, the modified Arrhenius kinetics predicts the glassy stability and flow processes in the rubbery regime (Palzer, 2005 & 2010; Sablani, Syamaladevi, & Swanson, 2010). The mechanical T_g is the thermodynamic parameter used to distinguish the glassy and glass transition regions. In a high-solid food polymer matrix, large scale motions of biopolymer segments are restricted in the glassy stage but diffusion of organic compounds increased the transport at elevated temperatures above T_g (Kasapis, 2009b).

Core-shell system of vitamin/biopolymer microcapsule technique is of interest as vitamin delivery system (Chiu & Solarek, 2009; Laovachirasuwan, Peerapattana, Srijesdaruk, Chitropas & Utsaka, 2010; Palma-Rodriguez, Agama-Acevedo, Gonzalez-Soto, Vernon-Carter, Alvarez-Ramirez, & Bello-Perez, 2013). In this study, the modified waxy maize starch carries lipid soluble vitamin, tocopherol acetate in high-solid contents to deserve a key role of the vitamin in the protection of bodily tissues from oxidation, assisting fertility, and maintaining immune and heart health (Buddrick, Jones, Morrison, Small, 2013; Lin, & Pascall, 2014). Spray drying allows the low viscosity of modified starch solution (Beirão-da-Costa, Duarte, Moldão-Martins, & Beirão-da-Costa, 2011; Gonzalez-Soto, da la Vega, García-Suarez, Agama-Acevedo, & Bello-Pérez, 2011) to form a glassy amylopectin network (Copeland, Blazek, Salman, & Tang, 2009; Jobling, 2004; Singh, Singh, Kaur, Sodhi, & Gill, 2003; Kasapis, Sablani, & Biliaderis, 2000) and

preserve the vitamin in microcapsules during storage and release (Parada & Aguilera, 2007; Turgeon & Rioux, 2011). Vitamin E release from spherical capsules was monitored in a broad range of 100°C. Thermomechanical analysis was employed to indicate physical changes in molecular mobility of polymeric matrices in terms of mechanical T_g and free volume fractions those parameters were then utilised to elucidate the vitamin release.

6.2 EXPERIMENTAL PROTOCOL

6.2.1 Materials

6.2.1.1 Waxy maize starch

A commercially modified waxy maize starch-Capsule® (MS) was supplied by National Starch & Chemical Pty. Ltd., Bangkok, Thailand. The white starch powder comprised 91% carbohydrate, 0.5% protein, 0.15% fat, <0.5% ash and 7.85% moisture.

6.2.1.2 α-Tocopheryl acetate

Vitamin E acetate [$C_{31}H_{52}O_3$, molecular weight 472.74 g/mol] in a yellow liquid form (96% purity) was obtained from Sigma-Aldrich Pty. Ltd. The vitamin was stored at low temperature (4°C).

6.2.1.3 Absolute ethanol

Ethanol is colourless liquid (more than 99% purity). The freezing point and boiling point of the solvent is -115°C and 78°C, respectively (Material Safety Data Sheet from the chemical supplier), so it allows us to employ mobility studies in a wide range of temperature (-30 to 70°C).

6.2.1.4 Chemical reagents

Vanillin, phosphoric acid solution (85%) and sulfuric acid (95%) were analytical-reagent grade. All reagents were used without further purification and Millipore type II water was used as eluent in all experiments.

6.2.2 Sample preparation

Maize starch dispersion was prepared by dissolving the powder in Millipore water, mixing for 2 hr, then heating at 70°C for 15 min to ensure thorough starch gelatinisation and encapsulate vitamin in a liquid form, as mentioned in the work of Fu, Wang, Li, & Adhikari (2012) and then holding at 4°C overnight. Before encapsulation, tocopheryl acetate was dissolved in absolute ethanol with the mixture being constantly stirred with a magnetic bar. In an aluminium-foil wrapped bottle, the heat-treated starch dispersion and vitamin in ethanol was optimised the final concentration containing the stock dispersions of 9.5% w/w starch with 0.5% w/w tocopheryl acetate. Homogenisation was carried out at 3,500 rpm for 5 min through a shear homogeniser (Model T25D, IKA®,Germany) to obtain a stable and uniform hydrophobic active core of tocopheryl acetate in starch solutions. The samples were then spray dried using a mini spray dryer (Model FT30MKIII, Keison products, Chelmsford, Essex, UK) with a 0.5 mm jet nozzle assembly. The spray dryer was equipped with a peristaltic pump, a cyclone separator, a hot air blower and an exhaust blower to produce microcapsules.

The drying operation was run by feeding treated starch solution at ambient temperature into the drying chamber where they were atomised by the hot air from the blower (inlet and outlet temperatures at 120°C and 75°C, respectively) in a downward co-current flow mode with the controlled air pressure of 250 kPa and the feed rate of 7.5 ml/min. The spray-dried microcapsules were separated by a cyclone driven by the exhaust blower and gathered in closed vials with a known weight. The powder products were then

immediately sealed in amber glass bottles, weighted and stored at -30°C in the dark for further experimental analysis.

6.2.3 Experimental analysis

6.2.3.1 Vitamin release studies

Vitamin release from microcapsules to ethanol was determined within 30 min for a range of temperature from -30 to 70°C. The 50 mg of microcapsules into twelve 25 ml beakers covered with aluminium foil for light protection and 5 ml of the organic solvent in beakers were separately incubated in a thermostatic water bath (Thermoline, Australia) for 30 min at an experimental temperature. Each beaker represented a different sampling time of release for every experimental temperature, and measurements were duplicated resulting in a total of twenty four beakers. The solvent was then added using micropipette to the beakers without mixing with starch powders and then the containers were promptly sealed with stretchable film to minimise solvent evaporation. The systems were still incubated in the water bath for immediately sampling of an aliquot thus setting the initial time of kinetic release. A known aliquot of ethanol contain the vitamin was collected, diluted with absolute ethanol of a known amount and then filtered using a Whatman No.4 filter paper of 20-25 μm pore size. The vitamin content in ethanol was quantified spectrophotometrically using a colorimetric method.

Colorimetric determination of tocopheryl aceatate using a Lamda 35 UV/Visible spectrophotometer (Perkin Elmer, MA, Singapore) was used to examine the vitamin release in the form of absorbance measurements. Tocopheryl acetate in ethanol was determined based on the reaction using the Sulfo-Phospho-Vanillin (SPV) method (Paramita, Bannikova, & Kasapis, 2015). According to the modified method, 100 μl of sample was placed in a glass tube then subjected to heating for 10 min at 100°C for a complete solvent removal. Residue was digested with 250 μl concentrated sulfuric acid

for 10 min at 100°C. Five milliliters of the SPV reagent, a mixture of 3 g of vanillin, 0.5 g of Millipore water and 2 l of concentrated phosphoric acid, were added and mixed vigorously to allow formation of a pink adduct.

The mixture was then incubated at ambient temperature for 30 min for complete colour formation. Final solutions were transferred into 1 cm glass cuvette for further reading of the vitamin absorbance at a set wavelength (λ_{max} = 525 nm). A standard curve was drawn by diluting vitamin in ethanol at a series of concentration up to 0.1%. The blank test remained colourless. Average values are reported from triplicates with standard deviations below $\pm$0.05.

6.2.3.2 Micro differential scanning calorimetry

Setaram Micro DSC VII (Seturau, Caluire, France) was used to perform the thermal event of gelatinisation for our materials. Starch solutions (total solids 10% w/w) both native form and resuspended microcapsules treated with gelatinisation at 70°C and then spray drying at an inlet temperature 120°C were accurately weighted about 850 mg samples with an equal amount of Millipore water in vessels. Sample was stabilised for 20 min at 20°C prior heating from 20 to 85°C at a scan rate of 1°C/min. Setaram propriety software was used to determine the initial, mid and end-gealtinisation temperature of endotherms. Results reported for thermal experiments are of individual traces selected as a representative of duplicates.

6.2.3.3 Dynamic oscillation measurements

A controlled strain rheometer ARG2 (TA Instrument, New Castle, DE) was used to examine the gelatinisation and subsequent structure formation of 10% (w/w) total solids content native starch and microcapsules heated at 70^{o}C before spray drying at an inlet temperature 120^{o}C. Small deformation experiments in shear were performed using a parallel-plate geometry of 40 mm in diameter in order to record the storage modulus ($G^{/}$,

elastic component) and loss modulus ($G^{//}$, viscous component) of the network as a function of temperature. Samples were introduced on a Peltier plate at 20°C, with the outer edge being covered throughout with a thin layer of low density silicon oil was performed by heating solutions to 85°C at a scan rate of 1°C/min and holding there for 20 min. The strain and angular frequency were set constantly during the heating ramp at 1% (within the linear viscoelastic region) and 1 Hz, respectively. Consistent results were obtained from duplicate experiments.

6.2.3.4 Dynamic mechanical measurements

A dynamic mechanical analyser (Perkin–Elmer DMA 8000, Waltham, MA, USA) was used to investigate the mechanical property of spray dried starch/vitamin E microcapsules in compression mode. The thermogram of a sinusoidal force resulted in a small deformation as a function of temperature yielding storage modulus ($E^{/}$), loss modulus ($E^{//}$), tan delta values, and the T_g was identified from the maximum peak in the loss tangent. The amplitude of the deformation was performed at a heating rate of 2°C/min from -100 to 140°C, with liquid nitrogen as the coolant. The measurement parameters were collected at a frequency of 1 Hz and a strain of 0.02%. Duplicate runs were recorded and low-variation averages are presented.

6.2.3.5 Wide angle X-ray diffraction

X-ray powder diffraction measurements were studied on D4 Advanced Bruker AXS (Karlsruhe, Germany) equipped with nickel-filtered Cu/Kα radiation source. Standard sample holders were carefully filled with approximately 0.5 g sample to determine its crystallinity. WAXD patterns between 5° and 90° (2θ) were recorded under the following conditions: an accelerating voltage of 40 kV, tube current of 40 mA and step-scan mode with a step size of 0.1°/min. The degree of crystallinity of samples (the area of crystalline region and area of amorphous region) was estimated using the method

described by Moreau, Bindzus, & Hill (2011) and the Bruker X-ray solutions software, Eva (DIFFRAC^{plus} Evaluation, version 10.0 revision 1). Results reported for WAXD measurements at ambient temperatures (22°C) are of individual traces selected as representative of duplicates.

6.2.3.6 Fourier transform infrared spectroscopy

Transmission FTIR of white powder samples were examined to identify molecular aspects of vitamin/starch microcapsules using a Perkin Elmer Spectrum 100 spectrometer (Perkin Elmer, MA, USA) equipped with MIRacle^{TM} ZnSe single reflection ATR plate. We ensured that sample loading was consistent throughout the various transmission runs. All sample spectra were collected within the wavenumber range of 4000-650 cm^{-1} by averaging 8 scans at 4 cm^{-1} resolution.

6.2.3.7 Conventional scanning electron microscopy and optical microscopy

Morphology of the specimens was observed by a scanning electron microscope, Philips XL30 SEM (Edwards High Vacuum, Sussex, England). The particles were deposited on conductive double-faced adhesive tape and subsequently sputter-coated with gold. SEM observations were performed with conditions of a high-vacuum mode at an operated voltage of 15 kV, spot size (from 4.5 to 5 nm) and observing distance at 10 mm resulting in high quality microscopic images of the present magnification at 3000X. An optical microscope (Nikon eclipse, Nikon H550s, Japan) with the cross polarisation during images was used to investigate the spray dried powder at 200X of a magnification.

6.2.3.8 Other physicochemical measurements

Particle size distribution of microparticles was determined with a laser light scattering method (Mastersizer 3000, Malvern Instruments, and Worcestershire, UK). Encapsulation yield (microcapsule weight to initial weight of starch plus vitamin), encapsulation efficiency (weight of tocopheryl acetate in capsule to initial weight of the vitamin) were calculated with an adapted methodology of Rocha, Fávaro-Trindade, & Grosso (2012) using absolute ethanol as solvent of the vitamin and a spectrophotometer (reading absorbance of the vitamin in the visible wavelength at 525 nm as explained in the previous section). Moisture content, water activity and colour profiles of the microcapsules were also obtained and results are reported in Table 6.1.

Table 6.1 Physicochemical characteristics[a] of waxy maize starch microcapsules spray-dried at an inlet temperature 120°C with and without tocopheryl aceatate

Sample	**MS**	**MS+tocopheryl acetate**
Encapsulation yield (%)	-	57.96±3.27
Encapsulation efficiency (%)	-	89.95±1.23
Moisture content (%) wet basis	10.82 ±0.20	10.47±0.06
Water activity	0.24	0.24
L* colour[b]	100	100
a* colour	-0.16	-0.21
b* colour	6.53	7.24
Particle size distribution (Dv 90) (μm)[C]	13±0.1	15±0.2

Note [a]n = 3

[b] L* = lightness axis (0 is black, 100 is white); a* = red-green axis ("+" values are red, "-" values are green, o is neutral); b* = blue-yellow axis ("+" values are yellow, "-" values are blue, o is neutral)

[c] Dv 90 refers to the maximum size of particle which 90% of the sample lies.

6.3 RESULTS AND DISCUSSION

6.3.1 Release mechanism of tocopheryl acetate/starch microcapsules

Small-scale mobility of vitamin release from the encapsulation could be obtained release profiles as a function of observing time and temperature of the material. It is important to first explore release mechanism in relation to the bioactive compound diffused from device behaving as semipermeable membrane (Kasapis, 2009a). As mentioned in Materials and Methods, this study aims to use the Sulfo-Phospho-Vanilin (SPV) method (Knigh, Anderson, & Rawie, 1972) to quantify the tocopheryl acetate activity. Reaction sequence in three steps suggests that the concentrated sulfuric acid reacts with the vitamin in the initial step to form a carbonium ion and then the phosphoric acid reacts with vanillin to produce a phosphate ester. Finally, the carbonium ion reacts with the carbonyl group of phosphovanillin to form a charged colour complex, which is absorbed at a maximum wavelength of 525 nm. A standard curve ($R^2 = 0.992$) obeying the Beer-Lambert plot up to 0.7 A is produced to demonstrate the relationship between the absorbance intensity and vitamin concentration. Ethanol served as a transport medium because of its high solvation capacity with tocopheryl acetate and lack of inference with the amorphous starch molecules (Lon, Lii, & Chang, 2005)

Fig. 6.1a compares the absorbance of vitamin diffusion within the maize starch matrix as a function of the time of observation. These clearly illustrate the considerable effect of experimental temperature on the release from -30 to 70°C with an increase in colour intensity within 2 min of all experimentations. Fig. 6.2b shows the release profile as a function of the broad temperature range employed presently to demonstrate a monotonic increase in reading absorbance and vitamin release (%). Plotting focused on

release in the first 2 min since longer timescales produced overlapping traces of observation.

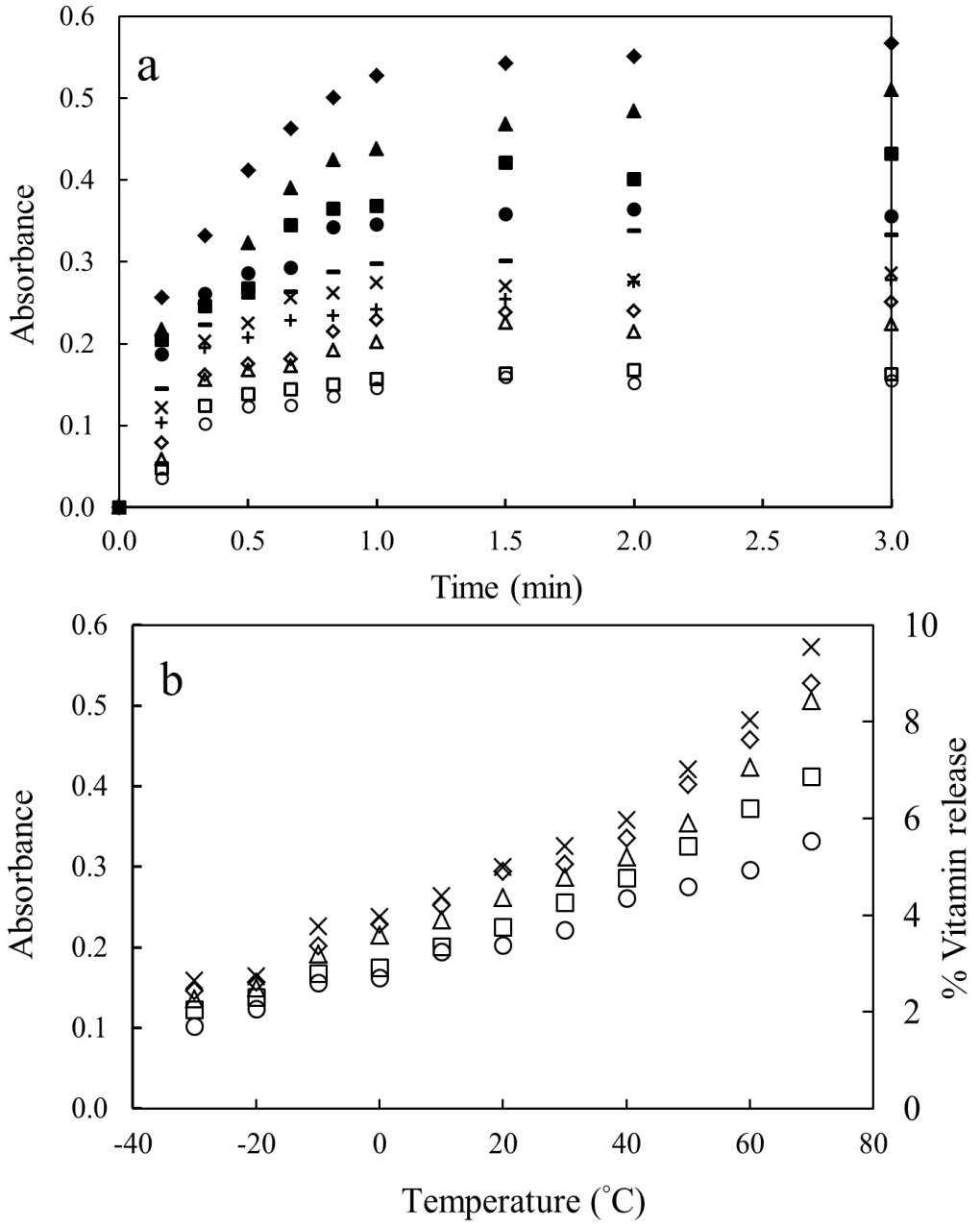

Fig. 6.1 Kinetic release of tocopheryl acetate from spray dried modified waxy maize starch microcapsules to ethanol (a) as a function of the time of observation at -30 (○), -20 (□), -10 (Δ), 0 (◊), 10 (+), 20 (x), 30 (-), 40 (●), 50 (■), 60 (▲) and 70 (♦)°C, and (b) as a function of experimental temperature for the periods of 20 (○), 30 (□), 50 (Δ), 60 (◊) and 120 (x) s

Next, we addressed the transport rate, determining the vitamin's diffusion in the medium of this investigation, by considering the concept of Fickian release described by the following power law equation (Ritger, & Peppas, 1987):

$$\frac{M_t}{M_\infty} = kt^n \tag{6.1}$$

where, M_t/M_∞ is the ratio release of a bioactive compound over the release time, t, k is a constant of the bioactive compound-biopolymer system, and n is the diffusion exponent for the release mechanism. For spherical geometries, perfect Fickian diffusion is characterised by an n-value of 0.43, Case II diffusion is defined by an n-value of 0.85 making the range of n-values between 0.43 and 0.85 anomalous transport, whereas low diffusion rates yield n-values below 0.43 describing a Less-Fickian release (Kuang, Oliveira, & Crean, 2010; Ritger, & Peppas, 1987).

Absorbance data in Fig. 6a was used to produce fundamental parameters from the gradient and intercept of the plot $ln\ M_t/M_\infty$ vs $ln\ t$ (s) in Equation (6.1). These fits are shown in Fig. 6.2, which allow estimation of the diffusion exponent and gel characteristic constant in our system. As reproduced in Table 6.2, all n-values are less than 0.43 for the experimental temperature range of -15 to 70°C. As for n values, Less-Fickian mechanism has also appeared in published reports in relation to the mobility of omega-3-fatty acids in the dense state of a vitrified carbohydrate matrix (Paramita, Bannikova, & Kasapis, 2015). Another possible explanation is the small mesh size of a complex three-dimensional network in condensed amylopectin matrix compared to the bulky structure of tocopheryl acetate leading to entrapment and reduction in the mass transport rate. It could be hypothesised that the vitamin release is controlled by the diffusion mechanism through macromolecular chain mobility of an amorphous wall material which will be further investigated using the concept of glassy dynamics.

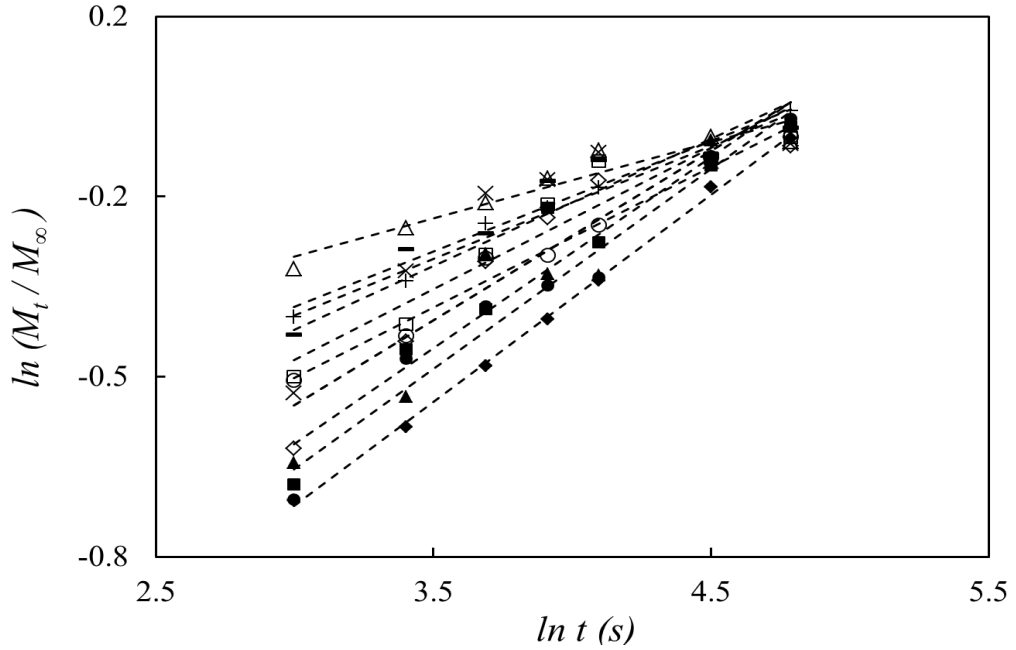

Fig. 6.2 Plot of *ln* (M_t/M_∞) vs *ln t* (s) for spray dried waxy maize starch plus tocopheryl acetate (at an inlet temperature 120°C) at -30 (○), -20 (□), -10 (Δ), 0 (◊), 10 (+), 20 (×), 30 (-), 40 (●), 50 (■), 60 (▲) and 70 (♦)°C

Table 6.2 Diffusion exponents (*n*) and gel characteristic constant (*k*) for the release of tocopheryl acetate from the high-solid waxy maize starch capsules

Temperature (°C)	Diffusion exponent (*n*)	Gel characteristic constant (*k*) × 10^{-2}
-30	0.23	8.3
-20	0.25	6.1
-10	0.21	8.1
0	0.17	14.6
10	0.19	12.2
20	0.17	21.7
30	0.22	10.4
40	0.24	6.1
50	0.28	5.4
60	0.30	3.5
70	0.39	1.5

6.3.2 Thermorheological profiles and glassy dynamics of waxy maize starch/tocopheryl acetate microcapsules

Conformational transitions subsequent to temperature of microcapsules could be investigated using micro differential scanning calorimetry providing enthalpy and thermodynamic transition temperatures. DSC studies (Fig. 6.3) have shown that thermograms of the native waxy maize starch dispersion at 10% (w/w) total solids create a broad endothermic transition temperature at 51.23, 61.65 and 67.65 for onset (T_o), peak (T_p) and conclusion (T_c), respectively. The overall enthalpy (ΔH_{gel}) is estimated at 0.83 J/g for irreversible changes in physicochemical properties including granular swelling, native crystallinity melting, loss of birefringence, and starch solubilisation (Marcotte, Sablani, Kasapis, Baik, & Fusteir, 2004; Muñoz, Pedreschi, Leiva, & Aguilera, 2015; Russel, 1987; Shanks & Gunaratne, 2011; Singh, Kaur, & McCarthy, 2007). Conversely, the thermal transition of 10% (w/w) resuspended microcapsule solution consisting of 9.5% waxy maize starch and 0.5% tocopheryl acetate produced following thermal induced structural conformation with heat treatment at 70°C and spray drying at 120°C inlet temperature has a complete loss of molecular order and crystallinity to interfere the release characteristic.

Dynamic oscillation in shear using the technique of temperature scan was performed to develop a structure of starch suspensions (10% (w/w) total solids) during controlled heating as illustrated in Fig. 6.3. At the temperature below 40°C, a native waxy maize starch solution shows a rapid rise in storage modulus (G') resulting from the heating temperature and reached a maximum at approximately 70°C ($T_{G'\ max}$). Similar pattern occurring as upward moving viscous modulus trace, G'' (data not shown) was because of gelatinisation of the starch fraction. Kong, Kasapis, Bao, & Corke (2009) concluded that starch granule swelling and leaching starch biopolymer chains based on the melting temperature had resulted in the partial loss of starch granule integrity and the formation of

a composite network of hydrated starch. During prolonged heating, a dynamic rheological test resulted in the increase of both moduli, indicating an extended rupture and disintegration of starch granules, melting of the crystalline region remaining in the swollen starch granules, and also weakening of inter-chain interactions of macromolecule mobility.

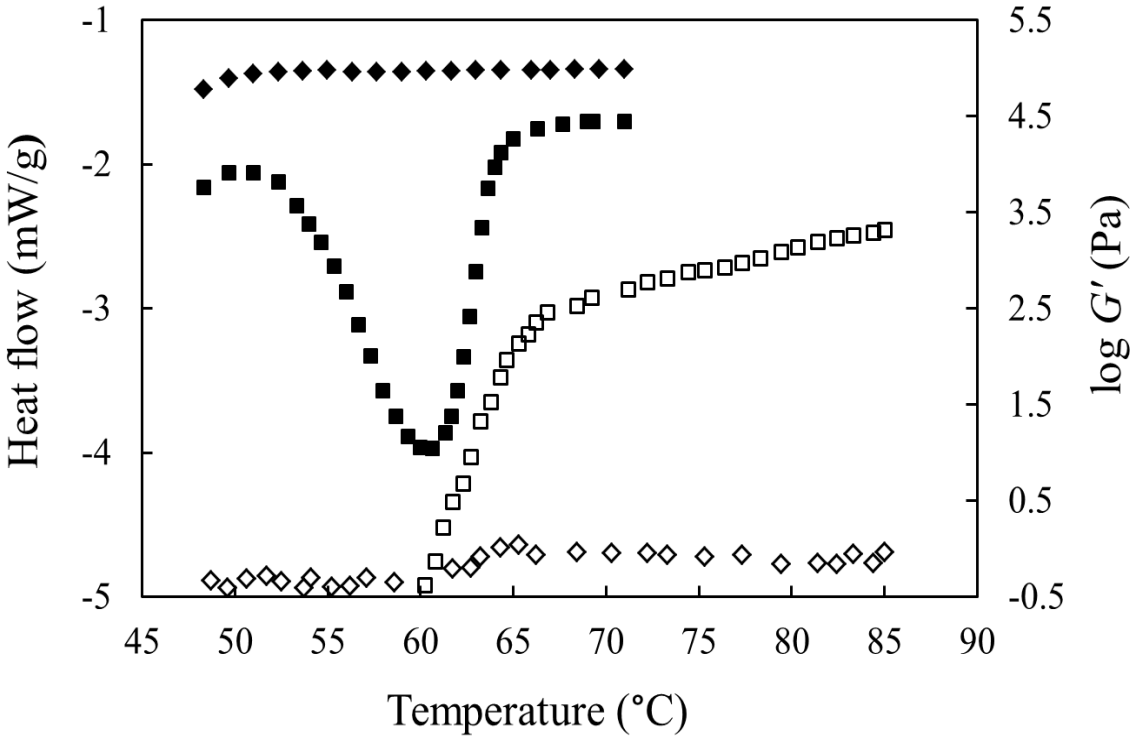

Fig. 6.3 Micro-DSC thermograms at a scan rate 1°C/min (close symbols) and storage modulus variation performing at a frequency of 1 Hz and a strain of 1% (open symbols) of 10% native waxy maize starch (■,□) and resuspended 9.5% modified waxy maize starch plus 0.5% tocopheryl acetate spray dried at an inlet temperature 120°C (♦,◊)

Regarding the process of spray drying, feed solutions of vitamin E/waxy maize starch at 10% (w/w) total solids as well as resuspended microcapsule solutions at the same total solids have relatively flat spectra during a temperature sweep. Using modified starch as encapsulating agent confers emulsifying properties between the vitamin and water leading to a very low viscoelasticity of a homogeneous mixture. It is suggested from literature of Duongthingoc, George, Katopo, Gorczyca, & Kasapis (2013) that biopolymer was treated with the current thermal conditions of the spray drier as discussed earlier from differential scanning calorimetry and the formation of three-dimensional network in rheology.

The material science of carbohydrate matrices relates to the molecular mobility of small organic molecules on temperature variation. The upward trend in the diffusion of the vitamin is shown by increasing the microcapsule temperature up to 70°C in Fig. 6.1b and the nature of the completely gelatinised starch matrix, from DSC as well as from rheological measurement in Fig. 6.3, elaborates the concept of glassy dynamics as a physical approach for the release of the micronutrient. This is reexamined in Fig. 6.4, reporting the heating profile in compression storage (elastic) element of a condensed waxy maize starch material (~90% w/w solids from data in Table 6.1) being spray dried at the inlet temperature of 120°C. Tan δ maximum, i.e. the ratio of E''/E', has been pinpointed here and it appears to be approximately -15°C. This refers to an empirical index of the mechanical T_g in relation to delivering the vitamin in a high-solid carrier (Panyoyai, Bannikova, Small, Shanks, & Kasapis, 2016).

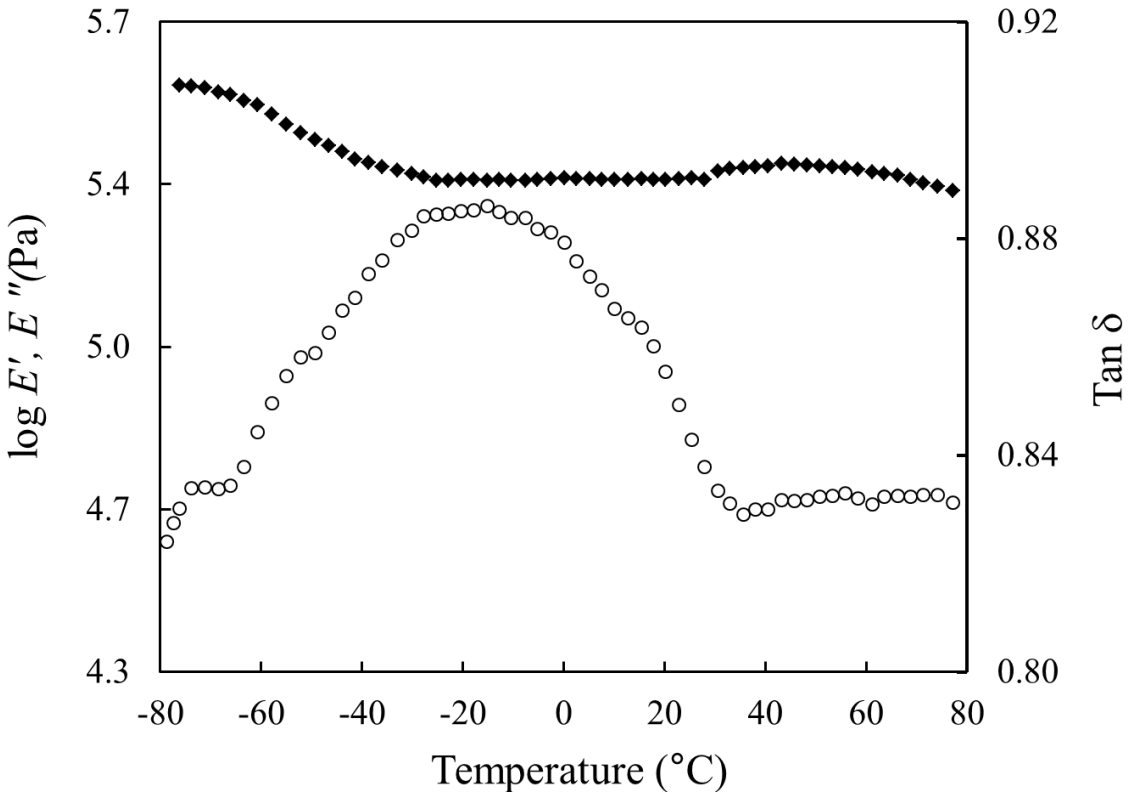

Fig. 6.4 Storage modulus (E'; ♦) and tan δ (○) variations as a function of temperature for waxy maize starch plus tocopheryl acetate spray dried at an inlet temperature 120°C (scan rate is 2°C/min; frequency is 1 Hz)

6.3.3 Molecular fingerprints and charaterisation of waxy maize starch/tocopheryl acetate systems

With the gained background of the biopolymer-vitamin system, physicochemical and morphological characteristics of vitamin E microcapsules spray-dried at 120°C were examined in comparison to a free vitamin counterpart and summarised in Table 6.1. Considerable encapsulation yield and high retention were produced from the amylopectin and micronutrients of the dried microcapsules thus minimising the effect of surface oil

(8.13%) to agglomerate powders on the interior of the drying chamber (Rocha, Fávaro-Trindade, & Grosso, 2012). Formulated vitamin powders also have low levels of moisture content and water activity, being stable against deterioration from chemical reactions and microorganisms (Anwar & Kunz, 2011: Jayasundera, Adhikari, Adhikari, & Aldred, 2011). The colorimetric parameters of the vitamin loaded powder are similar to the spray-dried starch powder, indicating a colour consistency of bright white shade. Finally, particle means diameter shows a small particle size at approximately 15 μm resulting from the droplet formation of low emulsion viscosity during atomisation.

X-ray diffraction analysis was performed to investigate the molecular aspects of the structure of waxy maize starch and spray dried powder with or without added vitamin. According to Fig. 6.5, starch obtained from the supplier shows an A-type crystallisation (Cai, Shi, Rong, & Hsiao, 2010) calculating the degree of crystallinity to be 11.33%. The material exhibited triple peaks at 14, 16 and 22° of the lowest diffractogram. When the material underwent gelatinisation following spray drying, this structure was affected by heat treatment resulting in a small tendency of crystallinity (1.02%) exhibiting clear reflections at 2θ Bragg angles between 10 and 30°. The morphology of starch in the addition of tocophryl acetate maintains the disorganised form (amorphous) profile of the spray dried starch matrix as well as tocopheryl aceate, indicating vitamin retention in the high-solid starch microcapsules. Diffraction analysis of all starch samples in this study reveals a specific pattern of the starch derivative like glucose, which is commonly present in modified starch as well as in a heterocyclic glucose attached to aromatic ring of tocopheryl acetate, with a well specified peak at approximately 43°.

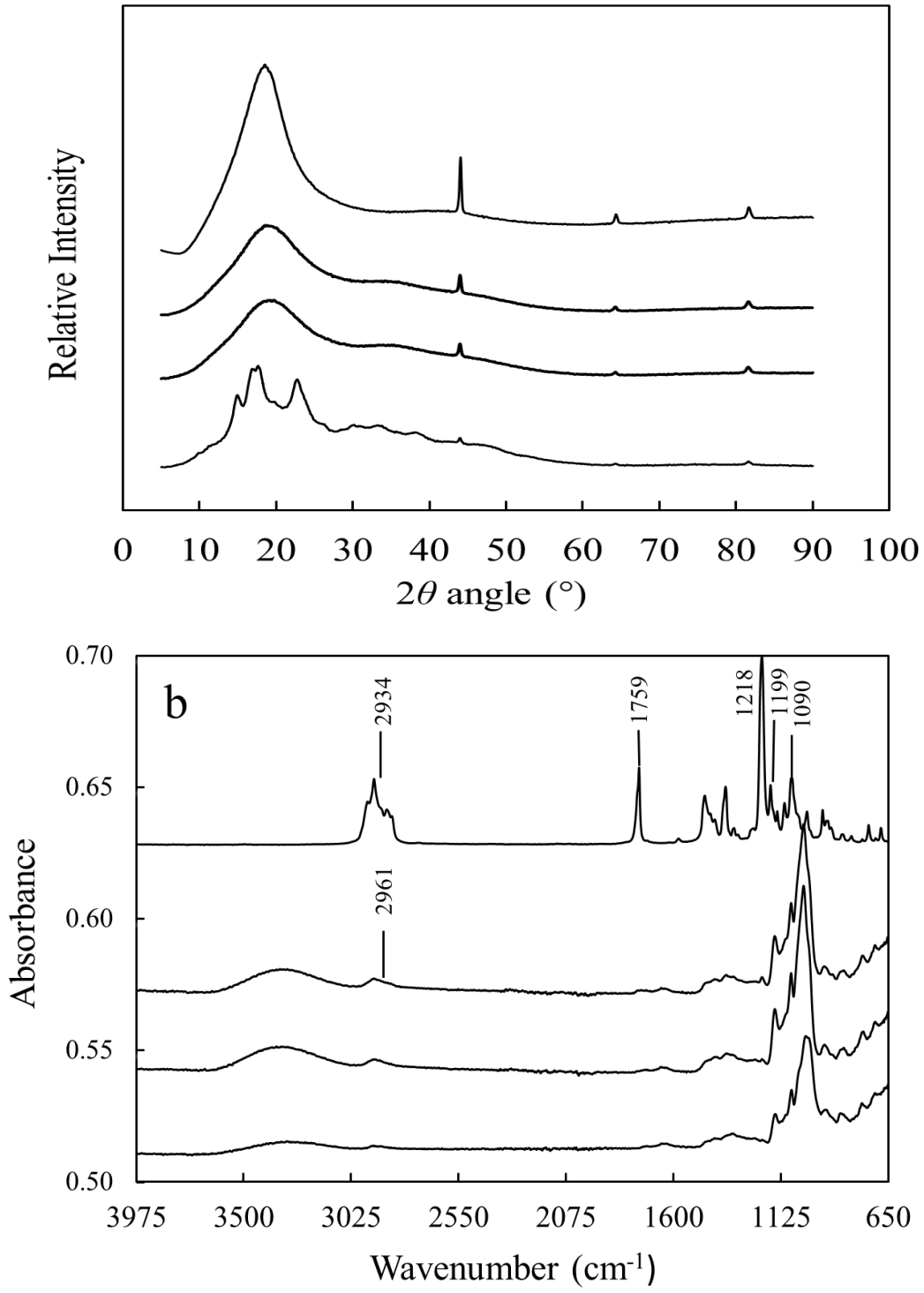

Fig. 6.5 X-ray diffractograms (a) and FTIR absorbance spectra (4000-650 cm^{-1}) (b) of waxy maize starch powder as received by supplier, spray dried maize starch at an inlet temperature 120°C , spray dried maize starch plus tocopheryl acetate (120°C), and tocopheryl acetate arranged successively upwards

In order to investigate possible intermolecular associations of tocopheryl aceate entrapped in waxy maize starch microcapsules, FTIR spectra identified the conformational characteristics of starch molecules of maize starch, spray dried materials and pure vitamin, as compared in Fig. 6.5. All the starch materials have an increase in intensity in the range 3600-3430 cm^{-1} which is hypothesised to be a great number of inter- and intra-molecular hydrogen bonds in capsule formation during the spray drying process. The starch spectrum is characterised by C-H bonds and CH_2 stretching at 2961 cm^{-1}, and C-O bonds in the range 1150-1000 cm^{-1}. There is similarity between the spectra of spray-dried microcapsules and vitamin having the same characteristic overlapping bands arising from CH_2 stretching variation modes between 2965 and 2875 cm^{-1}.The assignment bands of tocopheryl aceate is dominant in CH_2 stretching at 2934 cm^{-1}, C=O at 1759 cm^{-1}, C-O of CH_3COOR at 1218 cm^{-1}, C-O-C in the tocopherol ring at 1199 cm^{-1} and skeletal vibration of tocopherol rings at 1090 cm^{-1} (Gerasimov, Gubarera, Blokh, Cherkasova, & Berezovykw, 1984). This is a clear result that there are homogeneous microcapsules without obvious chemical associations.

Finally, The SEM observation of the surface topology of raw materials and spray dried waxy maize starch/tocopheryl acetate was examined using conventional electron and optical microscopy. In Fig. 6.6a, the morphology of commercial maize starch powder has an irregular polyhedron-shaped granule with a wide distribution of sizes ranging from 5 to 20 μm. The granule morphology appears to be aggregated and deformed upon starch modification.This contrasts strongly with the unshaped characteristic of tocopheryl acetate (Fig. 6.6b). Image obtained from spray-dried maize starch at 120°C in Fig. 6.6c. shows a relatively homologous particle size distribution that is less than 15 μm (Table 6.1) and roughness on the surface due to rapid evaporation of drops of liquid during the atomisation (Carneiro, Tonon, Grosso, & Hubinger, 2013; Rocha, Fávaro-Trindade, & Grosso, 2012).

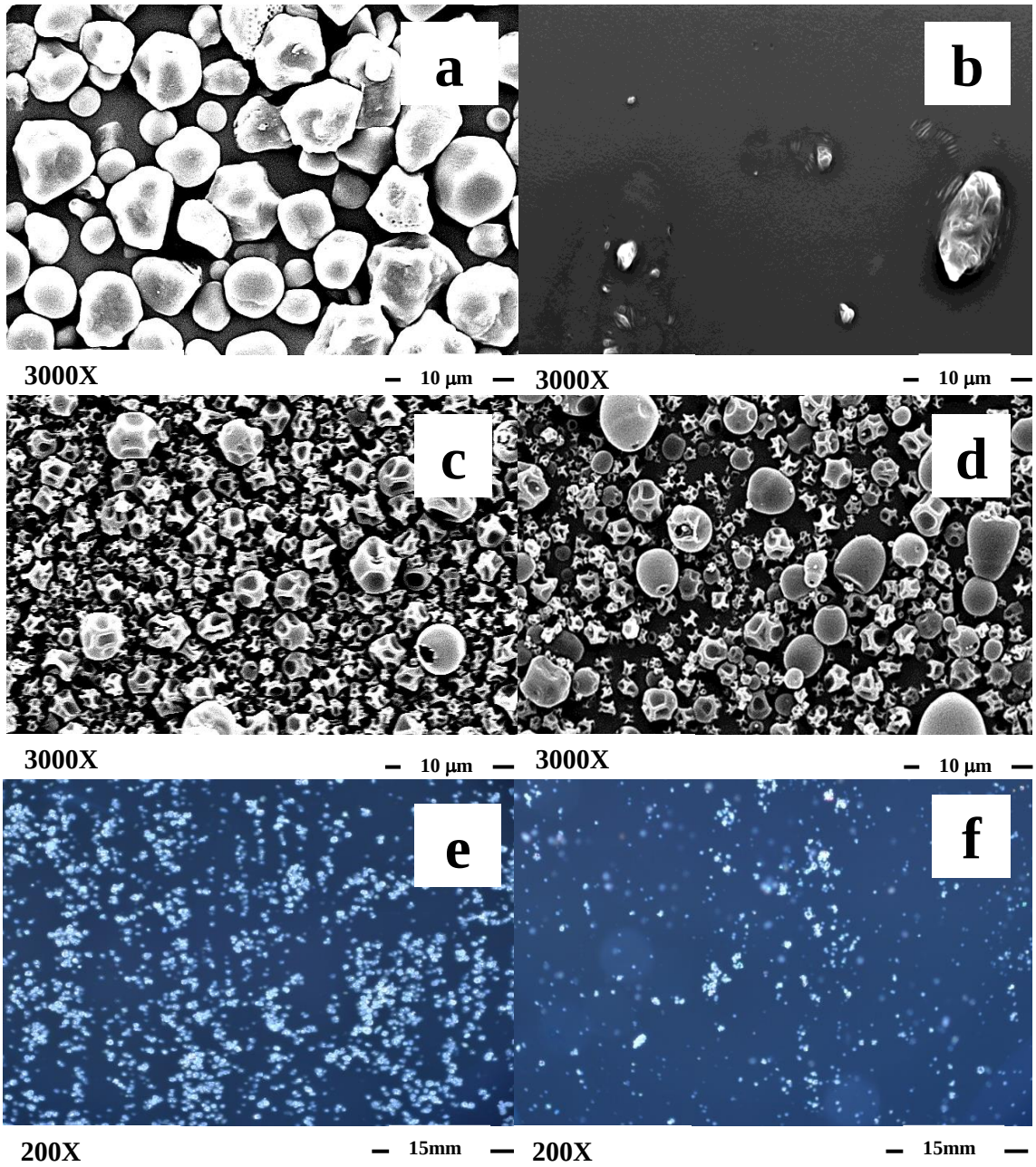

Fig. 6.6 SEM Micrographs of (a) waxy maize starch powder from supplier, (b) tocopheryl acetate, (c) spray dried waxy maize starch at an inlet temperature 120°C, (d) spray dried waxy maize starch plus tocopheryl acetate (120°C) at a magnification of 3000X, (e) optical observations of waxy maize starch powder from supplier, and (f) spray dried waxy maize starch plus tocopheryl acetate (120°C) at a magnification of 200X

It is evident that the encapsulated tocopheryl acetate by the spray dried starch wall also produced micro-size particles (Fig. 6.6d.), with smooth, spherical shape and less

imperfections. Observing the external morphology using the optical microscope, commercial waxy maize starch (Fig. 6.6e) illustrates birefringence of semi-crystallinity. The loss of birefringence tends to be minimised during heating in the presence of large amounts of water leading to granule transformation into formless cells (Fig. 6.6f).

6.3.4 Application of free volume theory to rationalise the diffusional mobility of tocopheryl acetate in starch based microcapsules

The material science of amorphous food matrices relates to the molecular mobility of small organic molecules on temperature variation. Ferry (1980) has shown for amorphous polymers above the T_g the fractional free volume increases linearly with temperature, which is expressed in the Williams, Landel and Ferry (WLF) equation:

$$\log a_T = -\frac{C_1^o (T - T_o)}{C_2^o + T - T_o} = -\frac{(B/2.303 f_o)(T - T_o)}{\left(f_o/\alpha_f\right) + T - T_o} \quad (6.2)$$

where, a_T is the shift factor of viscoelastic functions, C_1^0 and C_2^0 represent the WLF constants at a reference temperature, T_o, f_o is the fractional free volume at T_o (the ratio of free to total volume of the macromolecule), α_f is the thermal expansion coefficient, and B is usually set to 1.

In calculating the WLF parameters, i.e. factor a_T and fractional free volume, we replaced the value of T_g from the tan δ data in Fig. 6.4 as the reference temperature; therefore f_o is now f_g. Further, C_1^0 and C_2^0 were 7.53 and 59.48 deg^{-1}, respectively, from the literature for condensed starch metrix (Shrinivas & Kasapis, 2010). The remaining parameters of the WLF model, i.e. f_g and α_f, are 0.048 and 9.7×10^{-4} deg^{-1}, respectively. Fig. 6.7 depicts a non-exponential curve displaying a relationship in the progression of viscoelastic functions with changing temperature. It extends from -15 to 70°C, i.e. within the temperature range where, according to results in Fig. 6.3, the absence of energetic

barriers to conformational rearrangement prevents changes in the thermodynamic nature of the waxy maize starch matrix.

Based on Fig. 6.1 in relation to the diffusion of tocoperyl acetate within the matrix of spray dried starch, we considered a good linear relationship for the six readings of absorbance vs time. This section of the spectrum can be treated as a zero-order kinetic reaction with the gradient being constant at $k = dx/dt$ (Panyoyai, Bannikova, Small, Shanks, & Kasapis, 2016). A spectroscopic shift factor (log k_o/k) is then advanced covering the changing temperature range from -30 to 70°C, where k_o is the rate constant at the reference temperature of -10°C. Spectroscopic shift factors for the molecular transport of tocopheryl acetate as a function of experimental temperature are also plotted in Fig. 6.7, and modelled using a modified expression of the Arrhenius equation, which utilises a set of two experimental temperatures (Kasapis, 2000):

$$\log a_T = \frac{E_a}{2.303R}\left(\frac{1}{T} - \frac{1}{T_o}\right) \tag{6.3}$$

where, E_a is the activation energy of molecular reorientation from a glassy state to a glass transition, and R is the universal gas constant.

Results of the spectroscopic shift factor with temperature follow well Equation (6.3) returning a highly linear correlation (R^2 = 0.910). Activation energy for the diffusional mobility of the vitamin was thus estimated to be 17 kJ/mol, with the corresponding parameter for the biopolymer matrix at the T_g of -15°C being 127 kJ/mol. Treatment of results from Fig. 6.7 argues that although the glassy consistency of the starchy matrix controls vitamin transport, the structural relaxation of the two constituents, leading to molecular mobility of the active ingredient in microcapsules, follows distinct kinetic rates.

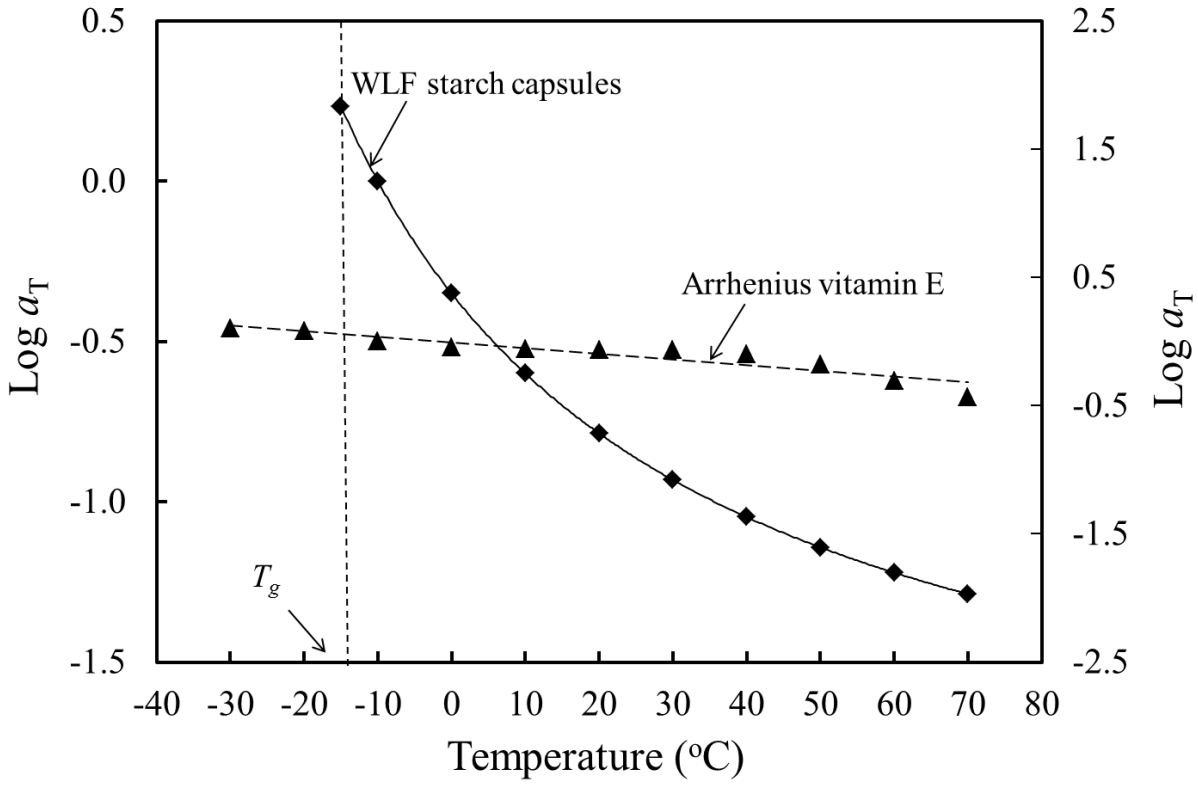

Fig. 6.7 Logarithmic shift factor (a_T) as a function of temperature for waxy maize starch-tocopheryl acetate microcapsules (left- y axis, ♦), and tocophyryl acetate being release from the starch matrix to ethanol (right y-axis, ▲), with the arrow indicating the estimated mechanical T_g from WLF equation

The concepts of free volume and reaction rate theories from Equations (6.2 & 6.3) unveil the molecular dynamics responsible for the diffusion of tocopheryl acetate within a waxy maize starch matrix spray dried at 120°C. Fick's second law can be further utilised to estimate the diffusion coefficient, D, of a vitamin within a solid-like macromolecular system in a glassy state and above T_g (Crank, 1975; Rehage, Ernst, & Fuhrmann, 1970). It describes the transport of such molecules from the core of the biopolymer matrix to the external collection tank due to a concentration-gradient differential. In this study, we considered spherical microcapsules well-mixed infinite sink, only diffusion in the radial direction (Meinder & van Vliet, 2009; Siepmann, & Siepmann, 2008) and regardless the

chemical interactions between vitamin and starch matrix. Earlier work in various our biomaterials demonstrated the release following relationship (Garbado, Rech, & Ayub, 2011):

$$ln\left(\frac{M_\infty - M_t}{M_\infty - M_i}\right) = ln\frac{6}{\pi^2} - \frac{D_{eff}\,\pi^2 t}{R^2} \quad (6.4)$$

where, M_i, M_t, and M_∞ denote the absolute amounts of the diffusant compound released at times zero, during experimentation and infinity/equilibrium at each experimental temperature (Fig. 6.1 in our case), and R is the radius of microcapsules (7.5 μm in Table 6.1).

Fig. 6.8 depicts values of the effective diffusion coefficient for tocopheryl acetate as a function of experimental temperature in spray-dried waxy maize starch microcapsules. These show a considerable decrease approximately half an order of magnitude from 18.34 × 10^{-14} m^2/s at 70°C to 9.3 × 10^{-14} m^2/s at the T_g (-15°C) of the system. Thereafter, i.e. at temperatures that lie within the solid-like glassy state, D_{eff} is at its minimum value. Variation in this essential parameter of the Fickian model follows closely progress in the fractional free volume of the starch matrix that is calculated from data in Fig. 6.7 and is also plotted in Fig. 6.8. Thus, values of the fractional free volume drop rapidly in the glass transition region, e.g. from 0.099 at 70°C, to a constant minimum within the glassy state, e.g. 0.037 at -15°C. Beyond -15°C, i.e. at the point of thermodynamic discontinuity, values of D_{eff} also increase to reflect the thermal effect on the malleable dense starch matrices and enhanced diffusional kinetics of the bioactive compound.

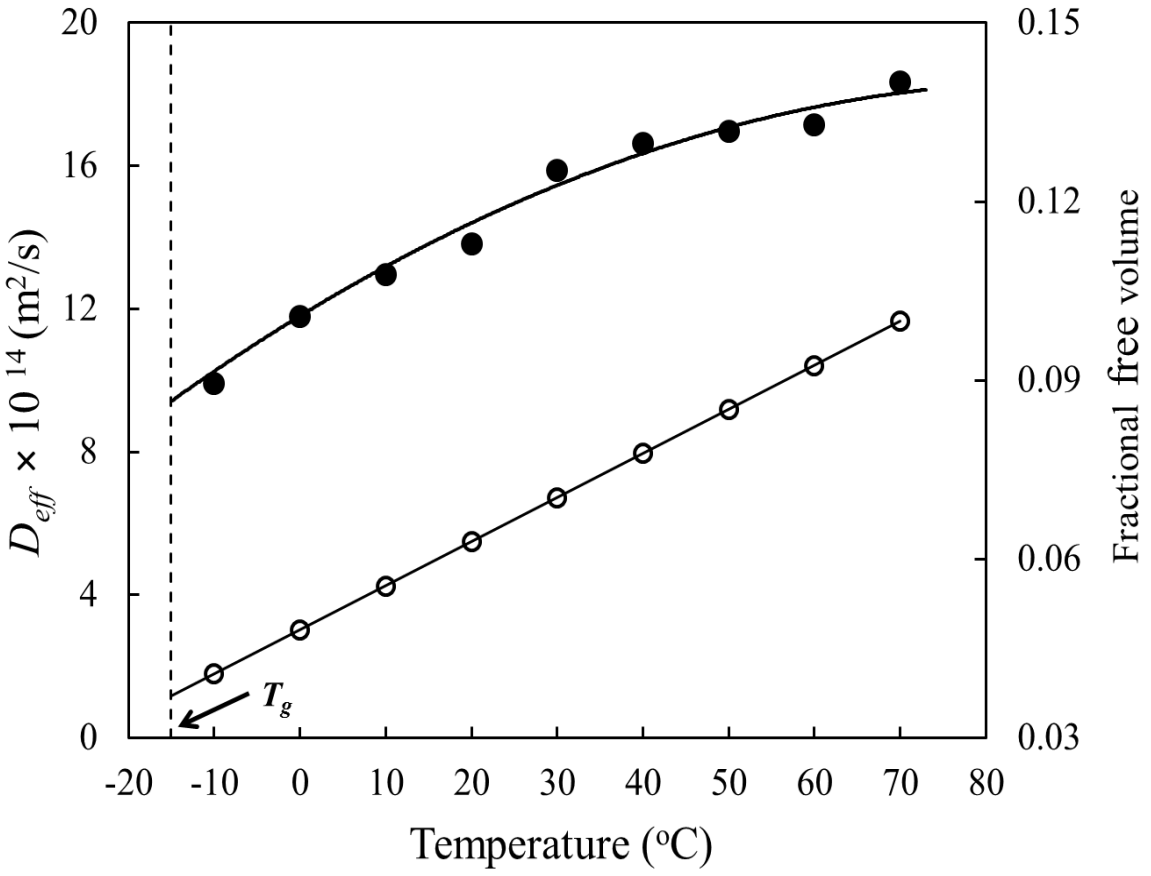

Fig. 6.8 Effective diffusion coefficient of tocopheryl acetate from spray dried waxy maize starch to ethanol as a function of temperature (●, left y-axis) and fractional free volume of the spray dried waxy maize starch matrix (at an inlet temperature 120°C) (○, right y-axis), with the arrow pinpointing the estimated mechanical T_g

6.4 CONCLUSIONS

Edible lipid-soluble vitamin microcapsules were prepared by employing waxy maize starch as a biopolymer encapsulating agent of tocopheryl acetate (vitamin E). The structure-function relationship was associated with the thermal and rheological properties of the matrix for vitamin release in order to allow recording of the diffusion of tocopheryl acetate at a broad time and temperature function. This study clearly demonstrates that the mechanical T_g has a strong influence on the release property as a result of the changing microcapsule viscoelasticity. The gelatinised starch has an amorphous domain in its structure facilitating application of the sophisticated synthetic polymer approach that was employed to characterise the diffusion around the T_g of the matrix. Furthermore, an extension of the free volume theory concerned with nutrient mobility during kinetic release was a core principle aiding the understanding of control release kinetics based on diffusion coefficient.

6.5 ACKNOWLEDGEMENTS

The authors wish to thank Mike Allan, Senior Research Assistant of Chemical Engineering for technical support in particle measurements and technical assistance of the Australian Microscopy and Microanalysis Research Facility within RMIT University. Thai Government Scholarship awarded to Naksit Panyoyai is duly acknowledged.

CHAPTER 7

CONCLUSIONS AND FUTURE WORK

ABSTRACT

Delivery of techno- and biofunctionality in all-natural processed foods is an area of steadily increasing fundamental and technological interest. One of the primary aspects in this field is the diffusion of bioactive ingredients that have been incorporated in high-solid biopolymer matrices. Organoleptic considerations dictate that the delivery vehicles incorporate a highly amorphous fraction in the polymer network. Molecular diffusion in the amorphous state is a complex process associated with the effect of T_g on the mobility of low molecular weight constituents. The four experimental chapters of this Thesis have documented the presence of a mechanical T_g in hydrocolloid/cosolute mixtures, and this has been modelled with the combined framework of the WLF equation/free volume concept. This approach has then formed the basis for a study of the inclusion of vitamins and monitoring their diffusional mobility from high solid matrices. Evidence of non-Fickian phenomena were observed that allowed estimation of the effective diffusion coefficient in these systems. From these investigations, it became apparent the literature lacks any rigorous reports on the relationship of matrix free volume and its effects on the transport phenomena of microconstituents. The contribution of the research reported in this Thesis is to develop such a relationship based on current experimental results and discuss its potential application to other published work.

7.1 CRITICAL DISCUSSION

Cohen & Turnbull (1959) advanced a theory that was extended by Duda (1985) in order to describe molecular diffusion phenomena in concentrated polymer systems on the basis of the free volume concept. As reproduced in Fig. 7.1, the total volume of a highly viscous liquid can be considered to consist of two regions, the actual volume occupied by the molecules and the space or free volume surrounding these molecules. However, it is difficult to correlate the total free volume of the system with molecular transport in the form of rheological properties and an effective diffusion coefficient because the occupied volume is independent of temperature and cannot be redistributed without overcoming a barrier of a high activation energy.

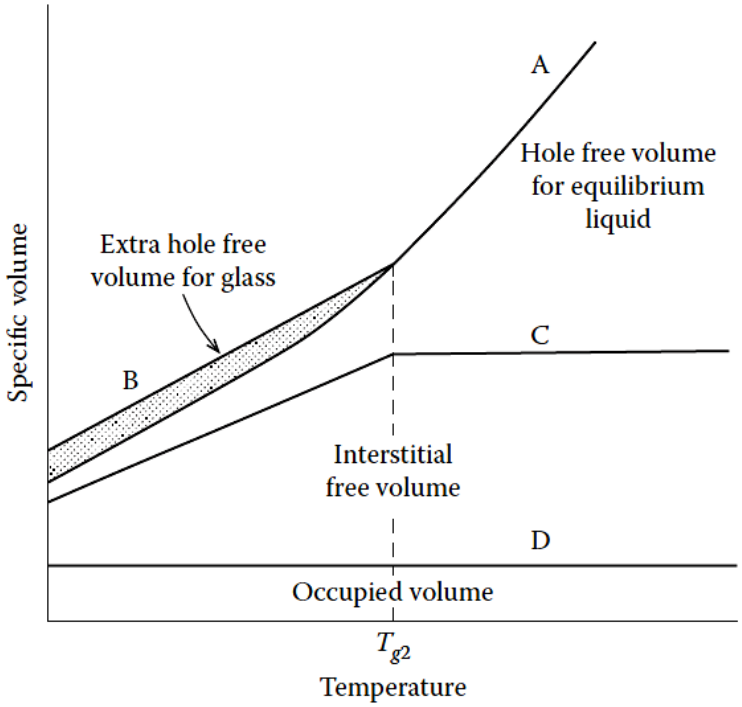

Fig. 7.1 Specific volume-temperature behaviour of a concentrated amorphous polymer ; A, volume of equilibrium liquid; B, volume of non-equilibrium liquid (glass); C, Total volume of occupied volume and interstitial free volume and D, occupied volume (Vrentas & Vrentas, 2013).

The remaining volume allotment, i.e. unoccupied free volume has been divided into interstitial free volume and hole free volume. Vrentas & Duda (1977a,b,c) believe that the interstitial free volume involves high activation energies with no cooperative movement in the diffusion processes. The remaining fraction of the unoccupied volume is the hole free volume. This is presumed to dictate molecular transport required for a relatively effortless distribution. Cavities of the free volume are pictured as being formed by general withdrawal of the surrounding viscous liquid molecules due to a random molecule migration. Following migration, generated voids are filled by the reverse process. Vrentas &Vrentas (2013) assumed that holes or vacancies are homogeneous expansions with no energy change along the vibrational pathways of the macromolecule. A basic concept in the free volume theory is that the polymer moves gradually by the migration of chain segments, and the relative size of the free volume holes is sufficient for the mobility of a small component.

Fig. 7.1 also illustrates the temperature dependence of the volume of a liquid. Upon cooling below the freezing point of a polymer melt, the random motion of the chain naturally slows. To maintain a thermodynamic equilibrium state, the specific volume of the melt decreases with decreasing temperature. If the liquid is cooled sufficiently fast but densification does not occur, crystallisation can be avoided to yield a non-equilibrium state. This glassy state will be formed at the critical point of T_g (Debenedetti & Stillinger, 2001). Below T_g, the amount of extra free volume in a glassy material exhibits qualitative characteristics such brittleness and rigidity. The diffusion coefficient in the excess free volume of the glass would be maintained constant if the amount of hole free volume is unchanged. In fragile porous liquids, however, a break will occur in the diffusivity vs temperature relationship in the vicinity of T_g and the diffusion processes in the glassy state will actually be faster than estimates determined from measurements in the glass transition region (Karel, Anglea, Buera, Karmas, Levi, & Roos, 1994).

Diffusion of small molecular solutes including monomers, oligomers, additives, contaminants or degradation products in polymer materials usually relates primarily to temperature, concentration and geometry of penetrants and polymers (Fang, Domenek, Ducruet, Réfrégiers, & Vitrac, 2013). Increasing temperature above T_g enhances the molecular diffusion reflecting Brownian movements and rotations of groups of atoms or polymeric segments around covalent bonds (Roudaut, Simatos, Champion, Contreras-Lopez & Le Meste, 2004). In addition to temperature, diffusion in polymers can be influenced by the penetrant which can be a good solvent for the polymer. Molecular transport in the concentrated polymer-penetrant system at penetrant weight fractions of less than 0.8 is a complex system because of the numerous degrees of freedom and complex intra-molecular and inter-molecular interactions. Geometry of penetrants and polymers also controls the rate of diffusion including penetrant size being comparable to the monomeric unit of a polymer, polymer molecular weight and polymer morphology particularly crystallinity, crosslink density, orientation and network structure. These factors render predictions of the diffusion coefficients in practical circumstances a complex task (Duda, 1985; Kou, 2000).

Measurements of the diffusion coefficient of small molecular penetrants in polymer often assume Fickian characteristics at temperatures above the T_g of the system. The use of a classical diffusion theory is fully sufficient for describing the mass transport and diffusion coefficients that can be calculated by sorption or permeation approaches. However, diffusion involving mechanisms based on the coupling or molecular migration diffusion processes near T_g would require more complex mechanistic theories such the free volume theory mentioned earlier. In biopolymeric systems, free volume concepts have been applied to model transport properties of small molecules in water sorption dynamics of bread crust (Meinders & van Vliet, 2009), glucose homopolymers (van der Sman & Meinders, 2013), polydextrose (Ribeiro, Zimeri, Yildiz, & Kokini, 2003) and the

drug release mechanisms of paclitaxel loaded in the biodegradable nanostructured hybrid polymer, called polyhedral oligosilsesquioxane thermoplastic polyurethane (Guo, Knight, & Mather, 2009).

In comparable time scales, the mobility of solvent molecules and the processes of polymer chain rearrangement take place simultaneously during viscoelastic diffusion. Non-Fickian phenomena are usually expected in mixed transport mechanisms at temperatures as high as 60°C above T_g, and including those near and below T_g (Duda, 1985). Anomalous behaviour as described by the power-law model (Korsmeyer, Gurney, Doelker, Buri, & Peppas, 1983; Ritger & Peppas, 1987), coupled diffusion-relaxation processes of water soluble vitamins and a special case of Less Fickian diffusion of vitamin E acetate have been now observed in micronutrient release from high-solid biopolymer matrices (Panyoyai, Bannikova, Small & Kasapis, 2016 & 2015; Panyoyai, Bannikova, Small, Shanks, & Kasapis, 2016, i.e. Chapters 3, 4, 5 & 6 of this Thesis). In the case of Less Fickian patterns, a "hopping" mechanism might enable large nonsticky vitamins to slide along polymer chains following polymer relaxation at long time scales in melted conditions (Cai, Panyukov, & Rubinstein, 2015). Table 7.1 summarises the vitamin release characteristic parameters of non-Fickian transport obtained from the work described in this Thesis.

Diffusion data in our high-solid systems were recorded at conditions of the glass transition region. At temperatures just above T_g, the extra hole free volume will relax very slowly towards a kinetically trapped equilibrium leading to an overall decrease in free volume (Vrentas & Duda, 1977a). Vitamins, like other small organic molecules, require certain activation energy to diffuse through limited free volume and the energy tends to increase with larger size. In our experimental systems, the vitamins have been homogenously dispersed in the glassy matrices hence allowing application of diffusion theory in accordance with the body of work discussed earlier.

Table 7.1 Release characteristics of vitamin-loaded high-solid polymer matrices

Vitamin	Matrix	Total solids %(w/w)	Matrix geometry	T_g (°C)	Diffusion exponent *n*	Diffusion coefficient (m^2/s)
Ascorbic acid	High-methoxy pectin/ polydextrose	80	Slab	-20	0.79-0.98	$7.9\text{-}9.7 \times 10^{-8}$
Thiamin hydrochloride	κ-carrageenan/ glucose syrup	85	Slab	-7	0.61-0.87	$3.0\text{-}12.0 \times 10^{-10}$
Nicotinic acid	Whey protein microcapsules	91	Sphere	30	0.42-0.85	$8.5\text{-}9.0 \times 10^{-15}$
Tocopheryl acetate	Modified waxy maize starch	90	Sphere	-15	0.17-0.39	$9.3\text{-}18.4 \times 10^{-14}$

Transport phenomena of the vitamins in this study are governed by a coupled diffusion that consists of the two components of self-diffusion and mutual (or tracer) diffusion. The former is the thermal motion of vitamin molecules in the high-solid matrix in relation to free volume considerations and relaxation processes in the matrix. The latter requires a common concentration gradient between matrix and solvent for diffusion to occur from the surface of the matrix to the liquid medium. Vitamin flow could be perturbed by the countercurrent flow of the liquid medium to solubilise the tracer, which was homogeneously dissolved within the high-solid carrier. The water content of up to 20% (w/w) in our mixtures result in a slow self-diffusion of the microconstituents due to interactions with hydroxyl groups of the macromolecules (Huang, Davies, & Lillford, 2011; Davies et al, 2010) and the tightly bound monolayer moisture in experimental conditions of low water activity (Sherwin & Labuza, 2006). Plasticisation and swelling effects were negligible during diffusion due to the polymer matrices being immiscible in the organic solvent hence having a low thermodynamic compatibility with the diffusion medium (Slade & Levine, 1993).

There are numerous free volume models developed to express the diffusion of traces in polymer solids. In 1959, Cohen and Turnbull presented an expression that relates the self-diffusion coefficient to the free volume of a condensed liquid or rigid sphere. Their work provided the theoretical framework for Fujita (1961) and Vrentas-Duda (1977) to describe the mobility of small concentrations of a penetrant (solvent, plasticizer) in highly concentrated solutions of a synthetic polymer. Later, Vrentas and Duda demonstrated the self-diffusion of organic solvents in glassy and rubbery polymers assuming that self-diffusion is defined as a single jumping unit of the solvent molecule into a small section jumping unit of a very long and flexible chain polymer. The free volume model has been further applied to drug release by Peppas & Reinhart (1983) by considering three components, i.e. drug, polymer and swelling medium hence being useful for the concentration-dependent diffusion observed in hydrogels. Structural parameters, drug size, swelling ratio and polymer molecular weight between crosslinks are included to explain the mechanism of drug diffusion through a swollen membrane.

The aforementioned free volume models include limiting assumptions for the explanation of our vitamin diffusional mobility. First, Vrentas and Duda primarily consider the self-diffusion coefficient without the driving force of tracer into the liquid tank. This complex model has many unknown parameters and these are currently unavailable in the food literature for the solving the proposed equation. Secondly, Pepas and Reinhart have considered changes in the purpose of free volume of the gel due to the solvent absorption rather than the state transition of the polymer subsequent to the vitrification phenomena observed presently.

In this Thesis, we introduce a Williams-Landel-Ferry (WLF) type of equation (1955) to advance a relationship between vitamin diffusion and biopolymer relaxation process. Vitamin diffusion in the concentrated biopolymer matrix is governed by its T_g, as follows:

$$-\log a_T = \frac{C'_{1g}(T - T_g)}{C'_{2g} + T - T_g} \tag{7.1}$$

$$C'_{1g} = \frac{B}{2.303 f_g} \tag{7.2}$$

$$C'_{2g} = \frac{f_g}{\alpha_f} \tag{7.3}$$

where, a_T is defined as the ratio of the relaxation phenomenon at T (K) to the relaxation at T_g by the time-temperature superposition principle, C'_{1g} and C'_{2g} are constants, B is a size parameter usually set to 1, f_g is the ratio of free to total volume of molecule at T_g, and α_f is the thermal expansion coefficient.

At high solute concentrations and in the vicinity of T_g, the solute diffusion coefficient of an appropriately sized small molecule probe in a rubbery polymer is most commonly described by the modified WLF equation (Ehlich & Sillescu, 1990; Guo, Knight, & Mather, 2009; Hall & Torkelson, 1998; Karel, Anglea, Buera, Karmas, Levi, & Roos, 1994; Ramesh, Davis, Zielinski, Danner, & Duda, 2011), as follows:

$$-\log a_{\mathrm{T}} = \log\left[D(T)/D(T_g)\right] \tag{7.4}$$

$$\log\left[\frac{D(T)}{D(T_g)}\right] = \frac{C'_{1g}(T - T_g)}{C'_{2g} + T - T_g} \tag{7.5}$$

where, D(T) and D(T_g) are diffusion coefficients above or at the T_g, and C'_1 and C'_2 are the WLF parameters of the matrix via the coupling parameter, ξ:

$$C'_{1g} = \xi C_{1g} \tag{7.6}$$

$$C'_{2g} = C_{2g} \tag{7.7}$$

Parameter, ξ, is the ratio of the critical hole free volume per mole of solvent jumping unit required for displacement of the small molecule jumping unit *(V_s*)* and the critical hole free volume per mole of polymer jumping unit required for displacement of the polymer (matrix) jumping unit *(V*)*. The coupling constant relates the intensity of interactions between primitive relaxation to physicochemical environment of the surrounding components (Kasapis, 2006). In general, it is also identified closely with the decoupling parameter (β), which is obtained from fundamental concepts of rheology and diffusion (Hong, 1995; Ramesh, Davis, Zielinski, Danner, & Duda, 2011).

According to the basic assumption of the free volume theory derived in Chapter 1, Section 1.3.2, reduction in temperature results in the vitrification of amorphous high-solid materials and the fractional free volume, $f = V_f / V_m$, defined as the ratio of the average free volume (V_f) over the corresponding molecular volume (V_m), is assumed to decrease linearly with temperature in accordance with the equation (Ehlich & Sillescu, 1990; Kasapis, 2001):

$$f = f_g + \alpha_f (T - T_g) \tag{7.8}$$

Substituting Equation (7.8) in Equation (7.5) and implementing a straightforward calculation provides a simple plotting scheme to test the validity of the following equation:

$$\log D(T) = \log D(T_g) + \frac{\xi}{2.303}\left(\frac{1}{f_g} - \frac{1}{f}\right) \tag{7.9}$$

Where f and f_g are fractional free volumes above or at the T_g derived from the WLF model of high-solid hydrocolloid matrices, and D(T) and D(T_g) are mutual diffusion coefficients of vitamin obtained from Fickian formulae.

The experimental results obtained in the various phase of the current study, have been summarised and presented in Fig. 7.2. In this the data for each concentration of vitamin and biopolymer matrices have been plotted.

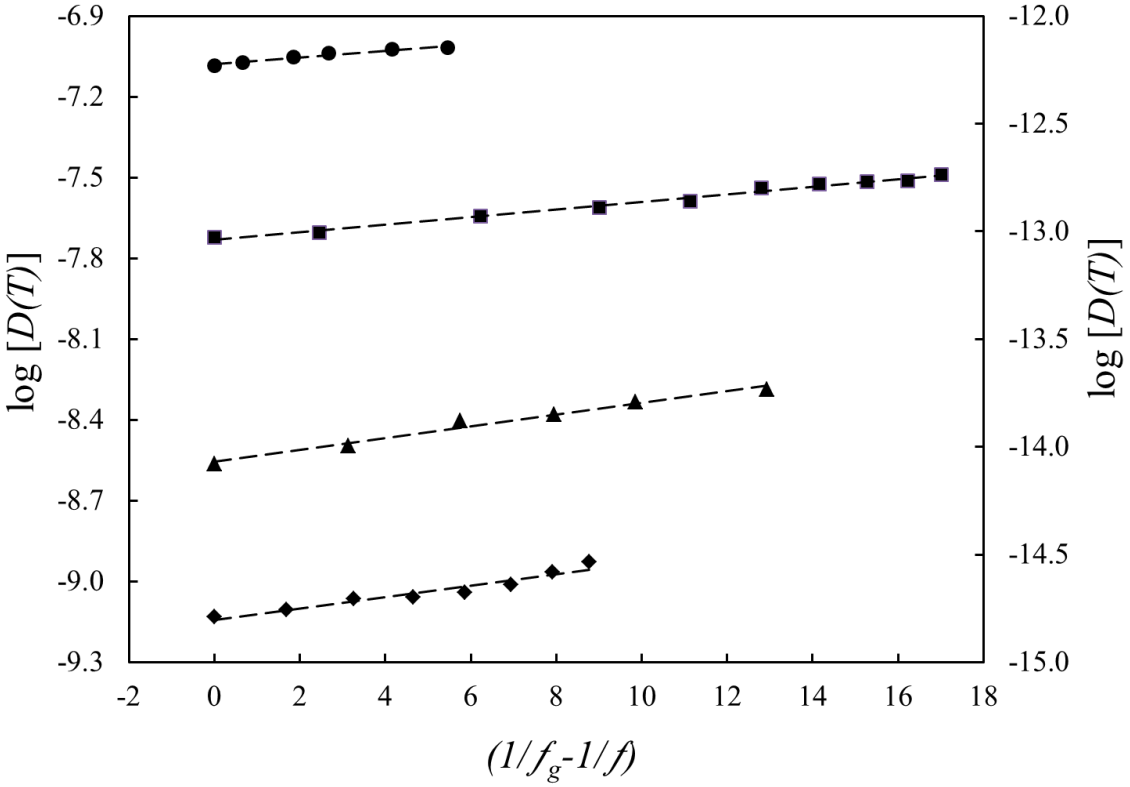

Fig. 7.2 Logarithmic effective diffusion coefficients of vitamin loaded in high-solid biopolymer systems as a function of inverse fractional free volume ($1/f_g$-$1/f$) within the glass transition region. Data are for ascorbic acid at 80% total solids high-methoxy pectin/polydextrose (●) and thiamin at 85% total solids κ-carrageenan/glucose syrup (♦) both plotted on the left y-axis, and nicotinic acid at 91% total solids whey protein isolate (▲) and tocopheryl acetate at 90% total solids modified waxy maize starch (■) both plotted on the right y-axis

According to Fig 7.2, a highly linear relationship was observed for log [*D(T)*] vs *(1/f_g-1/f)* (R^2 > 0.95) when fitting the WLF parameters of each high-solid matrix from data in Table 7.2 (below) into Equation (7.9), thus providing a guideline for the effect of

structural relaxation in the biopolymer matrix on the diffusional patterns of vitamin incorporated in the tertiary systems described in this Thesis.

Table 7.2 Modified WLF parameters of vitamins loaded in high-solids matrices

Vitamin	Matrix	Total solids %(w/w)	Modified WLF parameter			
			T_g	f_g	D_{Tg} (m^2/s)	ξ
Ascorbic acid	High-methoxy pectin /polydextrose	80	-20	0.040	8.07×10^{-8}	0.006
Thiamin hydrochloride	κ-carrageenan/ glucose syrup	85	-7	0.039	7.06×10^{-10}	0.009
Nicotinic acid	Whey protein microcapsules	91	30	0.029	8.99×10^{-15}	0.012
Tocopheryl acetate	Waxy maize starch microcapsules	90	-15	0.037	9.16×10^{-14}	0.008

As shown in Table 7.2, this approach allowed us able to calculate the effective diffusion coefficient at the T_g of the matrix using Equation (7.9). It was found that the lowest value of D_{Tg} is observed at the highest total solids content due to limitations of solvent diffusion into the condensed medium. In the context of solute diffusion according to the free volume concept (Vrentas & Duda, 1977a,b,c), parameter ξ, may be interpreted as the degree of translational diffusion of the solute coupled to the polymer matrix relaxation in a glass-forming system. Literature indicates that this parameter fitted to the modified WLF equation can be used to identify the extent of coupling between tracer molecule (dyes, drugs, essential oils) and a synthetic polymer matrix at temperatures above the respective T_g (Guo, Knight, & Mather, 2009; Hall & Torkelson, 1998; Tramón,

2014). For complete coupling ξ=1, which means that the average reorientation dynamics of the trace compound are identical to the polymer cooperative segmental dynamics. A combined rotational-translational process of diffusion occurs when the tracer mobility has a temperature dependence that is significantly lower than the average relaxation of the macromolecule near T_g. It has been suggested that the value of the coupling parameter increases on increasing the probe size in relation to the polymer mesh (Hall & Torkelson, 1998).

The assumption of dynamic coupling/decoupling between diffusant and matrix motion appears to be appropriate for interpreting our results. Free volume theory combined with an effective diffusion coefficient provides a physical explanation of transport phenomena in these glasses. Low values of the coupling parameter, i.e. high values of the decoupling parameter presented in Table 7.2 support the results in the various chapters of this Thesis indicate reduced cooperativity in the motion of hydrocolloids and vitamins. Applicability of this model to other biopolymer-nutrient or stimulant systems (e.g. essential fatty acids, antioxidants) is of interest to assist with the design of adjustable and controllable release of biofunctionality in natural biomaterials.

7.2 CONCLUSIONS

In this Thesis, delivery of bioactive compounds using food-grade hydrocolloid systems focused on the principles of structural design and process optimisation in order to enhance the stability and bioavailability of encapsulated microconstituents. The experiments have been designed to the investigate release characteristics, as an important function in delivery vehicles. This has required implementation of theoretical modelling for enhanced understanding of the physical processes controlling release. In doing so, we

developed novel hydrocolloid architectures to entrap essential compounds via gelification and encapsulation in order to stabilise vitamins in the condensed systems.

It was found that the structure of hydrocolloids is the physical factor that manipulates the mobility of small molecules. Large-scale motion of hydrocolloid based structure has been fundamentally elucidated in relation to glass dynamics for condensed systems that consist of gelling agents (high-methoxy pectin and κ-carrageenan) in the presence of cosolutes (glucose syrup and polydextrose) and spray dried microcapsules of whey protein and waxy maize starch. Based on dynamic oscillation measurements in-shear, these high-solid materials demonstrated a glass-to-rubber transition and metastable amorphous structure as a function of temperature. A discontinuity from a glassy solid to a rubbery high viscous material is well-defined as the T_g. This is a unifying concept of molecular mobility in polymer science that provides an interpretive framework for vitamin release in kinetically metastable systems of hydrocolloids as amorphous carriers.

It was found that diffusional mobility of vitamins depends heavily on change in the state of the hydrocolloids which were in the current study employed. Constrained glassy matrices require high energies of activation to deliver the micronutrients (ascorbic acid, thiamin, nicotinic acid and tocopheryl acetate), whereas macromolecular dynamics beyond vitrification accelerate mass transport. A spectroscopic shift factor was developed as a quantitative parameter for the systematic observation of vitamin release and this was utilised to indicate the relative mobility of microconstituents in comparison with the mechanical shift factor of condensed hydrocolloid networks. Temperature-dependent release patterns strongly confirm a limitation of a classical diffusive flux concept explained in terms of a concentration gradient and time according to a general Fick's second law.

In general, it was found that the release mechanism of hydrocolloid-vitamin systems obeys a non-Fickian diffusion. Power Law shows a diffusion controlled process in organic solvents on the basis of non-polymer swelling and lack of chemical interactions between components in the blend. Transport of vitamins occurs from the core of the biopolymer (self diffusion) to the perfect sink (mutual diffusion) and the diffusion rate accelerates at temperatures higher than the mechanical T_g. In addition to considerations of polymer relaxation, size of the diffusing molecule is an intrinsic factor that limits molecular mobility. Thus, the mobility of the bulky molecule of tocopheryl acetate entrapped in the amylopectin network was described as a special case of Less Fickian diffusion.

A critical advance achieved in this work is that the diffusion of vitamins is in qualitative agreement with the free volume theory. The concept of free volume describes the extra volume required for large-scale vibrational motions and string-like vibrations of a polymer chain. According to the theoretical model of Williams, Landel and Ferry, the free volume increases linearly with elevated temperature, and the T_g is defined as the position where the thermal expansion coefficient undergoes a discontinuity. We have highlighted this agreement with an upward trend for both fractional free volume and effective diffusion coefficient beyond the threshold of T_g. Thus, the current work offers insights into both the physics and the rate of bioactive-compound transport within a glassy network.

The Thesis further innovates by developing a mathematical model that provides for strong quantitative agreement between the diffusion coefficient of the vitamin and free volume of the hydrocolloid matrix. This yields the so-called coupling/decoupling parameter of polymeric motion and small-molecule diffusion. Values of the decoupling parameter range from 0.989 to 0.994 for the hydrocolloid-vitamin systems of this investigation demonstrats molecular decoupling between the two ingredients during the

process of diffusion. The results thus indicate that diffusion phenomena are the outcome of identifying an appropriate interstitial void within a polymeric cluster in order to jump in this void by a random redistribution of the free volume. The holes are then filled by the molecules of the bioactive compound without an overall energy change thus allowing passage from one cluster to the next. This process occurs rapidly in our systems leading to extensive diffusion, which however can be manipulated by altering the experimental constraints.

7.3 SUGGESTIONS FOR FUTURE WORK

It is interesting for both fundamental and technological reasons to observe glassy phenomena of hydrocolloid systems in relation to bioactive compound release. To further advance understanding in the field, particular relating to functional food products, biopolymer blending laws should be designed and applied in order to determine diffusion in relation to cosolute partition between the two polymeric phases. This will take advantage of enthalpic interactions between unlike hydrocolloid chains ("sticking together") and enthalpic interactions from chains being surrounded by others of the same type ("pushing apart"). It is assumed then that specific futures of the biphasic composites from low-solid gels to high-solid glasses can account for profiles of bioactive compound release.

A variety of analytical methods is required to examine diffusional processes in biopolymer gels. The current study utilised external methods of UV/Vis spectrophotometry coupled with chromogenic reactions to investigate the diffusion processes. Interactions between various ingredients in the blends were elucidated with Fourier transform infrared spectroscopy, wide angle X-ray diffraction and scanning electron microscopy. That was sufficient for the current systems of hydrocolloid/cosolute slabs or starch/whey protein microcapsules. In case that the other might be studied and in

which porosity is developed in fragile polymeric systems, relationships between shape or size of pores and internal molecular mobility should be examined. That would complement the concept of free volume developed by small deformation rheology in relation to the effective diffusion coefficient. For example, the technique of fluorescence recovery after photobleaching (FRAP) will provide useful insights into the molecular mobility of “drug” and “polymer strands” in low-solid systems with a high aqueous phase where there is mutual mobility of all ingredients given sufficient time of observation.

To design work directly applicable to functional foods or relevant biological systems, diffusion phenomena should be controlled to comply with release from a specific dosage form. Depending on delivery-vehicle requirements, formulations could be engineered where the aqueous solvent penetrates into the continuous polymeric network of a physically crosslinked alginate or carrageenan gel followed by the release of the bioactive compound. In this case, macromolecular swelling will become the mechanism of importance, and this will be reflected in a high free volume system that can be modelled by the predictions of the reaction rate theory. In the opposite case, where rearrangements of the polymeric network should remain at a minimum, delivery vehicles of chemically cross-linked gelatin gels could be designed to achieve a relatively low rate of diffusion meaning that the rate of microconstituent diffusion is much smaller than for the relaxation of local polymeric segments.

BIBLIOGRAPHY

Abad, L. V., Saiki, S., Kudo, H., Muroya, Y., Katsumura, Y., & de la Rosa, A. M. (2007). Rate constants of reactions of κ-carrageenan with hydrated electron and hydroxyl radical. *Nuclear Instruments and Methods in Physics Research Section B: Beam Interactions with Materials and Atoms, 265,* 410-413.

Abiad, M. G., Carvajal, M. T., & Campanella, O. H. (2009). A review on methods and theories to describe the glass transition phenomena: Applications in food and pharmaceutical products. *Food Engineering Reviews, 1,* 105-132.

Abraham, M. & Acree, Jr., W. E. (2013). On the solubility of nicotinic acid and isonicotinic acid in water and organic solvents. *The Journal of Chemical Thermodynamics, 61,* 74-78.

Adhikari, B., Howes, T., Bhandari, B. R., & Truong, V. (2001). Stickiness in foods: A review of mechanisms and test methods. *International Journal of Food Properties, 4,* 1-33.

Agilent Technologies (2013a). *The benefits of photodiode array in UV/Vis spectrophotometer*. Available from: http://www.chem.agilent.com/en-us/products-services/instruments-systems/molecular-spectroscopy/8453-uv-vis-diode-array-system/Pages/ photodiode_ array_benefits.aspx Accessed 14.04.13.

Agilent Technologies (2013b). *Agilent 140/240/280 Series AA*. Available from: http://www.chem.agilent.com/Library/usermanuals/Public/1547.pdf Accessed 30.12.13.

Ahmed, M., Akter, M. S., Lee, J., & Eun, J. (2010). Encapsulation by spray drying of bioactive compound, physiological and morphological properties from purple sweet potato. *LWT-Food Science and Technology, 43,* 1307-1312.

Al-Amri, I. S., Al-Adawi, K. M., Al-Marhoobi, I. M., & Kasapis, S. (2005). Direct imaging polysaccharide network at high levels of co-solute. *Carbohydrate Polymers, 61,* 379-382.

Al-Ani, M., Opara, L. U., Al-Bahri, D., & Al-Rahbi, N. (2007). Spectrophotometric quantification of ascorbic acid contents of fruit and vegetables using 2,4-dinitrophenylhydrazine method. *Journal of Food, Agriculture & Environment, 5,* 165-168.

Almrhag, O., George, P., Bannikova, A. Katopo, L., Chaudhary, D., & Kasapis, S. (2012a). Analysis on effectiveness of co-solute on the network integrity of high methoxy pectin. *Food Chemistry, 135,* 1455-1462.

Almrhag, O., George, P., Bannikova, A. Katopo, L., Chaudhary, D., & Kasapis, S. (2012b). Phase behavior of gelatin/polydextrose mixtures at high levels of solids. *Food Chemistry, 134,* 1938-1946.

Almrhag, O., George, P., Bannikova, A., Katopo, L., & Kasapis, S. (2012c). Networks of polysaccharides with hydrophilic and hydrophobic characteristics in the presence of co-solute. *International Journal of Biological Macromolecules, 51,* 138-145.

Almrhag, O., George, P., Bannikova, A. Katopo, L., Chaudhary, D., & Kasapis, S. (2013). Investigation on the phase behavior of gelatin/agarose mixture in an environment of reduced solvent quality. *Food Chemistry, 136,* 835-842.

Al-Ruqaie, I. M., Kasapis, S., & Abeysakera, R. (1997). Structural properties of pectin-gelatin gels. Part II: effect of sucrose/glucose syrup. *Carbohydrate Polymers, 34,* 309-321.

Anandharamakrishnan, C., Rielly, C. D. & Stapley, A. G. F. (2007). Effects of process variables on the denaturation of whey proteins during spray drying. *Drying Technology, 25,* 799-807.

Anandharamakrishnan, C., Rielly, C. D., & Stapley, A. G. F. (2008). Loss of solubility of α-lactalbumin and β-lactoglobulin during the spray drying of whey proteins. *Lebensmittel-Wissenschaft & Technologie, 41,* 270-277.

Andrade, E. N. daC. (1930). The viscosity of liquid. *Nature, 125,* 309-310.

Angell, C. A. (1988). Perspective on the glass transition. *Journal of Physics and Chemistry of Solids, 49,* 863-871.

Anwar, S. H., & Kunz, B. (2011). The influence of drying methods on the stabilization of fish oil microcapsules: comparison of spray granulation, spray drying and freeze drying. *Journal of Food Engineering*, *105,* 367-378.

Armfield Group (2014). *Food technology FT30MKIII spray dryer provisional.* Available from: http://discoverarmfield.com/en/products/view/ft30/spray-dryer
Accessed 02.09.14.

Arridge, R. G. C. (1975). The glass transition. In: *Mechanics of polymers*. Oxford: Clarendon Press. pp. 24-50.

Artiaga, R., López-Beceiro, J., Tarrío-Saavedra, J., Gracia-Fernández, Naya, S., & Mier, J. L. (2011). Estimating the reversing and non-reversing heat flow from standard DSC curves in the glass transition region. *Journal of Chemometrics, 25*, 287-294.

Auerbach, M. H., Craig, S. A. S., Howlett, J. F., & Hayes, K. C. (2007). Caloric availability of polydextrose. *Nutrition Reviews, 65,* 544-549.

Australian Microscopic and Microstructure Research Facility. (2013). *SEM in MyScope training for advanced research*.

Available from: www.ammrf.org.au/myscope/sem/ background

Accessed 13.04.13.

Baker, R. W. (1987). *Controlled release of biological active agents*. NY: John Wiley & Sons.

Ball, G. F. M. (2006). *Vitamins in food: Analysis, bioavailability, and stability.* Boca Raton: CRC Press. pp. 289-308.

Barbosa-Cánovas, G. V., Kokini, J. L., Ma, L., & Ibarz, A. (1996). The rheology of semiliquid foods. *Advances in Food and Nutrition Research,* 39, 1–69.

Batista, A. N. L., Batista Jr., J. M., Bolzani, V. S., Furlan, M., & Blanch, E. W. (2013). Selective DMSO-induced conformational changes in protein from Raman optical activity. *Physical Chemistry Chemical Physics, 15,* 20147-20152.

Bayarri, S., Rivas, I, Costell, E., & Durán, L. (2001). Diffusion of sucrose and aspartame in kappa-carrageenan and gellan gum gels. *Food Hydrocolloids, 15,* 67-73.

Beirão-da-Costa, S., Duarte, C., Moldão-Martins, M., & Beirão-da-Costa, M. L. (2011). Physical characterization of rice starch spherical aggregate produced by spray drying. *Journal of Food Engineering, 104,* 36-42.

Bell, L. N. & Hageman, M. J (1994). Differentiating between the effects of water activity and glass transition dependent mobility on a solid state chemical reaction: Aspartame degradation. *Journal of Agricultural and Food Chemistry, 42,* 2398-2401.

Bell, L. N. & White, K. L. (2000). Thiamin stability in solids as affected by the glass transition. *Journal of Food Science, 65,* 498-501.

Berry, G. C. & Fox, T. G. (1968). The viscosity of polymers and their concentrated solutions. *Advanced in Polymer Science, 5,* 261-357.

Bings, N. H., Bogaerts, A., & Broekaert, J. A. C. (2010). Atomic Spectroscopy: A review. *Analytical Chemistry, 82,* 4653-4681.

Boye, J. I., Alli, I., Ismali, A. A., Gibbs, B. F., & Konishi, Y. (1995). Factors affecting molecular characteristics of whey protein gelation. *International Dairy Journal, 5,* 337-353.

Brownlee, I. A. (2011). The physiological roles of dietary fiber. *Food Hydrocolloids, 25,* 238-250.

BRUKER AXS. (2013). *Diffraction solution D8 Advance.* Available from: http://ksanalytical.com/wp-content/uploads/2012/02/D8_ADVANCE_e_72dpi_05.pdf Accessed 13.04.13.

Brummer, R. (2006). *Rheology essentials of cosmetic and food emulsions*. Verlag Berlin Heldelberg: Springer. pp. 71-76.

Bryant, C. M. & McClements, D. J. (1998). Molecular basis of protein functionality with special consideration of cold-set gels derived from heat denatured whey. *Trends in Food Science & Technology, 9,* 143-151.

Buddrick, O., Jones, O. A. H., Morrison, P. D., & Small, D. M. (2013). Heptanes as a less toxic option than hexane for the separation of vitamin E from food products using normal phrase HPLC. *RSC Advances*, *3*, 24063-24068.

Buera, M. P., Roos, Y., Levine, H., Slade, L., Corti, H. R., Reid, D. S., Auffret, T., & Angell, A. C. (2011). State diagrams for improving processing and storage of foods, biological materials, and pharmaceuticals (IUPAC Technical Report). *Pure and Applied Chemistry, 83,* 1567-1617.

Bui, L. L. T. & Small D. M. (2007). The influence of formulation and processing on stability of thiamin in three styles of Asian noodles. *Food Chemistry, 102,* 1394-1399.

Bui, L. T. T., Small, D. M. & Coad, R. (2013). The stability of water-soluble vitamins and issues in the fortification of foods. In V. R. Preedy, V. R. Srirajaskanthan, & V. B. Patel (Eds), *Handbook of food fortification and health: From concepts to public health applications volume 1* (pp. 199-211). NY: Humana Press, Springer.

Burdock, G. A. & Flamn, W. G. (1999). A review of the studies of the safety of polydextrose in food. *Food and Chemical Toxicology, 37,* 233-264.

Burey, P., Bhandari, B. R., Howes, T., & Gidley, M. J. (2008). Hydrocolloid gel particles: formation, characterization and application. *Critical Reviews in Food Science and Nutrition, 48,* 361-377.

Busk, JR. G. C. & Labuza, T. P. (1979). A dye diffusion technique to evaluate gel properties. *Journal of Food Science, 44,* 1369-1372.

Cai, L., Panyukov, S., & Rubinstein, M. (2015). Hopping diffusion of nanoparticles in polymer matrices. *Macromolecules, 48,* 847-862.

Cai, L., Shi, Y., Rong, L. Hsiao, B. S. (2010). Debranching and crystallization of waxy maize starch in relation to enzyme digestibility. *Carbohydrate Polymers*, *81,* 385-393.

Campo, V. L., Kawano, D. F., da Silva Jr., D. B., & Carvalho, I. (2009). Carrageenan: Biological, chemical modification and structural analysis-A review. *Carbohydrate Polymers, 77,* 167-180.

Carneiro, H. C. F., Tonon, R. V., Grosso, C. R. F., & Hubinger, M. D. (2013). Encapsulation efficiency and oxidative stability of flaxseed oil microencapsulated by spray drying using different conbinations of wall materials. *Journal of Food Engineering*, *115,* 443-453.

Champion, D. Le Meste, M., & Simatos, D. (2000). Towards an improved understanding of glass transition and relaxations in foods; molecular mobility in the glass transition region. *Trends in Food Science & Technology, 11,* 41-55.

Chan, S. W., Mirhosseini, H, Taip, F. S., Ling, T. C., & Tan, C. P. (2013). Comparative study on the physicochemical properties of κ-carrageenan extracted from *Kappaphycus alvarezii* (doty) doty ex Silva in Tawau, Sabah, Malaysia and commercial k-carrageenans. *Food Hydrocolloids, 30,* 581-588.

Chaudhary, V., Small, D. M., & Kasapis, S. (2013a). Effect of a glassy gellan/polydextrose matrix on the activity of α-D-glucosidase. *Carbohydrate Polymers, 95,* 389-396.

Chaudhary, V., Small, D. M., & Kasapis, S. (2013b). Structural studies on matrices of deacylated gellan with polydextrose. *Food Chemistry, 137,* 37-44.

Chaudhary, V., Small, D. M., Shanks, R. A., & Kasapis, A. (2014). Enzymatic catalysis in a whey protein matrix at temperatures in the vicinity of glass transition. *Food Research International, 62,* 671-676.

Chávarri, M., Marañón, I., & Villarán, M. C. (2012). Encapsulation technology to protect probiotic bacteria. In E. C. Rigobelo (Ed.), *Probiotics*. http://www.intechopen.com/books/probiotics/probiotic-confectionery-products-preparation-and-properties. DOI: 10.5772/50046. Accessed 02.09.14

Chen, L., Remondetto, G. E., & Subirade, M. (2006). Food protein-based materials as nutraceutical delivery systems. *Trends in Food Science & Technology, 17,* 272-283.

Cheung, R. H. F., Marriott, P. J., & Small, D. M. (2007). CE methods applied to the analysis of micronutrients in foods. *Electrophoresis, 28,* 3390-3413.

Chiu, C. & Solarek, D. (2009). Modified of starch, In J. B. Roywhistler (Ed), *starch Technology* (pp. 629-655). NY: Academic Press.

Chinachoti, P. (1995). Carbohydrates: Functionality in foods. *American Journal of Clinical Nutrition, 61(supplement),* 922S-929S.

Chung, Y. & Lai, H. (2006). Molecular and granular characteristics of corn starch modified by HCl-methanol at different temperatures. *Carbohydrate Polymers, 63,* 527-534.

Clark, A. H., Kavanagh, G. M., & Ross-Murphy, S. B. (2001). Globular protein gelation-theory and experiment. *Food Hydrocolloids, 15,* 383-400**.**

Cohen, M. H. & Turnbull, D. (1959). Molecular transport in liquid and glasses. *The Journal of Chemical Physics, 31,* 1164-1169.

Copeland, L., Blazek, J., Salman, H., & Tang, M. C. (2009). Form and functionality of starch. *Food Hydrocolloids, 23,* 1527-1534.

Corradini, M. G. & Peleg, M. (2006). Prediction of vitamin loss during non-isothermal heat processes and storage with non-linear kinetic models. *Trends in Food Science & Technology, 17,* 24-34.

Craig, S. A. S., Holden, J. F., Troup, J. P., Auerbach, M. H., & Frier, H. I. (1998). Polydextrose as soluble fiber: physiological and analytical aspects. *Cereal Food World, 5,* 370-376.

Crank, J. (1975). Non-Fickian diffusion, in *The mathematic of diffusion* 2nd ed (pp 224-265). Oxford: Clarendon Press.

Creamer, L. K. & MacGibbon, A. K. H. (1996). Some recent advances in the basic chemistry of milk proteins and lipid. *International Dairy Journal, 6,* 539-568.

Davies, E., Huang, Y., Harper, J. B., Hook, J. M., Thomas, D. S., Burgar, I. M., & Lillford, P. J. (2010). Dynamics of water in agar gels studies using low and high resolution ^{1}H NMR spectroscopy. *International Journal of Food Science and Technology, 45,* 2502-2507.

Day, L., Seymour, R. B., Pitts, K. F., Konczak, I., & Lundin, L. (2009). Incorporation of functional ingredients into foods. *Trends in Food Science & Technology, 20,* 388-395.

de Wit, J. N. (1998). Nutrition and functional characteristics of whey proteins in food products. *Journal of Dairy Science, 81,* 597-608.

Debenedetti, P. G. & Stillinger, F. H. (2001). Supercooled liquids and the glass transition. *Nature, 410,* 259-267.

Department of Health and Aging, National Health and Medical Research Council, Ministry of Health, Australian Government. (2005). *Nutrient reference values for Australia and New Zealand including Recommended dietary intakes*. Available from: www.ag.gov.au/cca. Accessed 3.10.12.

Desai, K. G. H. & Park, H. J. (2005). Encapsulation of vitamin C in tripolyphosphate cross-linked chitosan microspheres by spray drying. *Journal of Microencapsulation, 22,* 179-192.

Deszczynski, M., Kasapis, S., MacNaughton, W., & Mitchell, J. R. (2002). High sugar/polysaccharide glasses: resolving the role of water molecules in structure formation. *International Journal of Biological Macromolecules, 30,* 279-282.

Deutsch, M. J. (1984). Vitamins and other nutrients. In S. Williams (Ed), *Official Methods of Analysis of the Association of Official Analysis Chemists* (pp.841-842). VA: AOAC international.

Devi, A. F., Liu, L. H., Hemar, Y., Buckow, R., & Kasapis, S. (2013). Effect of high pressure processing on rheological and structural properties of milk-gelatin mixtures. *Food Chemistry, 141,* 1328-1334.

Devi, N. & Kakati, D. K. (2013). Smart porous microparticles based on gelatin/sodium alginate polyelectrolyte complex. *Journal of Food Engineering, 117,* 193-204.

Dissanayake, M., Kasapis, S., Chaudhary, V., Adhikari, B., Palmer, M., & Meurer, B. (2012). Unexpected high pressure effects on the structural properties of condensed whey protein systems. *Biopolymers, 97,* 963-973.

Dissanayake, M., Kasapis, S., George, P., Adhikari, B., Palmer, M., & Meurer, B. (2013). Hydrostatic pressure effects on the structure properties of condensed whey protein/lactose systems. *Food Hydrocolloids, 30,* 632-640.

Distantina, S., Wiratni, Fahrurrozi, M., & Rochmadi (2011). Carrageenan properties extracted from *Eucheuma cottonii*, Indonesia. *World Academy of Science, Engineering and Technology, 54,* 738-742.

Dodson A. G. & Pepper, T. (1985). Confectionery technology and the pros and cons of using non-sucrose sweeteners. *Food Chemistry, 16,* 271-280.

Dole, M. N., Patel, P. A., Sawant, S. D., & Shedpure, P. S. (2011). Advanced applications of Fourier Transform Infrared Spectroscopy. *International Journal of Pharmaceutical Science Review and Research*, *7,* 159-166.

Doolittle, A. K. & Doolittle, D. B. (1957). Studies in Newtonian flow. V. Further verification of the free-space viscosity equation. *Journal of Applied Physics, 28,* 901-905.

Duda, J. L. (1985). Molecular diffusion in polymeric systems. *Pure & Applied Chemistry, 57,* 1681-1690.

Duongthingoc, D., George, P., Katopo, L., Gorczyca, E., & Kasapis, S. (2013). Effect of whey protein agglomeration on spray dried microcapsules containing *Saccharomyces boulardii*, *Food Chemistry, 141,* 1782-1788.

Duvvuri, P., Ko, G., Krommenhoek, N., & Sanchez, K. (2013). *Using X-ray diffraction to correlate physical appearance and chemical structure*. Available from: http://soe.rutgers.edu/files/xray.pdf Accessed 13.04.13.

Ehlich, D. & Sillescu, H. (1990). Tracer diffusion in the glass transition. *Macromolecules, 23,* 1600-1610.

Eitenmiller, R. R., Ye, L., & Landen, Jr, W. O. (2008). *Vitamin analysis for the health and food science, 2nd Ed.* Boca Raton: CRC Press. pp. 231-289.

Ellis, R. P., Cochrane, M. P., Dale, M. F. B., Duffus, C. M., Lynn, A., Morrison, I. M., Prentice, R. D. M., Swanston, J. S., & Tiller, S. A. (1998). Starch production and industrial use. *Journal of the Science of Food and Agriculture, 77,* 289-311.

ETS Laboratories®. (2013). *Fourier transform infrared spectrometer.* Available from: http://http://www.etslabs.com/analysis.aspx?id=%23JJUICPRF Accessed 13.04.13.

Etzel, M. R. (2004). Manufacture and use of dairy protein fractions. *Journal of Nutrition*, *134,* 996s-1002s.

European Pharmacopoeia. (2013). *Buffer solutions*. Available from: http:// lib.njutcm.edu.cn/buffer/4.1.3.%20Buffer%20solutions.pdf Accessed 13.04.13.

Evageliou, V., Kasapis, S., & Hember, M. W. N. (1998). Vitrification of κ-carrageenan in the presence of high levels of glucose syrup. *Polymer, 39,* 3909-3917.

Evageliou, V., Richardson, R. K., & Morris, E. R. (1999). Effect of pH, sugar type and thermal annealing of high-methoxy pectin gels. *Carbohydrate Polymers, 42,* 245-259.

Evans, J., Zulewska, J., Newbold, M., Drake, M. A., & Barbano, D. M. (2010). Comparison of composition and sensory properties of 80% whey protein and milk serum protein concentrates. *Journal of dairy Science, 93,* 1824-1843.

Fang, X., Domenek, S., Ducruet, V., Réfrégiers, M., & Vitrac, O. (2013). Diffusion of aromatic solutes in aliphatic polymers above glass transition temperature. *Macromolecules, 46,* 874-888.

Fang, Z. & Bhandari, B. (2010). Encapsulation of polyphenol-A review. *Trends in Food Science & Technology, 21,* 510-523.

FAO/WHO. (2004). *Human vitamin and mineral requirements*. Report of a joint FAO/WHO expert consultation in Bangkok, Thailand. Rome, Food and Agriculture Organization. pp. 130-139.

Favre, E. & Girard, S. (2001). Release kinetics of low molecular weight solutes from mixed cellulose ethers hydrogels: A critical experiment study. *European Polymer Journal, 37,* 1527-1532.

Fazaeli, M., Tahmasebi, M., & Djomeh, Z. E. (2012). Characterization of food texture: application of microscope technology. In A. Méndez-Vilas (Ed.), *Current microscopy contributions to advances in science and technology* vol. 2. (pp. 855-871). Badajoz: Spain.

Ferry, J. D. (1980). Dependence of viscoelastic behavior on temperature and pressure, in *Viscoelastic Properties of Polymers*, NY: John Wiley.

Ferry, J. D., Landel, R. F., & Williams, M. L. (1955). Extension of the Rouse theory of viscoelastic properties to undiluted linear polymers. *Journal of Applied Physics*, *26,* 359-362.

Fisher, P. & Windhab, E. J. (2011). Rheology of food materials. *Current Opinion in Colloid & Interface Science, 16,* 36-40.

Fox, P. F. (2001). Milk proteins as food ingredients. *International Journal of Dairy Technology, 54,* 41-55.

Fu, J-T., & Rao, M. A. (2001). Rheology and structure development during gelation of low-methoxyl pectin gels: the effect of sucrose. *Food Hydrocolloids, 15,* 93-100.

Fu, Z., Wang, L., Li, D., & Adhikari, B. (2012). Effects of partial gelatinization on structure and thermal properties of corn starch after spray drying. *Carbohydrate Polymers*, *88,* 1319-1325.

Fu, Z., Wang, L., Li, D., Zhou, Y., & Adhikari, B. (2013). The effect of partial gelatinization of corn starch on its retrogradation. *Carbohydrate Polymers, 97,* 512-517.

Fugita, H. (1961). Diffusion in polymer-diluent systems. *Fortschritte Der Hochpolymeren-Forschung*, 3, 1-47.

Funami, T. (2011). Next target for food hydrocolloid studies: Texture design of foods using hydrocolloid technology. *Food Hydrocolloid, 25,* 1904-1914.

Garbado, S., Rech, R., & Ayub, M. A. Z. (2011). Determination of lactose and ethanol diffusion coefficient in calcium alginate gel spheres: predicting values to be used in immobilized bioreactors. *Journal of Chemical & Engineering Data, 56,* 2305-2309.

García, L., Cova, A., Sandoval, A. J., Müller, A. J., & Carrasquel, L. M. (2012). Glass transition temperatures of cassava starch-whey protein concentrate systems at low and intermediate water content. *Carbohydrate Polomers, 87,* 1375-1382.

George, P., Kasapis, S., Bannikova, A., Mantri, N., Palmer, M., Meurer, B., & Lundin, L. (2013a). Effect of high hydrostatic pressure on the structural properties and bioactivity of immunoglobulins extracted from whey protein. *Food Hydrocolloids*, *32,* 286-293.

George, P., Lundin, L., & Kasapis, S. (2013b). Fundamental studies on the structural functionality of whey protein isolate in the presence of small polyhydroxyl compounds as co-solute. *Food Chemistry, 139,* 420-425.

Georget, D. M. R., Cairns, P., Smith, A. C., & Waldron, K. W. (1999). Crystallinity of lyophilized carrot cell wall components. *International Journal of Biological Macromolecules, 26,* 325-331.

Gerasimov, P. A., Gubarera, A. I., Blokh, E. L., Cherkasova, T. G., & Berezovykw, V. V. (1984). Physicochemical properties of α-tocopherol acetate. *Khimiko-farmatserticheskii Zhurnal. 19,* 1274-1276.

Gibbs, B. F., Kermasha, S., Alli, I., & Mulligan, C. N. (1999). Encapsulation in the food industry: a review. *International Journal of Food Science and Nutrition, 50,* 213-224.

Gibbson, G. R., & Roberfroid, M. B. (1995). Dietary modulation of the human colonic microbiota: introduction the concept of prebiotics. *Journal of Nutrition, 9,* 91401-91412.

Gill, P. S., Sauerbrunn, S. R., & Reading, M. (1993). Modulated differential scanning calorimetry. *Journal of Thermal Analysis, 40,* 931-939.

Gnanasambandam, R. & Proctor, A. (1999). Preparation of soy hull pectin. *Food Chemistry, 65,* 461-467.

Goff, H. D. (1992). Low-temperature stability and the glassy state in frozen foods. *Food Research International, 25,* 317-325.

Goff, H. D. (1994). Measuring and interpreting the glass transition in frozen foods and model systems. *Food Research International, 27,* 187-189.

Gonçalves, E. M. & da Piedade, M. E. M. (2012). Solubility of nicotinic acid in water, ethanol, acetone, diethyl ether, acetonitrile and dimethyl sulfoxide, The *Journal of Chemical Thermodynamics, 47,* 326-371.

Gonzalez-Soto, R. A., da la Vega, B., García-Suarez, F. J., Agama-Acevedo, E., & Bello-Pérez, L. A. (2011). Preparation of spherical aggregates of taro starch granules. *LWT-Food Science and Technology, 44,* 2064-2069.

Gotro, J. (2016). *Thermoset Characterization Part 14: Introduction to Dynamic Mechanical Analysis (DMA)* Available from: http://polymerinnovationblog.com/thermoset-characterization-part-14-introduction-dynamic-mechanical-analysis-dma/ Accessed 23.01.16.

Granado-Lorencio, F., Donoso-Navarro, E., Sánchez-Siles, L. M., Blanco-Navarro, I., & Pérez-Sacristán, B. (2011). Bioavilability of β-cryptoxanthin in the presence of phytosterols: In vitro and in vivo studies. *Journal of Agricultural and Food Chemistry, 59,* 11819-11824.

Gunasekaran, S. & Ak, M. M. (2000). Dynamic oscillatory shear testing of foods-selected applications. *Trends in Food Science & Technology, 11,* 115-127.

Gunasekaran, S., Ko, S., & Xiao, L. (2007). Use of whey proteins for encapsulation and controlled delivery applications. *Journal of Food Engineering, 83,* 31-40.

Guo, Q., Knight, P. T. & Mather, P. T. (2009). Tailored drug release from biodegradable stent coating based on hybrid polyurethanes. *Journal of Controlled Release, 137,* 224-233.

Hall, D. B. & Torkelson, J. M. (1998). Small molecule probe diffusion in thin and ultrathin supported polymer films. *Macromolecules, 31,* 8817-8825.

Hancock, B. C. & Zografi, G. (1997). Characteristics and significance of the amorphous state in pharmaceutical systems. *Journal of Pharmaceutical Science, 86,* 1-12.

Heelan, B. A. & Corrigan, O. I. (1998). Preparation and evaluation of microspheres prepared from whey protein isolate. *Journal of Microencapsulation*, *15,* 93-105.

Hermansson, A. M., Eriksson, E., & Jordansson, E. (1991). Effects of potassium, sodium and calcium on the microstructure and rheological behaviour of kappa-carrageenan gels. *Carbohydrate Polymers, 16,* 297-302.

Hicsasmaz, Z., Yazgan, Y., Bozoglu, F., & Katnas, Z. (2003). Effect of polydextrose-substitution on the cell structure of the high-ratio cake system. *LWT-Food Science and Technology, 36,* 441-450.

Hiegel, G. A., Abdala, M. H., Vincent Burke, S., & Beard, D. P. (1987). Methods for preparing aqueous solutions of chlorine and bromine for halogen displacement reactions. *Journal of Chemical Education, 64,* 156.

Hilliou, L., Wilhelm, M., Yamanoi, M. & Gonçalves, M. P. (2009). Strucatural and mechanical characterization of κ/ι-hybrid carrageenan gels in potassium salt using Fourier Transform rheology. *Food Hydrocolloids, 23,* 2322-2330.

Hind, A. (2011). *Agilent 101: An introduction to optical spectroscopy*. Available from: http://www.agilent.co.in/labs/features/2011_101_spectroscopy.html Accessed 30.12.2013.

Hong, S. (1995). Prediction of polymer/solvent diffusion behaviour using free-volume theory. *Industrial & Engineering Chemistry Research, 34,* 2536-2544. http://www.researchandmarkets.com/research/wjwckb/asia_pacific

Huang, Y., Davies, E., & Lillford, P. (2011). Effect of solutes and matrix structure on water mobility in glycerol-agar-water gel system: nuclear magnetic resonance approach. *Journal of Agricultural and Food Chemistry, 58,* 4078-4087.

Hutchinson, J. M. (1995). Physical aging of polymers. *Progress in Polymer Science, 20,* 703-760.

HyperPhysics. (2013). *Bragg spectrometer*. Available from: http://hyperphysics.phy-astr.gsu.edu/hbase/quantum/bragg Accessed 13.04.13.

Iijima, M., Hatakeyama, T., Takahashi, M., & Hatakeyama, H. (2007). Effect of thermal history on kappa-carrageenan hydrogelation by differential scanning calorimetry, *Thermochimica Acta*, *452,* 53-58.

Iijima, M., Nakamura, K., Hatakeyama, T., & Hatakeyama, H. (2000). Phase transition of pectin with sorbed water. *Carbohydrate Polymers, 41,* 101-106.

Imeson, A. P. (2000). Carrageenan, In G. O. Phillips & P. A. Williams (Eds.), *Handbook of hydrocolloids* (pp. 87-102). Abington : CRC Press.

International Life Science Institute. (1990). Safety assessment and potential health benefits of food components based on selected scientific criteria. ILSI North America Technical Committee on Food Components for Health Promotion. *Critical Reviews in Food Science and Nutrition, 39,* 203-316.

Jayasundera, M., Adhikari, B., Adhikari, R., & Aldred, P. (2011). The effect of protein types and low molecular weight surfactants on spray drying of sugar-rich foods. *Food Hydrocolloids, 25,* 459-469.

Jenkins, R. & Snyder, R. L. (1996). *Introduction to X-ray powder diffractometry*, NY: John Wiley & Sons, Inc, pp. 47-68.

Jiang, B. & Kasapis, S. (2011). Kinetics of a bioactive compound (caffeine) mobility at the vicinity of the mechanical glass transition temperature induced by gelling polysaccharide. *Journal of Agricultural and Food Chemistry, 59,* 11825-11832.

Jiang, Y. P., Guo, X. K., & Tian, X. F. (2005). Synthesis and NMR structural analysis of *o*-succinyl derivative of low-molecular-weight k-carrgeenan. *Carbohydrate Polymers, 61,* 399-406.

Jie, Z., Bang, L., Ming-jie, X., Hai-wei, L., Zu-kang, Z., Ting-song, W., & Craig, S. A. S. (2000). Studies on the effects of polydextrose intake on physiologic functions in Chinese people. *The American Journal of Clinical Nutrition, 72,* 1503-1509.

Jobling, S. (2004). Improving starch for food and industrial applications. *Current Opinion in Plant Biology, 7,* 210-218.

Jones, O. G. & McClements, D. J. (2010). Functional biopolymer particles: Design, fabrication, and applications. *Comprehensive Reviews in Food Science and Food Safety, 9,* 374-397.

Jones, P. J. & Jew, S. (2007). Functional food development: concept to reality. *Trends in Food Science & Technology, 18,* 387-390.

Josh, R. (1993). Functional characteristics of dairy proteins. *Trends in Food Science & Technology, 4,* 283-288.

Ju, Z. Y. & Kilara, A. (1998). Gelation of pH-aggregate whey protein isolate solution induced by heat, protease, calcium salt, and acidulant. *Journal of Agricultural and Food Chemistry*, *46,* 1830-1835.

Kaláb, M., Allan-Wojtas, D., & Shera Miller, S. (1995). Microscopy and other imaging techniques in food structure analysis. *Trends in Food Science & Technology, 6,* 177-186.

Kalogeras, I. M. (2011). A novel approach for analyzing glass-transition temperature vs composition patterns: Appication to pharmaceutical compound+polymer systems. *European Journal of Pharmaceutical Sciences, 42,* 470-483.

Karel, M., Anglea, S., Buera, P., Karmas, R., Levi, G., & Roos, Y. (1994). Stability-related transitions of amorphous foods. *Thermochimica Acta, 246,* 249-269.

Kasapis, S. (2000). Fundamental considerations in the comparison between thermal and non-thermal characterization of bioglasses. In I. Ahmed, H. S. Ramaswamy, S. Kasapis, & J. I. Boye (Eds.), *Novel food processing-effect on rheological and functional properties* (pp. 187-206). Boca Raton, CRC Press.

Kasapis, S. (2001a). Critical assessment of the application of the WLF/free volume theory to the structural properties of high solids systems: A review. *International Journal of Food Properties, 4,* 59-79.

Kasapis, S. (2001b). The use of Arrhenius and WLF kinetics to rationalise the rubber-to-glass transition in high sugar κ-carrageenan systems. *Food Hydrocolloids, 15,* 239-245.

Kasapis, S. (2004). Definition of a mechanical glass transition temperature for dehydrated foods. *Journal of Agricultural and Food Chemistry, 52,* 2262-2268.

Kasapis, S. (2006). Building on the WLF/Free Volume framework: Utilization of the coupling model the relaxation dynamics of the gelatin/cosolute system. *Biomacromolecules, 7, 1671*-1678.

Kasapis, S. (2006a). Composition and structure-function relationship in gums, In Y. H. Hui (Ed.), *Handbook of food science, technology and engineering* (pp.92-1 to 92-19). Boca Raton: CRC Press.

Kasapis, S. (2006b). Definition and applications of the network glass transition temperature. *Food Hydrocolloid, 20,* 218-228.

Kasapis, S. (2008a). Beyond the free volume theory: Introduction of the concept of cooperativity to the chain dynamics of biopolymers during vitrification. *Food Hydrocolloids, 22,* 84-90.

Kasapis, S. (2008b). Recent advances and future challenges in the explanation and exploitation of the network glass transition of high sugar/biopolymer mixtures. *Critical Review in Food Science and Nutrition, 48,* 185-203.

Kasapis, S. (2009a). Glass transitions in foodstuffs and biomaterials: Theory and measurements. In M. S. Rahman (Ed.), *Food properties handbook*, 2nd Ed. (pp. 207-245). Boca Raton, CRC Press.

Kasapis, S. (2009b). Unified application of the material-science approach to the structural properties of biopolymer co-gel throughout the industrially relevant level of solids. In S. Kasapis, I. T. Norton, & J. B. Ubblink (Eds), *Modern biopolymer science: bridging the divide between fundamental treatise and industrial applications* (pp. 225-260). NY: Academic Press.

Kasapis, S. (2012). Relation between the structure of matrices and their mechanical relaxation mechanisms during the glass transition of biomaterials: A review. *Food Hydrocolloids, 26,* 464-472.

Kasapis, S., Al-Alawi, A., Guizani, N., Khan, A. J., & Mitchell, J. R. (2000). Viscoelastic properties of pectin-co-solute mixtures at iso-free-volume states. *Carbohydrate Research, 329,* 399-407.

Kasapis, S., Al-Marhoobi, I. M. A., & Giannouli, P. (1999). Molecular order versus vitrification in high-sugar blends of gelatin and κ-carrageenan. *Journal of Agricultural and Food Chemistry, 47,* 4944-4949.

Kasapis, S., Al-Marhoobi, I. M., & Mitchell, J. R. (2003). Molecular weight effects on the glass transition of gelatin/cosolute mixtures. *Biopolymers, 70,* 169-185.

Kasapis, S., Al-Marhoobi, I. M., & Mitchell, J. R. (2003). Testing the validity of comparisons between the rheological and the calorimetric glass transition temperatures. *Carbohydrate Research, 388,* 787-794.

Kasapis, S., Al-Marhoobi, I. M., & Sworn, G. (2001). α and β mechanical dispersions in high sugar/acyl gallan mixture. *International Journal of Biological Macromolecules, 29,* 151-160.

Kasapis, S. & Mitchell, J. R. (2001). Definition of the rheological glass transition temperature in associated with the concept of iso-free-volume. *International Journal of Biological Macromolecules, 29,* 315-321.

Kasapis, S., Mitchell, J., Abeysekera, R., & MacNaughtan, W. (2004). Rubber-to-glass transitions in high sugar/biopolymer mixtures. *Trends in Food Science & Technology, 15,* 298-304.

Kasapis, S. & Shrinivas, P. (2010). Combined use of thermomechanics and UV spectroscopy to rationalize the kinetics of bioactive compound (caffeine) mobility in a high solids matrix. *Journal of Agricultural and Food Chemistry, 58,* 3825-3832.

Kee, D. D., Liu, Q., & Hinestroza, J. (2005). Viscoelastic (non-Fickian) Diffusion. *The Canadian Journal of Chemical Engineering, 83,* 913-923.

Knigh, J. A., Anderson, S., & Rawie, J. M. (1972). Chemical basis of the Sulfo-phospho-vanillin for estimating total serum lipids. *Clinical Chemistry, 18,* 199-202.

Kong, X., Kasapis, S., Bao, J., & Corke, H. (2009). Effect of gamma irradiation on the thermal and rheological properties of grain amaranth starch. *Radiation Physics and Chemistry*, *78,* 954-960.

Korsmeyer, R. W., Gurney, R., Doelker, E. M., Buri, P., & Peppas, N. A. (1983). Mechanism of solute release from porous hydrophilic polymers. *International Journal of Pharmaceutics, 198,* 15, 23-35.

Kou, J. H. (2000). Transport in polymer systems. In G. L. Amidon, E. M. Topp & P. I., Lee (Eds), *Transport process in pharmaceutical systems* (pp. 445-471). NY: CRC Press, M. Dekker.

Kovačevič, D., Mastanjević, K., & Kordić, J. (2011). Cryoprotective effect of polydextrose on chicken surimi. *Czech Journal of Food Science, 29,* 226-231.

Kuang, S. S., Oliveira, J. C., & Crean, A. M. (2010). Microencapsulation as a tool for incorporating bioactive ingredients into food. *Critical Review in Food Science and Nutrition, 50,* 951-968.

Kumagai, H., MacNaughtan, W., Farhat, I. A., & Mitchell, J. R. (2002). The influence of carrageenan on molecular mobility in low moisture amorphous sugars. *Carbohydrate Polymers, 48,* 341-349.

Labuza, T. P. & Hyman, C. R. (1998). Moisture migration and control in multi-domain foods. *Trends in Food Science & Technology, 9,* 47-55.

Labuza, T. P. & Ribos, D. (1982). Theory and application of Arrhenius kinetics to the prediction of nutrient losses in foods. *Food Technology, 36,* 67-74.

Labuza, T. P. (1984). Application of chemical kinetics to deterioration of food. *Journal of Chemical Education, 61,* 348-358.

Laovachirasuwan, P., Peerapattana, J., Srijesdaruk, V., Chitropas, P., & Utsaka, M. (2010). The physicochemical properties of a spray dried glutinous rice starch biopolymer. *Colloid and Surface B: Biointerfaces, 78,* 30-35.

Le Meste, M. L., Champion, D., Roudaut, G., Blond, G., & Simatos, D. (2002). Glass transition and food technology: A critical appraisal. *Journal of Food Science, 67,* 2444-2458.

Leśková, E., Kubíková, J., Kováćiková, E., Košická, M., Porubská, J., & Holćíková, K. (2006). Vitamin losses: Retention during heat treatment and continual changes expressed by mathematical models. *Journal of Food Composition and Analysis*, *19,* 252-276.

Lesmes, U. & McClements, D. J. (2009). Structure-function relationships to guide rational design and fabrication of particulate food delivery systems. *Trends in Food Science & Technology, 20,* 448-457.

Lin, S. & Pascall, M. A. (2014). Incorporation of vitamin E into chitosan and its effect on the film foaming solution (viscosity and drying rate) and the solubility and thermal properties of the dried film. *Food Hydrocolloids*, *35,* 78-84.

Liu, P., Yu, L., Liu, H., Chen, L., & Li, L. (2009). Glass transition temperature of starch studied by a high-speed DSC. *Carbohydrate Polymers, 77,* 250–253.

Liu, Y., Bhandari, B., & Zhou, W. (2006). Glass transition and enthalpy relaxation of amorphous food saccharides: A review. *Journal of Agricultural and Food Chemistry, 54,* 5701-5717.

Lon, J., Lii, C., & Chang, Y. (2005). Change of granular and molecular structures of waxy maize and potato starches after treated in alcohols with or without hydrochloric acid. *Carbohydrate Polymers, 59,* 507-515.

Loret, C., Ribelles, P., & Lundin, L. (2009). Mechanical properties of κ-carrageenan in high concentration of sugar solutions. *Food Hydrocolloids, 23,* 823-832.

Lukaski, H. C. (2004). Vitamin and mineral status: Effects on physical performance. *Nutrition, 20,* 632-644.

Maltini, E., Torreggiani, D., Venir, E., & Bertolo, G. (2003). Water activity and the preservation of plant foods. *Food Chemistry, 82,* 79-86.

Malvern, (2014). *Mastesizer 3000 smart particle sizing*. Available from: http://www.malvern.com/en/products/product-range/mastersizer-range/mastersizer-000/default.aspx?gclid=CMOM69T8w8ACFRIHvAod2aIAjw. Accessed 03.09.14.

Marcotte, M., Sablani, S. S., Kasapis, S., Baik, O., & Fusteir, P. (2004). The thermal kinetics of starch gelatinization in the presence of other cake ingredients. *International Journal of Food Science and Technology*, *39,* 807-810.

Mártinez-Ruvalcuba, A., Sánchez-Díaz, J. C., Becerra, F., Cruz-Barba, L. E., & González-Álvarez, A. (2009). Swelling characterization and drug delivery kinetics of polyacrylamide-co-itaconic acid/chitosan hydrogels. *eXPRESS Polymer Letter*, *3,* 25-32.

May, C. D. (1990). Industrial pectins: Sources, production and applications. *Carbohydrate Polymers, 12,* 79-99.

McClements, D. J., Decker, E. A., Park., Y., & Weiss, J. (2009). Structural design principles for delivery of bioactive components in nutraceuticals and functional food. *Critical Review in Food Science and Nutrition, 49*, 577-606.

McIntosh, G. H., Regester, G. D., Lelue, R. K., Royle, P. J., & Smithers, G. W. (1995). Dairy proteins protect against dimethylhydrazine-induced intestinal cancers in rats. *Journal of Nutrition*, *125,* 809-816.

Meinders, M., B., J. & van Vliet, T. (2009). Modeling water sorption dynamics of cellular solid food systems using free volume theory. *Food Hydrocolloids, 23,* 2234-2242.

Mellan, I. (1977). *Industrial solvents handbook*, 2nd ed., HJ: Noyes Data Corporation.

Michel, A-S., Mestdagh, M. M., & Axelos, M. A. V. (1997). Physico-chemical properties of carrageenan gels in presence of various cations. *International Journal of Biological Macromolecules, 21,* 195-200.

Míčková, K, Čopìková, J., & Synytsya, A. (2007). Determination of polydextrose as a fat replacer in butter. *Czech Journal of Food Science, 25,* 25-31.

Mimouni, A., Deeth, H. C., Whittaker, A. K., Gidley, M. J., & Bhandari, B. R. (2009). Rehydration process of milk protein concentrate powder monitored by static light scattering. *Food Hydrocolloids, 23,* 1958-1965.

Monsoor, M. A., Kalapathy, U., & Proctor, A. (2001). Improved method for determination of pectin degree of esterification by diffuse reflectance Fourier transform infrared spectroscopy. *Journal of Agricultural and Food Chemistry, 49,* 2756-2760.

Moore, R., Clark, D. W., & Vodopich, D. (1998). *Botany, 2nd Eds*. NY: WCB/McGraw-Hill.

Moreau, L., Bindzus, W., & Hill, S. (2011). Influence of salts on starch degradation: Part II-salt classification and caramelisation. *Starch/Stärke, 63,* 676-682.

Morris, V. J. & Chilvers, G. R. (1983). Rheological studies of specific cation forms of kappa carrageenan gels. *Carbohydrate Polymers, 3,* 129-141.

Muñoz, L. A., Pedreschi, F., Leiva, A., & Aguilera, J. M. (2015). Loss of birefringence and swelling behavior in native starch granules: Microstructural and thermal properties. *Journal of Food Engineering, 152,* 65-71.

Nakano, T., Sugimoto, Y., Ibrahim, H. R., Toba, Y., Aoe, S., & Aoki, T. (2000). Preparation and characterization of milk calcium salts by using casein phosphopeptide. *Preparative Biochemistry and Biotechnology, 30,* 155-166.

Natural History Museum UK. (2013). *Philips XL30 field emission SEM*. Available from: http://www.nhm.ac.uk/research-curation/science-facilities/analytical-imaging/imaging/ high-resolution-sem/xl30/index.html Accessed 13.04.13.

Nelson, K. A. & Labuza, T. P. (1994). Water activity and food polymer sciences: implications of state on Arrhenius and WLF models in predicting shelf life. *Journal of Food Engineering, 22,* 271-289.

Nickerson, M. T. & Paulson, A. T. (2005). Time-temperature studies of κ-carrageenan gelation in the presence of high levels of co-solutes. *Carbohydrate Polymers, 61,* 231-237.

Nickerson, M. T., Paulson, A. T., & Speers, R. A. (2004). A time-temperature rheological approach for examining food polymer gelation. *Trends in Food Science & Technology, 15,* 569-574.

Nishinari, K. & Watase, M. (1992). Effects of sugars and polyols on the gel-sol transition of kappa-carrageenan gels. *Thermochimica Acta*, *206,* 149-162.

Nishinari, K., Watase, M., Williams, P. A., & Phillips, G. O. (1990). κ-carrageenan gels: Effect of sucrose, glucose, urea and guadinine hydrochloride on the rheological and thermal properties. *Journal of Agricultural and Food Chemistry, 38,* 1188-1193.

Noel, T. R., Ring, S. G., & Whittam, M. A. (1990). Glass transition in low-moisture foods. *Trends in Food Science & Technology, 1,* 62-67.

Nussinovitch, A. (2005). Production, properties, and applications of hydrocolloid cellular solids. *Molecular Nutrition & Food Research, 49,* 195-213.

Olkku, J. & Rha, C. (1978). Gelatinisation of starch and wheat flour starch: A review. *Food Chemistry*, 3, 293-317.

Ottaway, P. B. (1993). *The technology of vitamins in food.* London: Chapman and Hall, p. 259.

Ottley, C. (2000). Nutritional effects of new processing technology. *Trends in Food Science & Technology*, 11, 422-425.

Pachapurkar, D. & Bell, L. N. (2005). Kinetics of thiamin degradation in solutions under ambient storage conditions. *Journal of Food Science, 70,* C423-C426.

Palma-Rodriguez, H. M., Agama-Acevedo, E., Gonzalez-Soto, R. A., Vemon-Carler, E. J., Alvarez-Ramirez, J., & Bello-Perez, L. A. (2013). Ascorbic acid microencapsulation by spray drying in native and acid-modified starches from different botanical sources. *Starch/Stärke, 65,* 584-592.

Palzer, S. (2005). The effect of glass transition on the desired and undesired agglomeration of amorphous food powders. *Chemical Engineering Science, 60,* 3959-3968.

Palzer, St. (2010). The relation between material properties and supra-molecular structure of water-soluble food solids. *Trends in Food Science & Technology, 21,* 12-25.

Panyoyai, N., Bannikova, A., Small, D. M. & Kasapis, S. (2015). Controlled release of thiamin in a glassy κ-carrageenan/glucose syrup matrix. *Carbohydrate Polymers*, *115,* 723-731.

Panyoyai, N., Bannikova, A., Small D. M., & Kasapis, S. (2016). Diffusion kinetics of ascorbic acid in a glassy matrix of high-methoxy pectin with polydextrose. *Food Hydrocolloids, 53,* 293-302.

Panyoyai, N, Bannikova, A., Small, D. M., Shanks, R. A., & Kasapis, S. (2016). Diffusion of nicotinic acid in spray-dried capsules of whey protein isolate. *Food Hydrocolloids, 52,* 811-819.

Papiz, M. Z., Sawyer, L., Eliopoulos, E. E., North, A. C. T., Findlay, J. B. C., Sivaprasadarao, R., Jones, T. A., Newcomer, M. E., & Kraulis, P. J. (1986). The structure of β-lactoglobulin and its similarity to plasma retinol-binding protein. *Nature, 324,* 383-385.

Parada, J. & Aguilera, J. M. (2007). Food microstructure affects the bioavilability of several nutrients. *Journal of Food Science, 72,* R21-R32.

Paramita, V. D., Bannikova, A., & Kasapis, S. (2015). Release mechanism of omega-3 fatty acid in κ-carrageenan/polydextrose undergoing glass transition. *Carbohydrate Polymers*, *126,* 141-149.

Patel, A, R. & Velikov, K. P. (2011). Colloidal delivery system in foods: A general comparison with oral drug delivery. *LWT-Food Science and Technology, 44,* 1958-1964.

Pelegrine, D. H. G. & Gomes, M. T. M. S. (2012). Analysis of whey protein solubility at high temperatures. *International Journal of Food Engineering*, 8, Article 23. DOI: 10.1515/1556-3758.1265.

Peppas N. A. & Reinhart, C. T. (1983). Solute diffusion in swollen membrane. I. A new theory. *Journal of Membrane Science, 15,* 275-287.

Peppas, N. A. (1985). Analysis of Fickian and non-Fickian drug release from polymers. *Pharmaceutica Acta Helvetiae, 60,* 110–111.

Perkin-Elmer, (2013a). *Dynamic Mechanical Analysis (DMA) A Beginner's Guide*. Available from: http://www.perkinelmer.com/CMSResources/Images/44-74546GDE_IntroductionToDMA.pdf Accessed 02.09.14.

Perkin-Elmer, (2013b). *FT-IR and FT-NIR spectrometers*. Available from: http://www.perkinelmer.com.cn/cmsresources/images/46-4472bro_spectrum100ftir.pdf Accessed 13.04.13.

Perkin-Elmer, (2013c). *Lambda 25/35/45 UV/Vis spectrophotometer*. Available from: http://www.perkinelmer.com/Content/relatedmaterials/brochures/bro_lambda253545.pdf Accessed 13.04.13.

Polymer Scienence Learning Centre, University of Southern Mississippi. (2013). *Differential Scanning Calorimetry*. Available from: http://www.pslc.ws/macrog/dsc.htm Accessed 14.04.13.

Pothakamury, U. R. & Barbosa Cánovas, G. V. (1995). Fundamental aspects of controlled release in foods. *Trends in Food Science & Technology, 6,* 397-406.

Prakash, S., Huppertz, T., Karrchuk, O., & Deeth, H. (2010). Ultra-high-temperature processing of chocolate flavoured milk. *Journal of Food Engineering, 96,* 179-184.

Prasad, P. S. S., Rajasree, K. P., Khan, K. A., & Reddy, M. N. (1997). Colorimetric determination of thiamine hydrochloride using Alizarin Brilliant Violet R. *Indian Journal of Pharmaceutical Sciences, 59,* 194-196.

Radosta, S., Boczek, P., & Grossklaus, R. (1992). Composition of polydextrose® before and after intestinal drgradation in rats. *Starch/Stärke*, *4,* 150-153.

Rahman, M. S. (2006). State diagram of foods: Its potential use in food processing and product stability. *Trends in Food Science & Technology, 17,* 129-141.

Rahman, M. S. (2010). Food stability determination by macro-micro region concept in the state diagram and by defining a critical temperature. *Journal of Food Engineering*, *99,* 402-416.

Rajan, K. (2011). *Analytical techniques in biochemistry and molecular biology*. NY, Springer, p. 286.

Raemy, A. & Lambelet, P. (1991). Thermal behavior of foods. *Thermochimica Acta, 193,* 417-439.

Ramesh, N., Davis, P. K., Zielinski, J. M., Danner, R. P. & Duda, J. L. (2011). Application of Free-Volume theory to self-diffusion of solvents in polymers below the glass transition temperature: A review. *Journal of Polymer Science Part B, Polymer Physics, 49,* 1629-1644.

Raninen, K., Lappi, J., Mykkänen, H., & Poutanen, K. (2011). Dietary fiber type reflects physiological functionality: Comparison of grain fiber, inulin, and polydextrose. *Nutrition Reviews*, *69,* 9-21.

Rawle, A. (2014). *Basic principles of particle size analysis.* Available from: http://golik.co.il/Data/BasicPrinciplesofParticlesize_1126925513.pdf Accessed 03.09.14.

Rehage, G., Ernst, O., & Fuhrmann, J. (1970). Fickian and non-Fickian diffusion in high polymer systems, *Discussion of the Faraday Society, 49,* 208-221.

Relkin, P. & Shukat, R. (2012). Food protein aggregates as vitamin-matrix carriers:Impact of processing conditions. *Food Chemistry, 134,* 2141-2148.

Renzetti, S.,Voogt, J. A., Oliver, L., & Meinders, M. B. J. (2012). Water migration mechanisms in amorphous powder material and related agglomeration propensity. *Journal of Food Engineering, 110,* 160-168.

Research & Markets (2015). *Asia Pacific Vitamins (Neutraceuticals) market-trends and forecast up to 2019.* Available from: http://www.prnewswire.com/news-releases/asia-pacific-vitamins-nutraceuticals-market-2015---trends-and-forecast-up-to-2019-300080201.html Accessed 24.01.16.

Ribeiro, C., Zimeri, J. E., Yildiz, E., & Kokini, J. L. (2003). Estimation of effective diffusivities and glass transition temperature of polydextrose as a function of moisture content. *Carbohydrate Polymers, 51,* 273-280.

Richardson, R. & Kasapis, S. (1998). Rheological methods in the characterization of food biopolymers. In D. Wetsel & G. Charalambous (Eds.), *Instrumental methods in food and beverage analysis* (p. 13). Elsevier Science: B.V.

Righetto, A. M. & Netto, F. M. (2006). Vitamin C stability in encapsulated green west Indian cherry juice and in encapsulated synthetic ascorbic acid. *Journal of the Science of Food and Agriculture, 86,* 1202-1208.

Ritger, P. L. & Peppas, N. A. (1987a). A simple equation for description of solute release I. Fickian and non-Fickian release from non-swellable devices in the form of slabs, spheres, cylinders or discs. *Journal of Controlled Release, 5,* 23-36.

Ritger, P. L. & Peppas, N. A. (1987b). A simple equation for description of solute release II. Fickian and anomalous release from swellable device. *Journal of Controlled Release*, *5,* 37-42.

Rocha, G. A., Fávaro-Trindade, C. S. & Grosso, C. R. F. (2012). Microencapsulation of lycopene by spray drying: characterization, stability and application of microcapsules. *Food and Bioproducts Processing, 90,* 37-42.

Roos, Y. H. (1995). Characterization of food polymer using state diagrams. *Journal of Food Engineering, 24,* 339-360.

Roos, Y. H. (2003). Thermal analysis, state transitions and food quality. *Journal of Thermal Analysis and Calorimetry, 71,* 197-203.

Roos, Y. H. (2010). Glass transition temperature and its relevance in food processing. *Annual Review of Food Science and Technology, 1,* 469-496.

Roudaut, G., Simatos, D., Champion, D., Contreras-Lopez, E., & Le Meste, M. (2004). Molecular mobility around the glass transition temperature: A mini review. *Innovative Food Science and Emerging Technology, 5,* 127-134.

Rudraraju, V. & Wyandt, C. M. (2005). Rheology characterization of microcrystalline cellulose/sodium carboxymethyl cellulose hydrogels using a controlled stress rheometer Part I. *International Journal of Pharmaceutics, 192,* 53-61.

Russel, P. (1987). Gelatinisation of starches of different amylose/amylopectin content. A study by differential scanning calorimetry. *Journal of Cereal Sciences, 6,* 133-145.

Sablani, S. S., Al-Belushi, K., Al-Marhubi, I., & Al-Belushi, R. (2007). Evaluating stability of vitamin C in fortified formula using water activity and glass transition. *International Journal of Food Properties, 10,* 61-71.

Sablani S. S., Datta, A. K., Rahan, S., Qaboos, S., & Mujumdar, A. S. (2006). *Handbook of food and bioprocess modeling techniques.* NY: CRC Press. p. 246.

Sablani, S. S., Kasapis, S., & Rahman, M. S. (2007). Evaluating water activity and glass transition concepts for food stability. *Journal of Food Engineering, 78,* 266-271.

Sablani, S. S., Syamaladevi, R. M., Swanson, B. G. (2010). A review of methods, data and applications of state diagrams of food systems. *Food Engineering Reviews*, *2,* 168-203.

Savadkoohi, S., Bannikova, A., Kasapis, S., & Adhikari, B. (2014). Structural behavior in condensed bovine serum albumin systems following applications of high pressures. *Food Chemistry, 150,* 469-476.

Schmidl, M. K. (1993). Food products for medical purpose. *Trends in Food Science & Technology, 4,* 163-168.

SETARAM. (2014). *Micro DSC III high sensitivity DSC and calorimetry.* Available from: http://files.instrument.com.cn/17img/old/literature/C63213.pdf Accessed 02.09.14.

Shalaev, E. Y. & Kanev, A. N. (1994). Study of the solid-liquid state diagram of the water-glycine-sucrose system. *Cryobiology, 31,* 374-382.

Shalmashi, A. & Eliassi, A. (2008). Solubility of L-(+)-ascorbic acid in water, ethanol, methanol, propan-2-ol, acetone, acetonitrile, ethyl acetate and tetrahydrofuran from (293-323) K. *Journal of Chemical Engineering Data*, 53, 1332-1334.

Shanks, R. A. & Gunaratne, L. M. W. (2011). Gelatinization and retrogradation of thermoplastic starch characterized using modulated temperature differential scanning calorimetry. *Journal of Thermal Analysis and Calorimetry, 106,* 93-99.

Sharma, D., George, P., Button, P. D., May, B. K., & Kasapis, S. (2011). Thermomechanical study of the phase behaviour of agarose/gelatin mixtures in the presence of glucose syrup as co-solute. *Food Chemistry, 127,* 1784-1791.

Shen, Z., Apriani, C., Weerakkody, R., Sanquansri, L., & Augustin, M. A. (2011). Food matrix effects on in vitro digestion of microencapsulated tuna oil powder. *Journal of Food Agricultural & Food Chemistry*, *59*, 8422-8449.

Sherwin, C. P. & Labuza, T. P. (2006). Beyond water activity and glass transition: A broad perspective on the manner by which water can influence reaction rates in foods, In M. P., Buera, J., Welti-Chanes, P. J., Lillford, & H. R., Corti (Eds), *Water properties of food, pharmaceutical and materials* (pp. 343-376). NY: CRC Press, Taylor & Francis Group.

Shrinivas, P. & Kasapis, S. (2010). Unexpected phase behavior of amylose in a hight solids environment. *Biomacromolecules, 11,* 421-429.

Shu, B., Yu, W., Zhao, Y., & Liu, X. (2006). Study on microencapsulation of lycopene by spray-drying. *Journal of Food Engineering, 76,* 664-669.

Siepmann, J. & Siepmann, F. (2008). Mathematical modeling of drug delivery. *International Journal of Pharmaceutics, 364,* 328-343.

Siepmann, J. & Siepmann, F. (2012). Modeling of diffusion controlled drug delivery. *Journal of Controlled Release, 161,* 351-362.

Sigma-Aldrich. (2013). *Chemical structure of L-ascorbic acid, thiamine hydrochloride, nicotinic acid and tocopherol.* Available from: http://www.sigmaaldrich.com. Accessed 11.12.14.

Sila, D. N., van Buggenhout, S, Duvetter, T, Fraeye, I, de Roeck, A., van Loey, A., & Hendrickx, M. (2009). Pectins in processed fruits and vegetables: Part II-Structure–function relationships. *Comprehensive Reviews in Food Science and Food Safety, 8,* 86-104.

Singh, B. & Chauham, N. (2009). Modification of psyllium polysaccharides for use in oral insulin delivery. *Food Hydrocolloids, 23,* 928-935.

Singh, J., Kaur, L., & McCarthy, O. J. (2007). Factors influencing the physico-chemical morphology, thermal and rheological properties of some chemically modified starches for food applications- A review. *Food Hydrocolloids, 21,* 1-22.

Singh, N., Singh, J., Kaur, L., Sodhi, N. S., & Gill, B. S. (2003). Morphological, thermal and rheological properties of starches from different botanical sources. *Food Chemistry, 81,* 219-231.

Slade. L. & Levine, H. (1991). Beyond water activity: Recent advances based on an alternative approach to the assessment of food quality and safety. *Critical Reviews in Food Science and Nutrition, 30,* 115-360.

Slade, L. & Levine, H. (1993). Water relationship in starch transitions. *Carbohydrate Polymers,* 21, 105-131.

Spray Analysis and Research services. (2014). *Laser Diffraction Particle Analyzer*. Available from: http://www.sprayconsultants.com/laser-diffraction.asp Accessed 03.09.14.

Stojanovic, Z. & Markovic, S. (2012). Determination of particle size distribution by laser diffraction. *Techniques-New materials, 21,* 11-20.

Stowell, J. D. (2009). Polydextrose. In S. S. Cho, & P. Samuel (Eds.), *Fiber ingredients: Food applications and health benefits* (pp.137-196). Boca Raton : CRC Press.

TA Instruments. (2013a). *AR-G2 Rheometer.* Available from: http://cit.kuleuven.be/smart/infrastructure/documents/AR-G2.pdf Accessed 13.04.13.

TA Instruments. (2013b). *Differential Scanning Calorimetry.* Available from: http://www.tainstruments.com/pdf/brochure/thermal_analysis.pdf Accessed 13.04.13.

Tabilo-Munizaga, G. & Barbosa-Cánovas, G. V. (2005). Rheology for the food industry. *Journal of Food Engineering, 67,* 147-156.

Takhar, P. S. (2008). Role of glass-transition on fluid transport in porous food materials. *International Journal of Food Engineering, 4,* DOI:10.2201/1556-3578.

Teleki, A., Hitzfeld, A., & Eggersdorfer, M. (2013). 100 Years of vitamins: the science of formulation is the key to functionality. *KONA Powder and Particle Journal, 30,* 144-163.

Thakur, B. R., Singh, R. K., & Handa, A. K. (1997). Chemistry and uses of pectin-A review. *Critical Reviews in Food Science and Nutrition, 37,* 47-73.

The Royal Society of Chemistry. (2013a). *Electron microscope*. In *Modern chemical techniques* (pp. 160-171). Available from: http://media.rsc.org/Modern%20chemical%20techniques/MCT6%20Electron%20microscopy.pdf Accessed 14.04.13

The Royal Society of Chemistry. (2013b). *Ultraviolet/visible spectroscopy*, in *Modern chemical techniques* (pp. 92-115). Available from: http://media.rsc.org/Modern%20chemical%20techniques/MCT4%20UV%20and%20visible%20spec.pdf Accessed 14.04.13

Thermo Nicolet Corporation. (2001). *Introduction to Fourier Transform Infrared Spectroscopy*. Madison: USA. pp. 1-8.

Tien, C. L., Letendre, M., Ispas-Szabo, P., Mateescu, M. A., Delmas-Patterson, G., Yu, H.-L., & Lacroix, M. (2000). Development of biodegradable films from whey proteins by cross-linking and entrapment in cellulose. *Journal of Agricultural and Food Chemistry, 48,* 5566-5577.

Tolstoguzov, V. (2008) Food polymer, In J. M. Aguilera & José Lillford (Eds.), *Food materials sciences principle and practice* (pp. 21-44). NY, Springer.

Totosaus, A., Montejano, J. G., Salazar, J., & Guerrero, I. (2002). A review of physical and chemical protein-gel induction. *International Journal of Food Science and Technology, 37,* 589-601.

Tramón, C. (2014). Modeling the controlled release of essential oils from a polymer matrix-A special case. *Industrial Crops and Products, 61,* 23-30.

Turgeon, S. & Rioux, L. (2011). Food matrix impact on macronutrients nutritional properties. *Food Hydrocolloids, 25,* 1915-1924.

Tütüncü, M. A. & Labuza, T. P. (1996). Effect of geometry on the effective moisture transfer diffusion coefficient. *Journal of Food Engineering, 30,* 433-447.

Ubbink, J., Burbidge, A., & Mezzenga, R. (2008). Food structure and functionality: A soft matter perspective. *Soft Matter, 4,* 1569-1581.

Ubbink, J. & Krüger, J. (2006). Physical approaches for the delivery of active ingredients in foods. *Trend in Food Science & Technology, 17,* 244-254.

van Boekel, M. A. J. S. (2008). Kinetic modeling of food quality: A critical review. *Comprehensive Reviews in Food Science and Food Safety, 7,* 144-158.

van Buggenhout, S., Sila, D. N., Duvetter, T., van Loey, A., & Hendrickx, M. (2009). Pectins in processed fruits and vegetables: Part III texture engineering. *Comprehensive Reviews in Food Science and Food Safety, 8,* 105-117.

van de Velde, K. & Kiekens, P. (2002). Biopolymers; Overview of several properties and consequence on their applications. *Polymer Testing, 21,* 433-442.

van der Put, T. A. C. M. (2010). Theoretical derivation of the WLF-and annealing equations. *Journal of Non-crystalline Solid, 356,* 394-399.

van der Sman, R. G. M. & Meinders, M. B. J. (2013). Moisture diffusivity in food materials. *Food Chemistry, 138,* 1265-1274.

van der Sman, R. G. M., & van der Goot, A. J. (2009). The science of food structuring. *Soft Matter, 5,* 501-510.

van de Voort, F. R. (1992). Fourier transform infrared spectroscopy applied to food analysis. *Food Research International, 25,* 397-403.

van Vliet, T., Lakemond, C. M. M., & Visschers, R. W. (2004). Rheology and structure of milk protein gels. *Current Opinion in Colloid & Interface Science, 9,* 298-304.

Velikov, K. P. & Pelan E. (2008). Colloidal delivery systems for micronutrients and nutraceuticals. *Soft Matter, 4,* 1964-1980.

Verdonck, E., Schaap, K., & Thomas, L. C. (1999). A discussion of the principles and applications of Modulated Temperature DSC (MTDSC). *International Journal of Pharmaceutics, 192,* 3-20.

Vergnaud, J. M. (1991). Liquid transport processes in polymeric materials. NJ: Prentice Hall.

Vrentas, J. S. & Duda, J. L. (1977a). Diffusion in polymer-solvent systems. I. Reexamination of the free volume theory. *Journal of Polymer Science Part B, Polymer Physics Edition,15,* 403-416.

Vrentas, J. S. & Duda, J. L. (1977b). Diffusion in polymer-solvent systems. II. A predictive theory for the dependence of diffusion coefficients on temperature, concentration, and molecular weight. *Journal of Polymer Science Part B, Polymer Physics Edition,15,* 417-439.

Vrentas, J. S. & Duda, J. L. (1977c). Diffusion in polymer-solvent systems. III. Construction of Deborah number diagrams. *Journal of Polymer Science Part B, Polymer Physics Edition,15,* 441-453.

Vrentas, V. & Vrentas, C. (2013). Parameter in consecutive equations in *Diffusion and mass transfer* (pp. 99-148). Boca Raton: CRC Press, Taylor & Francis Group.

Walter, P. (1994). Vitamin requirements and vitamin enrichment of foods. *Food Chemistry, 49,* 113-117.

Ward, I. M. & Hadley, D. W. (1993). Experimental studies of linear viscoelasticity behaviour as a function of frequency and temperature: Time-temperature equivalence. *An Introduction to the Mechanical Properties of Solid Polymers* (pp. 84-108). Chi Chester : John Wiley.

Wijaya, M., Small, D. M., & Bui, L. (2011) *Microencapsulation of ascorbic acid for enhanced long-term retention during storage.* Technical report number DSTO-TR-2504. Division, Defense Science and Technology Organisation, Fishermans Bend, Victoria, Australia.

Willats, W. G. T., Knox, P. J., & Mikkelsen, J. (2006). Pectin: New insights into an old polymer are starting to gel. *Trends in Food Science & Technology*, *17,* 97-104.

Williams, M. L., Landel, R. F. & Ferry, J. D. (1995). The temperature dependence of relaxation mechanisms in amorphous polymers and other glass-forming liquids. *Journal of the American Chemistry Society, 77,* 3701-3707.

Wilson, N. & Shah, N. P. (2007). Microencapsulation of vitamins. *ASEAN Food Journal*. *14,* 1-14.

Yang, N., Liu, Y., Ashton, J., Gorczyca, E., & Kasapis, S. (2013). Phase behavior and *in vitro* hydrolysis of wheat starch in mixture with whey protein. *Food Chemistry, 137,* 76-82.

Yoshii, H., Neoh, T. L., Furata, T., & Ohkawara, M. (2008). Encapsulation of proteins by spray drying and crystal transformation method. *Drying Technology, 26,* 1308-1312.

Yu, Z. & Quinn, P. J. (1994). Dimethyl sulfoxide: A review of its applications in cell biology. *Bioscience Report, 14,* 259-281.

Zarzycki, R., Modrzejewska, Z. & Nawrotek, K. (2010). Drug release from hydrogel matrices. *Ecological Chemistry and Engineering, 17,* 117-136.

Zhou, Y. & Roos, Y. H. (2012a). Stability and plasticizing and crystallization effects of vitamins in amorphous sugar systems. *Journal of Agricultural and Food Chemistry, 60,* 1075-1083.

Zhou, Y. & Roos, Y. H. (2012b). Stability of α-tocopherol in freeze-dried sugar-protein-oil emulsion solids as affected by water plasticization and sugar crystallization. *Journal of Agricultural and Food Chemistry, 60,* 7497-7505.

Zobel, H. F. (1988). Molecules to granules: a comprehensive starch review. *Starch/Stärke*, *40,* 44-50.